

SYNTHESIS AND CHARACTERISATION OF  
HYPERCROSSLINKED POLYMER  
MICROPARTICLES AND THEIR  
FUNCTIONALISED DERIVATIVES

PhD Thesis

NORHAYATI ABDULLAH

MAY 2013

## **Declaration of Copyright**

The copyright of this thesis belongs to the author under the terms of the United Kingdom Copyright Act as qualified by University of Strathclyde Regulation 3.51. Due acknowledgement must always be made of the use of any material contained in, or derived from, this thesis.

## **Acknowledgements**

The work reported herein was carried out in the Department of Pure and Applied Chemistry, University of Strathclyde, through full-time study, and was funded by the Government of Malaysia through the Ministry of Higher Education (MOHE). Permission to register for a PhD degree, and financial support provided by the University, is gratefully acknowledged.

The author wishes to express her gratitude to Prof Peter Cormack for his phenomenal supervision of the research, constant support and meticulous checking of manuscripts. Also, to Prof Sherrington a thousand thanks for the knowledge sharing, ideas and experiences.

The author would like to thank her colleagues within the Polymer Group at Strathclyde for their encouragement and constant support. The advice offered by colleagues is particularly appreciated.

The author is grateful to Mr Gavin Bain, Mrs Denise Gilmour and Mr Jim Morrow for their assistance in the analytical support laboratories. The production of all specimens in the Departmental Workshop was of the highest quality, for which the author is grateful.

Last, but not least, the author would like to say thank you very much to her family members for their support during the period of study.

## List of Abbreviations

ADP	Aqueous dispersion polymerisation
acac	Acetylacetone
A-HXL	Aminated hypercrosslinked polymer
AIBN	2-2'Azobisisobutyronitrile
BET	Brunauer, Emmett and Teller
DCE	1,2-Dichloroethane
DVB	Divinylbenzene-80
EGDMA	Ethylene glycol dimethacrylate
EtOH	Ethanol
EVB	Ethylvinylbenzene
FTIR	Fourier-Transform Infra-Red
Hept	Heptane
HXL	Hypercrosslinked
HXLNAD	Hypercrosslinked non-aqueous dispersion polymer
IEC	Ion-exchange capacity
MeOH	Methanol
NAD	Non-aqueous dispersion
PAA	Poly(acrylic acid)
PHXL	Partially hypercrosslinked
PSt	Polystyrene
PVP	Poly( <i>N</i> -vinylpyrrolidone)
RT	Room temperature
SAX	Strong anion-exchange
SCX	Strong cation-exchange
SEM	Scanning electron microscopy
S-HXL	Sulfonated hypercrosslinked polymer
SSA	Specific surface area
St	Styrene
VBC	4-Vinylbenzyl chloride

## Abstract

High specific surface area, microporous polymer particles were prepared successfully by using gel-type precursor particles, derived from non-aqueous dispersion (NAD) polymerisations of monomers in ethanol, in hypercrosslinking reactions. The precursor particles (containing 1 wt% of crosslinker) were close to monodisperse, spherical, had relatively narrow size distributions ( $\sim 3\text{-}4\ \mu\text{m}$ ), and were isolated in high yields ( $\sim 90\%$ ) when a ‘delayed addition’ methodology was applied. Such particles were essentially non-porous in the dry state, having only a very low nominal specific surface area ( $\sim 2\ \text{m}^2/\text{g}$ ).

NAD polymers with pendent chloromethyl groups were treated with  $\text{FeCl}_3$  in 1,2-dichloroethane (DCE) at  $80\ ^\circ\text{C}$ . Hypercrosslinked particles with remarkably high specific surface areas ( $\sim 1600\ \text{m}^2/\text{g}$ ) were isolated successfully, even although the quality of the particles was reduced upon hypercrosslinking. As an alternative hypercrosslinking strategy, gel-type NAD precursors were treated with a low level of  $\text{FeCl}_3$  in a non-swelling solvent in order to stabilise the spherical particles prior to exhaustive hypercrosslinking. Through this approach, high quality hypercrosslinked particles with narrow particles size distributions were successfully obtained. Polymers with high specific surface areas (up to  $\sim 1300\ \text{m}^2/\text{g}$ ) were prepared in this manner and the specific surface areas could be tuned depending upon the chlorine content of the swellable precursors prior to the exhaustive hypercrosslinking step.

The hypercrosslinked particles then were functionalised in such a way as to give strong cation-exchange (SCX) resins and strong anion-exchange (SAX) resins. For the SCX resins, satisfactory ion-exchange capacities (IECs) were obtained by treating the polymers with concentrated sulfuric acid as a sulfonating agent. In parallel with this work, SAX resins were prepared by treatment of the chloromethyl-containing polymers with dimethylbutylamine as an aminating agent. The IEC of the SAX materials could be tuned depending on the level of chlorine present in the hypercrosslinked polymers.

## List of Figures

- Figure 2.1: An example of step-growth polymerisation
- Figure 2.2: Chain-growth polymerisation of styrene
- Figure 2.3: Decomposition of AIBN into two 2-cyanopropyl radicals and nitrogen gas.
- Figure 2.4: Three steps in the polymerisation of polystyrene: initiation, chain propagation and chain termination.
- Figure 2.5: A crosslinked network of styrene and EGDMA where the polymer chains are linked together through covalent bonds.
- Figure 2.6: Schematic representation of suspension polymerisation: (a) the mixture of monomer, porogen and initiator; (b) aqueous continuous phase containing suspension stabiliser.
- Figure 2.7: Schematic representation of dispersion polymerisation.
- Figure 2.8: Pore types; (a) open pores; (b) closed pores
- Figure 2.9: Flow chart of members of macroporous materials
- Figure 2.10: Crystal structure of zeolite Type A (left)<sup>[38]</sup> and Type X (right).<sup>[39]</sup>
- Figure 2.11: Schematic representation of carbon materials: [a] activated carbon,<sup>[41]</sup> and [b] carbon nanotube.<sup>[42]</sup>
- Figure 2.12: The MOF-5 structure and its topology. (a) The MOF-5 structure shown as  $ZnO_4$  tetrahedra (blue polyhedra) joined by benzene dicarboxylate linkers (O, red and C, black) to give an extended 3D cubic framework with interconnected pores of 8 Å aperture width and 12 Å pore (yellow sphere) diameter. (Yellow sphere represents the largest sphere that can occupy the pores without coming within the van der Waals size of the framework). (b) The topology of the structure (primitive cubic net) shown as a ball-and-stick model. (c) The structure shown as the envelopes of the  $(OZn_4)O_{12}$  cluster (red truncated tetrahedron) and benzene dicarboxylate (BDC) ion (blue slat). Note that opposing slats are all at 90 °C.<sup>[54]</sup>
- Figure 2.13: Representative structure of the first member of the COF family<sup>[61]</sup>
- Figure 2.14: (a) Chemical structure of PIM-1. (b) Molecular model of PIM-1 showing its highly contorted, rigid structure.<sup>[73]</sup>

- Figure 2.15: Schematic illustration of sample preparation using SPE.  
(1) Conditioning; (2) Loading; (3) Washing; (4) Elution.
- Figure 3.1: Schematic representation of the synthesis procedures used in the production of a two-stage non-aqueous dispersion (NAD) precursor.
- Figure 3.2: SEM images for polystyrene (NA03) and Poly(St-*co*-VBC) (NA05) prepared in ethanol by a one-stage NAD polymerisation.
- Figure 3.3: FTIR spectra of poly(St-*co*-VBC-*co*-EGDMA) with fixed St/VBC feed ratio (50/50 wt%) in total monomer feed, (a) 1 wt% of EGDMA based on total monomer feed and (b) 6 wt% of EGDMA based on total monomer feed.
- Figure 3.4: SEM images of poly(St-*co*-VBC-*co*-EGDMA) at different monomer concentration in the first stage and second stages, respectively. JAG09 (0.263 g/mL / 0.263 g/mL), NA13 (0.211 g/mL / 0.216 g/mL), NA11 (0.201 g/mL / 6.5 g/mL), JAG20 (0.263 g/mL / 0.263 g/mL) and NA170 (0.316 g/mL / 0.316 g/mL).
- Figure 3.5: SEM images of poly(St-*co*-EGDMA-*co*-VBC) at different amount of initiator . JAG20 (3.045 mmol), NA162 (6.090 mmol) and NA169 (9.135 mmol)
- Figure 3.6: Particle size distribution of Poly(St-*co*-VBC-*co*-EGDMA) by non-aqueous dispersion (NAD) polymerisation at different initiator concentrations.
- Figure 3.7: Types of stirrers that used in the production of two-stage NAD precursor particles. [a] Four-blade PTFE type. [b] Two-blade metal type. [c] Three-blade metal type.
- Figure 3.8: SEM images of poly(St-*co*-VBC-*co*-EGDMA) obtained using different types of stirrers, where JAG27= four-blade PTFE type and NA11= two-blade metal type.
- Figure 3.9: Particle size distribution of Poly(St-*co*-VBC-*co*-EGDMA) prepared by non-aqueous dispersion (NAD) polymerisation with different solvent compositions (EtOH/Toluene = 100/0, 90/10, 85/15, 75/25).
- Figure 3.10: SEM images of poly(St-*co*-EGDM-*co*-VBC) particles prepared by a two-stage NAD polymerisation with fixed EGDMA content (1 wt%)

and St/VBC feed ratio (25/75) in different ethanol/toluene volume ratios. Ethanol/toluene content (v/v): (a) 100/0 (b) 90/10 (c) 85/15 (d) 75/25.

- Figure 3.11: Particle size distribution for poly(St-co-VBC-co-EGDMA) particles produced with varying EGDMA contents and fixed St/VBC feed ratio, (50/50 wt%).
- Figure 3.12: SEM images for poly(St-co-EGDMA-co-VBC) particles with fixed St/VBC feed ratio (50/50) (a) 1 wt%, (b) 2 wt% and (c) 6 wt%.
- Figure 3.13: SEM images for poly(St-co-VBC-co-EGDMA) at different monomer concentrations and amount of initiator.
- Figure 3.14: Particle size distribution for poly(St-co-VBC-co-EGDMA) particle prepared with varying monomer and amount of initiator at fixed St/VBC feed ratio, (10/90 wt%) and EGDMA content (1 wt%).
- Figure 4.2: Schematic representation of the synthesis procedures used in the production of aqueous dispersion polymerisation (ADP) precursor particles.
- Figure 4.2: FTIR spectra of (a) poly(St-co-VBC-co-EGDMA), (b) polystyrene and (c) poly(St-co-VBC).
- Figure 4.3: SEM images of ADP precursor particles: from left to right, polystyrene (NA84), poly(St-co-VBC) (NA92) with 5% of VBC, and poly(St-co-VBC-co-EGDMA) (NA99) with 0.1 wt% of EGDMA and 5% of VBC, respectively
- Figure 4.4: Particle size distribution of various precursor polymers synthesised by aqueous dispersion polymerisation (ADP).
- Figure 4.5: Synthesis of ADP precursors using PVP and PAA as a steric stabiliser in ethanol/water (95/5, v/v).
- Figure 4.6: Synthesis of poly(St-co-VBC) using PVP as a stabiliser in ethanol/water (95/5, v/v) and St/VBC = 95/5 (w/w).
- Figure 4.7: SEM image of poly(St-co-VBC) with a 95/5 (w/w) St/VBC ratio, using PVP as a stabiliser.

- Figure 4.8 : SEM images of ADP precursor particles, illustrating the effect of stirring. No stirring during polymerisation (NA96), and stirring started after second monomer addition added (NA99).
- Figure 4.9: Microscopy image of nucleated particles before a second (delayed) addition added.
- Figure 4.10: SEM images of ADP precursor particles; effected of feeding time.
- Figure 4.11: SEM images of ADP precursor particles produced in a two-stage polymerisation (NA94; poly(*St-co-VBC*) and NA99; Poly(*St-co-VBC-co-EGDMA*) and a one-stage polymerisation (NA97; poly(*St-co-VBC*)).
- Figure 4.12: SEM images of precursor particles of poly(*St-co-EGDMA-co-VBC*) and the effect of the presence of styrene. NA110: No styrene added in a second stage; NA96: styrene added in a second stage.
- Figure 4.13: SEM images of precursor particles of poly(*St-co-EGDMA-co-VBC-*) and the effect of VBC presence in the first stage of ADP. Values in the brackets are the ratios of styrene and VBC in monomer feed. Figure 4.14: Images of reaction mixture after polymerisation with 50% of VBC (NA129): (a) Before precipitation, and (b) After precipitation.
- Figure 4.15: SEM images of poly(*St-co-VBC-co-EGDMA*) particles prepared with varying VBC contents and fixed EGDMA content (0.1 wt%). VBC ratio in a second stage: (a) 80%; (b-i) 50%; (b-ii) 5%; (c-i) 20%; (c-ii) 5%; (d) 5% and (e) 30%.
- Figure 4.16: FTIR spectra of poly(*St-co-VBC-co EGDMA*) particles prepared with varying VBC contents.
- Figure 4.17: SEM images of poly(*St-co-EGDMA-co-VBC*) particles with 0.1 wt% of EGDMA at varying *St/VBC* ratios. Values in the brackets is percentage of VBC in the monomer feed.
- Figure 4.18: SEM images of poly(*St-co-EGDMA-co-VBC*) particles with 1 wt% of EGDMA at varying *St/VBC* ratios. Values in the brackest is percentage of VBC in the monomer feed.

- Figure 5.1: Hypercrosslinking of gel-type precursor particles *via* Friedel-Crafts alkylations.
- Figure 5.2: SEM images of poly(St-*co*-VBC-*co*-EGDMA) precursor particles prepared by NAD polymerisation with different St/VBC feed ratios and fixed EGDMA content (1 wt%); JAG20, JAG09 and JAG27, and their hypercrosslinked derivatives; HXLJAG20, HXLJAG09, HXLJAG27 hypercrosslinked after 60 min swelling time; HXLNA69, HXLNA70 and HXLNA71 hypercrosslinked after 15 min swelling time at 80 °C in DCE/Heptane (100/0) respectively.
- Figure 5.3: SEM images of poly(St-*co*-VBC-*co*-EGDMA) precursor particles prepared by NAD polymerisation with different St/VBC feed ratios and fixed EGDMA content (1 wt%); JAG20, JAG09 and JAG27 and their hypercrosslinked derivatives; HXLNA62, HXLNA61, HXLNA60 synthesised without stirring; HXLNA69, HXLNA70 and HXLNA71 synthesised whilst stirring, in DCE at 80 °C.
- Figure 5.4: SEM images of poly(St-*co*-VBC-*co*-EGDMA) precursor particles prepared by NAD polymerisation with different St/VBC feed ratios and fixed EGDMA content (1 wt%); JAG20, JAG09 and JAG27 and their hypercrosslinked derivatives; HXLJAG20, HXLJAG09, HXLJAG27 hypercrosslinked at 80 °C; HXLNA79, HXLNA67 and HXLNA80 hypercrosslinked at 60 °C, in DCE.
- Figure 5.5: SEM images of poly(St-*co*-VBC-*co*-EGDMA) precursor particles prepared by NAD polymerisation with different St/VBC feed ratios and fixed EGDMA content (1 wt%); JAG20, JAG09 and JAG27 and their hypercrosslinked derivatives; HXLNA79, HXLNA67, HXLNA80 hypercrosslinked with stirring; HXLNA77, HXLNA68 and HXLNA78 hypercrosslinked without stirring, at 60 °C in DCE.
- Figure 5.6: SEM images of precursor particles prepared by NAD polymerisation at fixed EGDMA content (1 wt%) and St/VBC ratio (90/10), NA171, and its hypercrosslinked derivative HXLNA172 prepared with no stirring during swelling time. Hypercrosslinking was at 80 °C for 18 h.

- Figure 5.7: SEM images of precursor particles prepared by NAD polymerisation at fixed EGDMA content (1 wt%) and St/VBC ratio (90/10), NA171, and its hypercrosslinked derivatives: HXLNA182 (80 °C, 18 h), HXLNA181 (RT, 18 h) and HXLNA179 (RT, 30 min), prepared with stirring during swelling.
- Figure 5.8: SEM images of poly(St-*co*-VBC-*co*-EGDMA) precursor particles prepared by NAD polymerisation with different St/VBC w/w ratios and fixed EGDMA content (1 wt%); JAG20, JAG09 and JAG27, and their hypercrosslinked derivatives synthesised in different solvent system: HXLJAG20, HXLJAG09 and HXLJAG27 in DCE/Heptane (100/0 v/v); HXLNA65, HXLNA64 and HXLNA63 in DCE/Heptane (50/50 v/v), at 80 °C.
- Figure 5.9: SEM images of poly(St-*co*-VBC-*co*-EGDMA) precursor particles prepared by NAD polymerisation with different St/VBC w/w ratios and fixed EGDMA content (1 wt%); JAG20, JAG09 and JAG27, and their hypercrosslinked derivatives: HXLNA65, HXLNA64 and HXLNA63 prepared with stirring; HXLNA74, HXLNA75 and HXLNA76 prepared without stirring, at 80 °C in DCE/heptane.
- Figure 5.10: SEM images of poly(St-*co*-VBC-*co*-EGDMA) precursor particles prepared by NAD polymerisation with a fixed St/VBC feed ratio (50/50) and fixed EGDMA content (6 wt%); NA45, and the hypercrosslinked derivative prepared without stirring; HXLNA58, in DCE at 80 °C.
- Figure 5.11: Dependence of the specific surface area (blue line) and chlorine content (red line) of the hypercrosslinked particles on the hypercrosslinking reaction time. HXLNAD NA136 (10 min); HXLNAD NA137a (30 min); HXLNAD NA135a (60 min) HXLNAD NA135b (180 min); XHLNAD NA135c (360 min); HXLNAD JAG23 (1080 min) and HXLNAD NA137b (1440 min).
- Figure 5.12: FT-IR spectra of hypercrosslinked particles with fix EGDMA contents (1 wt%) and St/VBC = 10/90 prepared with variable hypercrosslinking reaction times; (a) 0 min (b) 10 min (c) 15 min (d)

30 min (e) 60 min (f) 180 min (g) 360 min (h) 1080 min and (i) 1440 min.

Figure 5.13: SEM images of swellable poly(St-co-VBC-co-EGDMA) particles prepared by ADP with 1 wt% of EGDMA at varying St/VBC ratios (VBC content in monomer feed is shown in brackets).

Figure 5.14: SEM images of hypercrosslinked poly(St-co-VBC-co-EGDMA) particles with 1 wt% of EGDMA at varying St/VBC ratios (VBC content in monomer feed is shown in brackets)

Figure 5.15: Schematic representation of a one-step and a two-step hypercrosslinking process.

Figure 5.16: SEM images of NAD precursor particles (NA174) and their partially hypercrosslinked derivatives (PHXLNA187-PHXLNA191) prepared using different non-swelling solvent in the partial hypercrosslinking step. (a) PHXLNA187-PHXLNA188 in heptane (2 wt% of FeCl<sub>3</sub>), (b) PHXLNA189 in methanol (16.5 wt% of FeCl<sub>3</sub>) and (c) PHXLNA190-PHXLNA191 in hexane (11 wt% of FeCl<sub>3</sub>).

Figure 5.17: FT-IR spectra of NAD precursor particles (blue line) and partially hypercrosslinked particles prepared using different synthesis approaches in different non-swelling solvents. [a] NAD174 and PHXLNA187, [b] NAD174 and PHXLNA188, [c] NAD174 and PHXLNA189, [d] NAD174 and PHXLNA190 and [e] NAD174 and PHXLNA191.

Figure 5.18: FT-IR spectra of NAD precursor particles (blue line), their partially hypercrosslinked derivatives which were hypercrosslinked at RT (brown line) and their fully hypercrosslinked derivatives (pale blue line).

Figure 5.19: FT-IR spectra of NAD precursor particles (blue line), their partially hypercrosslinked derivatives where the partial hypercrosslinking has been conducted at 60 °C (green line), and the fully hypercrosslinked derivative (pink line).

Figure 5.20: SEM images of NAD precursor particles, their partially hypercrosslinked derivatives and their fully hypercrosslinked

derivatives. (a) NA174 and NA 171- NAD precursor particles. (b) PHXLNA190 (11 wt% of FeCl<sub>3</sub>, RT, 18 h), PHXLNA191 (11 wt% of FeCl<sub>3</sub>, 80 °C, 18 h), PHXLNA194 (11 wt% of FeCl<sub>3</sub>, RT, 30 min), PHXLNA195 (5 wt% of FeCl<sub>3</sub>, RT, 18 h) - partially hypercrosslinked particles, and (c) HXLNA193 HXLNA192, HXLNA196, HXLNA197 and HXLNA199 - fully hypercrosslinked particles.

Figure 6.1: Reaction schemes showing the two distinct routes into the production of sulfonated hypercrosslinked (HXLNAD-SCX) polymer

Figure 6.2: FT-IR spectra of a hypercrosslinked polymer and its sulfonated derivatives produced at different reaction times in the presence of 5 mL of sulfuric acid at 60 °C: NA142 (HXL polymer) and NA146-NA147 (HXLNAD-SCX polymers).

Figure 6.3: FT-IR spectra of hypercrosslinked polymer and its sulfonated derivatives synthesised at different reaction times in the presence of 30 mL of sulfuric acid at 60 °C: NA142 (HXL polymer) and NA149-NA151 (HXLNAD-SCX polymers).

Figure 6.4: Dependence of IEC on reaction time in the presence of 5 mL of sulfuric acid at 60 °C.

Figure 6.5: Dependence of IEC on reaction time in the presence of 30 mL of sulfuric acid at 60 °C.

Figure 6.6: SEM images of (a) swellable NAD precursor JAG27, (b) hypercrosslinked polymer NA142 and its derivatives after sulfonation reactions (c-e) at a fixed amount of sulfuric acid (5 mL) and at different reaction times: (c) NA145 - 3 h, (d) NA146 - 5 h and (e) NA146 - 18 h, respectively.

Figure 6.7: SEM images of (a) swellable NAD precursor JAG27 (b) hypercrosslinked polymer NA142 and its derivatives after sulfonation (c-e) at a fixed amount of sulfuric acid (30 mL) and at different reaction times: (c) NA151 - 3 h, (d) NA149 - 5 h and (e) NA150 - 18 h, respectively.

- Figure 6.8: Specific surface areas (SSA) of sulfonated polymers obtained upon treatment of a non-sulfonated precursor with variable amount of sulfuric acid and for different reaction times.
- Figure 6.9: Highly schematic representation of a sulfone-bridge forming reaction.
- Figure 6.10: SEM images of sulfonated hypercrosslinked polymers derived from a range of hypercrosslinked precursors (value in the bracket shows the percentage of St/VBC used in synthesis of swellable NAD precursor).
- Figure 6.11: Ion-exchange capacity of different sulfonated hypercrosslinked polymers.
- Figure 6.12: Specific surface area data for the different sulfonated hypercrosslinked polymers.
- Figure 6.13: SEM images of sulfonated hypercrosslinked polymers synthesised *via* a four step synthetic strategy. NA171 - NAD precursor particles; PHXNAD NA194 - partially hypercrosslinked particles; HXLNAD NA196 - fully hypercrosslinked particles and HXLNAD-SCX NA198 - sulfonated hypercrosslinked particles.
- Figure 7.1: Synthesis of aminated hypercrosslinked (HXLNAD-SAX) polymers *via* the amination of a hypercrosslinked precursor (HXLNAD
- Figure 7.2: FTIR spectra of a hypercrosslinked polymer and its aminated derivatives, with variable reaction times using a 5% molar excess of DMBA at 85 °C: NA141 (HXL polymer - green line); NA152-3 h (blue line), NA153-5 h (black line) and NA157-18 h (red line) are HXLNAD-SAX polymers.
- Figure 7.3: Specific surface areas of aminated hypercrosslinked polymers prepared using various amount of DMBA and different reaction times.
- Figure 7.4: Ion-exchange capacities of aminated hypercrosslinked polymers prepared using various amount of DMBA and variable reaction times.
- Figure 7.5: SEM images of (a) swellable NAD precursor, (b) hypercrosslinked polymer and (c)–(e) hypercrosslinked polymers aminated with 5% molar excess of DMBA at different reaction times: HXLNAD-SAX NA152-3 h, HXLNAD-SAX NA153-5 h and HXLNAD-SAX NA157-18 h, respectively.

Figure 7.6: SEM images of (a) swellable NAD precursor, (b) hypercrosslinked polymer and (c)-(e) hypercrosslinked polymers aminated with 10% molar excess of DMBA at different reaction times: HXLNAD-SAX NA158-3 h, HXLNAD-SAX NA159-5 h and HXLNAD-SAX NA160-18 h, respectively.

Figure 7.7: Specific surface areas of hypercrosslinked polymers before and after amination of polymers with variable chloromethyl contents.

## List of Tables

- Table 3.1: Characterisation data of NAD precursor particles prepared *via* a one-stage NAD polymerisation. [a] Mass of St +VBC=100% total monomer feed in the feed. [b] Calculated from the image analysis in SEM (using Minitab software).
- Table 3.2: Characterisation data for precursor particles prepared with varying EGDMA contents in a two-stage NAD polymerisation in ethanol. [a] Mass of St +VBC=100% total monomer feed in the feed. [b] Based on total monomer in the feed.
- Table 3.3: Characterisation data of NAD precursor particles prepared *via* a two-stage NAD polymerisation. [a] Mass of St +VBC=100% total monomer feed in the feed. [b] Calculated from the image analysis in SEM (using Minitab software).
- Table 3.4: Effect of stirrer type on the production of poly(St-*co*-VBC-*co*-EGDMA) by a two-stage NAD polymerisation with fixed St/VBC ratio (50/50; w/w) and 1 wt% of EGDMA. [a] Calculated from the image analysis in SEM (using Minitab software).
- Table 3.5: Characterisation data for precursor particles prepared in a two-stage NAD polymerisation. [a] Mass of St +VBC=100% total monomer feed in the feed. [b] EGDMA contents based on total monomer in the feed.
- Table 3.6: Characterisation data for precursor particles prepared with varying EGDMA contents in a two-stage NAD polymerisation. [a] Mass of St +VBC=100% total monomer feed in the feed. [b] based on total monomer in the feed.
- Table 3.7: Characterisation data for precursor particles prepared with varying monomer concentration and amount of initiator in a two-stage NAD polymerisation. [a] Based on total monomer feed.
- Table 4.1: Characterisation data for polymers synthesised during experiments designed to explore the effect of stirring on the ADP. [a] Mass of St +VBC=100% total monomer feed in the feed. [b] EGDMA content based on total monomer in the feed. [c] Average particle diameter  $\pm$

standard deviation (S.D.) calculated from the image analysis in SEM (using Minitab software).

Table 4.2: Characterisation data for polymers synthesised during experiments designed to explore the effect of feeding time. [a] Mass of St +VBC=100% total monomer feed in the feed. [b] EGDMA content based on total monomer in the feed. [c] Average particle diameter  $\pm$  standard deviation (S.D.) calculated from the image analysis in SEM (using Minitab software).

Table 4.3: Characterisation data for polymers synthesised during experiments to explore the effect of styrene added in a second stage in a ADP, with fixed EGDMA content (0.1 wt%). a) Mass of St +VBC=100% total monomer feed in the feed. [b] Average particle diameter  $\pm$  standard deviation (S.D.) calculated from the image analysis in SEM (using Minitab software).

Table 4.4: Characterisation data for polymer synthesised during experiments to explore the effect of VBC added in a second stage in an ADP, with fixed EGDMA content (0.1 wt%). a) Mass of St +VBC=100% total monomer feed in the feed. [b] Average particle diameter  $\pm$  standard deviation (S.D.) calculated from the image analysis in SEM (using Minitab software).

Table 4.5: Characterisation data for polymers synthesised during experiments to explore the effect of the VBC ratio in a second stage with varying VBC content and fixed EGDMA content (0.1 wt%). [a] Mass of St +VBC=100% total monomer feed in the feed. [b] Percentage of VBC based on total VBC in the feed. [c] Average particle diameter  $\pm$  standard deviation (S.D.) calculated from the image analysis in SEM (using Minitab software).

Table 4.6: Characterisation data for polymers synthesised during experiments to explore the effect of the VBC ratio in a second stage in a two-stage ADP. [a] Mass of St +VBC=100% total monomer feed in the feed.[b] based on total monomer in the feed.

- Table 4.7: Characterisation data for ADP precursor particles prepared with varying EGDMA content in the monomer feed. [a] Mass of St +VBC=100% total monomer feed in the feed, with varying EGDMA content (0.1 wt% and 1 wt% ), respectively.
- Table 5.1: Synthesis data for NAD particles and their hypercrosslinked derivatives at different swelling times. [a] Mass of St +VBC = 100% total monomer feed in the feed; EGDMA is 1 wt% based on total monomer in the feed. [b] Average particle diameter  $\pm$  standard deviation (S.D.) calculated from the image analysis in SEM (using Minitab software). [c] For the hypercrosslinked particles relative to the mass of the corresponding NAD (non-hypercrosslinked) precursor particles.
- Table 5.2: Porosimetry-derived characterisation data for NAD precursor particles and their hypercrosslinked derivatives synthesised in DCE using different swelling times. Data computed from the N<sub>2</sub> sorption isotherms and BET theory.
- Table 5.3: Synthesis data for NAD precursor particles and their hypercrosslinked derivatives synthesised either with or without stirring at 80 °C in DCE. [a] Mass of St +VBC = 100% total monomer feed in the feed; EGDMA is 1 wt% based on total monomer in the feed. [b] Average particle diameter  $\pm$  standard deviation (S.D.) calculated from the image analysis in SEM (using Minitab software). [c] For the hypercrosslinked particles relative to the mass of the corresponding the NAD (non-hypercrosslinked) precursor particles.
- Table 5.4: Porosimetry-derived characterisation data for NAD precursor particles and their hypercrosslinked derivatives synthesised either with or without stirring at 80 °C in DCE. Data computed from nitrogen sorption isotherms and BET theory.
- Table 5.5: Synthesis data for NAD precursor particles and their hypercrosslinked derivatives which were hypercrosslinked at different temperatures in DCE. [a] Mass of St +VBC = 100% total monomer feed in the feed; EGDMA is 1 wt% based on total monomer in the feed. [b] Average

particle diameter  $\pm$  standard deviation (S.D.) calculated from the image analysis in SEM (using Minitab software). [c] For the hypercrosslinked particles relative to the mass of the corresponding NAD (non-hypercrosslinked) precursor particles.

Table 5.6: Porosimetry-derived characterisation data for NAD precursor particles and their hypercrosslinked derivatives which were hypercrosslinked at different temperatures in DCE. Data computed from nitrogen sorption isotherms and BET theory.

Table 5.7: Synthesis data for NAD precursors and their hypercrosslinked derivatives prepared with and without stirring during hypercrosslinking at 60 °C in DCE. [a] Mass of St +VBC = 100% total monomer feed in the feed; EGDMA is 1 wt% based on total monomer in the feed. [b] Average particle diameter  $\pm$  standard deviation (S.D.) calculated from the image analysis in SEM (using Minitab software). [c] For the hypercrosslinked particles relative to the mass of the corresponding NAD (non-hypercrosslinked) precursor particles.

Table 5.8: Porosimetry-derived characterisation data for NAD precursors and their hypercrosslinked derivatives prepared with or without stirring at 60 °C in DCE. Data computed from nitrogen sorption isotherms and BET theory.

Table 5.9: Synthesis data for an NAD precursor and its hypercrosslinked derivatives prepared with and without stirring during swelling. Hypercrosslinking at 80 °C in DCE. St/VBC: 10/90 and EGDMA is 1 wt% based on total monomer in the feed. [a] Average particle diameter  $\pm$  standard deviation (S.D.) calculated from the image analysis in SEM (using Minitab software). [b] For the hypercrosslinked particles relative to the mass of the corresponding NAD (non-hypercrosslinked) precursor particles.

Table 5.10: Porosimetry-derived characterisation data for an NAD precursor and its hypercrosslinked derivatives prepared with stirring during

swelling. Hypercrosslinking at 80 °C in DCE. Data computed from nitrogen sorption isotherms and BET theory.

Table 5.11: Synthesis data of NAD precursors and their hypercrosslinked derivatives hypercrosslinked at 80 °C in either neat DCE or in a mixture of DCE and heptane. [a] Mass of St +VBC = 100% total monomer feed in the feed; EGDMA is 1 wt% based on total monomer in the feed. [b] Average particle diameter  $\pm$  standard deviation (S.D.) calculated from the image analysis in SEM (using Minitab software). [c] For the hypercrosslinked particles relative to the mass of the corresponding NAD (non-hypercrosslinked) precursor particles.

Table 5.12: Porosimetry-derived characterisation data NAD precursors and their hypercrosslinked derivatives, hypercrosslinked at 80 °C in either neat DCE or DCE/Heptane (50/50), Data computed from nitrogen sorption isotherms and BET theory.

Table 5.13: Synthesis and characterisation data for NAD precursor particles and their hypercrosslinked derivatives prepared with and without stirring during the reaction course, at 80 °C in a mixed solvent system. [a] Mass of St +VBC = 100% total monomer feed in the feed; EGDMA is 1 wt% based on total monomer in the feed. [b] Average particle diameter  $\pm$  standard deviation (S.D.) calculated from the image analysis in SEM (using Minitab software). [c] For the hypercrosslinked particles relative to the mass of the corresponding the NAD (non-hypercrosslinked) precursor particles.

Table 5.14: Porosimetry-derived characterisation data for NAD precursor particles and their hypercrosslinked derivatives prepared with and without stirring at 80 °C in DCE/Heptane (50/50). Data computed from nitrogen sorption isotherms and BET theory.

Table 5.15: Synthesis data for NAD precursor particles and their derivatives hypercrosslinked at 80 °C in DCE. [a] Mass of St +VBC = 100% total monomer feed in the feed. [b] Average particle diameter  $\pm$  standard deviation (S.D.) calculated from the image analysis in SEM (using Minitab software). [c] For the hypercrosslinked particles relative to

the mass of the corresponding NAD (non-hypercrosslinked) precursor particles.

Table 5.16: Porosimetry-derived characterisation data for NAD precursor particles and their hypercrosslinked derivatives prepared with different EGDMA contents at 80 °C in DCE. Data computed from nitrogen sorption isotherms and BET theory.

Table 5.17: Synthesis data for ADP particles hypercrosslinked at 80 °C in DCE. [a] Mass of St +VBC = 100% total monomer feed in the feed. [b] Average particle diameter  $\pm$  standard deviation (S.D.) calculated from the image analysis in SEM (using Minitab software).[c] For the hypercrosslinked particles relative to the mass of the corresponding ADP (non-hypercrosslinked) precursor particles.

Table 5.18: Porosimetry-derived characterisation data for swellable ADP precursor and their derivatives which were hypercrosslinked at 80 °C in DCE. Data computed from nitrogen sorption isotherms and BET theory.

Table 5.19: Synthesis data for the partial hypercrosslinking of swellable precursors in non-swelling solvents. [a] percentage of FeCl<sub>3</sub> used relative to the molar ratio CH<sub>2</sub>Cl groups in the precursor.

Table 5.20: Characterisation data for polymer synthesised *via* partial hypercrosslinking reactions. [a] % Cl content after reaction. [b] Computed from nitrogen sorption isotherms and BET theory. [c] For the hypercrosslinked particles relative to the mass of the corresponding NAD (non-hypercrosslinked) precursor particles. [d] NAD precursor particles. [e] % Cl content before reaction.

Table 5.21: Characterisation data for swellable precursors, their partially hypercrosslinked derivatives and their fully hypercrosslinked derivatives. [a] Porosity data computed from nitrogen sorption isotherms and BET theory. [b] For the partially hypercrosslinked particles relative to the mass of the corresponding NAD (non-hypercrosslinked) precursor particles, or for the fully

hypercrosslinked particles relative to the mass of the corresponding partially hypercrosslinked particles.

- Table 6.1: Synthesis data for sulfonated hypercrosslinked polymers prepared with different reaction time and varying amounts of sulfuric acid. [a] Based on 1:1 molar ratio  $C_{17}H_{16}:C_{17}H_{17}SO_3$ .
- Table 6.2: Synthesis data for sulfonated hypercrosslinked polymer. [a] Based on 1:1 molar ratio  $C_{17}H_{16}:C_{17}H_{17}SO_3$ .
- Table 6.3: Characterisation data for sulfonated hypercrosslinked polymers produced *via* a four step synthetic strategy.
- Table 7.1: Synthesis data for aminated hypercrosslinked polymers prepared using various amount of DMBA and variable reaction times. [a] Based on 1:1 molar ratio of  $C_9H_9Cl:C_{15}H_{24}N$ .
- Table 7.2: Synthesis data for aminated hypercrosslinked polymer at different chlorine residue and fixed 5% molar excess of DMBA.[a] Based on 1:1 molar ratio of  $C_9H_9Cl:C_{15}H_{24}N$ .

# Contents

Declaration of Copyright	II
Acknowledgements	III
List of Abbreviations	IV
Abstract	V
List of Figures	VI
List of Tables	XVI

## CHAPTER I

### INTRODUCTION

1.0 Background and Motivation	2
1.1 Problems and Opportunities	3
1.2 Objectives of the Study	5
1.3 Glossary Important Terms and Terminology	5
1.4 Structure of the Thesis	6
References	9

## CHAPTER II

### LITERATURE REVIEW

2.0 Summary	12
2.1 Polymer Synthesis	12
2.1.1 Step-Growth Polymerisation	13
2.1.2 Chain-Growth Polymerisation	13
2.1.2.1 Free Radical Polymerisation (FRP)	13
2.1.3 Crosslinked Polymers	16
2.2 Techniques for the Synthesis of swellable Precursor Polymers	17
2.2.1 Suspension Polymerisation	17
2.2.2 Precipitation Polymerisation	18
2.2.3 Dispersion Polymerisation	18

2.2.3.1	Process Description in Dispersion Polymerisation	21
2.2.3.2	Solvent	23
2.2.3.3	Monomer	23
2.2.3.4	Initiator	24
2.2.3.5	Stabiliser	24
2.3	Macroporous Materials	25
2.4	Zeolites	27
2.5	Carbon Materials	29
2.6	Metal-Organic Frameworks (MOFs)	30
2.7	Covalent Organic Frameworks (COFs)	33
2.8	Macroporous Polymers	34
2.8.1	Polymers with Intrinsic Microporosity (PIMs)	35
2.8.2	Hypercrosslinked Polymers	37
2.8.2.1	Preparation of Hypercrosslinked Polymers	38
2.9	Functionalised Polymers	43
2.9.1	Linear polymers	44
2.9.2	Crosslinked Polymers	45
2.9.3	Preparation of Functionalised Polymers	46
2.9.3.1	Functionalised Crosslinked Resins	47
2.9.3.2	Functionalised Hypercrosslinked Resins	49
2.10	Applications of Hypercrosslinked Polymers and Functionalised Hypercrosslinked Polymers	51
2.10.1	Solid-Phase Extraction (SPE)	51
2.10.2	Method For Solid Phase Extraction (SPE)	53
2.11	Conclusions	54
	References	56

## **CHAPTER III**

### **NON-AQUEOUS DISPERSION (NAD) POLYMERISATION**

3.0	Summary	64
-----	---------	----

3.1	Introduction to Dispersion Polymerisation	64
3.2	Aim of this Work	64
3.3	Research Methodology and Preliminary Work	66
3.3.1	Materials	66
3.3.2	Materials	66
3.3.3	Equipment	66
3.3.4	Characterisation	67
3.3.5	Optical Microscopy	67
3.3.6	Scanning Electron Microscopy (SEM)	67
3.3.7	Fourier-Transform Infra-Red Spectroscopy (FTIR)	67
3.3.8	Elemental Microanalysis	68
3.4	Resin Synthesis	68
3.4.1	One-Stage Polymerisations	68
3.4.2	Two-Stage Polymerisations	69
3.5	Results and Discussion	70
3.5.1	One-Stage NAD Polymerisations	70
3.5.2	Two-Stage NAD Polymerisations	72
	3.5.2.1 FTIR Spectroscopy	72
	3.5.2.2 Effect of Initial Monomer Concentration	73
	3.5.2.3 Effect of amount of Initiator	77
	3.5.2.4 Effect of Stirrer Type	79
	3.5.2.5 Effect of Solvent Composition	81
	3.5.2.6 Effect of EGDMA Concentration	85
	3.5.2.7 Optimisation	87
3.6	Conclusions	89
	References	91

## **CHAPTER IV**

### **AQUEOUS DISPERSION POLYMERISATION (ADP)**

4.0	Summary	94
4.1	Introduction to Aqueous Dispersion Polymerisation	94
4.2	Aim of this Work	94

4.3	Research Methodology and Preliminary Work	95
4.3.1	Materials	95
4.3.2	Equipment	95
4.3.3	Characterisation	96
4.3.3.1	Optical Microscopy	96
4.3.3.2	Scanning Electron Microscopy (SEM)	96
4.3.3.4	Fourier-Transform Infra-Red Spectroscopy (FTIR)	96
4.3.3.5	Elemental Microanalysis	96
4.4	Resin synthesis	97
4.5	Results and Discussion	98
4.5.1	Aqueous Dispersion Polymerisation Particles	98
4.5.2	Effect of Type of Stabiliser	100
4.5.3	Nucleation Stage	101
4.5.4	Effect of Stirring	102
4.5.5	Effect of Feeding Time for Second (Delayed) Addition	105
4.5.6	Two-Stage and One-Stage ADP	109
4.5.7	Effect of Styrene Added in Second Stage	110
4.5.8	Effect of VBC Added in First Stage	111
4.5.9	Effect of VBC ratio in First Stage and Second Stage of ADP	114
4.5.10	Effect of Crosslinker Content	119
4.6	Conclusions	122
	References	124

## **CHAPTER V**

### **HYPERCROSSLINKED POLYMERS**

5.0	Summary	126
5.1	Introduction to Hypercrosslinked Particles	126
5.2	Aims Of Work	127
5.3	Experimental	127
5.3.1	Materials	127

5.3.2	Equipment	127
5.3.3	Characterisation	127
5.3.3.1	Scanning Electron Microscopy (SEM)	128
5.3.3.2	Fourier-Transform Infra-Red(FT-IR) Spectroscopy	128
5.3.3.3	Optical Microscopy	128
5.3.3.4	Elemental Microanalysis	128
5.3.3.5	Nitrogen Sorption Porosimetry Analysis	129
5.3.3.6	Solubility Tests	129
5.4	Procedures/Methodology	129
5.4.1	Synthesis of Gel-Type, NAD Precursor Particles	129
5.4.2	Partial Hypercrosslinking of NAD Precursor Particles	130
5.4.3	Hypercrosslinking of NAD Particles	130
5.5	Results and Discussion	131
5.6	Hypercrosslinked Non-Aqueous Dispersion Precursor Particles	131
5.6.1	Effect of Swelling Time on the Hypercrosslinking Particles	132
5.6.2	Effect Upon the Hypercrosslinked Particles of Stirring During Hypercrosslinking	136
5.6.3	Effect of Hypercrosslinking Temperature Upon the Hypercrosslinked Particles	139
5.6.4	Effect Upon the Hypercrosslinked Particles by Stirring at 60 °C During Hypercrosslinking	142
5.6.5	Effect Of Stirring During Swelling	145
5.6.6	Effect of Solvent System on the Hypercrosslinked Particles	148
5.6.7	Effect of Stirring and a Mixed Solvent System on the Hypercrosslinking Particles	152
5.6.8	Effect of EGDMA Content of the Particles	155
5.6.9	Effect of Hypercrosslinking Reaction Time on Specific Surface Areas and Chlorine Content	157
5.7	Hypercrosslinking of Aqueous Dispersion Polymerisation (ADP) Precursor Particles	160

5.8	Optimisation	164
5.8.1	Partial Hypercrosslinking of Swellable Precursors	165
5.8.2	Full/Exhaustive Hypercrosslinking of Partially Hypercrosslinked Particles	172
5.9	Conclusions	178
	References	180

## **CHAPTER VI**

### **STRONG CATION-EXCHANGE POLYMERS**

6.0	Summary	182
6.1	Introduction to Strong Cation-Exchange Resins	182
6.2	Aims of Work	182
6.3	Experimental	183
6.3.1	Materials	183
6.3.2	Equipment	183
6.3.3	Characterisation	183
6.3.4	Scanning Electron Microscopy (SEM)	183
6.3.5	Fourier-Transform Infra-Red (FT-IR) Spectroscopy	184
6.3.6	Elemental Microanalysis	184
6.3.7	Nitrogen Sorption Porosimetry Analysis	184
6.3.8	Titration Analysis	185
6.4	Procedures/Methodology	185
6.4.1	Synthesis of Gel-Type NAD Precursor Polymers	185
6.4.2	Partial Hypercrosslinking of NAD Precursor Polymers	186
6.4.3	Hypercrosslinking of NAD Polymers	186
6.4.4	Sulfonation of Hypercrosslinked Polymers	186
6.5	Results and Discussion	187
6.5.1	Three Steps Strategy for the Production of Sulfonated Hypercrosslinked Polymers	189
6.5.1.1	FT-IR Analysis	189
6.5.1.2	Ion-Exchange Capacity (IEC)	190

6.5.1.3 Physical Form of Sulfonated Hypercrosslinked Polymers	192
6.5.1.4 Specific Surface Areas of Sulfonated Hypercrosslinked Polymers	194
6.5.1.5 Sulfonation of Other Hypercrosslinked Polymers	198
6.5.2 Four Steps Strategy for the Production of Sulfonated Hypercrosslinked Polymers	201
6.6 Conclusions	203
References	204

## **CHAPTER VII**

### **STRONG ANION-EXCHANGE POLYMERS**

7.0 Summary	206
7.1 Introduction to Strong Anion-Exchange Polymers	207
7.2 Aims of Work	207
7.3 Experimental	207
7.3.1 Materials	207
7.3.2 Equipment	207
7.3.3 Characterisation	
7.3.3.1 Scanning Electron Microscopy (SEM)	207
7.3.3.2 Fourier-Transform Infra-Red (FT-IR) Spectroscopy	207
7.3.3.3 Elemental Microanalysis	208
7.3.3.4 Nitrogen Sorption Porosimetry Analysis	208
7.4 Procedures/Methodology	
7.4.1 Synthesis of Gel-Type NAD Precursor Polymers	209
7.4.2 Hypercrosslinking of NAD Polymers	209
7.4.3 Amination of Hypercrosslinked Polymers	210
7.5 Results and Discussion	210
7.5.1 FT-IR Spectroscopy	212
7.5.2 Specific Surface Areas of Aminated Hypercrosslinked Polymers	212

7.5.3	Ion-Exchange Capacity (IEC) And Nitrogen Content	213
7.5.4	Physical Form of Hypercrosslinked Aminated Polymers	215
7.5.5	Amination of Hypercrosslinked Polymers with Variable Chloromethyl Contents	216
7.6	Conclusions	219
	References	220

## **CHAPTER VIII**

### **GENERAL CONCLUSION AND FUTURE WORK**

8.0	Conclusions	222
8.1	Future Work	224

## ***CHAPTER ONE***

## **1.0 Background and Motivation**

Hypercrosslinked polymers were classified as a new generation of porous polymers due to the fact that they differ from traditional macroporous polymers, and such materials introduced by Davankov's group<sup>[1]</sup>. Such materials display ultra-high surface specific areas ( $>1000 \text{ m}^2/\text{g}$ ) and have high contents micropore,<sup>[2]</sup> morphological features and features which arise from the nature of the hypercrosslinking process in which an expanded framework possessing internal void volume is generated. They also have capability to uptake polar and non-polar solvents. Besides the properties mentioned already, hypercrosslinked polymers are stable in use and inexpensive to produce, since commodity monomers and crosslinkers, for example styrene and divinylbenzene (DVB), are usually used in their preparation. Their unusual and attractive properties has led to hypercrosslinked materials being chosen as candidates for applications such as ion-exchange resins,<sup>[3]</sup> solid-phase extraction,<sup>[4]</sup> catalysis,<sup>[5]</sup> *etc.* Hypercrosslinked materials with micron-sized dimensions and narrow particle size distribution that can be packed into chromatography columns can lead to highly efficient chemical separations, such as in solid-phase extraction and high performance liquid chromatography (HPLC).

Precursor polymeric particles which are produced *via* suspension polymerisation, emulsion polymerisation and also precipitation polymerisation are commonly used in the preparation of hypercrosslinked polymers. Each synthesis technique has its own disadvantages and advantages. Nowadays, dispersion polymerisation has been investigated widely as an alternative method for preparing monodisperse polymeric particles in the micron-sized range in single step.<sup>[6, 7, 8]</sup> This is because such particles meet requirements that are needed in various applications, particularly in separation science, for example in high performance liquid chromatography (HPLC) and solid-phase extraction (SPE). In terms of chemical separation, highly efficient separation is important, for example in waste water treatment. Thus, narrow particle size distributions become important in the applications area in addition to the need for high specific surface area. In this study, good quality particles in the micron sized range

were prepared successfully using the non-aqueous dispersion (NAD) polymerisation technique and used as swellable precursors in hypercrosslinking reactions.

Functional groups have been implanted into hypercrosslinked polymers in order to achieve desired effects. Functionalised polymers were used as ion-exchange media in a few decades ago but were used more systematically after the introduction of Merrifield's solid-phase peptide synthesis.<sup>[9]</sup> This was the first step towards the preparation of a functional polymer for specific use in important applications such as ion-exchangers,<sup>[2, 10, 11]</sup> solid-phase peptide synthesis,<sup>[12]</sup> chelating agents,<sup>[13]</sup> solid-phase extraction,<sup>[3]</sup> *etc.* Such polymers possess many attributes which makes them attractive for use in combinatorial as well as automated syntheses. They can be recycled, are cost-effective to produce and non-toxic and odourless.

### **1.1 Problems and Opportunities**

Dispersion polymerisation is a very promising technique for the production of monodisperse particles in the micron-size range. However, such polymerisations can be difficult to control when a comonomer, known as a “problematic” monomer, is used. For example, a polar monomer or a crosslinking agent can interfere with particles nucleation. Also, small amounts of “problematic” monomer present in the reaction medium can broaden particle size distribution and lead to irregular particles even coagulation. To overcome this problem, a new method has been developed by Winnik *et al.*,<sup>[14]</sup> a two-stage methodology which involve delayed addition of the “problematic” monomer after the nucleation stage of the reaction has passed. Thus, such monomers cannot interfere with particle nucleation.<sup>[14, 15, 16, 17]</sup> In this study, three monomers (a functional monomer and a crosslinker were employed in addition to styrene) were polymerised using a similar methodology. In addition, aqueous dispersion polymerisation (ADP) has been explored in this study as an alternative to NAD polymerisation,<sup>[18]</sup> with a two-stage methodology also being developed.

Apart from facing a challenge when a second monomer is added into a dispersion polymerisation, the particles can also encounter a problem during the preparation of

hypercrosslinked particles in that some polymers chains may be soluble in the thermodynamically “good” solvent used in the hypercrosslinking reaction. As far as the works in this field are concern, there is a lack of publications regarding the production of precursor polymeric particles *via* dispersion polymerisation for the preparation of hypercrosslinked polymers. Although work has been carried out in house,<sup>[17]</sup> the particle quality was not so good even although the particles were in the micron-size range. Therefore, efforts have to be dedicated to overcoming the problems that were encountered in the published work, and these efforts are described herein.

Attempts were made to study the dependence of specific surface area and the percentage chlorine content on the course of the reaction in order to be in a position to tune the specific surface area and the percentage of reactive moieties remaining after hypercrosslinking to facilitate post-polymerisation chemical modifications.

Overall, in this study a two-stage dispersion polymerisation methodology, similar to that introduced by Winnik *et al.*, was applied in non-aqueous dispersion (NAD) polymerisation as well as aqueous dispersion polymerisation (ADP). Three monomers, styrene, ethylene glycol dimethacrylate (EGDMA) and vinylbenzyl chloride (VBC) were chosen to probe the effect of a comonomer and a third-monomer on particles formation, instead of the two monomers that were employed elsewhere.<sup>[14, 15]</sup> The research also continues to study the effect of crosslinker content on the precursors. Efforts were also made to increase the size of the particles that could be produced.

For hypercrosslinked particles, various aspects were explored with a view to study the best operating parameters that may influence the quality of the final product. The work focuses in overcoming the problems which can arise during hypercrosslinking reactions; several parameters such as solvent system, swelling time, reaction temperature, reaction time, stirring and crosslinker content, were probed. New route for preparation hypercrosslinked particles also was exploited to increase the quality of the particle.

The next step was the introduction of functional groups into the hypercrosslinked particles by chemical modification. The focus was upon imparting ion-exchange groups into the hypercrosslinked particles, and several methods were explored in this regard.

## 1.2 Objectives of the study

The aims of this study were to investigate the potential of dispersion polymerisation as a route to hypercrosslinked particles, and exploration of routes for functionalisation of the particles. In particular, the aims were to:

- Optimise non-aqueous dispersion (NAD) polymerisation
- Optimise aqueous dispersion polymerisation (ADP)
- Optimise hypercrosslinking reactions involving swellable precursor produced by NAD polymerisation and ADP
- Functionalise hypercrosslinked polymers

## 1.3 Glossary Important Terms and Terminology

Various terms and terminology that are important and used frequently in this thesis are as follows:

**Dispersion:** A finely distributed mixture of two or more insoluble (or slightly soluble) phases.

**Dispersion medium:** The component of a dispersion that is higher in quantity. It is also known as the dispersed medium, internal medium or continuous medium. The word “phase” is used synonymously with the word “medium”.

**Particle:** A small object that behaves as a whole unit in terms of its transport and properties.

**Hyperscrosslinked particle:** New type of porous material with permanently porous structure and high specific surface area ( $> 1000 \text{ m}^2/\text{g}$ ).

**Monodisperse particles:** Particles with a uniform distribution where all particles have the same size, shape and structure.

**Polydisperse particles:** A group of particles with a wide particle size distribution.

**Micropore:** Porous material with pore size less than 2 nm in diameter.

**Mesopore:** Porous material with pore size in between 2 nm-50 nm in diameter.

**Macropore:** Porous material with pore size more than 50 nm in diameter.

**Functionalised polymer:** Polymer with functional group attached.

**Strong cation-exchange:** Resins that derive their functionality from the ability to exchange cations.

**Strong anion-exchange:** Resins that derive their functionality from the ability to exchange anions.

#### **1.4 Structure of the Thesis**

The research works have been carried out and discussed in different chapters as follows:

**Chapter 1:** This chapter introduces the thesis. The background to the project, motivation, problems and opportunities, objectives, important terms and terminology and the structure of the thesis are presented. Also, this chapter provides an insight into the originality, contribution and innovation of the work.

**Chapter 2:** This chapter reviews different aspects of the literature that are related to dispersion polymerisations, hypercrosslinking reactions as well as functionalised polymers. Theories, development, approaches in application and comments on dispersion polymerisation, hypercrosslinking reactions and also functionalised polymers are thoroughly reviewed in this chapter.

**Chapter 3:** This chapter describes the synthesis route that was adopted in non-aqueous dispersion (NAD) polymerisation. Details of methods, materials and the main equipment employed in NAD polymerisations are discussed. The data analyses as well as the steps undertaken for analysis of the particles are also discussed. This includes FTIR, SEM and elemental microanalysis.

**Chapter 4:** In this chapter, aqueous dispersion polymerisation (ADP), which is an alternative route to produce polymer precursors in micron size for hypercrosslinking reactions, is described. The synthetic route as well as the methods, materials and all the equipment that were used are discussed. Additionally, FTIR, SEM and elemental microanalysis results were included in this chapter.

**Chapter 5:** This chapter presents the research methodology for the hypercrosslinking reactions which were adopted in this work. Detailed analysis data and characterisation of the particles using BET, SEM, elemental microanalysis, FTIR are discussed in this chapter.

**Chapter 6:** This chapter presents the sulfonation of hypercrosslinked particles. Methodology for producing sulfonated hypercrosslinked particles, detailed discussion and characterisation of the particles (SEM, elemental microanalysis, FTIR and BET), their application, particularly in solid-phase extraction (SPE), are presented.

**Chapter 7:** The penultimate chapter presents aminated hypercrosslinked particles. Methodology for amination reactions and all the detailed analyses and characterisation, such as SEM, FTIR, BET and elemental microanalysis, are presented.

**Chapter 8:** The final chapter draws the general conclusions and provides suggestion for further work.

## References

- [1] V. A. Davankov, M. M. Llyin, M. P. Tsyurupa, G. I. Timofeeva and L. V. Dubrovina, *Macromolecules* **1996**, *29*, 8398-8402.
- [2] N. Fontanals, P. A. G. Cormack and D. C. Sherrington, *J. Chromatogr. A* **2008**, *1215*, 21-28.
- [3] D. Bratkowska, N. Fontanals, F. Borrull, P. A. G. Cormack, D. C. Sherrington and R. M. Marcé, *J. Chromatogr. A* **2010**, *1217*, 3238-3242.
- [4] N. Fontanals, R. M. Marcé and F. Borrull, *J. Chromatogr. A* **2007**, *1152*, 14-31.
- [5] S. E. Lyubimov, A. A. Vasil'ev, A. A. Korlyukov, M. M. Ilyin, S. A. Pisarev, V. V. Matveev, A. E. Chalykh, S. G. Zlotin and V. A. Davankov, *React. Funct. Polym.* **2009**, *69*, 755-758.
- [6] D. Horák, *J. Polym. Sci.: Part A: Polym. Chem.* **1999**, *37*, 3785-3791.
- [7] H. Qi, W. Hao, H. Xu, J. Zhang and T. Wang, *Colloid Polym. Sci* **2009**, *287*, 243-248.
- [8] A. J. Paine, W. Luymes and J. McNulty, *Macromolecules* **1990**, *23*, 3104-3109.
- [9] R. B. Merrifield, *J. Am. Chem. Soc.* **1963**, *85*, 2145-2150.
- [10] B. Gong, L. Li and J. Zhu, *Anal. Bioanal. Chem.* **2005**, *3825*, 1590-1594.
- [11] C. A. Toro, R. Rodrigo and J. Cuellar, *React. Funct. Polym.* **2008**, *68*, 1325-1336.
- [12] K. C. Wood, S. M. Azarin, W. Arap, R. Pasqualini, R. Langer and P. T. Hammond, *Bioconjugate Chem.* **2008**, *19*, 403-405.
- [13] S. D. Alexandratos, R. Beauvais, J. R. Duke and B. S. Jorgensen, *J. Appl. Polym. Sci.* **1998**, *68*, 1911-1916.
- [14] J. S. Song, F. Tronc and M. A. Winnik, *J. Am. Chem. Soc.* **2004**, *126*, 6562-6563.
- [15] J. S. Song, L. Chagal and M. A. Winnik, *Macromolecules* **2006**, *39*, 5729-5737.
- [16] J. S. Song and M. A. Winnik, *Macromolecules* **2005**, *38*, 8300-8307.

[17] N. Fontanals, P. Manesiotis, P. A. G. Cormack and D. C. Sherrington, *Adv. Mater.* **2008**, *20*, 1298-1301.

[18] K. P. Lok and C. K. Ober, *Can. J. Chem.* **1985**, *63*, 209-216.

## ***CHAPTER TWO***

**2.0 Summary**

This review presents an overview of the literature concerning porous materials, particularly hypercrosslinked polymers. As a new generation of the porous materials, hypercrosslinked polymers have a number of attractive properties and can be chemically modified to introduce new functional groups for specific uses. Routes to prepare the precursors that can be used in post-polymerisation steps to produce hypercrosslinked polymers and their functionalised derivatives are presented in this review. The review concludes with a discussion of the technique that was employed in the preparation of hypercrosslinked polymers, as well as a discussion of the functionalisation of hypercrosslinked polymers.

**2.1 Polymer Synthesis**

In polymer science, one of the fundamental pieces of knowledge is to understand polymer synthesis. Generally speaking, a monomer is a small structural unit and a polymer is a large molecule constructed from the union of these monomer units. The process to convert monomers to polymer is called polymerisation, and there are two distinct classes of polymerisation: step-growth polymerisation and chain-growth (addition) polymerisation.

In 1929, Wallace Hume Carothers introduced the distinction between “addition polymerisation” and “condensation polymerisation”.<sup>[1]</sup> However, in 1952, the term condensation was replaced by the term “step-growth” by Paul Flory.<sup>[2]</sup> Today, it is logical to speak of step-growth polymerisation rather than condensation polymerisation since some polymers grow by a step-reaction mechanism without the elimination of a small molecule (e.g., polyurethanes).

### 2.1.1 Step-Growth Polymerisation

Step-growth polymerisation is used for monomers bearing functional groups such as COOH, -OH and -NH<sub>2</sub>. Normally, the polymers grow either without the elimination of a small molecule or with the elimination of a small molecule as a by-product, usually water (Figure 2.1).

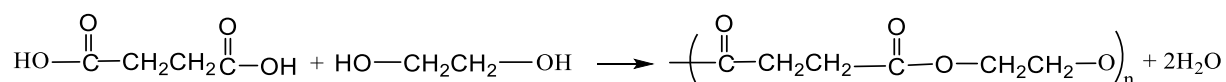


**Figure 2.1: An example of step-growth polymerisation**

### 2.1.2 Chain-Growth Polymerisation

In a typical chain-growth polymerisation, monomers are converted to polymer by the action of either a free radical or ionic initiator on a double bond or triple bond in the monomers. The monomers link up with other monomers to form polymer. The final product has same chemical composition as the starting material and, normally, no elimination of a small molecule occurs (Figure 2.2).

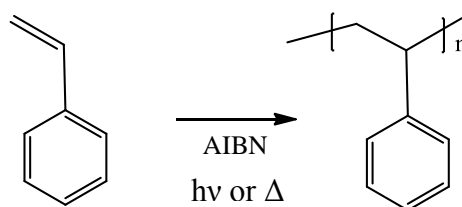


**Figure 2.2: Chain-growth polymerisation of styrene**

#### 2.1.2.1 Free Radical Polymerisation (FRP)

Free radical polymerisation is a type of chain-growth polymerisation, along with anionic and cationic polymerisation. Nowadays, the most important synthetic method which is available for the conversion of monomer to polymer is a free radical polymerisation. This method is a variant of chain-growth polymerisation. It is

exploited widely in industry, particularly in the commercial production of important plastics. Many vinyl monomers, such as styrene, ethylene and methyl methacrylate can be polymerised very effectively *via* this method. This technique has a number of advantages including the facts that it is relatively safe and easy to perform, even on a large scale. In addition, typically it results in high yields of product and can be performed under mild reaction conditions (20-150 °C). It can also tolerate a wide variety of solvents, including water, various functional groups (which are present in many monomers) as well as impurities in the system. For these reasons, free radical polymerisation was used as the method of choice for polymerisations in the present study.

Generally speaking, free radical polymerisation consists of three steps: initiation, chain propagation and chain termination. The initiation is triggered by a radical initiator, such as an azo compound or peroxides, either photolytically or thermally. One commonly used azo compound is 2,2'-azobisisobutyronitrile (AIBN) which decomposes into a pair of 2-cyanopropyl radicals and nitrogen gas; the 2-cyanopropyl radicals act as initiator radicals (Figure 2.3).

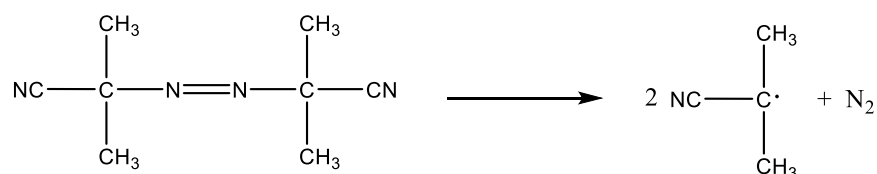
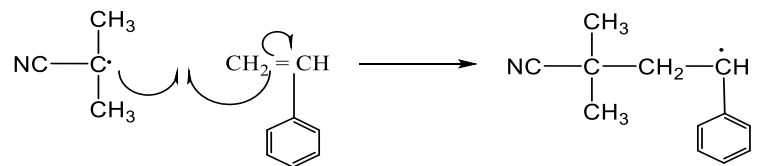
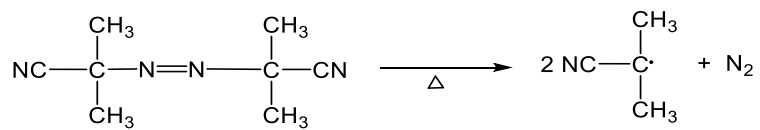


**Figure 2.3: Decomposition of AIBN into two 2-cyanopropyl radicals and nitrogen gas.**

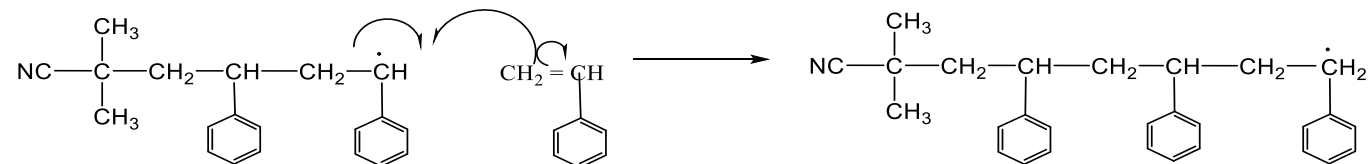
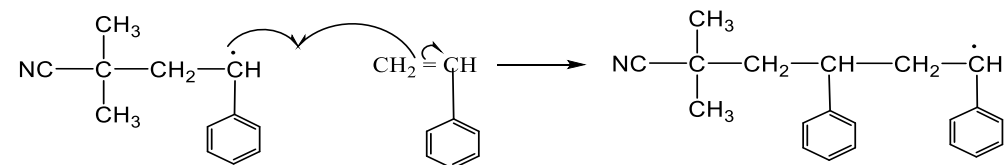
The radical reacts with a monomer in the initiation step and the growth of the polymer chain is then started. Initiation is followed by chain propagation (Figure 2.4) as illustrated by the conversion of styrene to polystyrene, and the combination of the radicals in two polymer chains terminates the growth process.

Termination occurs in free radical polymerisation either by radical-radical coupling or disproportionation. Some monomers terminate exclusively by combination, for instance styrene, whereas some monomers terminate by both mechanisms, for example poly(methyl methacrylate) (PMMA).

### Initiation



### Chain propagation



### Chain termination

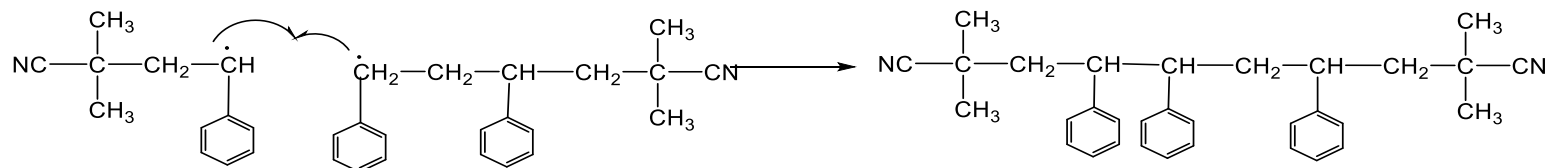
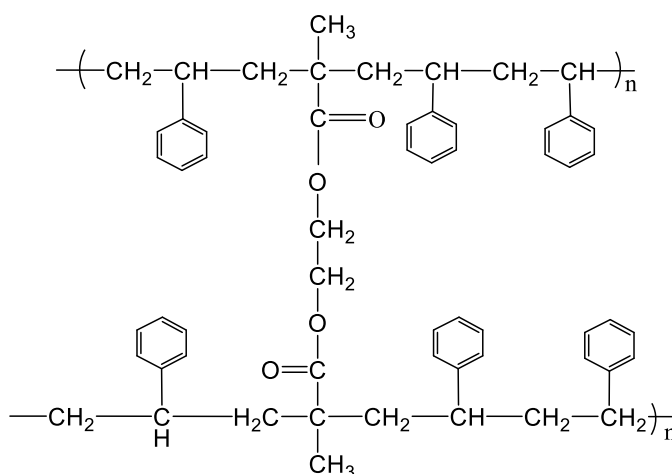


Figure 2.4: Three steps in the polymerisation of polystyrene: initiation, chain propagation and chain termination.

### 2.1.3 Crosslinked Polymers

Whereas linear polymers can be described as independent random coil macromolecules, the chains in crosslinked polymer are linked together chemically. Such polymers consist of an infinite network of interconnected linear polymers, where at least one of the monomers used must have two reactive groups. Monomers which consist of more than one vinyl group have an ability to combine or link together two polymer chains and are called crosslinking agents. A scheme illustrating styrene with the addition of the crosslinking agent ethylene glycol dimethacrylate (EGDMA) is shown in Figure 2.5.

Crosslinked polymers have numerous applications in areas such as solid-phase extraction (SPE), high performance liquid chromatography (HPLC), *etc.* Chemical crosslinking of the polymer confers strength and insolubility to the polymers, and polymer particles crosslinked with crosslinking agents such as divinylbenzene (DVB), ethylene glycol dimethacrylate (EGDMA), *etc.*, have good mechanical strength and can withstand high pressures (1000-5000 psi).<sup>[3]</sup> If there is a low degree of crosslinking, such as 1-2 wt% in the particles that are prepared by dispersion polymerisation (discussed later in Chapters 3 and 4), the particles have a tendency to swell and are thus not especially well suited for flow-through applications involving high pressures, however they should provide better access for hypercrosslinking (discussed later in Chapter 5).



**Figure 2.5: A crosslinked network of styrene and EGDMA where the polymer chains are linked together through covalent bonds.**

## **2.2 Techniques for the Synthesis of swellable Precursor Polymers**

Polymer particles can be synthesised in many ways, resulting in particles with different size and morphology. These polymerisation techniques include suspension polymerisation, precipitation polymerisation, emulsion polymerisation and dispersion polymerisation. The current body of work described in this thesis involves the study of lightly crosslinked polymer resins. To explain the synthesis and structure of these polymers, an introduction to simple polymer chemistry as well as a description of the polymerisation protocols used in the present study will be discussed later in this chapter. In connection to hypercrosslinked polymers and functionalised polymers, a chloromethylated polystyrene precursor could be prepared by copolymerisation of styrene (St) and vinylbenzylchloride (VBC) together with a crosslinker (e.g., ethylene glycol dimethylacrylate (EGDMA)) in a free radical polymerisation such as suspension polymerisation, precipitation polymerisation or dispersion polymerisation.

### **2.2.1 Suspension Polymerisation**

The technique of suspension polymerisation allows particles to be produced in a highly reproducible manner and is therefore used widely on a laboratory scale and on a large-scale in industry. In this technique, the monomer is dispersed as spherical liquid droplets in a continuous phase, which is normally water for most hydrophobic monomers. The mixture contains the dissolved initiator, suspension stabiliser (which is dissolved in the aqueous phase), and a water-soluble polymer as a surface active species in order to maintain monomer droplets. Then, continuous stirring is applied to maintain a stable suspension, and typically the reaction is heated at 80 °C for several hours.<sup>[4]</sup> The spherical liquid monomer droplets are converted into hard, glassy polymer particles during this reaction time, and with retention of the spherical symmetry of the original droplets (Figure 2.6). This technique can allow particles to be produced on large scale, however the broad particle size distribution obtained (50 µm – 1000 µm) may give disadvantages in some applications.

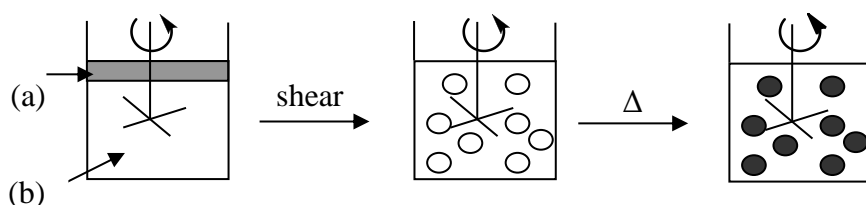


**Figure 2.6: Schematic representation of suspension polymerisation: (a) the mixture of monomer, porogen and initiator; (b) aqueous continuous phase containing suspension stabiliser.**

### 2.2.2 Precipitation Polymerisation

This type of polymerisation enables the production of monodisperse polymer beads, as does dispersion polymerisation, emulsion and seeded emulsion polymerisation. This technique is particularly interesting, because it does not require any surfactants to achieve monodisperse polymer beads.

At the beginning of the reaction, the precipitation polymerisation consists of a homogeneous solution of monomer, crosslinking agent, and initiator dissolved in an organic solvent (e.g., acetonitrile). Polymer formation itself can be characterised by two steps: a nucleation stage and a growth stage. When the reaction begins, oligomers are produced. Then, after a certain time, these soluble oligomers begin to aggregate, forming swollen microgels, resulting in the formation of colloidally stable particle nuclei. Each seed grows by steady capture of oligomer radicals by pendent vinyl groups on the particles' surfaces, and subsequent desolvation follows. This effect prevents any further nucleation and therefore monodisperse particles are obtained. The particles obtained are substantially smaller than the particles obtained by suspension polymerisation; 0.1  $\mu\text{m}$ -10  $\mu\text{m}$  is typical.

### 2.2.3 Dispersion Polymerisation

Micron-sized, monodisperse particles can be prepared by seeded emulsion polymerisation or by activated swelling.<sup>[5]</sup> Unfortunately, both methods are complex, time consuming and sometimes very difficult to implement on a large scale. Thus, dispersion polymerisation has become one of the most popular techniques for

preparing monodisperse particles in the micron-sized range. It is similar to precipitation polymerisation, but different in that a stabiliser is employed during the polymerisation. The polymerisation begins with a homogeneous solution of monomer, crosslinking agent, stabiliser and initiator dissolved in an appropriate solvent (e.g., ethanol). When the polymerisation proceeds, a heterogeneous mixture is formed and during this time the soluble oligomers begin to aggregate, forming swollen microgels, resulting in the formation of colloidally stable particle nuclei. Each seed grows by steady capture of oligomer radicals by pendent vinyl groups on the particles surfaces and then grows as the mature particles.

Dispersion polymerisation is an attractive method for producing micron-sized monodisperse polymer particles in a single batch process. There have been many studies about dispersion polymerisation, and the particles produced by this method have found in several applications, such as in the medical field, HPLC and SPE.<sup>[6]</sup> Dispersion polymerisation has been exploited widely over the past two decades because of the scientific and commercial interest in such particles; research into their preparation is active until today. However, one of the biggest challenges in dispersion polymerisation is to obtain particles in the micron-size range and particles which are monodisperse. This is because this size range lies between the diameter range of particles which can be produced by conventional emulsion polymerisation (0.06-0.7  $\mu\text{m}$ ) in a batch process, and suspension polymerisation (50-1000  $\mu\text{m}$ ).<sup>[6]</sup>

Therefore, dispersion polymerisation has been investigated widely as an alternative method for preparing monodisperse polymeric particles in the micron-sized range in one single step.<sup>[7-8]</sup> This method was developed originally in the early 1970s<sup>[9]</sup> but, stimulated by the work of Lok and Ober, it can deliver monodisperse, micron-sized particles in one step,<sup>[10]</sup> and gained particular interest in the late 1990s.<sup>[11-13]</sup> Ober and Lok have reported on the production of 1-10  $\mu\text{m}$  monodisperse copolymer particles consisting of styrene and *n*-butyl methacrylate with ethanol-water as the polymerisation medium. They used poly(acrylic acid) and benzoyl peroxide as a stabiliser and initiator, respectively.

Most of the published examples in this area involve common vinyl monomers such as styrene, methyl acrylates, and their copolymers, with stabilisers such as poly(*N*-vinylpyrrolidone) (PVP) and poly(acrylic acid) (PAA) in polar media, usually alcohols.<sup>[14-15]</sup> Instead of polar media, a large variety of non-aqueous dispersion (NAD) polymerised could be obtained in non-polar media such as supercritical carbon dioxide.<sup>[11, 16-17]</sup>

Recently, many researchers extended the concept of dispersion polymerisation in mixed solvent systems, as a method of forming monodisperse polymer microspheres either in methanol/water, ethanol/water or isopropanol/water.<sup>[18-22]</sup> These researchers studied this method in order to control the particle size and/or gain narrow particle size distributions.

Even though the invention of dispersion polymerisation suggests great opportunities for the preparation of monodisperse, micron-sized polymeric resins, and the method can be large-scale in the preparation of such particles, over the last two decades researchers have encountered big challenges in dispersion polymerisation when functional groups or crosslinking agents are employed. A dispersion polymerisation is highly sensitive to small changes in the reaction parameters involved in the course of polymerisation, and this can result in broad particle size distributions or gross changes in the final particle size when a second monomer is added into polymerisation.

Dispersion polymerisations have also failed when a crosslinker is employed. Odd-shape particles and broad particle size distributions, as well as flocculation or coagulation of the product is often reported.<sup>[23-24]</sup> Dispersion polymerisation may lead to monodisperse particles, but the crosslinking agent normally needs to be used at levels of below 1 wt%.

Thus, several methods have been proposed by many authors for the production of monodisperse polymer particles with narrow particle size distribution, as well as easily controllable particle sizes, in order to address the above-mentioned problems.

Jiang *et al.*<sup>[25]</sup> used the seeded polymerisation technique in order to control particle size in dispersion polymerisation. They reported that secondary nucleation (new particles) can be prevented by using this method. Similarly, Camli and co-workers<sup>[26]</sup> prepared macroporous polymers by modified seeded polymerisation to obtain monodisperse particles. Even though these methods could prevent secondary nucleation from occurring, the methods involved multistep polymerisation and were time consuming.

Winnik and co-workers<sup>[18-20, 22]</sup> introduced a new method which is known as a “two-stage” dispersion polymerisation method, in order to address these problems. In this method, they used late/delayed addition of a second monomer after the end of nucleation stage of the reaction. Under appropriate conditions, monodisperse, polymeric particles with narrow particle size distributions were obtained. Recently, Song and Winnik<sup>[18]</sup> reported that when DVB or EGDMA were added at the end of the nucleation stage, monodisperse particles could be obtained.

Yang *et al.*<sup>[23]</sup> proposed a seed-swelling technique as a method for the preparation of crosslinked polystyrene microsphere up to 3 wt% of crosslinker and, similarly to Kim *et al.*,<sup>[27]</sup> they used the same technique to obtain the particles in relatively narrow particle size distributions. Highly crosslinked micron-sized particles were successfully prepared by Lee and co-workers<sup>[28]</sup> with up to 20 wt% of crosslinker being employed in a dispersion polymerisation in which monodisperse polystyrene particles were prepared.

### **2.2.3.1 Process Description in Dispersion Polymerisation**

Figure 2.7 shows a schematic representation of the formation of polymer particles in dispersion polymerisation. In dispersion polymerisation, the monomer and the initiator are both soluble in a thermodynamically good solvent but the solvent is a thermodynamically poor for the resulting polymer. At the beginning of the reaction, the reaction mixture is a homogeneous solution of monomer(s) with initiator and dispersant in the solvent. Oligomer radicals are formed in solution by initiation and

propagation. These oligomers then reach the critical chain length to precipitate to form nuclei and, later, these nuclei aggregate to form large particles. At the same time, they absorb some monomer, initiator or polymeric stabiliser until monosized beads are obtained. This stage is called the nucleation stage, or the point of phase separation, and it is usually finished within a few minutes only. It depends on the solvency of the medium.<sup>[29]</sup> The polymerisation process can be divided into two stages, a “nucleation stage”, which is a very short stage but very complex, and also very sensitive, and a second stage which is known as a “particles growing” stage. The second stage is relatively long, simple and robust.<sup>[22]</sup>

As dispersion polymerisation proceeds, the polymer separates out and the reaction then continues in a heterogeneous manner; this stage is well known as the particle growth stage. In this stage, the numbers of particles remains virtually constant. Once the number of particles reaches a certain level, the oligomers and nuclei precipitate onto the particles’ surfaces without the formation of new, stable particles and this leads to the formation of spherical particles in the region of about 0.1-10  $\mu\text{m}$ .<sup>[20, 30]</sup> If new, stable particles are obtained during the polymerisation, this results in a broad particle size distribution. All the stable particles grow at the same rate, and all of them have an equal probability of trapping oligomer radicals and the polymer molecules formed in the heterogeneous phase. Hence, the diameter of the particles obtained is determined by the number of stable seed particles per unit volume and is directly related to the molecular weight of precipitating oligomer chains.<sup>[29]</sup> Thus, correlation between bead size and molecular weight is typical of a dispersion polymerisation. Besides this point, the bead size also can be adjusted *via* solvency mechanism, monomer, initiator or stabiliser.

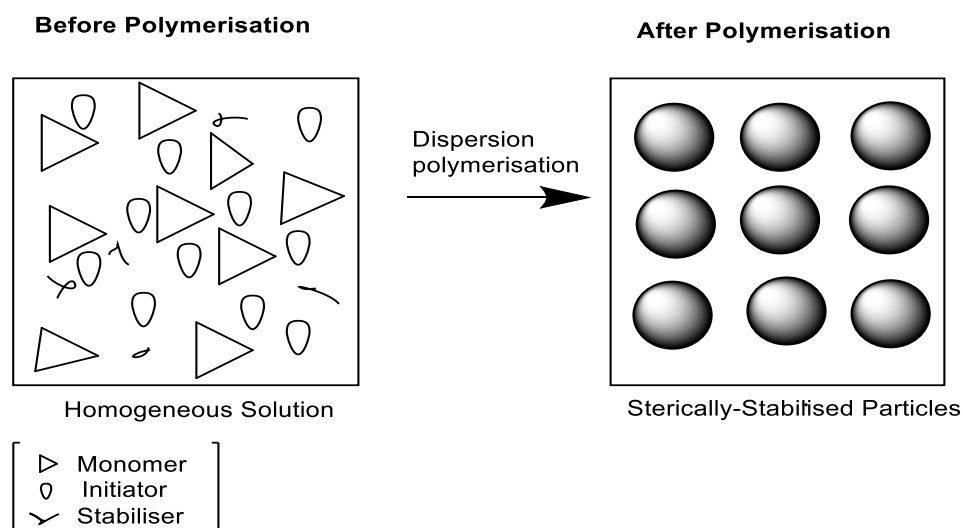


**Figure 2.7: Schematic representation of dispersion polymerisation.**

### 2.2.3.2 Solvent

For a typical dispersion polymerisation, the medium that is chosen has simultaneously to be a good solvent for the given monomer but a non-solvent for the polymer formed. The solvent is especially important in dispersion polymerisation because it has an influence upon the final properties of the dispersion, such as the average particle size, morphology and particle size distribution.<sup>[21, 31-32]</sup> Generally speaking, any changes in the system which tend to enhance the solubility of the polymer initially formed will tend to increase the bead size of the final product. Thus, the particle size increases when the solvency of the medium is decreased.

### 2.2.3.3 Monomer

The initial monomer concentration in the polymerisation has a major influence on the final size of the particles. This was demonstrated in a few studies<sup>[16, 33]</sup> which demonstrated that when the concentration of monomer increases the final particle size increases also. Hence, the polarity of the medium depends on the initial monomer concentration. Moreover, in the continuous phase, the monomer concentration affects the size of the particles by altering the critical chain length by changing the nuclei formation rate and the rate of adsorption of stabiliser.

#### **2.2.3.4 Initiator**

Initiator type and concentration also have a great influence on the final size of particles.<sup>[15, 34]</sup> In order to obtain small and stable dispersion particles, the selection of a suitable initiator becomes an important aspect. The nucleation stage in the dispersion polymerisation can be determined by the concentration and decomposition rate of the initiator which determines the rate of production of free radicals in the medium.<sup>[33]</sup> At higher initiator concentrations, a greater number of oligomeric radicals would be created, thus the polymerisation is started with more radicals per unit volume. Therefore, lower molecular weight polymer is obtained which leads to fewer nuclei but which are larger in diameter.

#### **2.2.3.5 Stabiliser**

Stabiliser plays a crucial role in the formation of stable particles in dispersion polymerisation. The stabilisation of particles is determined by the rate and extent of adsorption of the stabiliser on the particles' surfaces. Some papers have reported that the type of stabiliser has an influence on the formation of particles.<sup>[21, 31]</sup> In non-aqueous dispersion (NAD) polymerisation, the selection of stabiliser is one of the primary factors that should be considered. Classical, low-molecular weight surfactant is not efficient as a stabiliser for an NAD system, especially ionic surfactants. Therefore, the most successful type of stabiliser for use with an NAD system is based on "block" or graft copolymers.<sup>[35]</sup> For example, the simple case of an A-B type block copolymer, where the A block is soluble in the dispersing solvent medium, which acts as a stabilising moiety, and the B block is the insoluble block which has a tendency to be adsorbed or anchored into the dispersed (polymeric) phase.

Besides this point, the concentration of stabiliser also has an effect on the particle size. When the concentration of stabiliser increases, the particle size also increases. However, upon adding more stabilisers into the system, monodisperse particles are not obtained. This can be explained by the amount of stabiliser on the particles' surfaces exceeding the saturation value.<sup>[21]</sup>

### 2.3 Macroporous Materials

Macroporous materials are defined as solids containing pores. The pores persist even in the dry state. Generally speaking, macroporous materials have a porosity of between 2-95% , where “porosity” means the volume ratio of pore space to the total volume of the material.<sup>[36]</sup> The term ‘macroporous’ was established many decades ago and it simply implies that the materials have permanent porosity; it does not imply the presence of any particular pore size. The ability of macroporous solids to interact with atoms, ions and molecules, not only on their surfaces but also throughout the bulk of the material, is attractive in science and technology. Thus, it is not surprising, to find that applications of macroporous materials, such as zeolites, involve catalysis, separation processes, ion-exchange and many applications which benefit from the higher order that can be achieved in solids. Macroporous materials have been used in various applications from daily necessities, for example purification of drinking water by the macroporous ceramics or activated carbon, to use in modern industry, such as for waste water treatment.

Pores can be classified into two types: open pores, which connect to the surface of the materials, and closed pores which are isolated from the outside and which do not allow the access of external fluids (Figure 2.8). Usually, penetrating open pores (having at least two openings located on two side of the macroporous material) is required for catalysis, filtration, separation or membranes, and materials with closed pores are required in lightweight structural applications, thermal insulation, *etc.* Pores can have different shapes and morphology such as spherical, cylindrical and slit types, and complex shapes for pores, for example hexagonal shape are also known.<sup>[37]</sup>

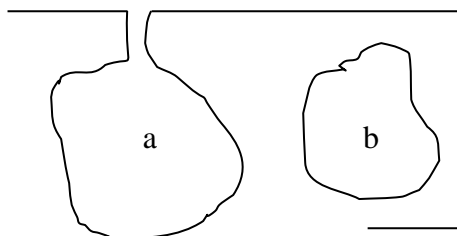


**Figure 2.8: Pore types; (a) open pores; (b) closed pores**

Different applications of macroporous materials require different pore sizes. For instance, zeolites or silica gels are used for gas separation or catalyst supports due to their atomic scale pores that meet the requirement for those applications. The International Union of Pure and Applied Chemistry (IUPAC) have recommended that classification of the porous materials by pore size should be as follows: micropores are smaller than 2 nm in diameter, mesopores from 2 to 50 nm and macropores larger than 50 nm.

Macroporous materials, also known as molecular sieves, which covers the microporous, mesoporous and the macroporous domain, depend upon their pore dimension. The ability to perform a desired function in a particular application relates directly to the particle size distribution, and shapes and volumes of the void spaces in the macroporous materials. Over recent years, the need to create uniformity within pore size, shape, and volume has steadily increased because it can lead to superior application properties. For instance, a zeolite, which is a material with uniform micropores, can separate molecules on the basis of their size by selectively adsorbing a small molecule from a mixture containing molecules too large to enter its pores. Clearly, the ability of the solid to separate molecules of differing sizes would be limited by a pore size distribution. Besides this point, the presence of atoms in the material also has an influence in molecules separation process. For example, molecular sieves comprising aluminosilicate are hydrophilic and thus can take up water from organic solvents, whereas molecular sieves comprising pure silica are hydrophobic and can take up organic components from water.

The development of advanced macroporous materials having channels of tuneable dimensions at the atomic, molecular and nanoscale has become a fast-growing interdisciplinary field since microporous zeolites were discovered. This has resulted in materials with new or improved properties. Figure 2.9 depicts a flow chart of members of macroporous materials. Each material has its own relative advantages and disadvantages that will be discussed further in a next section.

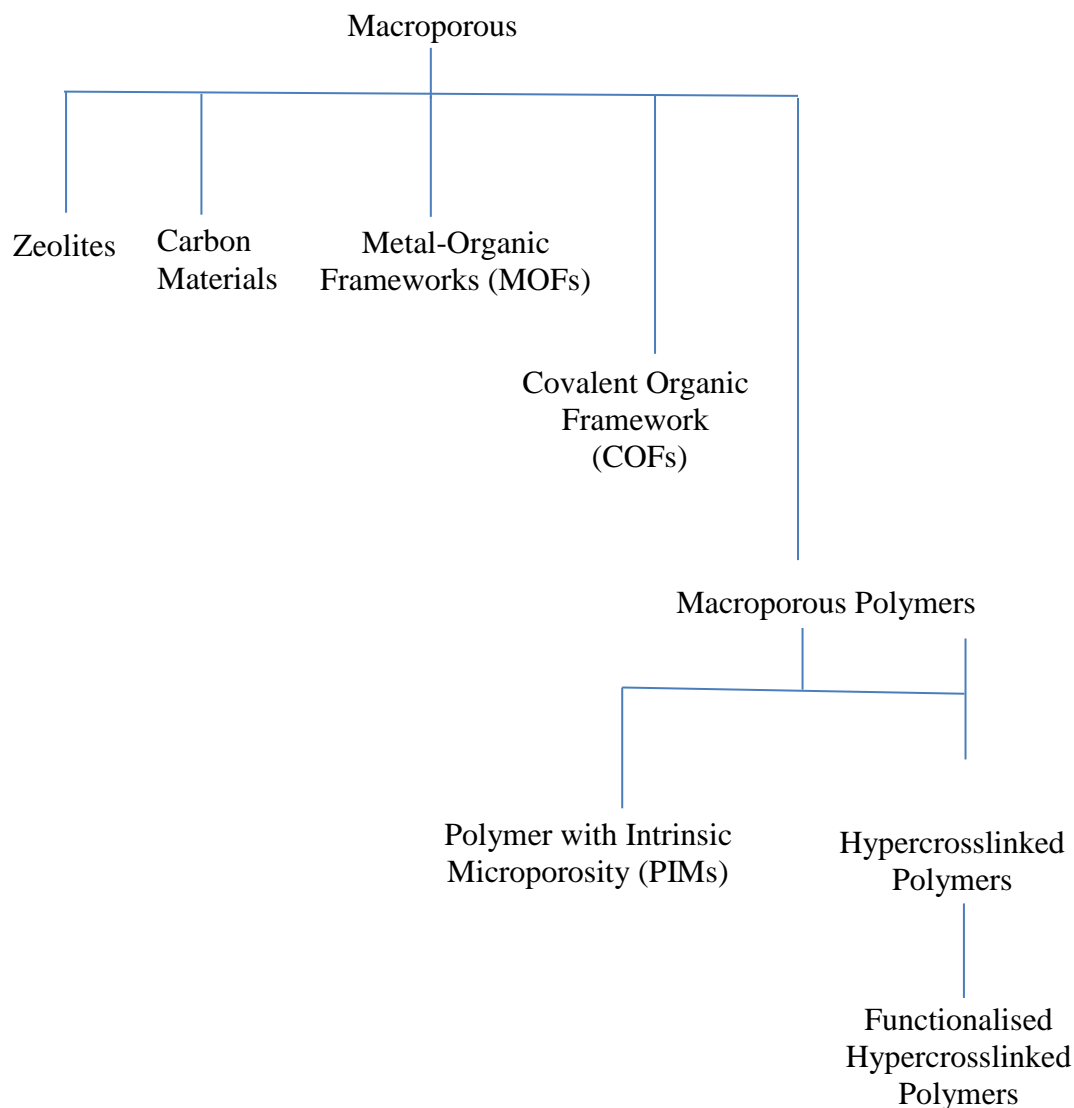


**Figure 2.9: Flow chart of members of macroporous materials**

## 2.4 Zeolites

Zeolites are three-dimensional silicate structures built of  $\text{TO}_4$  tetrahedra sharing all four corners, where T typically indicates  $\text{Si}^{4+}$  or  $\text{Al}^{3+}$  ions. The tetrahedral units can be linked in a great number of different network topologies due to the fact that the T-O-T bonds are more flexible than O-T-O. These tetrahedra are the basic building blocks for various zeolite structures, such as zeolite type A and type X, which are the most common commercial adsorbents (Figure 2.10). In zeolite type A, the cages

possess the form of a truncated octahedron, and are connected with each other through the square faces in a cubic framework, while in type X the cages are connected through the hexagonal faces.

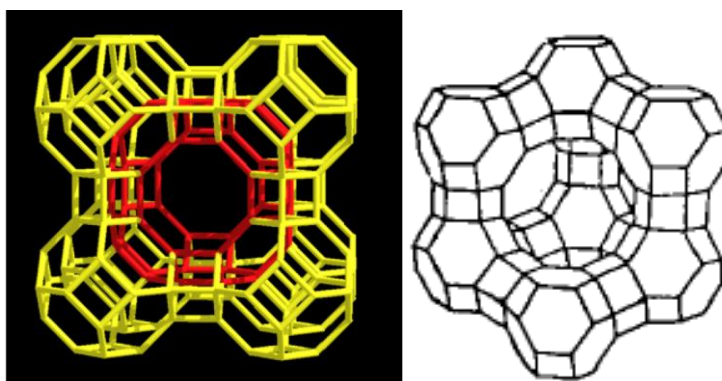


**Figure 2.10: Crystal structure of zeolite Type A (left)<sup>[38]</sup> and Type X (right).<sup>[39]</sup>**

Zeolites were discovered by a Swedish mineralogist 255 years ago.<sup>[40]</sup> Some zeolites can be found in nature, however most of them are produced synthetically usually by the hydrothermal crystallisation of aluminosilicate gels. They also consist of a robust, crystalline silica ( $\text{SiO}_2$ ) framework. Zeolites are the aluminosilicate members of the family of microporous solids known as “molecular sieves”, and have a very open microporous structure with different frameworks types depending on the assembly of the tetrahedral building units. This assembly is determined by the Si to Al ratio. At some places in the framework,  $\text{Si}^{4+}$  is substituted with  $\text{Al}^{3+}$  and the framework carries a negative charge, and loosely held cations that sit within the cavities preserve the electrical neutrality of the zeolite structure.

Zeolites have a rigid, three-dimensional crystalline structure (similar to a honeycomb) consisting of a network of interconnected tunnels and cages. These channels are large enough to allow exchange of certain ions, or to absorb water and small molecules without breaking down the structure (the channels, typically 0.3-0.7 nm in diameter, are slightly larger than a water molecule). Zeolites in general have high specific surface area (SSA) (up to  $925 \text{ m}^2/\text{g}$ ) and their rigid framework limits shrinking and swelling.

Because of these attractive properties, zeolites have been applied intensively in many applications, from daily basis household uses to technical purposes like water treatment, catalysis, gas adsorption and ion-exchange. Nevertheless, this material has some limitations in terms of the molecular size of species which can enter the network which is obviously limited by the size of the pore apertures or of the channel intersection.

## 2.5 Carbon Materials

A great variety of carbon materials are appearing in the literature, for example activated carbon, carbon nanotubes and carbon nanofibers (Figure 2.11). These materials consist of benzene-like carbon hexagons with  $sp^2$ -hybridized carbon atoms, but a difference between them is the way in which these hexagons are arranged in the materials. Carbonaceous structures have varieties surface texture and porosity, which can be modulated through the synthetic route.

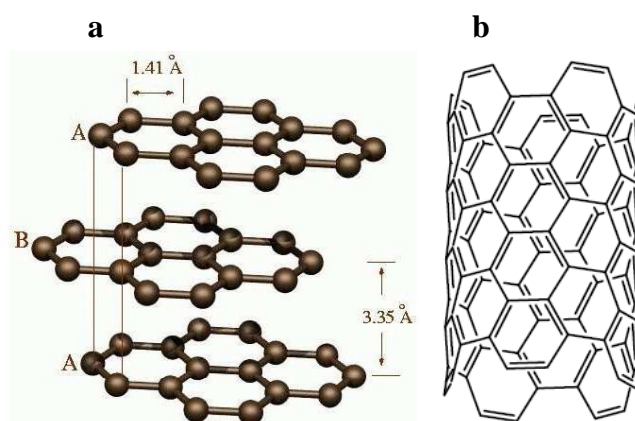


**Figure 2.11: Schematic representation of carbon materials: [a] activated carbon,<sup>[41]</sup> and [b] carbon nanotube.<sup>[42]</sup>**

The ability of charcoal to adsorb contaminants from water has been well known for thousands of years. Nowadays, activated carbon is mostly used as a catalyst<sup>[43]</sup> and adsorbent.<sup>[44]</sup> Traditionally, activated carbon has been produced from wood, peat, coal and waste of vegetable origin, such as fruit stone, nutshell, *etc.*

Regular grades of activated carbons have specific surface area (SSA) up to 1500 m<sup>2</sup>/g, dependent upon the precursor materials and post-carbonisation treatment. The porosity of the activated carbon is obtained by chemical activation, during or prior to the carbonisation of the organic precursor through either reaction with an oxidising gas or with inorganic chemical such as phosphoric acid.<sup>[45]</sup> In addition, activated carbons have SSA up to 3000 m<sup>2</sup>/g,<sup>[46]</sup> which is generally obtained by heat treatment at high temperature (~800 °C). Activated carbon possesses a highly disordered array of graphitic platelets and is a twisted network of carbon layer planes, crosslinked by an extended network of aliphatic carbon. This results in a continuum of interlayer spaces, ranging from distances which are similar to the spacing in graphite up to sizes which can form micropores.

A new synthetic method has been developed to produce carbon with a uniform pore size distribution. In this case, an inorganic macroporous template like a silica matrix<sup>[47]</sup> is used to define the porosity of the carbon materials. An organic or hydrocarbon precursor is adsorbed on the macroporous silica and then subjected to pyrolysis. Later, the template is removed chemically, leaving well-ordered pores of uniform size in the carbon material.

Activated carbon and macroporous carbon materials have found use in many applications, such as in water purification, metal extraction and waste water treatment due to their high SSA and microporosity. Activated carbons possesses a broad pore size distribution ranging from microporous (<2 nm) to mesoporous (between 2 nm-50 nm) to macroporous (>50 nm)<sup>[48]</sup> which give limitation in certain applications. The surfaces area also very heterogeneous in terms of chemical functionality; oxygen- and nitrogen-containing functional groups.

## **2.6 Metal-Organic Frameworks (MOFs)**

Metal organic frameworks (MOFs) are highly macroporous crystalline molecular structures composed of two major components: a metal ion linked by organic molecules yielding an open framework structure. The choice of linker and metal ion

has a significant effect on the structure as well as properties of the MOF. They have recently shown considerable promise in a wide range of applications, including hydrogen storage,<sup>[49]</sup> catalysis<sup>[50]</sup> and ion-exchange.<sup>[51]</sup> MOFs can be systematically built for desired applications, including particular configurations that are stable and macroporous and which can be used to trap other molecules in a cage-like structure. Indeed, the strong metal-oxygen bond confers exceptional robustness to the framework, a framework which does not collapse after removal of the solvent molecules incorporated during reaction. The ability to prepare MOFs with adjustable pore size, shape and functionality has led to their use in many applications and recently, MOFs produced by a new method are currently being trailed for natural gas storage in heavy duty vehicles.<sup>[52]</sup>

Open networks comprising metal-organic units gained attention in the 1990s, but the inability of these materials to maintain permanent porosity and avoid structural rearrangement upon guest removal or guest exchange (leading to complete collapse of the framework, such as in the case of frameworks of the metal bipyridine type) was a big issue.<sup>[53-54]</sup> However, MOFs that exhibit permanent porosity have now been prepared. The outstanding work performed by Yaghi and co-workers<sup>[55]</sup> in this class of crystalline materials was responsible for the real breakthrough of MOFs. They found that the use of carboxylate rigid organic ligands to link with metal-ions was ideal to form extended frameworks with structure stability and high porosity.

The first such solid was MOF-5 (Figure 2.12), which consists of metal-carboxylate subunits ( $Zn^{+}$  and 1,4-benzenedicarboxylate) as nodes of a framework and of organic linker in desired network topology, and has a microporous volume larger than any known zeolite.<sup>[53]</sup> MOF-5 units ( $Zn_4O(CO_2)_6$ ) containing four  $ZnO_4$  tetrahedra with a common vertex and six carboxylate C atoms define an octahedral secondary building units (SBUs), and are then joined by benzene links. This type of microporous material is the most studied of all organic framework due to its high SSA (2900  $m^2/g$ ) and pore volume (1-2  $cm^3/g$ ).<sup>[54]</sup> In practice, MOF-5 was prepared from Zn(II) and benzenedicarboxylate (BDC) acid under conditions pre-determined to yield octahedral secondary building units (SBUs) *in situ*. SBU as a structural entity was

adopted from zeolite structure analysis in order to aid the process of structure prediction.

Today, a great variety of different MOFs have been synthesised and characterised, for instance a magnesium-based metal organic framework (Mg-MOF-74) and an iron terephthalate (MOF-235).<sup>[56-57]</sup> Recently, BASF research scientists developed an innovative method for solvent-free industrial-scale manufacture of these materials on a large scale.<sup>[52]</sup> This step-change makes this class of microporous material much more attractive for industrial use. The cost of production of organic ligands limits the interest of industry to a reduced number of MOF structures. In addition, chosen of organic and building block of a MOF are crucial due to have an influence on properties of the product. Also, such materials can suffer from limited long-term stability at high temperature.

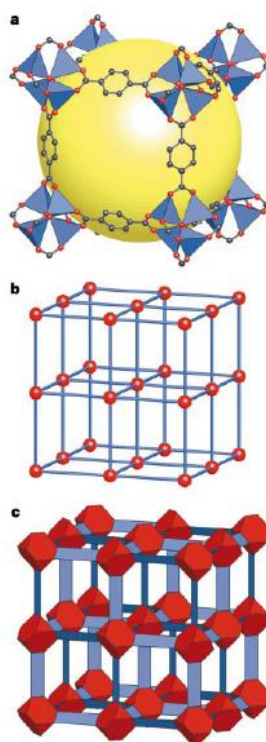


**Figure 2.12: The MOF-5 structure and its topology. (a) The MOF-5 structure shown as  $ZnO_4$  tetrahedra (blue polyhedra) joined by benzene dicarboxylate linkers (O, red and C, black) to give an extended 3D cubic framework with interconnected pores of 8 Å aperture width and 12 Å pore (yellow sphere) diameter. (Yellow sphere represents the largest sphere that can occupy the pores without coming within the van der Waals size of the framework). (b) The topology of the structure (primitive cubic net) shown as a ball-and-stick model. (c) The structure shown as the envelopes of the  $(OZn_4)O_{12}$  cluster (red truncated tetrahedron) and benzene dicarboxylate (BDC) ion (blue slat). Note that opposing slats are all at 90 °C.<sup>[54]</sup>**

## 2.7 Covalent Organic Frameworks (COFs)

The design and synthesis of crystalline molecular blocks into extended structures by strong covalent bonds is becoming commonly practiced in the synthesis of metal-organic frameworks, wherein transition metal-oxide bonds (e.g., Zn-O) join organic units to make highly robust and microporous structures.<sup>[58-60]</sup> This provided the stepping stone for the development of alternative microporous materials that constitute macroporous, crystalline organic frameworks. The first covalent organic framework (COF) was reported in 2005.<sup>[61]</sup>

Unlike MOFs which contain heavy metals, COF structures are contain entirely light elements (H, B, C and O) linked by strong covalent bonds (B-O, C-C and B-C) such as those found in diamond or boron carbides. These materials have rigid structures, low densities (one member of this class has the lowest density reported for a crystalline solid),<sup>[62]</sup> exhibit permanent porosity with SSAs surpassing those of well-known zeolites and macroporous silicates, and also thermal stability (up to 600 °C). The first members of this class, COF-1 [ $(C_3H_2BO)_6 \cdot (C_9H_{12})_1$ ] and COF-5 ( $C_9H_4BO_2$ ) (see Figure 2.13) have been synthesised using a simple “one pot” condensation reaction of discrete molecules known to produce six- and five-membered rings. This reaction was carried out under mild reaction condition and resulted in high yields of products (71-73%).<sup>[61]</sup>

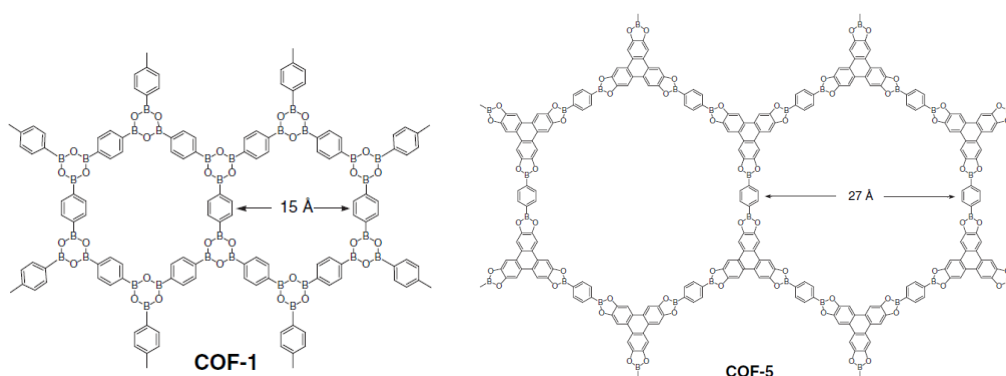


Figure 2.13: Representative structure of the first member of the COF family.<sup>[61]</sup>

The SSA for COF-1 and COF-5 were 711 m<sup>2</sup>/g and 1590 m<sup>2</sup>/g, respectively. Since the initial report, a number of other studies have described crystalline boroxine or boronate-ester COFs, with SSAs up to 4210 m<sup>2</sup>/g in some cases (COF-103),<sup>[62]</sup> SSA values which are surpassing those of well-known zeolite or macroporous silicate. The development of COFs, while still in its early stage, has exhibited great potential for application in the field of hydrogen storage and capture of carbon dioxide,<sup>[63]</sup> but due to their non-uniformity morphology, for instance platelets, spherical and irregular spherical structure are known,<sup>[62]</sup> they are limited in other applications.

## 2.8 Macroporous Polymers

Polymeric materials are often used in various applications such as in ion-exchange, polymer supports or chromatography columns due to their stability and the possibility of a wide range of surface functionalisation. Thus, polymer-based materials have become important today due to their attractive features compared to the other materials.

Macroporous polymers with permanent porosity even in the dry state have been around for several decades. According to Okay,<sup>[29]</sup> these conventional resins, called ‘macroporous’ or ‘macroreticular’ were made by radical copolymerisation of styrene in the presence of divinylbenzene (DVB) using suspension polymerisation. Macroporous polymer networks form because phase separation occurs during the course of free radical crosslinking copolymerisation in the presence of inert diluent. At the same time, the crosslinker (e.g., DVB) ties together linear chains of styrene at various points to fix the structure of the crosslinked polymer. When the copolymerisation proceeds, the pores are formed in the space where the diluent was found. Using an appropriate organic solvent such as toluene, copolymerisation of styrene and divinylbenzene (DVB) can yield polymer beads. After the development of macroporous networks in a few decades, it became necessary to distinguish new materials from the conventional materials; these new materials have come to be called ‘macroporous polymers’.<sup>[64]</sup>

In contrast to gel-type polymer resins, these materials do not swell in any solvents neither (thermodynamically good or bad solvents) but do allow access to the interior because they possess a permanent macroporous structure.<sup>[65]</sup> These characteristics of macroporous polymer resins facilitate any reagent to penetrate within the empty pore structure of the polymer. In addition, this type of resin is also rigid due to the high degree of crosslinking. Their rigidity and pore structure allow them to be used in any solvents and this specific characteristic may lead to further application of the macroporous resins, for example as resin supports and for packing into small or large columns.

Macroporous, crosslinked polymers are interesting materials for numerous separation processes; therefore, they are used widely in the ion-exchange field, as specific adsorbents in solid-phase extraction (SPE) and as stationary phases in liquid chromatography.<sup>[66-67]</sup> Unfortunately, this type of macroporous has some limitation which is associated with mechanical and chemical stability. In recent years, in order to overcome the issues that can arise from conventional macroporous polymers, an effort was made by the researchers in which an advanced technology and a new class of macroporous polymer has been developed.<sup>[68-69]</sup>

### **2.8.1 Polymers with Intrinsic Microporosity (PIMs)**

By exploiting the concept of intrinsic microporosity from amorphous organic materials similar to that of activated carbon, the first polymer with intrinsic microporosity (PIM) was reported in 2004. This new class of microporous organic material which is termed “polymer with intrinsic microporous” (PIM) and has relatively rigid, “awkward shaped” backbones, was developed by Budd and co-workers.<sup>[69]</sup> Such materials were developed upon a concept of designing highly rigid and contorted macromolecules to ensure inefficient packing in the solid state, resulting in interconnected intermolecular voids in the solid state.<sup>[37, 48, 69-71]</sup>

Even though these materials possess amorphous structures similar to activated carbon, in terms of surface chemistries they offer well-defined surfaces compared to

activated carbon. The apparent microporosity is termed 'intrinsic' due the fact that it does not depend on the history of the material but instead is dependent upon the molecular structure. PIMs are generated solely through the processing and such materials forms robust solids either in membrane or powder form.

PIM-1 (Figure 2.14) was the first generation of soluble PIM that was produced in robust solid form (membrane or powder), with the SSA of 600-900 m<sup>2</sup>/g.<sup>[69]</sup> This soluble PIM (soluble in solvent such as chloroform and tetrahydrofuran) is prepared from the dioxane-forming reaction between 5,5',6,6'-tetrahydroxy-3,3,3'-trimethyl-1,1'-spirobisindane and tetrafluoro-terephthalonitrile (double aromatic nucleophilic substitution).

Microporosity in such materials arises from the association of the macromolecule during precipitation from the solvent. PIM-1 also offers a greater thermal, chemical stability, and extremely rigid. In addition, the SSA of these materials can be tuned over the range 600-1760 m<sup>2</sup>/g. However, the SSA of PIMs are depend upon the form of the material and the SSA is greater in the powder form compared to the film.<sup>[60]</sup> Given the ability to generate soluble PIMs (film forming, microporous), such materials offer highly selective gas separation membranes and have potential for heterogeneous catalysis and hydrogen storage.<sup>[48, 71-72]</sup>

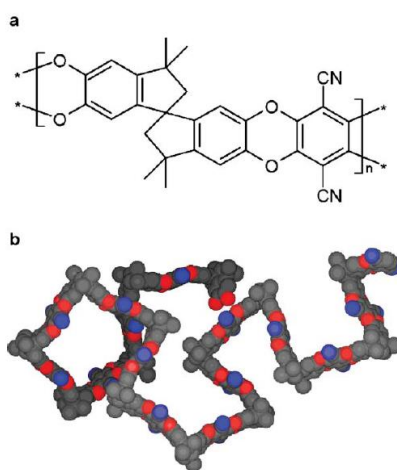


**Figure 2.14: (a) Chemical structure of PIM-1. (b) Molecular model of PIM-1 showing its highly contorted, rigid structure.**<sup>[73]</sup>

## 2.8.2 Hypercrosslinked Polymers

Three-dimensional polystyrene networks are used widely as sorbents and supports in industry and academia. The synthesis of such materials can yield three distinct types of network depending upon the synthesis conditions. The first consists of homogeneous networks in which styrene copolymers with divinylbenzene (DVB) or other divinyl monomers are obtained by free radical polymerisation without any micro-phase separation of the initial homogeneous system in the absence of diluent (e.g., loose network of vulcanized rubber). The second group consists of heterogeneous networks. These materials are obtained by copolymerisation of styrene with a relatively high amount of divinylbenzene in the presence of a solvent which is a thermodynamically good solvent for the monomer but a thermodynamically bad solvent for the polymer which is formed. The last group consists of hypercrosslinked networks; these differ from the known types of homogeneous and heterogeneous networks. The resins obtained in this third group have been thoroughly studied.<sup>[35, 74-76]</sup>

Distinctly different from conventional styrene-divinylbenzene copolymers, hypercrosslinked polymers are a new generation of microporous polymers which are obtained by extensive post-crosslinking of polymer chains in the presence of a good solvent, preferably by introducing numerous methylene bridges between aromatic rings. This material can be produced in two ways: by using an 'internal' bis-electrophile<sup>[68]</sup> or an 'external' bis-electrophile in conjunction with either preformed linear chains or preformed lightly crosslinked gels.<sup>[77]</sup>

Many research groups have probed the porous structure of hypercrosslinked polystyrene and found that polymers of this type can be classified as a new hypercrosslinked family distinct to conventional macroporous styrene-divinylbenzene (St-DVB) copolymers.<sup>[74]</sup> Hypercrosslinked polymers have a rigid three-dimensioned open network and these polymers display extraordinarily high specific surface areas ( $>1000 \text{ m}^2/\text{g}$ ) and high micropore contents,<sup>[78]</sup> which arise from the nature of the hypercrosslinking process in which an expanded framework

possessing internal void volume is generated. They have a capability to uptake polar and non-polar solvents, from hexane to methanol to water.

Besides the properties mentioned already, hypercrosslinked polymers are highly stable to air and water, inexpensive to produce since commodity monomers and crosslinkers are usually used in their preparation, their pore structure can be finely tuned, chemical modification is facile and the technology is scalable. These features render hypercrosslinked polymers as attractive candidates in many applications. For instance, chromatography columns packed with hypercrosslinked materials of micron-sized dimensions and narrow particle size distributions lead to highly efficient chemical separations, particularly in solid-phase extraction.<sup>[79]</sup>

### 2.8.2.1 Preparation of Hypercrosslinked Polymers

The hypercrosslinked polymer was introduced by Davankov *et al.* and they have intensively studied the preparation of such materials, pore structure, various properties as well as the application of hypercrosslinked polymers.<sup>[67-68, 80]</sup> In pioneering work, hypercrosslinked polystyrene networks were prepared by extensive post-polymerisation crosslinking of linear polystyrene (PSt) chains or swollen, gel-type styrene-divinylbenzene copolymers. In addition, various bifunctional compounds as crosslinking agents, such as chloromethyl methyl ether, *bis*-chloromethylated benzene and biphenyl have been used to introduce such bridges using Friedel-Crafts catalysts to generate ‘external’ bis-electrophiles. This led to the introduction of a large number of methylene bridges between aromatic rings in which every phenyl group of the polystyrene coils were involved in intramolecular crosslinks. The products obtained are conformationally rigid, display high specific surface areas (>1000 m<sup>2</sup>/g), an ability to sorb polar and non-polar solvents, and were characterised by an exceptionally rigid open-network structure of high permeability.<sup>[35]</sup>

In order to get more regular networks and permanently porous functionalised styrene copolymers in the polymer bulk, Hradil *et al.*<sup>[81]</sup> employed tetrachloromethane

(which is less carcinogenic reagent) as a crosslinker along with a Friedel-Craft catalyst (aluminium or ferric chloride) in post-crosslinking reactions. In this reaction, the short dichloromethylene bridges which were introduced reinforced the structure of the polymers and gave specific surface areas around 998 m<sup>2</sup>/g.

The original preparation of hypercrosslinked polymers is typically a single pot procedure where both chloromethylation of polystyrene and the hypercrosslinking reaction was performed in a single step.<sup>[82]</sup> However, this method has been extended by a procedure in which chloromethylation and hypercrosslinking processes are performed separately, and similar effects can be achieved compared to the single pot procedure. This technique has an advantage where the precursor polymers can be used as relative intermediates, such as for anion-exchange materials.

Jerabék and co-workers<sup>[83-84]</sup> has used two reaction steps to probe in more detail the formation of bridges resulting from conversion of chloromethyl groups into methylene bridges, by using commercial polymers and imparting varying degrees of hypercrosslinking into gel-type and macroreticular precursors. They found that at the start of hypercrosslinking, more than 72% of the chloromethyl groups were converted rapidly into methylene bridges, and after that residual chloromethyl groups become inaccessible due to the chloromethyl groups being located in sterically hindered positions. Changes to the molar ratio of the catalysts and chloromethyl groups influence the course of the reaction. At low catalyst concentrations, the process of conversion of chloromethyl groups into methylene bridges was also low because the formation of crosslinks was not very effective for the enforcement of the skeleton rigidity. SSA for those particles was shown to be remarkably high, more than 1000 m<sup>2</sup>/g. According the authors, evaluation of surface area based on the monolayer adsorption capacity of hypercrosslinked resins is not quite correct because the porosity of the hypercrosslinked resins arises mainly from micropores. Thus, the sorption proceeds through a pore filling mechanism rather than the formation of an adsorbed layer.

Preparation of macroporous styrene (St)-vinylbenzylchloride (VBC) copolymers has been reported by Guyot *et al.*<sup>[65]</sup> The polymerisations were performed by using a procedure in which macroporous styrene (St)-divinylbenzene (DVB) resins were prepared in the presence of a porogen by suspension polymerisation. The resulting beads were functionalised by grafting a St-VBC copolymer *via* a post-copolymerisation exploiting residual double bonds. Similarly, Sherrington and co-workers<sup>[85]</sup> prepared Davankov-type resins using a gel-type resin and porous resin, incorporating vinylbenzyl chloride (VBC) and divinylbenzene (DVB) into polymer chains using direct terpolymerisation by conventional suspension polymerisation. Then, they extended the procedure, whereby the chloromethyl substituents present in the precursors were used to perform hypercrosslinking reactions in the presence of a Friedel-Crafts catalyst generated 'internal' electrophile.

In this work, they were manipulating Friedel-Craft catalysts ( $\text{FeCl}_3$ ,  $\text{AlCl}_3$  and  $\text{SnCl}_4$ ) and found that  $\text{FeCl}_3$  was by far the most effective catalyst. Also, they reported that intensive microporosity was generated in hypercrosslinked polymers within 15 minutes of initiating the reaction, with high specific surface areas of  $\sim 1200 \text{ m}^2/\text{g}$  being realised for gel-type resins. After 18 hours, the specific surface area approached  $2000 \text{ m}^2/\text{g}$ . For porous resins, a bimodal pore size distribution was found in the resins, with the original macropores of the precursor being joined by micropores that were formed during the hypercrosslinking reaction, thereby allowing facile preparation of such resins with specific surface areas up to  $1200 \text{ m}^2/\text{g}$ .

In the same year, Macintyre *et al.*<sup>[86]</sup> prepared near monodisperse chloromethylated polystyrene precursor microspheres *via* surfactant-free emulsion polymerisation. The microparticles (400 nm in diameter) were essentially non-porous in the dry state ( $\sim 20 \text{ m}^2/\text{g}$ ). However, upon hypercrosslinking, monodisperse, porous hypercrosslinked particles were obtained which showed extremely high specific surface areas up to  $\sim 1200 \text{ m}^2/\text{g}$ . Such particles were able to sorb thermodynamically good and bad solvents such as toluene, *n*-hexane and water, and thus displayed all the characteristics of Davankov-type resins. The authors also reported that the relationship between surface area and VBC content was essentially linear. This

shows that by adjusting the content of VBC in the precursors, the specific surface area of the near monodisperse microparticles can be adjusted up to  $\sim 1300 \text{ m}^2/\text{g}$ . Other research works dealing with poly(styrene-*co*-divinylbenzene-*co*-vinylbenzyl chloride) have also been reported since then.<sup>[74, 87]</sup>

It is possible to control both the specific surface area and the degree of hydrophilicity of hypercrosslinked beads by appropriate choice of the VBC isomer composition used during synthesis of the precursor gel-type resins.<sup>[77]</sup> Fontanals *et al.* prepared two different types of gel-type precursors by using either *p*-vinylbenzyl chloride (*p*-VBC) or a mixture of VBC isomers ( $\sim 70\%$  *m*-;  $\sim 30\%$  *p*-) with 2 wt% of DVB in suspension polymerisation. Both resins showed differences in specific surface area and degree of hydrophilicity in which the specific surface area of the hypercrosslinked resin containing the mixture of isomers was up to  $\sim 2000 \text{ m}^2/\text{g}$  and for *p*-VBC up to  $\sim 900 \text{ m}^2/\text{g}$ .

This new hypercrosslinked polymer (called HXLGp) showed hydrophilic character due to the presence of hydroxyl moieties. The application of the hypercrosslinked polymers as sorbents in the solid-phase extraction (SPE) of polar phenolic compounds was tested. The results showed that the recoveries of analytes were higher for the resins containing *p*-VBC, and such resins then were compared to other commercially available sorbents.<sup>[88]</sup> Other research groups have reported similar types of hypercrosslinked resins, and have evaluated such resins in SPE using polar compounds and also compared them to commercially available sorbents. However, the specific surface area of the resins were lower rather than reported by Fontanals.<sup>[88]</sup>

Research groups from China<sup>[74, 87, 89]</sup> have prepared hypercrosslinked resins with bimodal pore size distributions and controllable microporosity. They found that by changing the concentration of VBC and the porogen type, it was possible to tune the microporosity. These factors have significant influences on specific surface area, average pore size and the total pore volume of the final products.

Conventionally, hypercrosslinked resins have been prepared with hydrophobic character arising from styrene-divinylbenzene in their skeletons. Therefore, particularly for SPE sorbents, they are most effective in the retention of non-polar compounds rather than polar compounds. Thus, in order to overcome such limitations several sorbents that have both high specific surface area and hydrophilicity have been developed.<sup>[88]</sup> Recently, Bratkowska *et al.*<sup>[90]</sup> synthesised new hypercrosslinked polymers with hydroxyl moieties in place to confer hydrophilic character. Such materials were then evaluated as novel sorbents for the retention of polar pollutants using SPE. The precursors were used directly in hypercrosslinking reactions, and were obtained by an optimised precipitation polymerisation involving delayed monomer addition. Then, the hypercrosslinked polymers were obtained by a modified Davankov protocol. They found that the sorbents performed very well, and when compared to commercial materials, their performance was significantly better. The authors also reported that recoveries of analytes in real samples were higher, even for the most polar compounds.

Typically, precursors are prepared by suspension polymerisation, but have a broad particle size distribution. As an alternative, there is an interest in producing the particles in which the particle size lies between emulsion and suspension polymerised particles, e.g., in the low micrometer size range. For this reason, Fontanals *et al.* investigated the hypercrosslinked polymers which were produced from precursor materials which were prepared *via* either a non-aqueous dispersion (NAD) polymerisation or a precipitation polymerisation (PP). In the case of NAD polymerisation, polymers with high specific surface areas ( $>1,600 \text{ m}^2/\text{g}$ ) were produced in yields from 50-77%.<sup>[91]</sup> However, the NAD precursor polymers that were produced were polydisperse and the surfaces of the particles were also rough and contaminated, although such particles were spherical and were in the range low micrometer. In contrast to the NAD particles, the precipitation polymerisation particles were near monodisperse and perfectly spherical. The specific surface areas of the hypercrosslinked variant, were somewhat lower ( $\sim 1300 \text{ m}^2/\text{g}$ ) than the NAD particles and were isolated in lower yield as well. Both the NAD particles and the PP particles were able to sorb significant levels of both hydrocarbon solvents and water.

This proves that those materials exhibited the characteristics of hypercrosslinked resins. Besides this point, the authors tested the PP resins, and variant, thereof, in SPE applications, for example as anion-exchangers for the pH-tuneable, selective extraction of analytes from complex environmental samples.<sup>[88-89]</sup> They found that satisfactory analyte recoveries and clean chromatogram profiles were obtained.

Ordinarily, hypercrosslinked resins are in bead form, however, they can also be found in other forms, such as in monolith and fiber. Urban *et al.*<sup>[92]</sup> reported the preparation of hypercrosslinked porous polymer monoliths. Hypercrosslinked monolith polymers have been prepared from poly(styrene-*co*-vinylbenzyl chloride-*co*-divinylbenzene) precursors *via* Friedal-Crafts catalysed hypercrosslinking reactions. They explored the factors that affect the formation of networks of small pores within the monolith, such as concentration of catalyst and temperature. Even although the specific surface areas were favourable to other polymer-based monoliths (600 m<sup>2</sup>/g), this value is still lower compared to hypercrosslinked beads. Hypercrosslinked polymers in fiber form have also been reported in the literature.<sup>[93]</sup> Compared to the initial fiber, the hypercrosslinked fiber exhibited high specific surface area, but the value (200 m<sup>2</sup>/g) was still low when compared to hypercrosslinked beads.

## 2.9 Functionalised Polymers

Functional polymers are macromolecules to which chemical functional groups are attached, and they can be utilised as reagents, protecting groups, catalysts, *etc.* The attachment of functional groups to polymers is the first step toward the preparation of functional polymers for a specific use. The polymer properties can be modified either by chemical reactions/modifications on pendent functional groups or by changing the physical nature of the polymers, for example their physical form, porosity and solvation behaviour.

The efficiency with which functional groups can be introduced into polymers by chemical reactions is dependent on the nature of the polymer backbone, degree of

crosslinking, pore-volume and pore-size of the polymers, solvation and swelling behaviour and also the hydrophobic-hydrophilic balance in the polymer. Chemical modifications of polymers can be accomplished by using either phase transfer catalysis techniques<sup>[94-95]</sup> or under classical conditions.<sup>[78, 90]</sup>

Functionalised polymers were used as ion-exchange media in the 1930s. However, their systematic use started a few years later after Merrifield's solid-phase peptide synthesis was introduced.<sup>[96]</sup> This was the first step towards the preparation of a functional polymer for a specific application, in wider applications such as in ion-exchangers<sup>[78, 97-98]</sup>, solid-phase peptide synthesis<sup>[99]</sup>, chelating agents<sup>[100]</sup>, solid-phase extraction,<sup>[90, 101]</sup> *etc.* Such polymers possess many attributes which makes them attractive for use in combinatorial as well as automated syntheses. They can be recycled, are cost-effective and environmentally friendly.

Functionalisation of polymers has been demonstrated using polystyrene (PS),<sup>[78]</sup> polytetrafluoroethylene (PTFE),<sup>[102]</sup> poly(ethylene terephthalate) (PET), polyethylene (PE),<sup>[103]</sup> poly( $\alpha$ -hydroxyacids) (PAH), polypyrrole (PP),<sup>[104]</sup> polydimethylsiloxane (PDMS),<sup>[105]</sup> and poly(methyl methacrylate) (PMMA), *inter alia*.<sup>[106]</sup> There are several methods available to functionalise polymer surfaces. These different methods include generating new reactive species on a surface, and the use of functional groups contained in the polymer material. These functional groups can be from residual functionalities unconsumed by the polymerisation procedure, or from functional groups introduced during polymerisation. The use of a functional polymer depends upon the chemical constitution of the polymer and also the physical properties of the polymer, in which the macromolecule can be a linear species or alternatively a crosslinked polymer called a resin.<sup>[107]</sup>

### **2.9.1 Linear polymers**

The use of functionalised linear polymers is growing in interest, particularly when the separation of the polymer from the rest of the components is not necessary or when the polymer must be soluble to permit working in a homogeneous phase for the

polymer to perform its function.<sup>[108]</sup> Soluble polymer substrates are useful for chemical reactions since diffusion control problem are minimised and the reactions can be carried out under homogeneous conditions. The reactions are also not influenced significantly by the polymer backbone size and can proceed to high conversion because the accessibility of functional groups is equal. Besides, the characterisation of polymer is facile.

Despite having the many advantages mentioned above, in some applications the use of linear, soluble polymers may give rise to some disadvantages such as difficulty in separation of the polymers from low molar mass species. Even though ultrafiltration or precipitation can be used to separate them, the recovery of the polymers by these methods may not be easy nor quantitative. Another problem that can arise with the use of linear polymers is gel formation.

### **2.9.2 Crosslinked Polymers**

Crosslinked polymers offer many advantages over linear polymers in terms of properties depending upon the degree of crosslinker present in the system and the method of preparation. In addition, they can be characterised in terms of specific surface area, average pore diameter and total pore volume. The solubility, extent of swelling, pore size, mechanical stability and specific surface area for such polymers are determined to a significant extent by their degree of crosslinking.

Since crosslinked polymers are insoluble in all solvents, they provide ease of processing. They can be prepared in a spherical form which does not coalesce when placed in a suspending solvent. Thus, they can be easily separated from low molar mass contaminants by simple filtration and can be washed with various solvents. Polymers in a bead form that have a low degree of crosslinking can swell extensively and thereby expose their reactive groups to the soluble reagents. In contrast, polymers beads with higher crosslinker content may be prepared with very porous structures. This allows the solvents and reagents to penetrate the inside of the beads to contact the reactive groups.

Unfortunately, using crosslinked polymers also offer disadvantages. For example, not all the reagents can penetrate with ease into the crosslinked network, especially larger reagents which may only be able to react at some of the more accessible sites located on the surface of the polymer or within the larger pores. The introduction of functional groups into the polymers beads may also remove some of the original pore volume.

### **2.9.3 Preparation of Functionalised Polymers**

Polystyrene is the polymer most widely used as a carrier of functional groups, although many polymer types, as mentioned before, including both aliphatic and aromatic organics as well as inorganic polymers have been employed as supports. These latter polymers have met with limited success for reasons such as lack of reactivity, unsuitable physical properties of the final polymers, or degradation of the polymer chain. In principle, polystyrene successfully fulfils the major requirement for a solid support, and has many advantages over other polymers such as its compatibility with most organic solvents, which allows easy access of functional groups to the reagent and the solvents, as well as good mechanical and chemical stability. Polystyrene also undergoes facile functionalisation through the aromatic ring by electrophilic aromatic substitution, and the polystyrene is also readily available commercially. Instead of polystyrene, chloromethylated polystyrene is used widely for the chemical modification of polystyrene beads for the preparation of new functionalised polymers, because functional groups can be introduced by either electrophilic aromatic substitution reactions or nucleophilic aliphatic substitution reactions.

Recent developments in polymer technology have led to the development of new ion-exchange resins as well as polymeric adsorbents. Ion-exchange resins are now most commonly based on crosslinked polystyrene, where the crosslinking agent is usually, though not exclusively, divinylbenzene (DVB). The ion-exchange resins can be organised into two types depending on the charge of the counter-ion with which they exchange (anion or cation counter-ion). The preparation of two types of these

resins is quite similar, and consists of two or three stages. Preparation involving two stages starts with the synthesis of the crosslinked copolymer and ends with the addition of functional groups/ion-exchangeable.<sup>[98, 109-110]</sup> Microporous ion-exchangers are often prepared in the three steps: 1) Synthesis of a swellable polymer precursor; 2) Hypercrosslinking of the swellable precursor; 3) Introduction of the functional groups in a third stage.<sup>[78, 101]</sup>

### 2.9.3.1 Functionalised Crosslinked Resins

The early cation-exchange resins were based on phenol-formaldehyde resins which contain polyfunctional ion-exchangers in a single material. This type of material has disadvantages in that its exchange-capacity varies with pH and the ion-exchange groups have different rates of exchange and affinity due to the fact that they consist of different groups in a single material. Therefore, in 1951 Pepper *et al.* introduced a monofunctional cation-exchange resin by sulfonating crosslinked polystyrene to overcome the problems arising in the use of polyfunctional resins.<sup>[110]</sup> They prepared polystyrene-co-divinylbenzene *via* suspension polymerisation, and excess concentrated sulfuric acid was used as a sulfonating agent. They reported that the exchange rate was not a surface phenomenon because it depends upon the particle size of the resins where the rate of sulfonation increases with decreasing particle size as well as decreasing degree of crosslinking.

Cuellar *et al.* probed the effect of crosslinking degree on the sulfonation rate, as well as the proportion of isomers on the cation-exchange capacity.<sup>[98]</sup> In their work, poly(styrene-*co*-DVB) was synthesised with varying DVB content and with two types of commercial DVB. Then, the polymer was treated with hot sulfuric acid to obtain the cation-exchange resins. The authors reported that increasing the DVB content led to a decrease in the rate of sulfonation, as was also reported by Pepper *et al.*<sup>[110]</sup> They also found that not only was sulfonation a surface process, but also that the sulfonating agent penetrated into the polymer interior.

Beside this point, the isomers present in DVB also influence to the sulfonation reaction, such as *para*-isomers present in commercial DVB is non-polar. Therefore, the sulfonating agent would be unable to penetrate into polymer interior, and thus the polymer remains unsulfonated. However, they did not report the specific surface area of the polymer.

Instead of concentrated sulfuric acid as a classical sulfonating agent, other sulfonating agents such as chlorosulfonic acid can also be employed to introduce sulfonic acid groups into crosslinked polymers. Theodoropoulos *et al.*<sup>[111]</sup> has been studied the sulfonation of crosslinked polymers using chlorosulfonic acid. In this study, they reported that sulfone-type crosslink formation occurred during sulfonation at high concentrations of sulfonating agent, and the sulfonated polymer that is prepared has intermediate ion-exchange capacity.

In contrast to cation-exchangers, for anion-exchangers, conventional preparations of anion-exchangers is based upon chloromethylation of crosslinked polystyrene with a reagent such as either chlorodimethylether (CME) or bis-chloromethylether (BCME). Then, the subsequent resin is treated with amines in an amination process to produce anion-exchange resins. However, these reagents have been listed as strong carcinogenic agents. Therefore, a new method for the preparation of anion-exchangers was introduced by Xu *et al.* to overcome this problem.<sup>[112]</sup> In their work, acetyl groups were introduced, rather than chloromethyl groups, by treatment of resin with either acetyl chloride or acetic anhydride in the presence of a Friedel-Crafts catalyst. Then, the acetylated intermediate is treated with ammonia or amines in the presence of a reducing agent and can be readily converted to a strong anion-exchange moiety.

They have also reported that secondary amino-containing resins have very high exchange capacity compared to same type of commercial resins, and that quaternary ammonium resins have medium exchange capacity. Unfortunately, for primary amino-containing resins, they found that the exchange capacity was very low but still high enough for practical use. In terms of water content, which reflects the

hydrophilicity of resins (adsorption), such resins show relatively low water contents compared to those of commercial resins; for strong anion-exchange resin the water content is higher. Even though in this work they successfully synthesised anion-exchange resins, the reducing agent used is not practical because the reducing agent is expensive and somewhat toxic.

### **2.9.3.2 Functionalised Hypercrosslinked Resins**

Hypercrosslinked ion-exchange resins have received great attention because this class of polymer provides many advantages in terms of higher specific surface area, higher chemical and mechanical stability, *etc.* Moreover, hypercrosslinked polymers coupled with ion-exchangers can offer mixed-mode sorbents which have high retentivity as well as selectivity.

Fontanals *et al.*<sup>[78]</sup> successfully modified hypercrosslinked polymer micro-spheres (HXLPPs) with 1,2-ethylenediamine (EDA) and piperazine to produce new hypercrosslinked sorbents with weak anion-exchange capacity (HXLPP-WAX). The performance of these mixed-mode sorbents were successfully evaluated in the solid-phase extraction (SPE) of a range of analytes from chemically complex real water samples. They reported that the performance of such sorbents were superior compared to commercial sorbents. This fact can be ascribed to the high specific surface area presence of ion-exchange groups and the low particle size. These functionalised particles enabled essentially 100% recovery of acidic compounds. In 2010, for the first time, they successfully employed the same sorbents in on-line solid-phase extraction-liquid chromatography (SPE-LC), to achieve automated determination with an effective clean-up.<sup>[79]</sup> In this study, such sorbents were percolated with a large volume of ultrapure, river and effluent sewage water samples and the resins were provided almost 100% recovery of the most acidic compounds studied. Furthermore, they reported clean chromatograms. This proved that ion-exchange interactions enabled the removal of the compounds with weak acidic, neutral and basic properties from the sample matrix.

Pan *et al.* modified commercial hypercrosslinked microporous by using dimethylamine as aminating agent.<sup>[113]</sup> This weak anion-exchange sorbent was capable of adsorbing aromatic acids from aqueous solution, where hydrogen-bonding interactions that arise should be regarded as a paramount contributor to increasing the adsorption capacities of aromatic acids on the modified hypercrosslinked resins. Even though the adsorption capacity of such resins is significant, the authors did not report the selectivity of the resins.

Instead of using WAX, weak cation-exchange (WCX) groups can also be tethered to the sorbent. Bratkowska *et al.* successfully synthesised hypercrosslinked polymer microspheres with weak cation-exchange character.<sup>[90]</sup> They used carboxylic acid moieties derived from the comonomer methacrylic acid as a WCX, and then investigated this new type of sorbent in more detail with respect to an application in an off-line SPE protocol for the selective extraction of basic compounds from complex environmental samples. They reported that this was the first time that hypercrosslinked polymers had been exploited as WCX for the SPE of basic pharmaceuticals. In this study, they found that this new type of sorbent enables essentially quantitative recovery of analytes, plus satisfactory selectivity was achieved. The performance of such a sorbent was then compared to the commercial sorbents. Overall, HXLPP-WCX was better than the commercial ones in terms of selectivity as well as extraction efficiency, and proved to be highly effective for the preconcentration of basic analytes present in the complex environmental water samples.

Instead of ion-exchange sorbents being used in SPE, they were also employed in field of biology. Šálek *et al.* prepared hypercrosslinked polymers coupled with strong cation-exchange (SCX) character for the electrochemical detection of proteins.<sup>[114]</sup> They used dispersion polymerisation with Ober's modified procedure to prepare poly(styrene-*co*-divinylbenzene) microspheres as the precursors and then hypercrosslinked the precursors using a modified Davankov procedure by employing an external electrophile as a crosslinking agent. In this work, they functionalised the hypercrosslinked polymers with H<sub>2</sub>SO<sub>4</sub> as a sulfonating agent to produce strong

cation-exchange sorbents. They claimed that sulfonic acid groups enable immobilisation of biomolecules, and an antibody was tethered to the surface of magnetic microspheres. The system served as the construction of an electrochemical immunosensor for the detection of ovalbumin protein, and such a system offers promising scope for the detection of biomarkers specific to various diseases.

Another research group used hypercrosslinked polymers to deliver the sulfonated particles. They synthesised a precursor *via* free radical suspension polymerisation, and then hypercrosslinked the precursors before modification using strong cation-exchange chemistry by using acetylsulfuric acid as a sulfonating agent.<sup>[115]</sup> The modified resins that were synthesised retained their original microporous structure and spherical morphology, and had sulfonic acid groups as hydrophilic groups and active sites. In this work, the modified resins were employed as sorbents for the removal of toxic metal ions from water. The researchers found that such materials have very good adsorption capacity for metal ions due to the synergic effects of microporous structure and active sites. Moreover, these modified resins could be recycled several times with very low loss of adsorption capacity. However, they did not report on the selectivity of such resins.

## **2.10 Applications of Hypercrosslinked Polymers and Functionalised Hypercrosslinked Polymers**

Hypercrosslinked polymers, as well as their functionalised variants, have a broad range of potential applications in many distinct areas such as solid-phase extraction (SPE), chromatography, catalysis, *etc.* In this PhD study, the performance of such materials will eventually be tested and evaluated in SPE and other areas of application. Presently, these particles are undergoing evaluation as ion-exchange resins in the laboratory of a collaborator.

### 2.10.1 Solid-Phase Extraction (SPE)

Sample preparation is an important step in many analytical procedures, not only to achieve detection limits but also to clean the sample matrix prior to analysis. Sample preparation should be fast, efficient and easily automated. SPE is the most popular sample preparation technique for liquid samples, and this technique has already replaced liquid-liquid extraction (LLE) because LLE requires the use of large quantities of organic solvents. SPE has been used extensively as a way to purify and pre-concentrate desired components from complex matrices, such as environmental and biological samples.

Even though many materials can be used as an SPE sorbent, such as silica-based and carbon-based materials, nevertheless, polymeric sorbents are the most suitable because they have a few extraordinary characteristics, for example chemical stability and a broad range of attractive physico-chemical characteristics. The conventional polymeric sorbents are macroporous PS-DVB which have a hydrophobic structure along with specific surface areas less than 1000 m<sup>2</sup>/g. The hydrophobic character of the sorbent contributes interactions with the analytes, in principle through Van der Waals forces and  $\pi$ - $\pi$  interactions of the aromatic rings. Specific surface areas for such sorbents are one of the primary parameters that control  $\pi$ - $\pi$  interactions with compounds; the higher specific surface area, the larger the number of  $\pi$ - $\pi$  sites available to interact with the compounds. Therefore, increasing the specific surface area can improve the extraction efficiency.

Highly crosslinked macroporous resins with high levels of crosslinking agent (DVB) have been prepared in order to increase the specific surface area as an alternative to conventional polymeric sorbents. Nevertheless, specific surface areas obtained for such materials are only around 800 m<sup>2</sup>/g.<sup>[29]</sup> Therefore, as an alternative, new hypercrosslinked polymers were successfully synthesised in which specific surface areas more than 1000 m<sup>2</sup>/g were obtained.<sup>[68]</sup> Since then, extraction efficiency of polymer sorbents has been improved.

Nowadays, functionalised hypercrosslinked polymers have received great attention as sorbents for SPE, since the modified resins allow more efficient extraction of polar analytes compared to the unmodified resins. The first modified resin used as a sorbent for the extraction of polar compounds was reported in 1995 by Fritz. In this work, the authors synthesised styrenic resins which were functionalised with sulfonic acid groups.<sup>[116]</sup> By introducing polar moieties, polar interactions between the resin and the analytes increased, as well as an increase in the contact with the aqueous solution and also with the analytes. Since then, many functionalised polymers, including functionalised hypercrosslinked polymers, have been reported in the literature. Some studies have shown that hypercrosslinked sorbents provide better recoveries compared to sorbents with lower degrees of crosslinking, due to such materials having greater specific surface areas. Today, some functionalised hypercrosslinked polymers have been commercialised, such as Styrosorb 2 m (910 m<sup>2</sup>/g) and Styrosorb MT-430 (1050 m<sup>2</sup>/g) from Purolite Int. (Pontyclun, UK), as well as HySphere-SH (> 1000m<sup>2</sup>/g) from Spark Holland (Emmen, The Netherlands).<sup>[88]</sup>

### **2.10.2 Method For Solid Phase Extraction (SPE)**

An SPE method usually consists of three to four successive steps, as depicted in Figure 2.15. In the first step the solid sorbent should be conditioned using an appropriate solvent, followed by the same solvent as the sample solvent. This step is paramount, as it enables the wetting of the packing material and the solvation of the functional groups. The next step is the percolation of the sample through the solid sorbent, with the sample volumes used ranging typically from 1 mL to 1 L. The third step (which is optional) is washing of the solid sorbent with an appropriate solvent, having low elution strength, to eliminate matrix components that have been retained by the solid sorbent, without displacing the analytes. The final step is the elution of the analytes of interest by an appropriate solvent, without removing the retained matrix components.

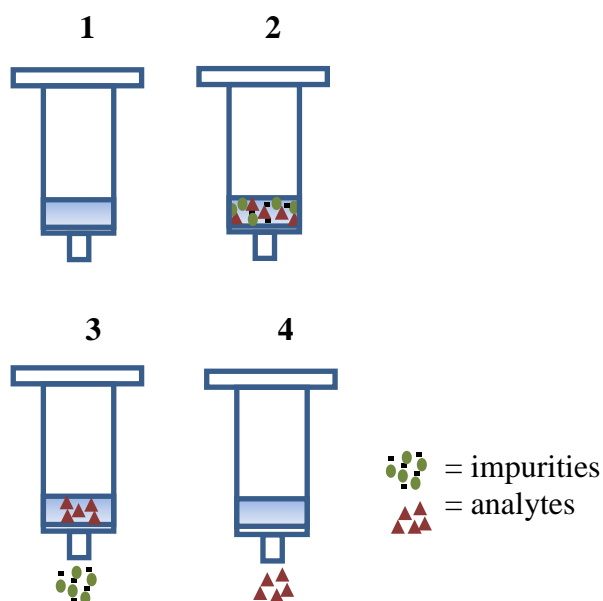


**Figure 2.15: Schematic illustration of sample preparation using SPE.**  
 (1) Conditioning; (2) Loading; (3) Washing; (4) Elution.

## 2.11 Conclusions

Non-aqueous dispersion (NAD) polymerisation is a more attractive route for the synthesis of beaded polymers compared to other techniques such as suspension polymerisation and precipitation polymerisation due to the many advantages offered, for example the beaded polymers can be prepared in the micron-size range, with narrow particle size distributions, and scale up can be very effective in terms of cost. This promising technique was applied in many applications, such as in the medical field, HPLC and SPE. However, there is still lack of publications regarding the preparation of hypercrosslinked polymers using this technique. Therefore, in the current study, NAD polymerisation will be employed in order to prepare swellable precursor polymers.

Distinctly different from conventional styrene-divinylbenzene copolymers, hypercrosslinked polymers are a new generation of microporous polymers which are

obtained from extensive post-crosslinking of polymer chains in a swollen state. Such materials have superior properties, such as extraordinarily high specific surface areas ( $>1000 \text{ m}^2/\text{g}$ ), high micropore contents, high stabilisation in air, water and moisture, their pore structure can be finely tuned, functionality can be introduced into polymers, and it is scalable technology compared to other microporous materials. To date, the preparation of hypercrosslinked polymers using precursor derived from a dispersion polymerisation technique, particularly non-aqueous dispersion (NAD) polymerisation, is still new. However, the materials that can be produced from a combination of both reactions are highly attractive.

## References

- [1] [http://en.wikipedia.org/wiki/Step-growth\\_polymerization](http://en.wikipedia.org/wiki/Step-growth_polymerization) in *Step-growth polymerization*, Vol. **2011**.
- [2] P. J. Flory in *Principles Of Polymer Chemistry*, Vol. Cornell University Press, New York, **1953**.
- [3] F. Limé in *Synthesis and Modification of Monodisperse Polymer Particles for Chromatography*, Phd Umeå University, Sweden, **2008**, p. 45.
- [4] D. C. Sherrington, *Chem. Comm.* **1998**, 2275-2285.
- [5] K.-C. Lee and H.-A. Wi, *J. Appl. Polym. Sci.* **2010**, *115*, 3092-3101.
- [6] S. Kawaguchi and K. Ito, *Adv. Polym. Sci.* **2005**, *175*, 299-328.
- [7] H. Qi, W. Hao, H. Xu, J. Zhang and T. Wang, *Colloid Polym. Sc.* **2009**, *287*, 243-248.
- [8] A. J. Paine, W. Luymes and J. McNulty, *Macromolecules* **1990**, *23*, 3104-3108
- [9] K. E. J. Barret, *Brit. Polym. J.* **1973**, *5*, 259-271.
- [10] C. K. Ober and K. P. Lok, *Macromolecules* **1987**, *20*, 268-273.
- [11] A. I. Cooper, W. P. Hems and A. B. Holmes, *Macromolecules* **1999**, *32*, 2156-2166.
- [12] D. Horák, *J. Polym. Sci: Part A: Polym. Chem.* **1999**, *37*, 3785-3791.
- [13] J. Lee and M. Senna, *Colloid Polym. Sci.* **1995**, *273*, 76-82.
- [14] Z. Xu, *J. Disper. Sci. Techno.* **2000**, *21*, 869-882.
- [15] A. J. Paine, W. Luymes and J. McNulty, *Macromolecules* **1990**, *23*, 3104–3109.
- [16] S. M. Klein, V. N. Manoharan, D. J. Pine and F. F. Lange, *Colloid Polym. Sci.* **2003**, *282*, 7-13.

- [17] C. Li, H. Liang, X. Zhu and X. Z. Kong, *Colloid Polym. Sci.* **2010**, 288, 1571-1580.
- [18] J. S. Song and M. A. Winnik, *Macromolecules* **2005**, 38, 8300-8307.
- [19] J. S. Song, F. Tronc and M. A. Winnik, *Polymer* **2006**, 47, 817-825.
- [20] J. S. Song, L. Chagal and M. A. Winnik, *Macromolecules* **2006**, 39, 5729-5737.
- [21] F. Zhang, Y. Bai, Y. Ma and W. Yang, *J. Colloid Interf. Sci.* **2009**, 334, 334-343.
- [22] J. S. Song, F. Tronc and M. A. Winnik, *J. Am. Chem. Soc.* **2004**, 126, 6562-6563.
- [23] W. Yang, W. Ming, J. Hu, X. Lu and S. Fu, *Colloid Polym. Sci.* **1998**, 276, 655-661.
- [24] J. W. Kim, B. S. Kim and K. D. Suh, *Colloid Polym. Sci.* **2000**, 278, 591-595.
- [25] S. Jiang, E. D. Sudol, V. L. Dimonie and M. S. El-Aasser, *J. Appl. Polym. Sci.* **2008**, 108, 4096-4107.
- [26] S. T. Camli, E. Unsal, A. Tuncel and S. Senel, *J. Appl. Polym. Sci.* **2004**, 92, 3685-3695.
- [27] J. W. Kim, C. H. Lee, J. B. Jun and K. D. Suh, *Colloids and Surfaces A: Physicochem. Eng. Aspects* **2001**, 194, 57-64.
- [28] K. C. Lee and H. A. Wi, *J. Appl. Polym. Sci.* **2010**, 115, 3092-3102.
- [29] O. Okay, *Prog. Polym. Sci.* **2000**, 25, 711-779.
- [30] R. Arshady, *Colloid Polym. Sci.* **1992**, 270, 717-732.
- [31] D. Horák and D. Šponarová, *J. Polym. Sci.* **2008**, 46, 6263-6272.
- [32] X. Zhang, S. Shen and L. Fan, *Polym. Bull.* **2008**, 61, 19-26.
- [33] H. Daniel, *Acta Polym.* **1996**, 47, 20-28.
- [34] D. Wang, V. L. Dimonie, E. D. Sudol and M. S. El-Aasser, *J. Appl. Polym. Sci.* **2002**, 84, 2721-2731.

- [35] M. P. Tsyurupa and V. A. Davankov, *React. Funct. Polym.* **2006**, *66*, 768-778.
- [36] K. Ishizaki, S. Komarnemi and M. Nanko in *Porous Material Process technology and Application* Kluwer Academia publisher, Dordrecht, The Netherlands, **1998**
- [37] N. B. McKeown, P. M. Budd and D. Book, *Macromol. Rapid Comm.* **2007**, *28*, 995-1001.
- [38] A. H. Roy, R. R. Broudy, S. M. Auerbach and W. J. Vining, *The Chemical Educator* **1999**, *4*, 1-14.
- [39] S. A. Johnson, E. S. Brigham, P. J. Ollivier and T. E. Mallouk, *Chem. Mater.* **1997**, *9*, 2448-2457.
- [40] E. Polat, M. Karaca, H. Demir and A. N. Onus, *J. Fruit Orn. Plant Res.* **2004**, *12*, 183-189.
- [41] A. A. El-Barbary in *First Principles Characterisation of Defects in Irradiated Graphitic Materials*, PhD University of Sussex, Brighton, **2005**.
- [42] B. M. Kemal in *Synthesis and Properties of Chemically Modified Carbon Nanotubes*, PhD Durham University, Durham, **2010**.
- [43] F. L. Cking, H. K. Ser, M. Jank and A. Ritter, *Wat. Res.* **1998**, *32*, 2607-2614.
- [44] N. Öztürk and T. E. Köse, *Desalination* **2008**, *223*, 174-179.
- [45] V. Sricharoenchaikul, C. Pechyen, D. Aht-ong and D. Atong, *J. Am. Chem. Soc.* **2008**, *22*, 31-37.
- [46] E. Raymundo-Piñero, K. Kierzek, J. Machnikowski and F. Béguin, *Carbon* **2006**, *44*, 2498-2507.
- [47] J. Pang, X. Li, D. Wang, Z. Wu, V. T. John, Z. Yang and Y. Lu, *Adv. Mater.* **2004**, *16*, 884-886.
- [48] N. B. McKeown, P. M. Budd, K. J. Msayib, B. S. Ghanem, H. J. Kingston, C. E. Tattershall, S. Makhseed, K. J. Rwynolds and D. Fritsch, *Chem. Eur. J.* **2005**, *11*, 2610-2620.
- [49] S. S. Han, W. Q. Deng and W. A. Goddard, *Angew. Chem. Int. Ed.* **2007**, *46*, 6289-6292.

- [50] F. X. L. i. Xamena, O. Casanova, R. G. Tailleux, H. Garcia and A. Corma, *J. Catal.* **2008**, *255*, 220-228.
- [51] W. G. Lu, L. Jiang, X. L. Feng and T. B. Lu, *Inorg. Chem.* **2009**, *48*, 6997-6999.
- [52] <http://www.ngvglobal.com/mofs-new-opportunities-for-gas-storage-for-alternative-propulsion-systems-1010> in *MOFs – New Opportunities for Gas Storage for Alternative Propulsion Systems*, **2011**.
- [53] M. E. Davis, *Nature* **2002**, *417*, 813-821.
- [54] O. M. Yaghi, M. O'Keeffe, N. W. Ockwig, H. K. Chae, M. Eddaoudi and J. Kim, *Nature* **2003**, *432*, 705-714.
- [55] J. L. C. Rowsell and O. M. Yaghi, *Micropor. Mesopor. Mat.* **2004**, *73*, 3-14.
- [56] Z. Bao, L. Yu, Q. Ren, X. Lu and S. Deng, *J. Colloid Interf. Sci.* **2011**, *353*, 549-556.
- [57] E. Haque, J. W. Jun and S. H. Jung, *J. Hazard. Mater.* **2011**, *185*, 507-511.
- [58] L. Feng and S. R. Batten, *Dalton T.* **2010**, *39*, 4485-4488.
- [59] G. Z. Yuan, W. Gen and Y. X. Ping, *Anal. Chem.* **2010**, *82*, 1365-1370.
- [60] B. S. Ghanem, M. Hashem, K. D. M. Harris, K. J. Msayib, M. Xu, P. M. Budd, N. Chaukura, D. Book, S. Tedds, A. Walton and N. B. McKeown, *Macromolecules* **2010**, *43*, 5287-5294.
- [61] A. P. Côté, A. I. Benin, N. W. Ockwig, M. O'Keefe, A. J. Matzger and O. M. Yaghi, *Science* **2005**, *310*, 1166-1170.
- [62] H. M. Elkaderi, J. R. Hunt, J. L. Mendoza-Cortés, A. P. Côté, R. E. Taylor, M. O'Keeffe and O. M. Yaghi, *Science* **2007**, *316*, 268-272.
- [63] H. Furukawa and O. M. Yaghi, *J. Am. Chem. Soc.* **2009**, *131*, 8875-8883.
- [64] K. A. Kun and R. Kunin, *J. Polym. Sci. Pol. Lett.* **1964**, *2*, 587-591.
- [65] A. Guyot, A. Revillon and Q. Yuan, *Polym. Bull.* **1989**, *21*, 577-584.
- [66] B. Gawdzik and J. Osypiuk, *Chromatography* **2001**, *54*, 323-327.

- [67] N. A. Penner, P. N. Nesterenko, M. M. Ilyin, M. P. Tsyurupa and V. A. Davankov, *Chromatographia* **1999**, *50*, 611-619.
- [68] V. A. Davankov, M. M. Llyin, M. P. Tsyurupa, G. I. Timofeeva and L. V. Dubrovina, *Macromolecules* **1996**, *29*, 8398-8402.
- [69] P. M. Budd, E. S. Elabas, B. S. Ghanem, S. Makhseed, N. B. McKeown, K. J. Msayib, C. E. Tattershall and D. Wang, *Ad. Mater.* **2004**, *16*, 456-459.
- [70] N. B. McKeown and P. M. Budd, *Macromolecules* **2010**, *43*, 5163-5176.
- [71] N. B. McKeown, P. M. Budd, B. Gahmen, K. J. Msayib, C. E. Tettershall, K. Mahmood, S. Tan, D. Book, H. W. Langmi and A. Walton, *Angew. Chem. Int. Ed.* **2006**, *45*, 1804-1807.
- [72] N. B. McKeown and P. M. Budd, *Chem. Soc. Rev.* **2006**, *35*, 675-683.
- [73] P. M. Budd, N. B. McKeown and D. Fritsch, *J. Mater. Chem* **2005**, *15*, 1977-1986.
- [74] S. Shen, X. Zhang and L. Fan, *Mater. Lett.* **2008**, *62*, 2392-2394.
- [75] N. Fontanals, R. M. Marcé, P. A. G. Cormack, F. Borrull and D. C. Sherrington, *J. Chromatogr. A* **2008**, *1191*, 118-123.
- [76] M. P. Tsyurupa, Z. K. Blinnikova and V. A. Davankov, *Russ. J. Phys. Chem. A* **2010**, *84*, 1767-1772.
- [77] N. Fontanals, J. Cortés, M. Galià, R. M. Marcé, P. A. G. Cormack, F. Borrull and D. C. Sherrington, *J. Polym. Sc: Part A: Polym. Chem.* **2005**, *43*, 1718-1727.
- [78] N. Fontanals, P. A. G. Cormack and D. C. Sherrington, *J. Chromatogr. A* **2008**, *1215*, 21-28.
- [79] N. Fontanals, P. A. G. Cormack, D. C. Sherrington, R. M. Marcé and F. Borrulla, *J. Chromatogr. A* **2010**, *1217*, 2855-2861.
- [80] A. V. Pastukhov, M. P. Tsyurupa and V. A. Davankov, *J. Polymer. Sci: Part B: Polym. Phys.* **1999**, *37*, 2324-2333.
- [81] J. Hradil and E. Králová, *Polymer* **1998**, *39*, 6041-6047.

- [82] M. P. Tsyurupa, T. A. Mrachkovskaya, L. A. Maslova, G. I. Timofeeva, L. V. Dubrovina, E. F. Titova, V. A. Davankov and V. M. Menshov, *React. Polym.* **1993**, *19*, 55-66.
- [83] P. Veverka and K. Jeřábek, *React. Funct. Polym.* **1999**, *41*, 21-24.
- [84] P. Veverka and K. Jeřábek, *React. Funct. Polym.* **2004**, *59*, 71-78.
- [85] J. H. Ahn, J. E. Jang, C. G. Oh, S. K. Ihm, J. Cortéz and D. C. Sherrington, *Macromolecules* **2006**, *39*, 627-631.
- [86] F. S. Macintyre, D. C. Sherrington and L. Tetley, *Macromolecules* **2006**, *39*, 5381-5383.
- [87] Q. Q. Liu, L. Wang, A. G. Xiao, H. J. Yu and Q. H. Tan, *Eur. Polym. J.* **2008**, *44*, 2516-2521.
- [88] N. Fontanals, M. Galià, P. A. G. Cormack, R. M. Marcé, D. C. Sherrington and F. Borrulla, *J. Chromatogr. A* **2005**, *1075*, 51-56.
- [89] Z. Xie, *Mater. Lett.* **2009**, *63*, 509-510.
- [90] D. Bratkowska, R. M. Marcé, P. A. G. Cormack, D. C. Sherrington, F. Borrulla and N. Fontanals, *J. Chromatogr. A* **2010**, *1217*, 1575-1582.
- [91] N. Fontanals, P. Manesiotis, P. A. G. Cormack and D. C. Sherrington, *Adv. Mater.* **2008**, *20*, 1298-1301.
- [92] J. Urban, F. Svec and J. M. J. Fréchet, *J. Chromatogr. A* **2010**, *1217*, 8212-8221.
- [93] L. D. Guang and Z. Y. Li, *Bull. Chem. Soc. Ethiop* **2007**, *21*, 397-404.
- [94] J. M. J. Fréchet and E. Eichler, *Polym. Bull.* **1982**, *7*, 345-331.
- [95] A. J. Hagen, M. J. Farrall and J. M. J. Fréchet, *Polym. Bull* **1981**, *5*, 111-116.
- [96] R. B. Merrifield, *J. Am. Chem. Soc.* **1963**, *85*, 2145-2150.
- [97] B. Gong, L. Li and J. Zhu, *Anal. Bioanal. Chem.* **2005**, *3825*, 1590-1594.
- [98] C. A. Toro, R. Rodrigo and J. Cuellar, *React. Funct. Polym.* **2008**, *68*, 1325-1336.

- [99] K. C. Wood, S. M. Azarin, W. Arap, R. Pasqualini, R. Langer and P. T. Hammond, *Bioconjugate Chem.* **2008**, *19*, 403-405.
- [100] S. D. Alexandratos, R. Beauvais, J. R. Duke and B. S. Jorgensen, *J. Appl. Polym. Sci.* **1998**, *68*, 1911-1916.
- [101] D. Bratkowska, N. Fontanals, F. Borrull, P. A. G. Cormack, D. C. Sherrington and R. M. Marcé, *J. Chromatogr. A* **2010**, *1217*, 3238-3242.
- [102] E. T. Kang, K. G. Neoh, K. L. Tan, B. C. Senn, P. J. Pigram and J. Liesegang, *Polym. Adv. Technol.* **1997**, *8*, 683-692.
- [103] M. Hong, J. Y. Liu, B. X. Li and Y. S. Li, *Macromolecules* **2011**, *44*, 5659-5665.
- [104] S. C. Wuang, K. G. Neoh, E. T. Kang, D. W. Pack and D. E. Leckban, *J. Mater. Chem.* **2007**, *17*, 3354-3362.
- [105] B. Huang, H. Wu, S. Kim, B. K. Kobilka and R. N. Zare, *Lab Chip* **2006**, *6*, 369-373.
- [106] A. Hirao and A. Matsuo, *Macromolecules* **2003**, *36*, 9742-9751.
- [107] A. Akelah and D. C. Sherrington, *Chem. Rev.* **1981**, *81*, 557-587.
- [108] A. Akelah and A. Moet in *Functionalized Polymers and Their Applications* (Ed. First), Chapman And Hall, London, **1990**.
- [109] P. Akkaramongkolporn, T. Ngawhirunpat and P. Opanasopit, *AAPS Pharm. Sci. Tech.* **2009**, *10*, 641-648.
- [110] K. W. Pepper, *J. Appl. Chem.* **1951**, *1*, 124-133.
- [111] A. G. Theodoropoulos, V. T. Tsakalos and G. N. Valkanas, *Polymer* **1992**, *34*, 3905-3909.
- [112] H. Xu and X. Hu, *React. Funct. Polym.* **1999**, *42*, 235-242.
- [113] B. C. Pan, Y. Xiong, A. M. Li, J. L. Chen, Q. X. Zhang and X. Y. Jin, *React. Funct. Polym.* **2002**, *53*, 63-72.
- [114] P. Šálek, L. Korecká, D. Horák, E. Petrovský, J. Kovářová, R. Metelka, M. Čadková and Z. Bílková, *J. Mater. Chem.* **2011**, *21*, 14783-14792.

[115] B. Li, F. Su, H. K. Luo, L. Liang and B. Tan, *Microporous Mesoporous Mater.* **2011**, *138*, 214-221.

[116] J. S. Fritz, P. J. Dumont and L. W. Schmidt, *J. Chromatogr. A* **1995**, *691*, 133-140.

[117] J. M. Cowie, *Polymers: Chemistry and Physics of Modern Materials*, Taylor & Francis Group, Florida, **2008**.

## ***CHAPTER THREE***

**3.0 Summary**

Dispersion polymerisation of styrene-EGDMA-VBC was investigated using ethanol as a dispersion medium, AIBN as an initiator, poly(*N*-vinylpyrrolidone) (PVP) as a stabiliser and ethylene glycol dimethacrylate (EGDMA) as a crosslinker. The effects of polymerisation parameters, such as the delayed addition technique, ethanol/toluene ratio in the polymerisation medium, monomer concentration, amount of initiator, types of stirrers as well as stirring during the nucleation stage and crosslinker concentration on the resulting particles' shape and size distribution were studied. All the polymerisation parameters were found to influence the final particles. Poly(St-*co*-VBC-*co*-EGDMA) with narrow particle size distributions, and spherical shape were prepared successfully in high yield in ethanol as polymerisation medium at moderate monomer and initiator concentration and low concentration of crosslinker, by using a four-blade, PTFE stirrer.

**3.1 Introduction to Dispersion Polymerisation**

Dispersion polymerisation is effectively a modified precipitation polymerisation in which flocculation is prevented by the addition of a stabiliser, and the initial solution formed is homogenous and contains monomers, stabiliser and initiator. Monodisperse, micron-sized polymer particles that are obtained from this technique are attractive materials, and have found many applications in areas such as bioseparation,<sup>[1]</sup> solid-phase extraction (SPE),<sup>[2-3]</sup> high performance liquid chromatography (HPLC),<sup>[4]</sup> as well as photonic crystal templating.<sup>[5]</sup> Also, they can be used as the precursors for post-polymerisation chemical modification reactions.

**3.2 Aim of Work**

The aims of the work were, in the first instance, to synthesise swellable, lightly crosslinked polymers by non-aqueous dispersion (NAD) polymerisation *via* a 'two-

stage' methodology. Dispersion polymerisation encounters serious problems when functional groups or crosslinking agents are employed since the method is highly sensitive to small changes in the reaction parameters involved in the course of polymerisation. This may result in broad particle size distributions or gross changes to the final particle size. Winnik and co-workers<sup>[6-9]</sup> introduced a 'two-stage' methodology to overcome this problem. In this method, a delayed addition of second monomer was performed in a reaction flask after the end of the nucleation stage of reaction. The advantage of using this method is that the nuclei formed in the nucleation stage are not affected by the second monomer. Thus, the particles can retain their spherical form and fall in the micron-sized range with narrow particle size distributions. In this study, an attempt was made to obtain monodisperse, micron-sized particles by incorporating vinylbenzyl chloride (VBC) and ethylene glycol dimethacrylate (EGDMA) as a co-monomer and a third-monomer, respectively, using a 'two-stage' methodology. Then, as a comparison to this method, one-stage polymerisation was also carried out.

Variants types/designs of stirrers were also investigated to ascertain the influence on the final particles in terms of particle morphology and size distribution. The effect of the type of stirrer on dispersion polymerisation is rarely reported elsewhere.

A systematic study has been carried out to probe how particle morphology is affected by solvent composition. For a typical dispersion polymerisation, the polymerisation medium that is chosen has simultaneously to be a good solvent for the given monomer but a non-solvent for the polymer formed. The solvent is especially important in dispersion polymerisation because it has an influence upon the final properties of the dispersion, such as the average particle size, morphology and particle size distribution.<sup>[10-11]</sup> Generally speaking, any change in the system which tends to enhance the solubility of the polymer tends to increase the bead size of the final product. Therefore, in this study, ethanol and an ethanol/toluene mixture were chosen as a solvent system in order to probe their effect on the final products.

Further investigations focussed on the crosslinker content, with the challenge being focused on increasing the crosslinker levels. In dispersion polymerisation, the presence of crosslinker has a big effect on the final product and, typically, the content of crosslinker that is used in dispersion polymerisation is very low (<2 wt%). Thus, increasing the crosslinker content would be valuable to investigate, particularly with respect to the effect of the EGDMA content on the products obtained by using a ‘two-stage’ methodology.

The polymers have to fulfil in-house requirements such as being micron-sized, nearly monodisperse and in spherical particulate form to allow their exploitation in hypercrosslinking reactions (discussed in chapter 5).

### **3.3 Research Methodology and Preliminary Work**

#### **3.3.1 Materials**

The reagents used for the polymer synthesis were styrene (99% grade) and ethylene glycol dimethacrylate (EGDMA) (98% grade), both supplied by Aldrich (Steinheim, Germany), 4-vinylbenzyl chloride (VBC) (95% grade) and divinylbenzene (DVB) (80% grade) supplied by Fluka (Steinheim, Germany), methanol (99.7% grade), ethanol (95% grade), toluene ( $\geq 99.3\%$  grade), Poly(*N*-vinylpyrrolidone) (PVP) 55 ( $M_w \sim 55,000$ ) and Triton X-305, used as a stabiliser and co-stabiliser, were supplied by Sigma-Aldrich (Steinheim, Germany). All reagents were used as received. The 2,2'-azobisisobutyronitrile (AIBN) (97% grade) used as initiator was supplied by BDH (Poole, UK); it was purified by recrystallisation from methanol at lower temperature.

#### **3.3.2 Equipment**

Polymerisations were performed in a five-necked, round-bottomed flask fitted with a flange, condenser, and overhead stirrer fitted with a PTFE stirrer with four blades. The round-bottomed flask was immersed in a thermostatically-controlled oil bath.

The final products obtained were centrifuged using IEC Centra® CL2 (International Equipment Company).

### **3.3.3 Characterisation**

Polymer characterisation is one of the analytical branches in polymer science and it is used to characterise polymers on a variety of levels. In this chapter, several methods were used to characterise the NAD particles.

### **3.3.4 Optical Microscope**

Optical microscopy (Olympus, Japan) was used in order to visualise the product particles at the end of the reactions. A few drops of polymer dispersion were deposited onto a microscope slide and the particles imaged once the solvent had evaporated.

### **3.3.5 Scanning Electron Microscopy (SEM)**

SEM was carried out using a Cambridge S-90. Micrographs were acquired at an accelerating voltage of 10.0 kV. A thin layer of sample was deposited onto a steel stub, which had been coated previously with conductive (copper), double-sided adhesive tape. Gold coating of the immobilised sample was then carried out. Coated samples were placed inside the SEM chamber and a vacuum was applied; this vacuum evacuated the chamber of any small particles that may have deflected the electrons and affected the SEM image that was obtained.

### **3.3.6 Fourier-Transform Infra-Red Spectroscopy (FTIR)**

All FTIR spectra were recorded on a Perkin-Elmer 1600 series FTIR Spectrometer. The method that was used involved placing polymer beads between two diamond plates in a diamond compression cell. The sample was scanned with a resolution of 4  $\text{cm}^{-1}$ ; an average of 16 scans was taken per sample.

### 3.3.7 Elemental Microanalysis

A small sample of each resin (30 mg) was submitted to the Microanalysis Laboratory at Strathclyde University and C, H and N contents were determined simultaneously using a Perkin Elmer 2400 analyser. The samples were wrapped in tin foil and combusted at 1800 °C in pure oxygen. The combustion products were catalysed and interferences removed before being swept into a detector zone where each element was separated and eluted as CO<sub>2</sub>, H<sub>2</sub>O and NO<sub>2</sub>. The signals were converted to a percentage of the elements.

For Cl analysis, approximately 5 mg of the sample was weighed into ashless filter paper, which was then fastened to a platinum rod. The sample was then combusted in an oxygen-filled flask containing a weak solution of H<sub>2</sub>O<sub>2</sub> (oxygen flask combustion method) and left to sit for 30 minutes. During this time, any halogen present is adsorbed into the solution in the form of halide. After adding 80 mL of ethanol and adjusting the pH to between 1.5 and 2, the resultant solution was titrated with mercuric nitrate solution using diphenylcarbazone as the indicator.

## 3.4 Resin synthesis

### 3.4.1 One-Stage Polymerisations

For one-stage NAD polymerisations, all the monomers, initiator, stabiliser and co-stabiliser were dissolved in ethanol in a 250 mL three-necked, round-bottomed flask equipped with overhead stirrer, condenser and a gas inlet. The solution was bubbled with nitrogen gas for 30 minutes after a homogeneous solution had formed at room temperature. The reaction flask was then placed in an oil bath set at 70 °C, and stirred mechanically using a two bladed metal stirrer at 160 rpm. The reaction was carried out for 24 hours. The particles that were obtained were centrifuged for 10 minutes at 3000 rpm and then washed 2 times in ethanol and 2 times in methanol (the particles were suspended in the appropriate wash solvent and centrifuged between each washing step). The particles then were filtered using vacuum filtration on a 0.22 µm nylon membrane filter and dried overnight in *vacuo* (60 mbar) at 40 °C.

### 3.2 Two-Stage Polymerisation

The synthetic procedure is outlined in Figure 3.1. In detail, for a two-stage NAD polymerisation, all the stabiliser, co-stabiliser, initiator and styrene, half of the VBC and half of the ethanol were added into a 500 mL five-necked, round-bottomed flask fitted with an overhead stirrer, condenser and nitrogen inlet. Once a homogenous solution had formed at room temperature, the solution was bubbled with nitrogen gas at room temperature for 30 minutes. The flask was then placed into an oil bath set at 70 °C, and stirred mechanically using a four bladed PTFE stirrer at 160 rpm. EGDMA and the second half of the VBC were dissolved in the second half of the ethanol at 70 °C under nitrogen. One hour after the start of the polymerisation, the hot solution containing EGDMA and VBC was added into the reaction flask. The reaction was continued for a further 24 hours. The particles that were obtained were centrifuged for 10 minutes at 3000 rpm and then washed 2 times in ethanol and 2 times in methanol (the particles were suspended in the appropriate wash solvent and centrifuged between each washing step). The particles were filtered using vacuum filtration on a 0.22 µm nylon membrane filter and dried overnight in *vacuo* (60 mbar) at 40 °C.

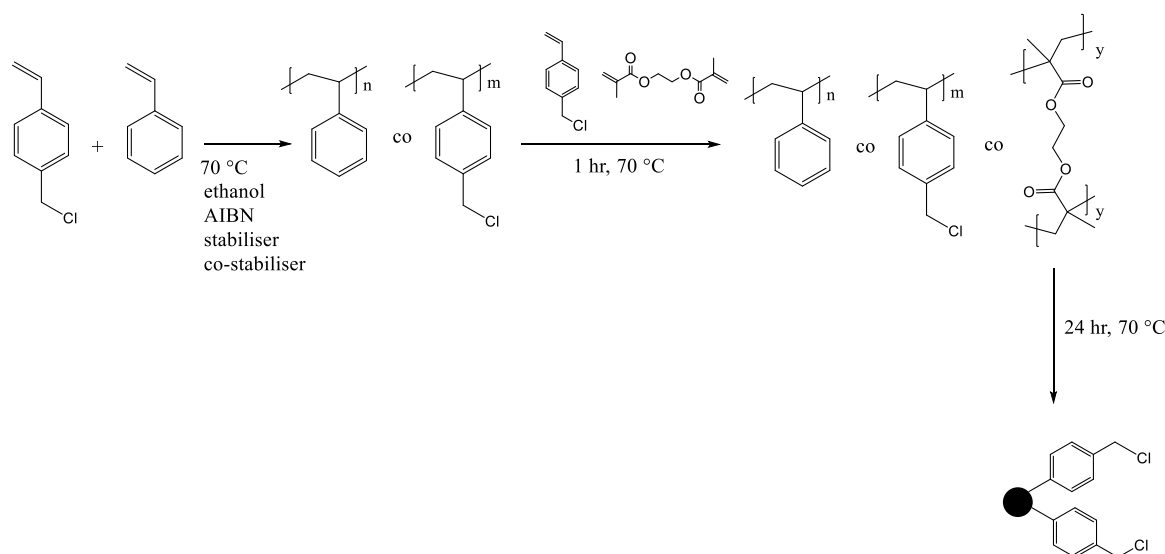


**Figure 3.1: Schematic representation of the synthesis procedures used in the production of a two-stage non-aqueous dispersion (NAD) precursor.**

### 3.5 Results and Discussion

All parameters affected on the final products to be discussed in detail in each section.

#### 3.5.1 One-Stage NAD Polymerisations

In the first instance, one-stage NAD polymerisations were performed to provide practical experience with the polymerisation techniques and to allow a comparison with the two-stage NAD polymerisations, which were performed later. Figure 3.2 shows the SEM images of polystyrene (NA03) and poly(St-co-VBC) (NA05) that were prepared by one-stage NAD polymerisations. The particles obtained were of reasonably good quality.

From Figure 3.2, it can be seen that when VBC was added as a co-monomer at a low level (NA05) there was a narrowing in the particle size distribution (Table 3.1) which emphasises the sensitivity of NAD polymerisation. The yield of NA05 was also higher than the yield of NA03 (Table 3.1). Whilst these experiments were useful and interesting, in order to produce lightly crosslinked polymer precursors with high VBC content, it was necessary to develop an efficient two-stage NAD polymerisation methodology.

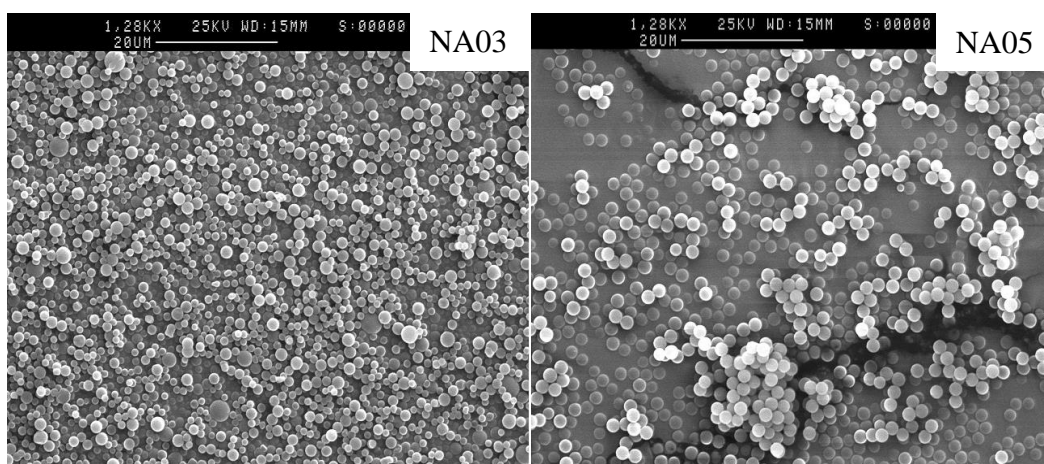


**Figure 3.2: SEM images for polystyrene (NA03) and Poly(St-co-VBC) (NA05) prepared in ethanol by a one-stage NAD polymerisation.**

**Table 3.1: Characterisation data of NAD precursor particles prepared *via* a one-stage NAD polymerisation. [a] Mass of St +VBC=100% total monomer feed in the feed. [b] Calculated from the image analysis in SEM (using Minitab software).**

Sample	Crosslinker	St/VBC ratio <sup>a</sup> (w/w)	Monomer concentration (g/mL)		Stirrer type	Average diameter particle size (μm) <sup>b</sup>	Yield (%)	Remarks
			1 <sup>st</sup> stage	2 <sup>nd</sup> stage				
NA03	No	100/0	0.268	No	Three blade-metal	2.65±1.83	21	Broad particles observed
NA05	No	99/1	0.268	No	Three blade-metal	2.37±0.89	58	Narrow particle size distribution

## 3.5.2 Two-Stage NAD Polymerisations

### 3.5.2.1 FTIR Spectroscopy

Figure 3.3 shows the comparison of FTIR spectra of poly(St-*co*-VBC-*co*-EGDMA) with varying EGDMA contents (Table 3.2). The presence of a band  $1265\text{ cm}^{-1}$  in both spectra can be ascribed to chloromethyl groups derived from VBC residues. As expected, signals arising from the ester groups of EGDMA residues was present at  $\sim 1730\text{ cm}^{-1}$ , and the intensity of this signal was increased as the EGDMA concentration in the feed increased from 1 wt% to 6 wt%. This indicates that EGDMA was successfully incorporated into both precursor polymers. Aromatic C-H stretches ascribed to polymerised styrene are present in both spectra.

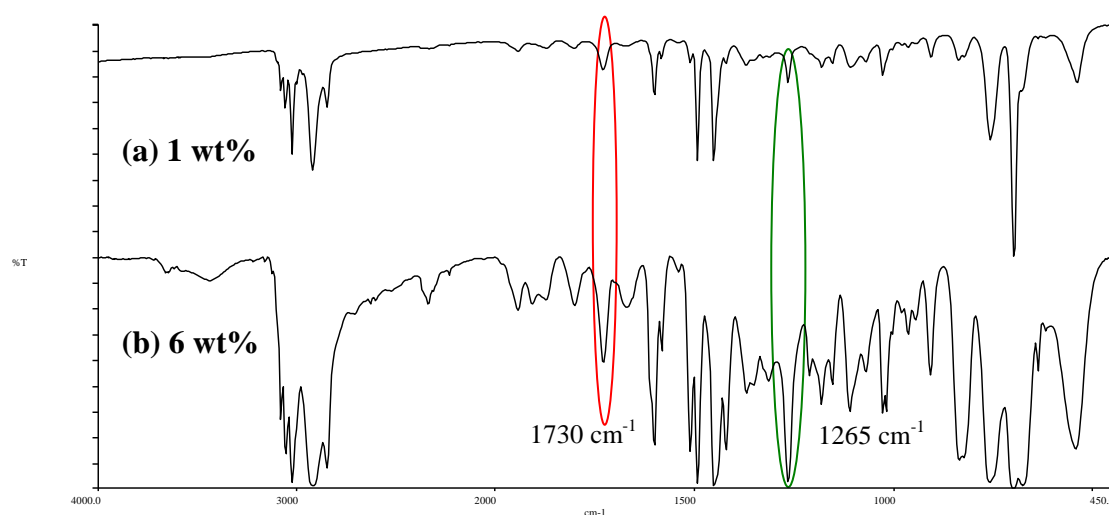


**Figure 3.3:** FTIR spectra of poly(St-*co*-VBC-*co*-EGDMA) with fixed St/VBC feed ratio (50/50 wt%) in total monomer feed, (a) 1 wt% of EGDMA based on monomer feed and (b) 6 wt% of EGDMA based on monomer feed.

**Table 3.2: Characterisation data for precursor particles prepared with varying EGDMA contents in a two-stage NAD polymerisation in ethanol. [a] Mass of St +VBC=100% total monomer feed in the feed. [b] Based on total monomer in the feed.**

Sample	Monomer concentration (g/mL)		Stirrer type	St/VBC ratio <sup>a</sup> (%)	Crosslinker <sup>b</sup> (w%)	Yield (%)	Remarks
	1 <sup>st</sup> stage	2 <sup>nd</sup> stage					
JAG27	0.268	0.268	Four blade-PTFE	50/50	1	83	Spherical and nearly monodisperse
NA45	0.268	0.268	Four blade-PTFE	50/50	6	13	Spherical and polydisperse

### 3.5.2.2 Effect of Initial Monomer Concentration

The initial monomer concentration is known to have a major influence on the final particle size.<sup>[12]</sup> Therefore, an effort was made to ascertain a suitable monomer concentration in this study by varying the concentration of monomer. Two-stage NAD copolymerisations of styrene, VBC and DVB/EGDMA were carried out in order to investigate the effect of varying the monomer concentration in the feed. For NA06 (Table 3.3), the reaction mixture became slightly turbid after a few minutes which this proved that a nucleation process occurred, however when delayed monomer addition added into the reaction vessel, the solution remained slightly turbid until the end of reaction. Assuming difference in monomer concentration at the first stage and second stages as well as the monomer concentration was insufficient (low concentration) contributed this result.

When the monomer concentration was identical (0.263 g/mL) in the first and second stages (Table 3.2; JAG09), even though a broad particle size distribution was obtained the particles retained their spherical form (Figure 3.4) and the yield was also satisfactory (Table 3.3). Similarly, very good quality, highly monodisperse particles were obtained in high yield was obtained when the monomer concentration was kept constant at 0.263 g/mL in each stage but with use of a different a type of

stirrer (Table 3.3(JAG20)) (the effect of the type of stirrer will be discussed in the next section).

When the concentration of monomers was changed slightly (Table 3.3), the quality of the final particles also changed (Figure 3.4 (NA13)) and the yield obtained was very low (Table 3.3). Instead, when difference in the monomer concentration is greater in the first and second stages (Table 3.3( NA11)), it also influences the final product in that particles were produced in low yield in a mixture of shapes such as oval and spherical forms (Figure 3.4 (NA11)). This shows that the monomer concentration in both stages is paramount in order to produce good quality particles with a narrow particle size distribution.

Additionally, an attempt was made to investigate the effect of increasing the monomer concentration. According to Tseng *et al.*,<sup>[13]</sup> increasing the monomer concentration affects the nucleation process in many ways. First, oligomers will grow longer before they precipitate when the solvency of the continuous phase increases and the propagation rate of the oligomer chain will increase. Another effect is the adsorption rate of stabiliser or co-stabiliser, which decreases due to the change in solvency of the polymerisation medium. All these factors contribute to an increase in the average nuclei particle size.

However, a contrasting result was obtained in this study when the monomer concentration was increased from 0.263 g/mL to 0.316 g/mL (Table 3.3 (NA170)) in both stages; very small particles with broad particle size distribution were obtained in low yield (Figure 3.4 (NA170)). This could be explained by the fact that the same amount of initiator was used in both experiments and it was expected that similar amounts of radicals were produced during each reaction. At a higher monomer concentration faster propagation rates result, hence more monomer units were added to each free radical prior to termination or chain transfer. Thus, when higher monomer concentration added in the reaction, there no enough amount of radicals for each monomer. Thus, small particles with a broad particle size distribution were obtained in low yield.

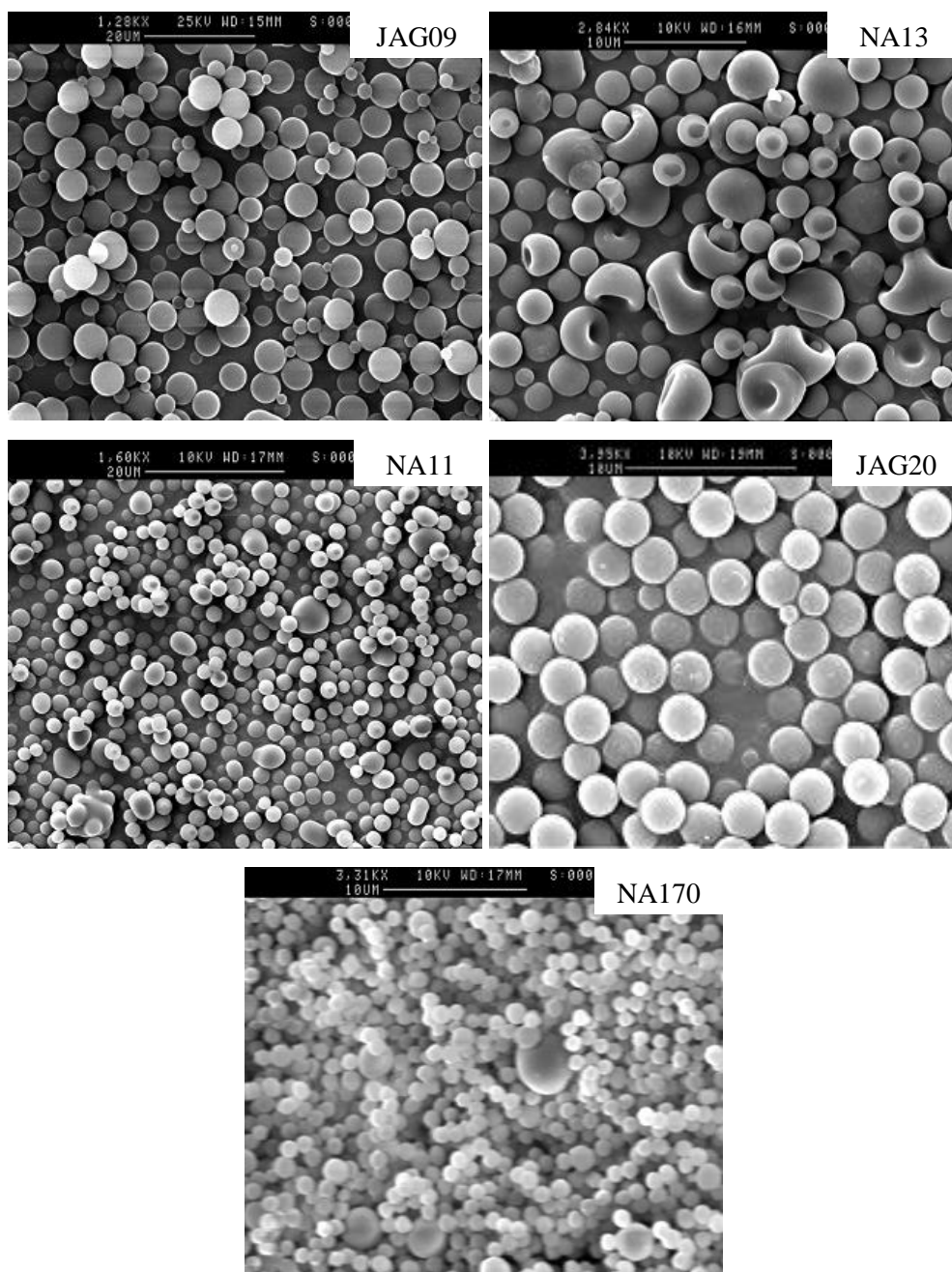


**Figure 3.4: SEM images of poly(St-co-VBC-co-EGDMA) at different monomer concentration in the first stage and second stages, respectively. JAG09 (0.263 g/mL / 0.263 g/mL), NA13 (0.211 g/mL / 0.216 g/mL), NA11 (0.201 g/mL / 6.5 g/mL), JAG20 (0.263 g/mL / 0.263 g/mL) and NA170 (0.316 g/mL / 0.316 g/mL).**

**Table 3.3: Characterisation data of NAD precursor particles prepared *via* a two-stage NAD polymerisation. [a] Mass of St +VBC=100% total monomer feed in the feed. [b] Calculated from the image analysis in SEM (using Minitab software).**

Sample	Crosslinker	St/VBC ratio <sup>a</sup> (w/w)	Monomer concentration (g/mL)		Stirrer type	Average diameter particle size (μm) <sup>b</sup>	Yield (%)	Remarks
			1 <sup>st</sup> stage	2 <sup>nd</sup> stage				
NA06	DVB	25/75	0.008	0.042	Three blade-metal	N/A	N/A	Solution cloudy until the end of reaction
NA09	EGDMA	50/50	0.263	0.263	Three blade-metal	4.49±1.67	77	Smooth particle surfaces Some particles aggregated Small particles observed Broad particle size distribution
NA13	EGDMA	50/50	0.211	0.216	Three blade-metal	2.94±1.18	6	Aggregated particles observed Broad particles size distribution
NA11	EGDMA	75/25	0.201	6.5	Three blade-metal	2.66±0.97	22	Smooth particle surfaces, not spherical Some particles aggregation observed
JAG20	EGDMA	90/10	0.263	0.263	Four blade-PTFE	2.40±0.40	89	Highly monodisperse
NA170	EGDMA	90/10	0.316	0.316	Four blade-PTFE	1.54±0.74	2	Spherical Small particle size

### 3.5.2.3 Effect of Amount of Initiator

Figure 3.5 shows a comparison of SEM micrographs of three poly(St-*co*-EGDMA-*co*-VBC) samples with 1 wt% EGDMA which were prepared in ethanol as a polymerisation medium with different amount of initiator (AIBN). The amounts of the other components and polymerisation conditions were kept the same except for NA162 and NA169 in which the stirring was started only after the second charge of monomer was added into the reaction flask. The initiator plays an important role in the polymerisation, particularly in the nucleation stage has reported elsewhere.<sup>[14-15]</sup> As shown in Figure 3.5, variation in the amount of AIBN from 2 wt% to 6 wt% used in order to produce good quality (spherical), highly monodisperse particles. When the amount of AIBN was increased from 2 wt% to 6 wt%, the quality of the particles significantly improved, particularly for NA162 and NA169.

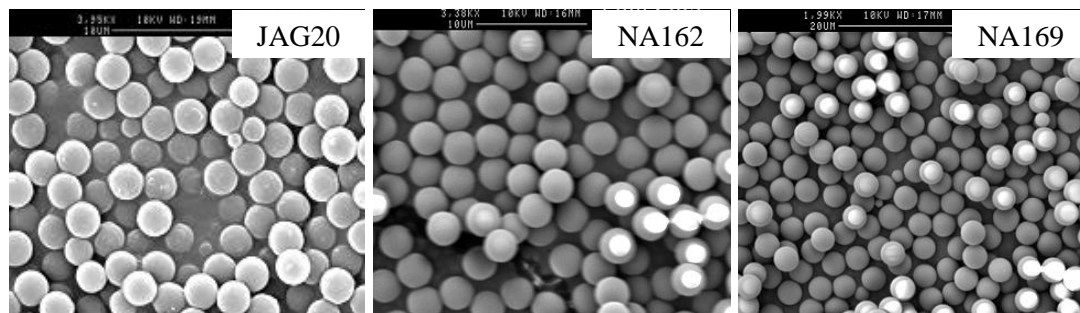


**Figure 3.5: SEM images of poly(St-*co*-EGDMA-*co*-VBC) at different amount of initiator . JAG20 (2 wt%), NA162 (4 wt%) and NA169 (6 wt%)**

Figure 3.6 shows the effect of the variation of amount of initiator from 2 wt% to 6 wt%. As can be seen, the average particle size changes with variation of the amount of AIBN. Increasing the amount of AIBN led to higher average size due to the fact that lower molecular weight polymer chains were formed which were more soluble in the medium. Paine *et al.*<sup>[14]</sup> have reported that larger particles are obtained at higher amount of initiator because lower molecular weight polystyrene was formed, thus making the graft poly(*N*-vinylpyrrolidone) (PVP)-polystyrene (PS) more soluble and less effective as a

stabiliser. Therefore, the adsorption of the grafted stabiliser onto the particles would be retarded, leading to larger particle sizes. Similar trends were observed in this study, where the average particle size increased when the amount of AIBN was increased. This fact could be supported by the assumption that a greater amount of AIBN leads to a greater rate of generation of unstable oligomeric radicals. Hence, it could lead to greater rate of coagulation, resulting in larger but fewer particles.

This fact may result from the role played by the oligomeric free radicals during the nucleation stage in which when the rate of formation of oligomeric radicals is much faster than the stabiliser absorption rate (attributed to the fast decomposition of the initiator). The oligomers would tend to aggregate, and then larger particle nuclei at various size would be formed before enough stabilisers adsorb to stabilise them.<sup>[13]</sup> But, when the amount of AIBN was increased up to 6 wt% (NA169), the particle sizes decreased somewhat. This result can be explained by considering that the stabilisation effect at higher amount of initiator improves; the rate of formation of oligomeric free radicals is slower than the stabiliser absorption rate, and resulting in the formation of smaller particles with broad particle size distributions.

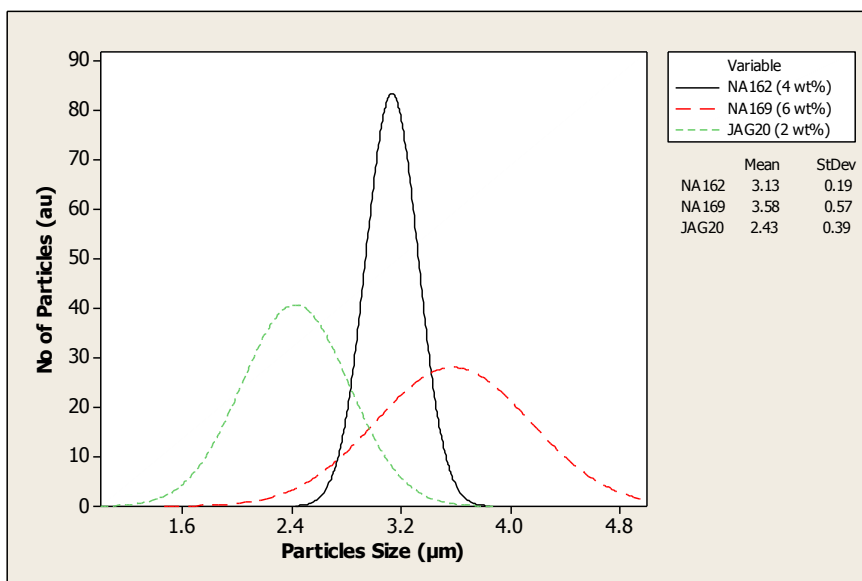


**Figure 3.6: Particle size distribution of Poly(St-co-VBC-co-EGDMA) by non-aqueous dispersion (NAD) polymerisation at different amount of initiator.**

### 3.5.2.4 Effect of Stirrer Type

Figure 3.7 shows the types of stirrers that were used in the NAD reactions for which the ratio of VBC to styrene was fixed at 50/50 (w/w) and 1 wt% of EGDMA was used for each reaction. For NA11, some aggregated particles were obtained in low yield at the end of reaction (Table 3.4) and non-spherical particles were observed (Figure 3.8). Poor results were also obtained when a similar type of stirrer (metal type) was used for NA13; aggregation of particles as well as a very poor yield was the outcome. The reaction mixture also turned yellow in colour after 16 hours due to corrosion of the metal stirrer. However, when the type of stirrer was changed to PTFE (Figure 3.7), discrete particles (JAG27) were obtained in high yield (94%), albeit with a narrow particle size distribution (Table 3.4), some rough particle surfaces and some particle fusion (Figure 3.8). This evidence shows that the stirrer type does influence the final products in NAD polymerisation. In our hands, the PTFE stirrer gave the best results.

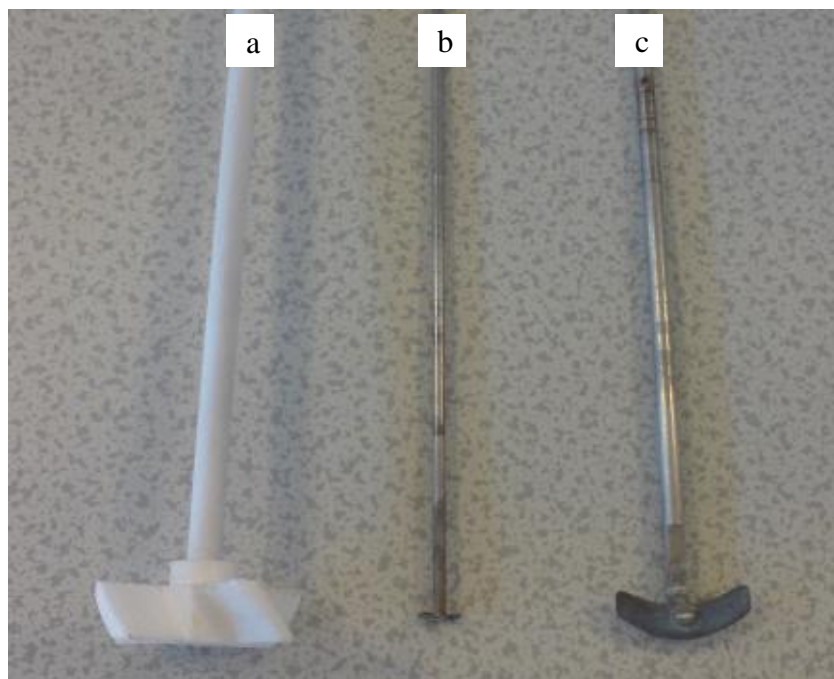


**Figure 3.7: Types of stirrers that used in the production of two-stage NAD precursor particles. [a] Four-blade PTFE type. [b] Two-blade metal type. [c] Three-blade metal type.**

**Table 3.4: Effect of stirrer type on the production of poly(St-co-VBC-co-EGDMA) by a two-stage NAD polymerisation with fixed St/VBC ratio (50/50; w/w) and 1 wt% of EGDMA. [a] Calculated from the image analysis in SEM (using Minitab software).**

Sample	Average particle size ( $\mu\text{m}$ ) <sup>a</sup>	Method	Stirrer type	Yield (%)	Remarks
NA11	2.66±0.97	Two-stage	Two-blade metal type	22	Aggregation
NA13	N/A	Two-stage	Three-blade metal type	6	Aggregation Solution turned yellow in colour
JAG27	3.41±0.57	Two-stage	Four-blade PTFE type	94	Highly monodisperse

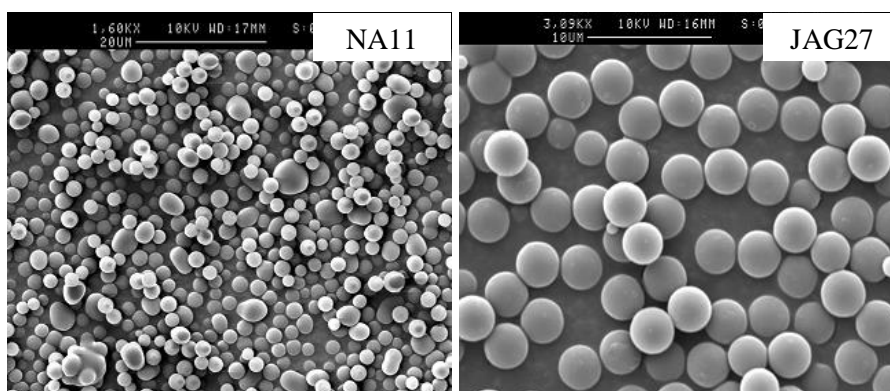


**Figure 3.8: SEM images of poly(St-co-VBC-co-EGDMA) obtained using different types of stirrers, where JAG27= four-blade PTFE type and NA11= two-blade metal type.**

Besides this point, stirring also has an effect on the nucleation stage. From our observation, when without stirring before the second monomer added into the reaction flask, nucleation process occurred around 15 minutes. In contrast, with stirring before the second monomer added into the reaction flask, longer nucleation time can be observed which the nucleation occurred almost half an hour. This fact could be

supported by the assumption that stirring has an influence on the formation of nuclei. The stirring could control the growing of the particles nucleation under diffusion-controlled conditions<sup>[16]</sup> which the growth of nucleation particles were controlled by the shear rate that produced during the stirring process.

In fact, radicals are generated in medium polymerisation and react with the soluble monomers to form the soluble oligomeric radicals before grow further by the addition of the monomer units. This process proceeds until they exceed their solubility limit in the polymerisation medium and then precipitate. However, in a case which stirring started at the beginning of the reaction, the shear rate controlled the radicals from react with the soluble monomers as well as controlling diffusion of the monomers into the nuclei. Thus, longer time occurred in the formation of nucleation particles.

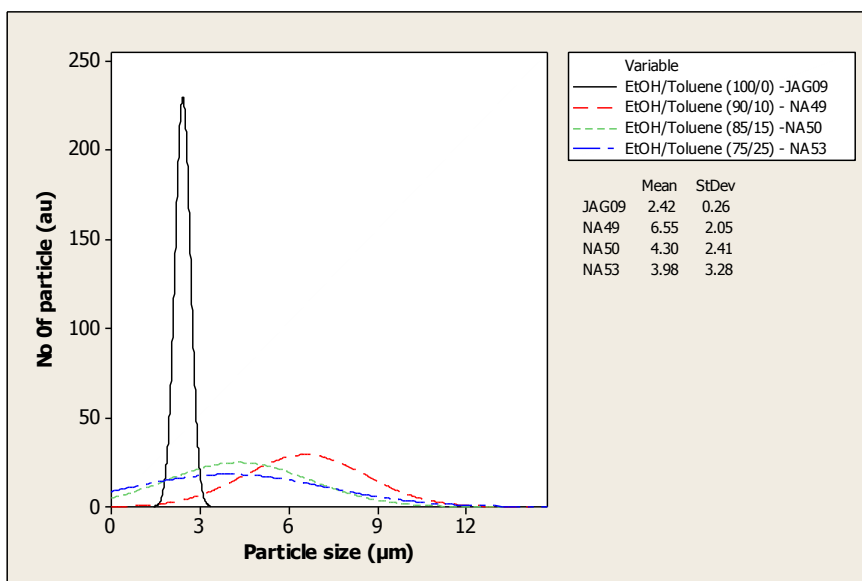
### **3.5.2.5 Effect of Solvent Composition**

The composition of the solvent dispersion media for the polymer is an important consideration for both the polymerisation processes and the final properties of particles (e.g., particle morphology, average particle size and particle size distribution). In this study, ethanol and an ethanol/toluene mixture were chosen as a medium for NAD polymerisations. It is well known that the solubility of monomer strongly depends upon the polarity of dispersion media. Thus, it has a direct effect on the average size and particle size distribution of the final particles. In the present study, the ethanol/toluene volume ratio was varied over a relatively narrow range (75/25, 85/15, 90/10, 100/0) in order to investigate the effect of solvency on average size and particle size distribution of polymer particles.

Figure 3.9 shows the particle size distribution of the poly(*St-co-VBC-co-EGDMA*) particles which were obtained from NAD polymerisations with varying ethanol/toluene volume ratios. Varying the ethanol/toluene volume ratio has significantly changed the average particle size and size range of the poly(*St-co-VBC-co-EGDMA*) particles. The

average particle size increased and then decreased back when the toluene content increased, but with broadening of the particle size distribution (Figure 3.9). This can be explained by an effect of solvent composition on the critical chain length for precipitation of nuclei in the early stage of polymerisation. In other words, better solvency led to longer chain lengths and larger particles, whereas a shorter critical chain length and smaller particles were favored for a thermodynamically bad solvent. Toluene is a thermodynamically good solvent for the polymer formed. When the toluene added in the continuous phase, this leads to an increase in the critical chain length of the oligomers, and delayed precipitation of polymer nuclei which are reduced in number. Thus, the particle nuclei will be less produced and consequently to the big particles formed. Therefore, at the higher toluene amount, more the particle sizes decrease because less the particle nuclei produced, and results bigger the particles formed. Beside this point, during the polymerisation time, network growth may therefore occur by reaction with neighbouring particles alongside longer nucleation stage to appear, resulting in broad particle size distributions.

In ethanol, particles with narrow particle size distribution and average particle size  $2.42 \pm 0.26 \mu\text{m}$  were obtained (Figure 3.9) which is proof that no second generation particles formed during the course of the polymerisation. The key feature of the NAD polymerisation is that the particle nucleation stage is very short (around a few minutes) which ensures a narrow particle size distribution. In this case, the nucleation stage was observed within 15 minutes after the start of the polymerisation and thus could contribute to the successful production of highly monodisperse particles when using ethanol as the polymerisation medium.



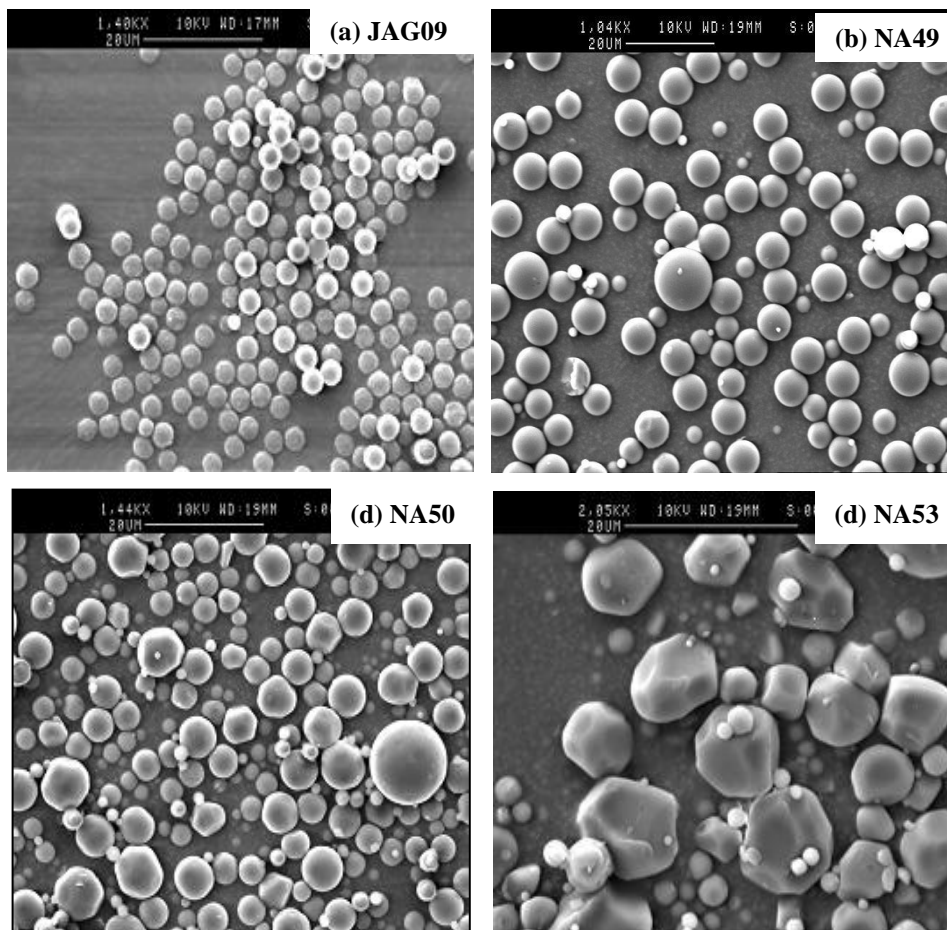
**Figure 3.9: Particle size distribution of Poly(St-co-VBC-co-EGDMA) prepared by non-aqueous dispersion (NAD) polymerisation with different solvent compositions (EtOH/Toluene = 100/0, 90/10, 85/15, 75/25).**

Figure 3.10 shows SEM images of poly(St-co-VBC-co-EGDMA) particles prepared by a two-stage NAD polymerisation at fixed EGDMA content (1 wt%) and St/VBC ratios (25/75). One can see clearly that when the toluene content was increased, many populations of small particles can be observed, which shows that secondary nucleation occurred during polymerisation as the result of this long nucleation stage. Some particle surfaces (Figure 3.10; a-c) are rough and contaminated with small particle deposited on the surfaces of particles.

Particle formation in mixed solvent systems also suffers from poor particle size uniformity. More non-spherical particles appeared when the toluene content was increased. When the toluene content reached up to 25% (v/v), deformation of particles was clearly observed. The particle yield (Table 3.5) also decreased when the toluene content was increased.

However, when the polymerisation takes place in ethanol, the particle quality was very good; the particles retain their uniformity (nearly monodisperse) (Figure 3.10; a) and the

yield obtained was also very satisfactory (97%) (Table 3.5). It is well known that the preparation of monodisperse particles around 5  $\mu\text{m}$  *via* dispersion polymerisation is particularly challenging.



**Figure 3.10: SEM images of poly(St-co-EGDM-co-VBC) particles prepared by a two-stage NAD polymerisation with fixed EGDMA content (1 wt%) and St/VBC feed ratio (25/75) in different ethanol/toluene volume ratios. Ethanol/toluene content (v/v): (a) 100/0 (b) 90/10 (c) 85/15 (d) 75/25.**

**Table 3.5: Characterisation data for precursor particles prepared in a two-stage NAD polymerisation. [a] Mass of St +VBC=100% total monomer feed in the feed. [b] EGDMA contents based on total monomer in the feed.**

Sample	Time (h)	Solvent (v/v)	St/VBC ratio <sup>(a)</sup> (wt%)	EGDMA <sup>b</sup> (wt%)	Yield (%)	Remarks
JAG09	24	EtOH/Toluene (100/0)	25/75	1	97	Nearly monodisperse
NA49	24	EtOH/Toluene (90/10)	25/75	1	86	Aggregation Polydisperse
NA50	24	EtOH/Toluene (75/25)	25/75	1	79	Dents on the particle surfaces Polydisperse
NA53	24	EtOH/Toluene (85/15)	25/75	1	68	Polydisperse  Dents on the particle surfaces Population of small particles observed

### 3.5.2.6 Effect of EGDMA Concentration

In the present work, EGDMA was selected as a crosslinking agent for styrene instead of divinylbenzene (DVB) since EGDMA has a more favourable reactivity ratio for reaction with styrene than DVB ( $r_{st} = 0.4$  and  $r_{EGDMA} = 0.64$  for styrene/EGDMA<sup>[17]</sup> and  $r_{st} = 0.15$  and  $r_{p-DVB} = 1.00$  for styrene/*p*-DVB.<sup>[18]</sup> Beside this point, different reactivity of the two double bonds in DVB also one of the other reasons EGDMA selected in the current study. DVB has four resonances which makes DVB less reactive but more stable, but only two resonances in EGDMA which makes EGDMA more reactive but less stable.

Table 3.6 shows the characterisation data for NAD particles prepared with varying EGDMA contents. When the EGDMA was increased from 1 wt% to 6 wt% and was added into the polymerisation one hour after the start of reaction, the particle size

decreased because at the higher EGDMA content, higher the crosslinked networks formed on the surfaces' particles compared to the particle containing the lower EGDMA content, resulting the monomers and the oligomer radicals difficult to diffuse from solution to the particles and resulted small particle size obtained as well as broad particle size distributions obtained (Figure 3.12).

Figure 3.12 shows the SEM photographs at given EGDMA concentrations based on total monomer weight. The population of small particles can be clearly observed (Figure 3.12; b and c); this suggests that secondary nucleation occurred during the reaction. However, the particles still retained their uniformity (spherical) in spite of the presence of EGDMA, which is a satisfactory outcome. The percentage yield that obtained also was very satisfactory, although for the particles synthesised with 6 wt% of EGDMA the yield was very low because some particles coagulated during the reaction and were lost (Table 3.6).

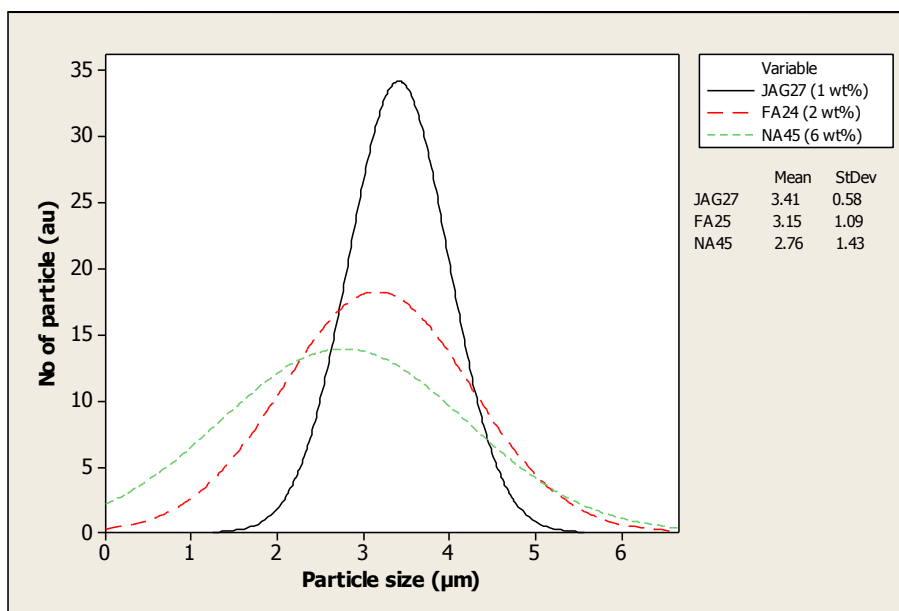


**Figure 3.11: Particle size distribution for poly(St-co-VBC-co-EGDMA) particles produced with varying EGDMA contents and fixed St/VBC feed ratio, (50/50 wt%).**

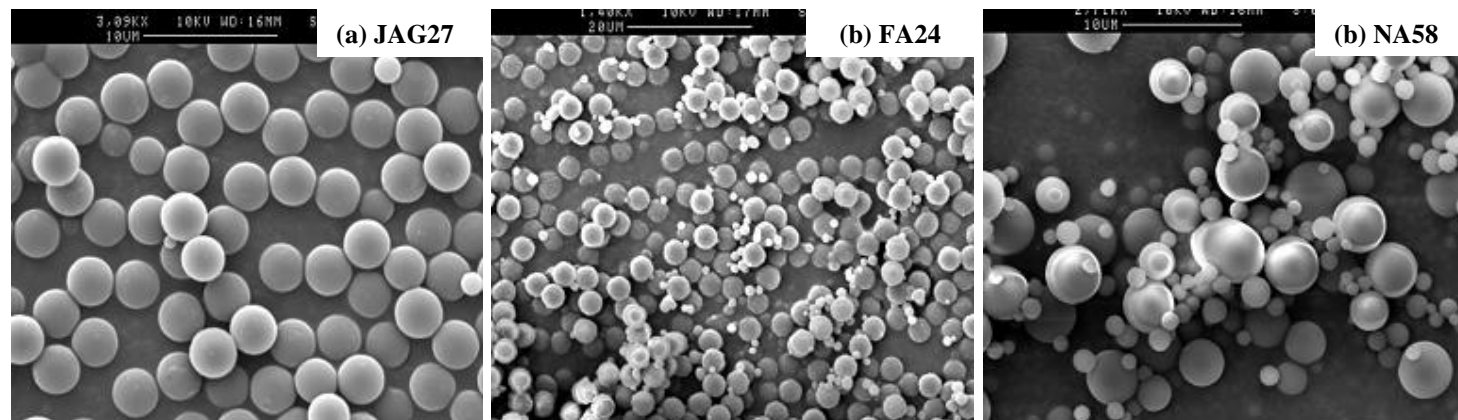


Figure 3.12: SEM images for poly(St-co-EGDMA-co-VBC) particles with fixed St/VBC feed ratio (50/50) (a) 1 wt%, (b) 2 wt% and (c) 6 wt%.

Table 3.6: Characterisation data for precursor particles prepared with varying EGDMA contents in a two-stage NAD polymerisation. [a] Mass of St +VBC=100% total monomer feed in the feed. [b] Based on total monomer in the feed.

Sample	Time (h)	Solvent	St/VBC ratio <sup>a</sup> (%)	Crosslinker <sup>b</sup> (w%)	Yield (%)	Remarks
JAG27	24	EtOH	50/50	1	83	Spherical Nearly monodisperse
FA24	24	EtOH	50/50	2	94	Spherical Nearly monodisperse
NA46	24	EtOH	50/50	5	N/A	Coagulation
NA45	24	EtOH	50/50	6	13	Spherical Polydisperse

### 3.5.2.7 Optimisation

As was discussed previously, the NAD particle size can be controlled by controlling the conditions of polymerisation. An attempt was made to optimise the NAD particle size. In this study, two conditions were chosen in which the monomer concentration and the amount of initiator were the parameters used to tune the particle size. Other conditions, such as solvent system (ethanol), crosslinker concentration (1 wt%), stirrer type (four blade PTFE) as well as constant stirring, kept constant in all the experiments.

The characterisation data of the NAD particles produced is listed in Table 3.7. As can be seen in Table 3.7, increasing the concentration of monomer (from 25 g to 30 g relative to solvent) and amount of initiator (from 2 wt% to 4 wt%) simultaneously, resulted in larger particles (NA171) being produced; the yield of particles was also high, and the quality of the particles was improved (Figure 3.13). This can be explained by the solvency of the medium as well as stabiliser being increased when more monomers were added into the reaction, plus increasing the amount of initiator leads to a lower molecular weight of particles because the numbers of radicals is increased in the polymerisation medium. When both parameters were increased simultaneously, this resulted in the formation of larger particles with narrow particle size distributions (Figure 3.14).

For NA174, the AIBN concentration was increased to 6 wt% while the monomer concentration kept constant, and as expected the particle sizes increased but with broadening of the particle size distribution (Figure 3.14). The broad particle size distribution is probably due to second nucleation occurring during the polymerisation, as can be seen in Figure 3.13 (the quality of the particles is as good as NA171, but a smaller particle population (second generation) also appeared).

When the AIBN amount was kept constant (NA173) but the monomer concentration was increased, the particle size and quality decreased (Figures 3.13 and 3.14) and the yield decreased to 19% (Table 3.7).

**Table 3.7: Characterisation data for precursor particles prepared with varying monomer concentration and amount of initiator in a two-stage NAD polymerisation. [a]  
Based on total monomer feed.**

Sample	AIBN (wt%) <sup>a</sup>	Monomer concentration (g/mL)	Particle size (μm)	Yield (%)
JAG20	2	0.5264	1.49-2.86	89
NA171	4	0.6316	2.91-3.82	89
NA174	6	0.6316	1.64-4.24	85
NA173	6	0.7368	1.83-2.66	19

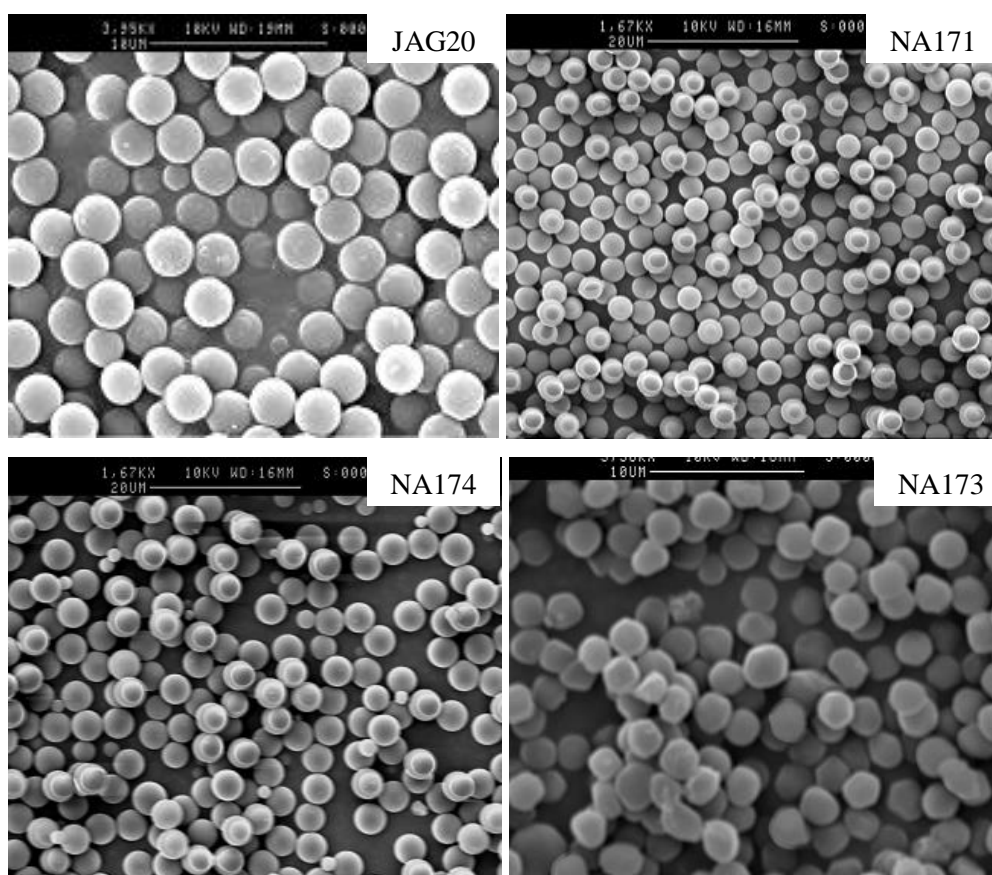


**Figure 3.13: SEM images for poly(St-co-VBC-co-EGDMA) at different monomer concentrations and amount of initiator.**

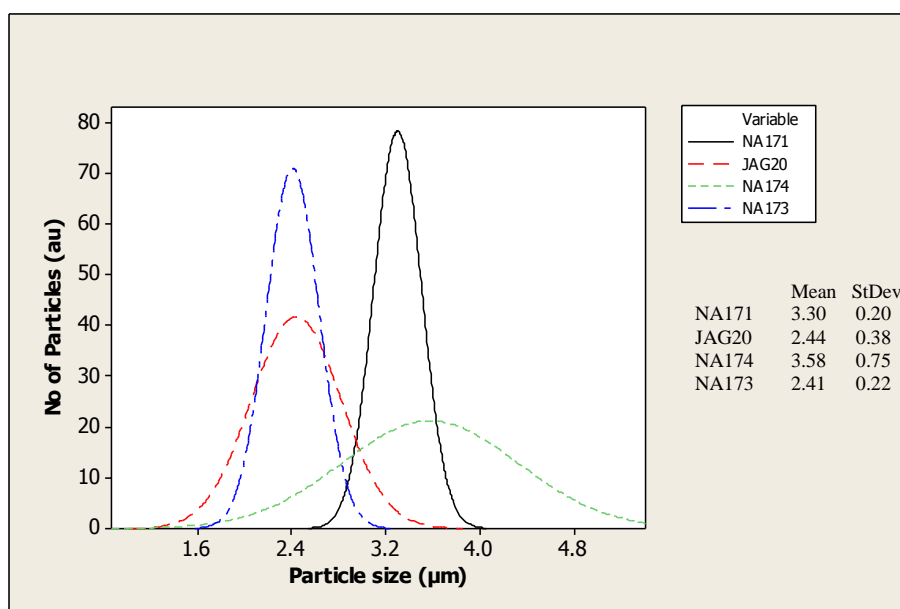


**Figure 3.14: Particle size distribution for poly(St-co-VBC-co-EGDMA) particle prepared with varying monomer concentrations and amount of initiator at fixed St/VBC feed ratio, (10/90 wt%) and EGDMA content (1 wt%).**

### 3.6 Conclusions

The original aim of the work was to synthesise poly(St-co-VBC-co-EGDMA) particles *via* non-aqueous dispersion (NAD) polymerisation in ethanol. The ideal scenario was using a ‘two-stage’ methodology/late addition in order to get monodisperse particles in the micron-sized range. In the present study, lightly crosslinked, nearly monodisperse poly(St-co-EGDMA-co-VBC) particles were prepared successfully by NAD polymerisation in ethanol as a polymerisation medium. The preparation of poly(St-co-VBC-co-EGDMA) was examined by investigating various reaction parameters such as solvent composition, types of stirrer as well as the effect of stirring during the nucleation stage, initial monomer concentration, amount of initiator and degree of crosslinker in polymer. The effect of these parameters was interrelated. Upon varying the various parameters, the morphology of the particles and the particle size distributions were changed as well.

The SEM images obtained for the particles indicated that the polymer particles had uniformity (spherical), smooth surfaces and narrow particle size distributions when synthesised in ethanol ( $2.4 \pm 0.26 \mu\text{m}$ ). However, when the solvent composition was

changed, the particle shape changed and very small particles were obtained. The average particle size was increased when the toluene content was increased but with a broadening of the particle size distribution.

Monomer concentration is one of the key factors that influences the final particles. Slightly different monomer concentration in each stage affected the particles in terms of particle size, particle size distribution and also morphology of the particles.

In contrast, the quality of the particles was improved when the amount of initiator was increased; the average particle size also increased and the particle size distribution narrowed at higher amount of initiator. In contrast, when the EGDMA content was increased the average particle size was decreased, although the particles still retained their spherical form. From FTIR data, EGDMA and VBC were shown to be successful incorporated into the polymers with the signals at  $\sim 1730\text{ cm}^{-1}$  and  $1265\text{ cm}^{-1}$ , respectively, being particularly diagnostic.

When a metal stirrer was changed to a PTFE stirrer, discrete particles were obtained in high yield (94%) with a narrow particle size distribution. Nucleation was also affected by stirring. A longer nucleation period was observed when stirring start at the beginning of the polymerisation.

With optimisation of the conditions of polymerisation, particles in the desired size range were obtained prior to hypercrosslinking reactions. Increasing the monomer concentration and amount of initiator simultaneously resulted in bigger particles (2.91-3.82  $\mu\text{m}$ ). Thus, the particle size could be controlled by controlling the conditions of the polymerisation. Overall, high quality particles with narrow particles size distribution were prepared successfully in ethanol *via* a two-stage NAD polymerisation methodology.

## References

- [1] H. Kawaguchi, *Prog. Polym. Sci.* **2000**, *25*, 1171–1210.
- [2] N. Fontanals, J. Cortés, M. Galià, R. M. Marcé, P. A. G. Cormack, F. Borrull and D. C. Sherrington, *J. Polym. Sci: Part A: Polym. Chem.* **2005**, *43*, 1718-1727.
- [3] N. Fontanals, P. A. G. Cormack and D. C. Sherrington, *J. Chromatogr. A* **2008**, *1215*, 21-28.
- [4] B. Gawdzik and J. Osypiuk, *Chromatography* **2001**, *54*, 594-597.
- [5] S. M. Klein, V. N. Manoharan, D. J. Pine and F. F. Lange, *Colloid Polym. Sci.* **2003**, *282*, 7-13.
- [6] J. S. Song, F. Tronc and M. A. Winnik, *J. Am. Chem. Soc.* **2004**, *126*, 6562-6563.
- [7] J. S. Song and M. A. Winnik, *Macromolecules* **2005**, *38*, 8300-8307.
- [8] J. S. Song, L. Chagal and M. A. Winnik, *Macromolecules* **2006**, *39*, 5729-5737.
- [9] J. S. Song, F. Tronc and M. A. Winnik, *Polymer* **2006**, *47*, 817-825.
- [10] D. Horák and D. Šponarová, *J. Polym. Sci.* **2008**, *46*, 6263-6272.
- [11] X. Zhang, S. Shen and L. Fan, *Polym. Bull.* **2008**, *61*, 19-26.
- [12] F. Zhang, Y. Bai, Y. Ma and W. Yang, *J. Colloid Interf. Sci.* **2009**, *334*, 334-343.
- [13] C. M. Tseng, Y. Y. Lu, M. S. El-Asser and J. W. Vanderhoff, *J. Polym. Sci: Part A: Polym. Chem.* **1986**, *24*, 2996-3008.
- [14] A. J. Paine, W. Luymes and J. McNulty, *Macromolecules* **1990**, *23*, 3104-3109.
- [15] J. Choi, S. Y. Kwak, S. Kang, S. S. Lee, M. Park, S. Lim, J. Kim, C. R. Choe and S. I. Hong, *J. Polym. Sci: Part A: Polym. Chem.* **2002**, *40*, 4368–4377.
- [16] S. Sajjadi, *Macromol. Rapid Comm.* **2004**, *25*, 882-887.

[17] N. Felorzabihi in *Mophorlogy And Interfaces In Polymer Blends Studied By Fluorescence Resonance Energy Transfer (FRET)*, PhD University of Toronto, Toronto, **2010**.

[18] K. C. Lee and H. A. Wi, *J. Appl. Polym. Sci.* **2010**, *115*, 3092-3102.

## ***CHAPTER FOUR***

**4.0 Summary**

Dispersion copolymerisation of styrene-EGDMA-VBC in an alcohol/water medium using a two-stage methodology has been investigated. The influence of parameters such as type of stabiliser, stirring, feeding time for the second addition, two-stage polymerisation versus one-stage polymerisation, effect of styrene added in a second stage, effect of VBC added in first stage, effect of the VBC ratio in each stage, and the crosslinker content on the resulting particles have all been studied. All the parameters were found to influence the nucleation stage as well as the final particles formed. Good quality and nearly monodisperse particles were prepared in this way using PVP as the stabiliser, very low crosslinker content, low VBC content, delayed stirring until the second addition and adding styrene in the first stage.

**4.1 Introduction to Aqueous Dispersion Polymerisation**

An increasing interest in aqueous dispersion polymerisation (ADP) can be related to the possibility of tailoring ADP to specific needs. The production of hydrophilic polymers and copolymers provides many commercial applications, particularly in the pharmaceutical and medical fields. Such polymerisations are quite interesting because heat transfer can be controlled more easily and high molar mass polymers can be produced in beaded form.

**4.2 Aims of this work**

The work's aims were to synthesise swellable, lightly crosslinked polymer resins by aqueous dispersion polymerisation (ADP) *via* a two-stage/delayed addition methodology. ADP was chosen as an alternative to an NAD polymerisation system in an attempt to retain integrity of the lightly crosslinked beads during hypercrosslinking reactions.

A systematic study has been carried out to optimise polymerisation conditions for ADP. In this study, an ethanol and water mixture was chosen (95/5 (v/v)) as a polymerisation medium.<sup>[1]</sup> Several parameters were changed to probe the effects on the final products. Then, the products were used directly in hypercrosslinking reactions to investigate the effects on morphology and quality of particles after hypercrosslinking reactions (to be discussed in the next chapter).

### **4.3 Research Methodology and Preliminary Work**

#### **4.3.1 Materials**

The reagents used for polymer synthesis were styrene (99% grade) and ethylene glycol dimethacrylate (EGDMA) (98% grade) supplied by Aldrich (Steinheim, Germany), 4-vinylbenzyl chloride (VBC) (95% grade) supplied by Fluka (Steinheim, Germany), methanol (99.7% grade), ethanol (95% grade), poly(*N*-vinylpyrrolidone) (PVP) 55 ( $M_w \sim 55,000$ ) and Triton X-305 used as a stabiliser and co-stabiliser, respectively, supplied by Sigma-Aldrich (Steinheim, Germany), poly(acrylic acid) (PAA) ( $M_w$  50,000; 25% aqueous solution) used as a stabiliser was supplied by Polyscience, Inc.. All reagents were used as received. The 2,2'-azobisisobutyronitrile (AIBN) (97% grade) used as initiator was supplied by BDH (Poole, UK). This initiator was purified by recrystallisation from methanol at low temperature.

#### **4.3.2 Equipment**

The polymer syntheses were performed in a five-necked round-bottomed flask fitted with a flange, condenser, and overhead stirrer with a four bladed PTFE stirrer. The reaction flask was immersed into a thermostatically-controlled oil bath. The final products obtained were centrifuged using IEC Centra® CL2 (International Equipment Company).

### **4.3.3 Characterisation**

Polymer characterisation is one of the analytical branches in polymer science and it is used to characterise polymers on a variety of levels. In this chapter, several methods were used to characterise the NAD particles.

#### **4.3.3.1 Optical Microscope**

Optical microscopy (Olympus, Japan) was used in order to visualise the product particles the end of the reactions. A few drops of polymer dispersion were deposited onto a microscope slide and the particles imaged once the solvent had evaporated.

#### **4.3.3.2 Scanning Electron Microscopy (SEM)**

SEM was carried out using a Cambridge S-90. Micrographs were acquired at an accelerating voltage of 10.0 kV. A thin layer of sample was deposited onto a steel stub, which had been coated previously with conductive (copper), double-sided adhesive tape. Gold coating of the immobilised sample was then carried out. Coated samples were placed inside the SEM chamber and a vacuum was applied; this vacuum evacuated the chamber of any small particles that may have deflected the electrons and affected the SEM image that was obtained.

#### **4.3.3.4 Fourier-Transform Infra-Red spectroscopy (FTIR)**

All FTIR spectra were recorded on a Perkin-Elmer 1600 series FTIR Spectrometer. The method that was used involved placing polymer beads between two diamond plates in a diamond compression cell. The sample was scanned with a resolution of 4  $\text{cm}^{-1}$ ; an average of 16 scans was taken per sample.

#### **4.3.3.5 Elemental Microanalysis**

A small sample of each resin (30 mg) was submitted to the Microanalysis Laboratory at Strathclyde University and C, H and N contents were determined simultaneously

using a Perkin Elmer 2400 analyser. The samples were wrapped in tin foil and combusted at 1800 °C in pure oxygen. The combustion products were catalysed and interferences removed before being swept into a detector zone where each element was separated and eluted as CO<sub>2</sub>, H<sub>2</sub>O and NO<sub>2</sub>. The signals were converted to a percentage of the elements.

For Cl analysis, approximately 5 mg of the sample was weighed into ashless filter paper, which was then fastened to a platinum rod. The sample was then combusted in an oxygen-filled flask containing a weak solution of H<sub>2</sub>O<sub>2</sub> (oxygen flask combustion method) and left to sit for 30 minutes. During this time, any halogen present is adsorbed into the solution in the form of halide. After adding 80 mL of ethanol and adjusting the pH to between 1.5 and 2, the resultant solution was titrated with mercuric nitrate solution using diphenylcarbazone as the indicator.

#### **4.4 Resin synthesis**

The synthetic procedure is outlined in Figure 4.1. In detail, for a typical two-stage ADP polymerisation, all of the stabiliser, co-stabiliser, and initiator, styrene and half of the VBC and solvent, were added into a 500 mL five-necked round-bottomed flask fitted with an overhead stirrer, condenser and nitrogen inlet. Once a homogenous solution had formed at room temperature, the solution was bubbled with nitrogen gas at room temperature for 30 minutes. The flask was then placed into an oil bath set at 70 °C and stirred mechanically using a four bladed PTFE-type stirrer at 120 rpm. EGDMA and VBC were dissolved in the second half of the solvent under nitrogen at 70 °C. One and half hours after polymerisation had begun the hot solution containing the EGDMA and VBC was added into reaction flask. The reaction was carried out for 24 hours in total. The particles that were obtained were centrifuged and washed 2 times in ethanol and 2 times in methanol with centrifugation for 10 minutes at 3000 rpm between each washing cycle. The particles were washed again with methanol and then filtered using vacuum filtration on a 0.22 µm nylon membrane filter and dried overnight in *vacuo* (60 mbar) at 40 °C.

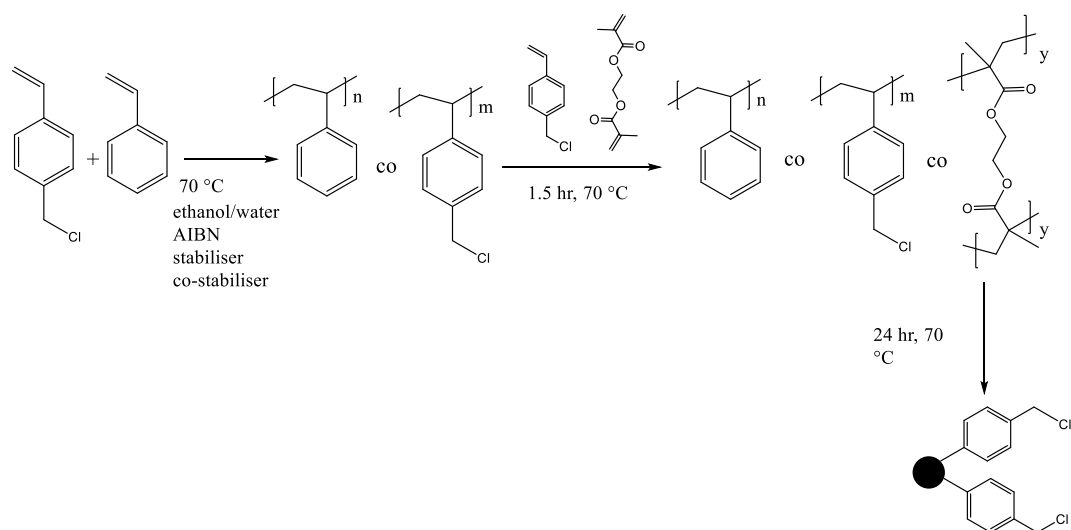


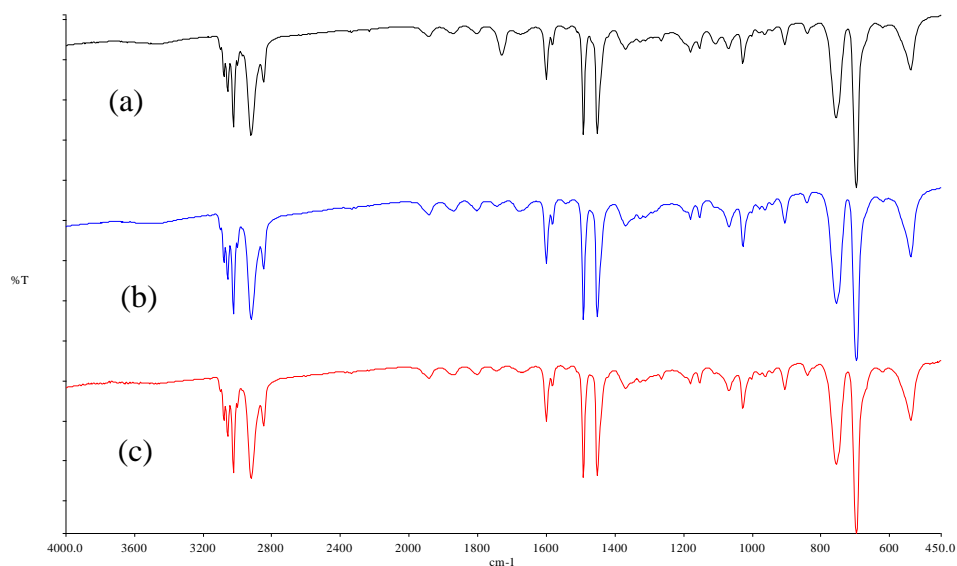
**Figure 4.1: Schematic representation of the synthesis procedures used in the production of aqueous dispersion polymerisation (ADP) precursor particles.**

## 4.5 Results and Discussion

All parameters affected on the final products to be discussed in detail in each section.

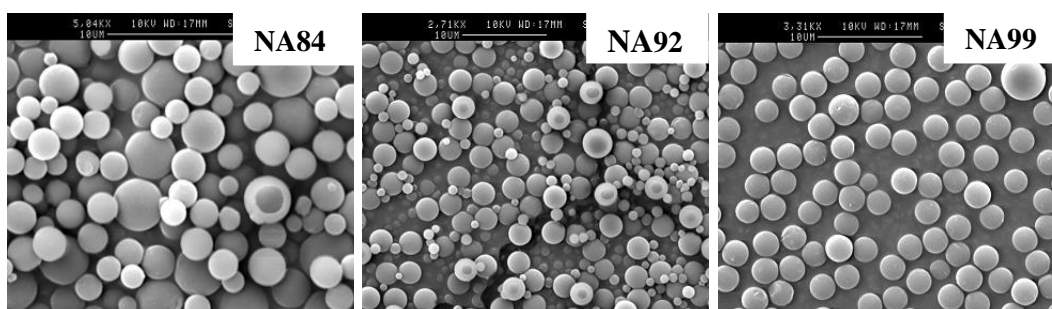
### 4.5.1 Aqueous Dispersion Polymerisation Particle

Figure 4.2 shows the FTIR spectra of: (a) poly(St-co-VBC-co-EGDMA), (b) polystyrene and (c) poly(St-co-VBC). The strong signals at  $700\text{ cm}^{-1}$  and  $750\text{ cm}^{-1}$  in all spectra arise from a *mono*-substituted aromatic ring (*i.e.*, from polystyrene aromatic residues). A low intensity signal at  $1265\text{ cm}^{-1}$  present in spectra (a) and (c) can be ascribed to chloromethyl groups; the low intensity of the signal is consistent with the low level of VBC (5%) used in the feed. A signal arising from the ester groups of EGDMA residues can be seen at  $1730\text{ cm}^{-1}$  in spectrum (a), which confirmed that EGDMA was successfully incorporated into this polymer.



**Figure 4.2:** FTIR spectra of (a) poly(St-co-VBC-co-EGDMA), (b) polystyrene and (c) poly(St-co-VBC).

Figure 4.3 shows the SEM images of the three precursor polymers synthesised *via* ADP. From these images, it can be seen that the quality of the particles is good, even though for NA84 (polystyrene) and NA92 (poly(st-co-VBC)) there is evidence of secondary nucleation. Surprisingly, nearly monodisperse ADP particles of good quality were obtained when EGDMA was added (NA99) in a delayed addition. This showed that EGDMA did not interfere with the particle growth stage.



**Figure 4.3:** SEM images of ADP precursor particles: from left to right, polystyrene (NA84), poly(St-co-VBC) (NA92) with 5% of VBC, and poly(St-co-VBC-co-EGDMA) (NA99) with 0.1 wt% of EGDMA and 5% of VBC, respectively

In addition, a narrower particle size distribution as well as slightly larger particles were obtained when EGDMA was added by delayed addition, compared to the particles synthesised without EGDMA (Figure 4.4). The presence of crosslinker in a

dispersion system normally interferes particle nucleation, however in this case the addition of EGDMA was delayed until the nucleation stage had passed. The yield of the particles that obtained did fall from 99% to 63% when the third monomer (EGDMA) was incorporated into polymer particles (Figure 4.4).

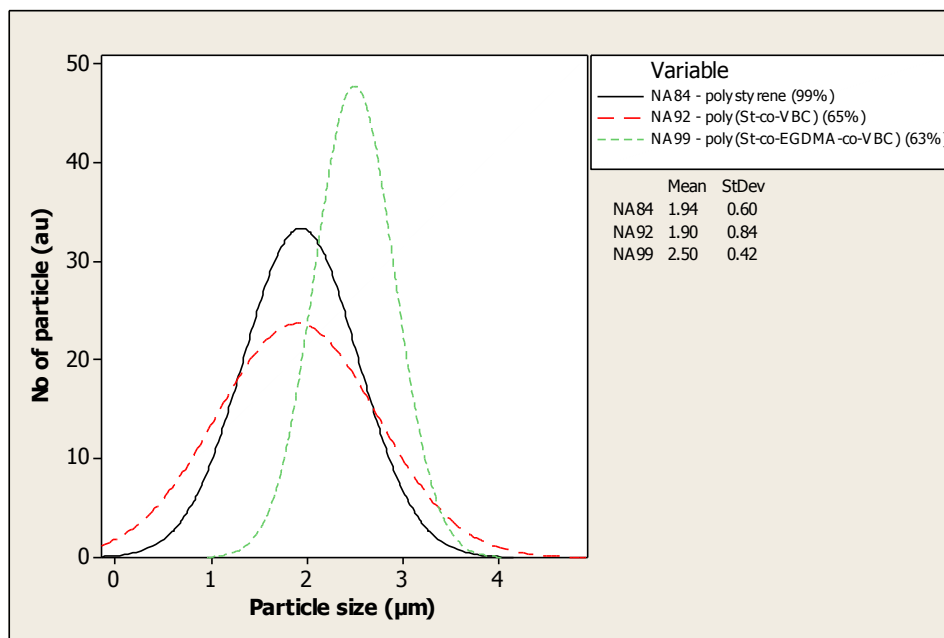


**Figure 4.4: Particle size distribution of various precursor polymers synthesised by aqueous dispersion polymerisation (ADP).**

#### 4.5.2 Effect of Type of Stabiliser

In dispersion polymerisation, the stabiliser used plays a crucial role. In this study, two types of stabilisers were studied poly(*N*-vinylpyrrolidone) (PVP) and poly(acrylic acid) (PAA) because they have been extensively used as stabilisers in dispersion polymerisation,<sup>[2-3]</sup> particularly in aqueous dispersion polymerisation.

In the first instance, linear polymers were synthesised using a 25/75 (w/w) ratio of St/VBC and with PVP as a stabiliser (Figure 4.5 (a)). At the end of the polymerisations no particles could be observed under a microscope. Assuming that this might be because PVP was not able to stabilise the nuclei formed in the nucleation stage or stabilise the particle growth during the growth stage. Therefore, the stabiliser was changed to PAA (Figure 4.5 (b)). PAA is an effective stabiliser and

used frequency in aqueous polymerisation.<sup>[3-5]</sup> Unfortunately, at the end of the polymerisation a similar result to before was obtained; no particles were formed. The results indicated that neither stabiliser was suitable under the conditions tested, therefore an attempt was made to probe further the other parameters which could influence the ADP.

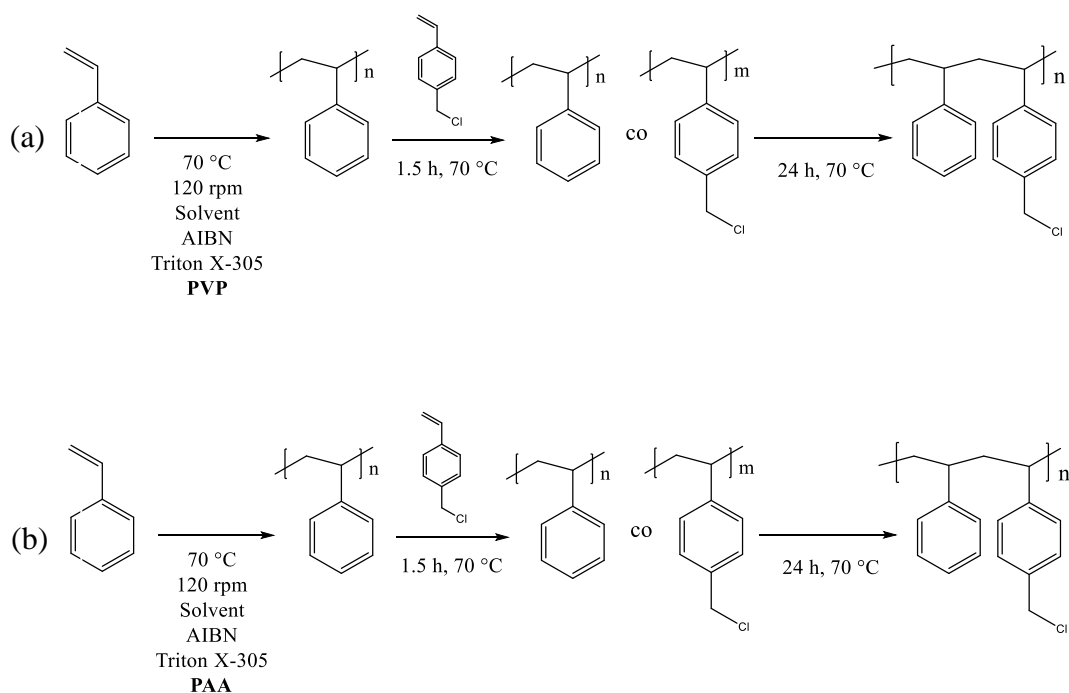


**Figure 4.5: Synthesis of ADP precursors using PVP and PAA as a steric stabiliser in ethanol/water (95/5, v/v).**

### 4.5.3 Nucleation Stage

It is well-known that the presence of water in the polymerisation medium will affect the nucleation process in terms of the partitioning of the components, such as initiator, monomer, solvent, oligomeric radicals and nuclei between the continuous phase and the polymer phase.<sup>[3, 6]</sup> However, to the best of our knowledge, the effect of stirring and the effect of feeding time for a delayed monomer addition on ADP has not been reported in the literature. Thus, a few experiments were carried out to probe these variables.

#### 4.5.4 Effect of Stirring

Given the previous evidence that the stabilisers that had been used in ADP did not influence the outcome of the ADP, a second attempt was made in which non-crosslinked polymers were synthesised, using PVP as stabiliser. In this reaction, a small amount of VBC was added in the first stage and stirring was used from the outset of the reaction, as outlined in Figure 4.6. After 1.5 hours nucleation was still not observed and the reaction was stopped. Surprisingly, 2 hours after the reaction was stopped, particle nucleation was observed in the reaction flask (it was noted that the reaction flask was still warm). Immediately, a delayed monomer added into the reaction flask as well as stirring started, and the polymerisation was carried out for 24 hours in total. Even though the yield of polymer was very poor (14%), good shape and nearly monodisperse particles were successfully produced (Figure 4.7). From this evidence, the stirring have a big influence to nuclei formed as well as to the final product because the shear rate which produced by stirring controlling the radicals from react with the soluble monomers in the solution mixture, and thus diffusion of the monomers into the nuclei was controlled. In other words, shorter time in the formation of the nucleation particles without the stirring, however longer time in the formation of the nucleation particles with the stirring. It shows that ADP has potential to produce monodisperse particles.

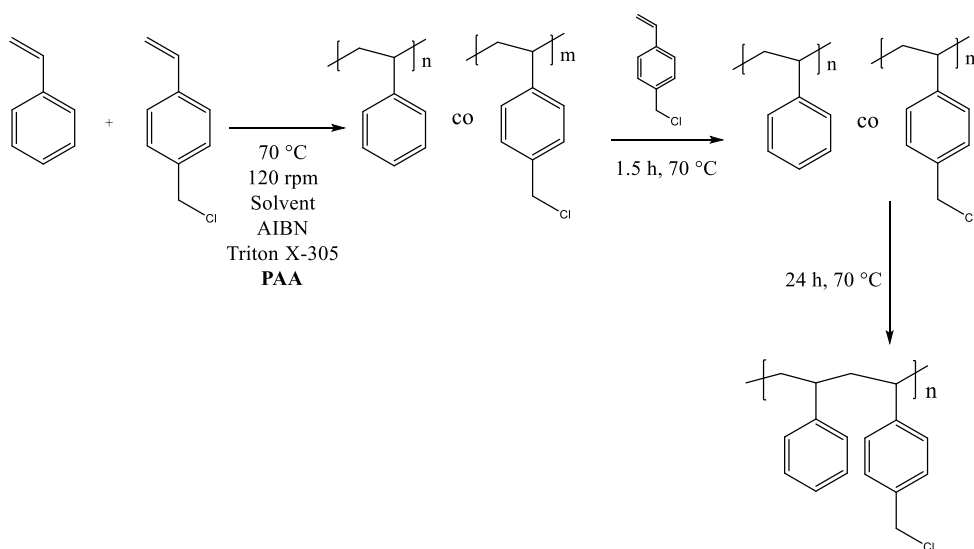


**Figure 4.6:** Synthesis of poly(St-co-VBC) using PVP as a stabiliser in ethanol/water (95/5, v/v) and St/VBC = 95/5 (w/w).

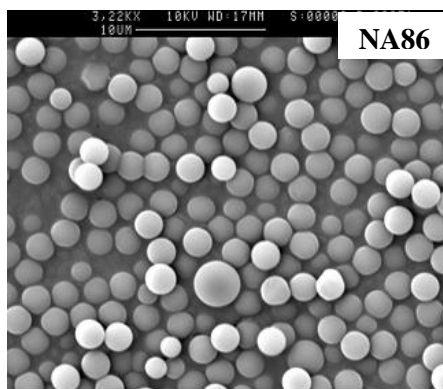


**Figure 4.7: SEM image of poly(St-co-VBC) with a 95/5 (w/w) St/VBC ratio, using PVP as a stabiliser.**

In contrast to NAD polymerisation, the nucleation stage of ADP lasted longer when the system was stirred. Particle nucleation could be observed more than 1 hour after the start of the reaction when stirring. This behaviour is not precisely understood, but in dispersion polymerisation, the nucleation stage is very complex and highly sensitive compared to the particle growth stage. Any changes to the polymerisation conditions can influence the nucleation of particles.

Table 4.1 shows the characterisation data for the crosslinked ADP precursor particles prepared with stirring and without stirring. Three conditions were used to probe the influence of stirring on the nucleation of particles: (1) stirring, (2) absence of stirring, and (3) stirring started after second monomer addition. When the stirring was delayed until after the second monomer addition, the nucleated particles (solution turned to a bit cloudy) could be observed around 4 to 15 minutes after the reaction started. However, when the stirring was applied from the beginning of the ADP reaction, nucleated particles takes longer to appear, but nearly monodisperse particles obtained. In a case without stirring during the course of the polymerisation, even although nucleated particles appeared in shorter and good particles produced successfully, but the second generation generated as can be seen in Figure 4.8. The yield obtained in the polymerisation without stirring higher (95%) than either with stirring started at the beginning of the polymerisation (63%), or stirring after the second delayed monomer added (65%) (Table 4.1).

**Table 4.1: Characterisation data for polymers synthesised during experiments designed to explore the effect of stirring on the ADP. [a] Mass of St +VBC=100% total monomer feed in the feed. [b] EGDMA content based on total monomer in the feed. [c] Average particle diameter  $\pm$  standard deviation (S.D.) calculated from the image analysis in SEM (using Minitab software).**

St/VBC ratio <sup>a</sup>	Sample	EGDMA (wt%) <sup>b</sup>	Stirring during polymerisation	Average particles size ( $\mu\text{m}$ ) <sup>d</sup>	Yield (%)	Remarks
25/75	NA90	No	Started after 2 <sup>nd</sup> addition	N/A	N/A	Nucleation was observed 15 min after the start of reaction 2 <sup>nd</sup> addition was performed 1 h after start of reaction Solution a bit cloudy after 2 <sup>nd</sup> addition
	NA92	No	Yes	1.90 $\pm$ 0.84	65	No nucleation was observed 1 hour after start of reaction Stirring was stopped and nucleation was observed 2 <sup>nd</sup> addition performed after 1.5 h after start of reaction Stirring start after 2 <sup>nd</sup> addition added
90/10	NA98	0.1	No	N/A	N/A	Nucleation stage was observed 15 min after start of reaction 2 <sup>nd</sup> addition performed 1 h after start of reaction Particles coagulated
95/05	NA94	No	NO	2.25 $\pm$ 0.98	79	Broad particle size distribution 2nd addition performed 1.5 h after start of the reaction
	NA99	0.1	Start after 2nd addition	2.50 $\pm$ 0.42	63	Nucleation stage was observed 15 min after start of the reaction Nearly monodisperse 2nd addition performed 1.5 h after start of the reaction
	NA100	0.1	No	3.05 $\pm$ 0.30	94	Nearly monodisperse 2nd addition performed 1.5 h after of reaction

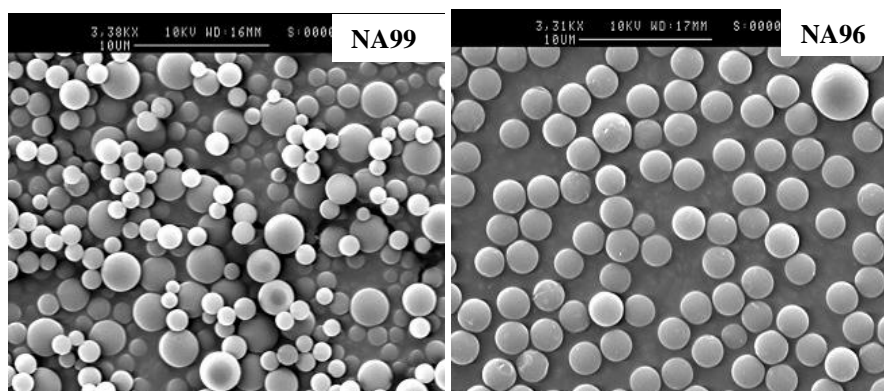


**Figure 4.8 : SEM images of ADP precursor particles, illustrating the effect of stirring. No stirring during polymerisation (NA96), and stirring started after second monomer addition (NA99).**

#### **4.5.5 Effect of Feeding Time for Second (Delayed) Monomer Addition**

The feeding time for a second (delayed) addition of monomer into the reaction flask can also influence the products formed. From a microscopy image (Figure 4.9) which the sample was taken from the solution mixture before the second addition added into the reaction, it can be seen small beads (some in spherical and another beads are not in good shape). Although the nucleated particles appeared within 1 hour after the reaction started, however, at this time the nucleation particles still not stable. Therefore, the presence of the second monomer/crosslinker within this period could be interferes the nucleation particles. From an observation, when the second addition occurred 1 hour after polymerisation had begun, no particles were observed under the microscope and the solution stayed cloudy until the end of the reaction (Table 4.2; NA89). This evidence shows that the monomers added in the second stage interfered with the nucleation particles.

Similar outcomes with NA98 (Table 4.2) were obtained when the second addition took place within 1 hour after polymerisation had begun; coagulated particles were obtained. This evidence shows that the nucleation of particles is highly sensitive process and that the nucleated particles are not sufficiently stable after one hour. Within this period, assuming that the nucleation stage is not complete, and that the number of particles is

not constant<sup>[7]</sup> any monomer addition within this time will disturb the nucleation particles.

When the delay addition (of EGDMA) took place after 1.5 hours, good quality, nearly monodisperse particles were obtained in satisfactory yield (Table 4.2; Figure 4.10: NA99 and NA100). This suggests that after 1.5 hours, the nucleated particles are stable enough to accommodate the addition of new monomer (i.e. a perturbation to the system). Therefore, addition of monomer after this time does not interfere with the particle growth. After the delayed addition, the reaction medium turns from cloudy to milky within a few minutes, and stays retain milky until the end of the reaction.

When no EGDMA was present, a broad particle size distribution was obtained (Figure 4.10: NA92 and NA94) and second generation particles were clearly generated during polymerisation. However, spherical particles can still be seen. Surprisingly, no secondary particles were generated in the cases NA99 and NA100 (Figure 4.10) when EGDMA was added to the reaction vessel 1.5 hours after the start of the reaction.

Satisfactory yields were obtained in every case, with a very good yield being recorded for NA100 (94%). The greatest average particle size recorded was around 3  $\mu\text{m}$ , which was recorded for the very same particles (Table 4.2).

**Table 4.2: Characterisation data for polymers synthesised during experiments designed to explore the effect of feeding time. [a] Mass of St +VBC=100% total monomer feed in the feed. [b] EGDMA content based on total monomer in the feed. [c] Average particle diameter  $\pm$  standard deviation (S.D.) calculated from the image analysis in SEM (using Minitab software).**

St/VBC ratio <sup>a</sup>	Sample	EGDMA (wt%) <sup>b</sup>	Stirring during polymerisation	Average particles size ( $\mu\text{m}$ ) <sup>c</sup>	Yield (%)	Remarks
95/05	NA94	No	No	2.25 $\pm$ 0.98	79	Broad size particle distribution 2 <sup>nd</sup> addition performed 1.5 h after start of the reaction Nucleation stage was observed 15 min after start of the reaction
	NA99	0.1	Start after 2 <sup>nd</sup> addition	2.50 $\pm$ 0.42	63	Nearly monodisperse 2 <sup>nd</sup> addition performed 1.5 h after start of the reaction
	NA100	0.1	No	3.05 $\pm$ 0.30	94	Nearly monodisperse 2 <sup>nd</sup> addition performed 1.5 h after start of reaction
25/75	NA92	No	Yes	1.90 $\pm$ 0.84	65	No nucleation was observed 1 hour after start of the reaction 2 <sup>nd</sup> addition performed after 1.5 h after start of reaction Stirring started after 2 <sup>nd</sup> addition
	NA84	1	Yes	N/A	N/A	No particles observed under microscope
90/10	NA98	0.1	No	N/A	N/A	No nucleation was observed 1 hour after start of the reaction 2 <sup>nd</sup> addition performed after 1.5 h after start of reaction Stirring started after 2 <sup>nd</sup> addition Particles coagulated

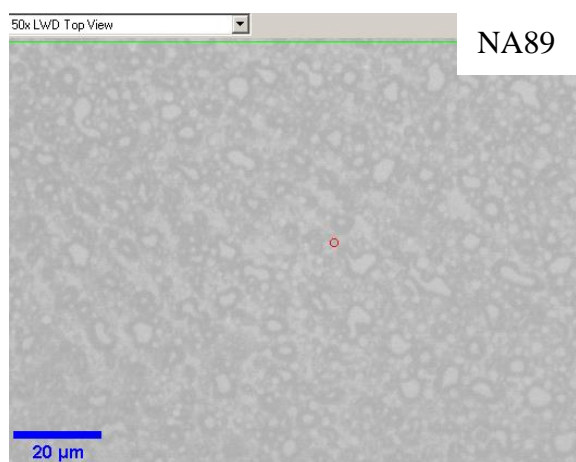


**Figure 4.9: Microscopy image of nucleated particles before a second (delayed) addition added.**

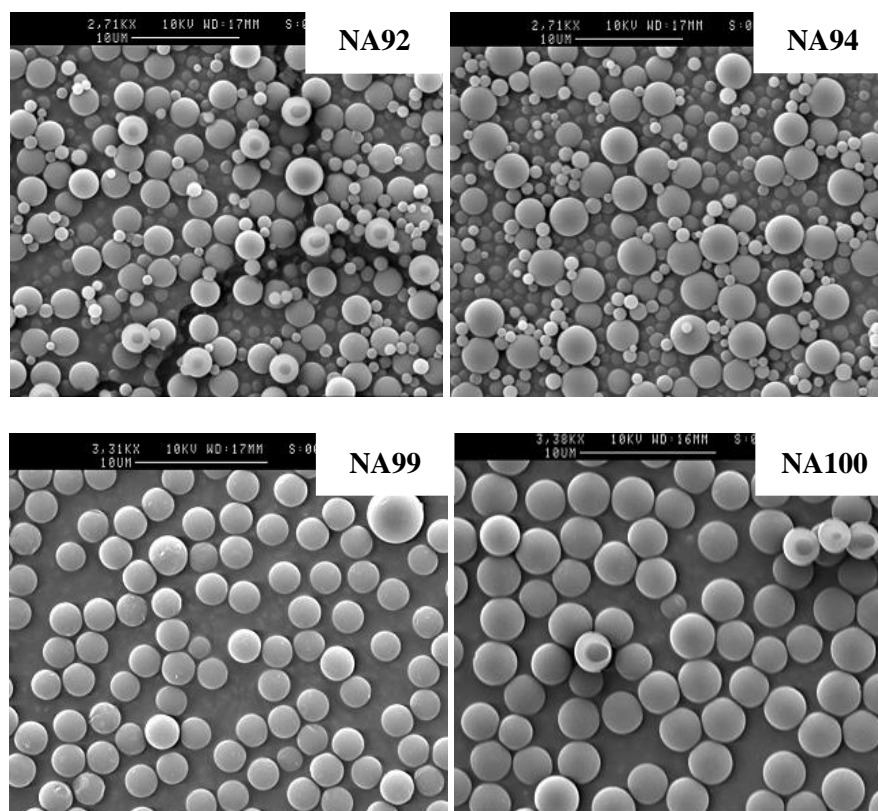


**Figure 4.10: SEM images of ADP precursor particles; effected of feeding time.**

#### **4.5.6 Two-Stage and One-Stage ADP**

Two-stage and one-stage polymerisations were also carried out to probe the effect on the final products. As can be seen in Figure 4.11 (NA94 and NA97), the linear

polymer precursor particles that were obtained in the two-stage (NA94) and one-stage polymerisation (NA97) processes are not much different from one another. Second generation (small) the particles were generated in both reactions. It is assumed that the longer nucleation time in both reactions contributed to the generation of the secondary particles.

When the crosslinker (EGDMA) was added into a two-stage polymerisation a narrow particle size distribution and spherical particles were obtained (Figure 4.11; NA99). In contrast, for one-stage polymerisation, with EGDMA present, coagulated particles were obtained. In fact, the swellability of the primary particles plays a crucial role in determining the shape and monodispersity of the final particles.<sup>[8]</sup> Figure 4.11; NA94 and NA97 shows the secondary nucleation occurred in the two-stage polymerisation and one-stage polymerisation which the polymer synthesised without EGDMA. In contrast, no secondary particles appeared when the polymer synthesised in a two-stage polymerisation which EGDMA added with a low level (delayed monomer) into the reaction vessel. In some cases, either a high levels of crosslinker added into the reaction vessel or the crosslinker added in a one-stage polymerisation, resulting coagulated particles were formed.<sup>[9]</sup> When the crosslinker was present at the beginning of the reaction it were disturbed the nucleation of particles. Moreover, it led to the formation of a crosslinked network on the surfaces of the particles and this makes it difficult for the monomers and also oligomer radicals to diffuse from solution to the particles.

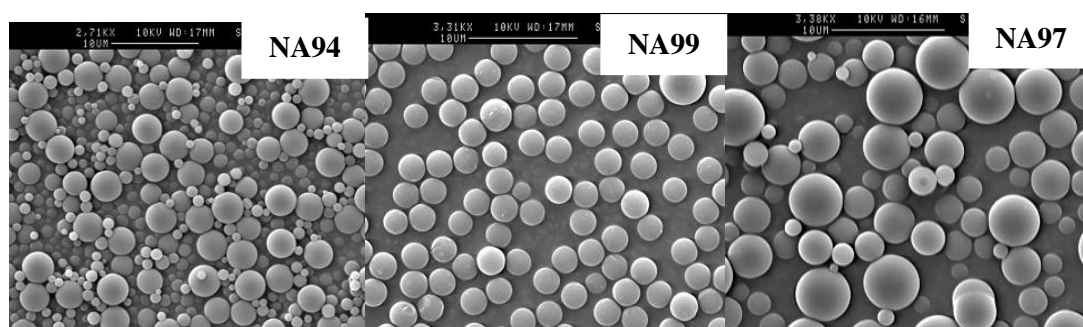


**Figure 4.11: SEM images of ADP precursor particles produced in a two-stage polymerisation (NA94; poly(St-co-VBC) and NA99; Poly(St-co-VBC-co-EGDMA) and a one-stage polymerisation (NA97; poly(St-co-VBC).**

#### 4.5.7 Effect of Styrene Added in Second Stage

Song *et al.* reported that they carried out dispersion polymerisations in ethanol/water mixture in which no styrene was added in the second stage.<sup>[7]</sup> However, the reason why styrene was not added in the second stage was not reported.

As can be seen clearly in Figure 4.12 (NA96), when styrene was added in the second stage, a second population of particles was produced. In contrast, no second populations/small particles were produced when no styrene was added in the second stage (Figure 4.12; NA110); here, the particle size also was increased, although the yield was a bit low (Table 4.3).

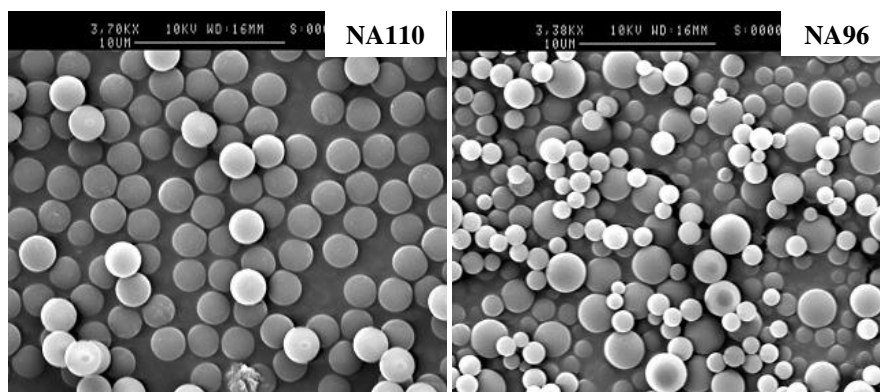


**Figure 4.12: SEM images of precursor particles of poly(St-co-EGDMA-co-VBC) and the effect of the presence of styrene. NA110: No styrene added in a second stage; NA96: styrene added in a second stage.**

**Table 4.3: Characterisation data for polymers synthesised during experiments to explore the effect of styrene added in a second stage in a ADP, with fixed EGDMA content (0.1 wt%). a] Mass of St +VBC=100% total monomer feed in the feed. [b] Average particle diameter  $\pm$  standard deviation (S.D.) calculated from the image analysis in SEM (using Minitab software).**

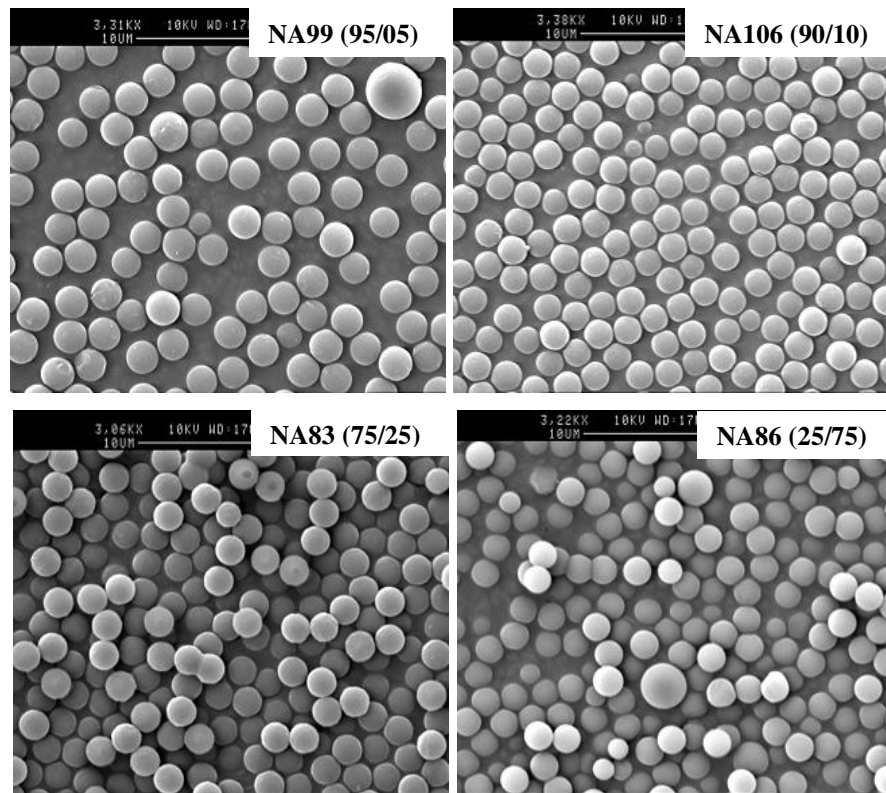
Sample	St/VBC ratio <sup>a</sup>	St added in 2 <sup>nd</sup> stage	Stirring during polymerisation	Average particle size ( $\mu\text{m}$ ) <sup>b</sup>	Yield (%)	Remarks
NA96	95/05	Yes	Started after 2 <sup>nd</sup> addition	1.80 $\pm$ 0.66	83	Second particle population observed
NA108	90/10	Yes	Started after 2 <sup>nd</sup> addition	N/A	N/A	No particles observed
NA110	90/10	No	Started after 2 <sup>nd</sup> addition	2.24 $\pm$ 0.13	63	Nearly monodisperse

#### 4.5.8 Effect of VBC Added in First Stage

A series of experiments was carried out to investigate the effect of the presence of VBC in the first stage. In dispersion polymerisation, the nucleation stage is very complex and highly sensitive,<sup>[1, 3, 8]</sup> and the presence of comonomer can interfere with particle nucleation, resulting in odd shape, and coagulation of particles. Surprisingly, in this study when VBC was employed in the first stage in the ADP series (less than 25%), the particles formed were highly monodisperse and of good quality (Figure 4.13 and Table 4.4). This similar results obtained with no VBC present in the first stage (Table 4.4 and Figure 4.13). This shows that VBC did not interfere with the nucleation stage.

However, for higher VBC content (25% and 75%), there no particles observed under microscope when VBC absent in the first stage (Table 4.4; NA111 and NA90). This contradicts previous reports from other research groups in which the presence of comonomer at the beginning of polymerisation was observed to interfere with the nucleation stage.<sup>[1, 7, 9]</sup> For series of VBC added in the first stage, the average particle size in range  $\sim 2 \mu\text{m}$ , and the yields obtained still satisfactory except for NA86.

**VBC present in first stage**



**No VBC present in first stage**

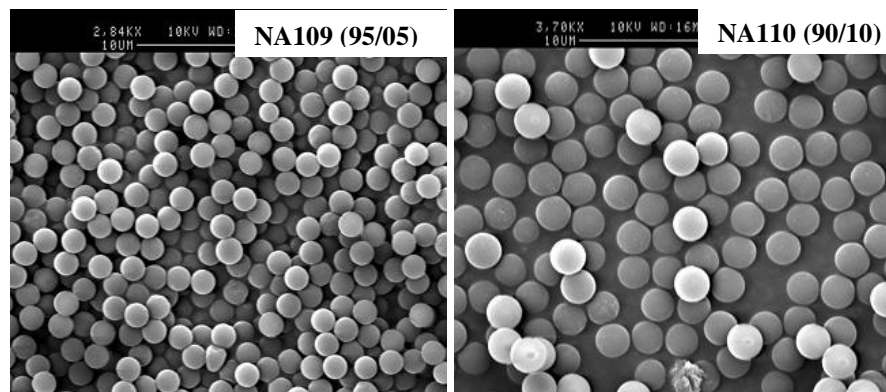


**Figure 4.13: SEM images of precursor particles of poly(St-co-EGDMA-co-VBC-) and the effect of VBC presence in the first stage of ADP. Values in the brackets are the ratios of styrene and VBC in monomer feed.**

**Table 4.4: Characterisation data for polymer synthesised during experiments to explore the effect of VBC added in a second stage in an ADP, with fixed EGDMA content (0.1 wt%). a) Mass of St +VBC=100% total monomer feed in the feed. [b] Average particle diameter  $\pm$  standard deviation (S.D.) calculated from the image analysis in SEM (using Minitab software).**

St/VBC ratio <sup>a</sup>	Sample	VBC added in 1 <sup>st</sup> stage	Average particles size ( $\mu\text{m}$ ) <sup>b</sup>	Yield (%)	Remarks
95/05	NA99	Yes	2.50 $\pm$ 0.42	63	Nearly monodisperse
	NA109	No	2.03 $\pm$ 0.12	57	Nearly monodisperse
90/10	NA106	Yes	2.03 $\pm$ 0.12	63	Nearly monodisperse
	NA110	No	2.24 $\pm$ 0.13	63	Nearly monodisperse
75/25	NA83	Yes	2.45 $\pm$ 0.06	68	Nearly monodisperse
	NA111	No	N/A	N/A	No particles observed under microscope
25/75	NA86	Yes	2.11 $\pm$ 0.33	14	Nearly monodisperse Nucleation observed 15 min after heating applied
	NA90	No	N/A	N/A	No particles observed under microscope

#### 4.5.9 Effect of VBC ratio in First Stage and Second Stage of ADP

Increasing VBC content provided a progressively increase content of chloro-methyl groups. Chloro-methyl groups very important in post-polymerisation (hypercrosslinking reaction) to determine specific surface areas of hypercrosslinked particles. Higher amount of VBC lead to greater specific surface area and total pore volume (to be discussed in next chapter). Therefore, the VBC content is one of the important parameters in precursor polymers synthesise.

Next, an attempt was made to probe the influence of the VBC ratio in the first stage and second stage of an ADP. As discussed in the previous section, when VBC was employed in the first stage at lower ratio, a satisfactory yield of highly monodisperse particles was obtained. However, when the VBC content was increased, the yield obtained was very poor. In other case, at higher VBC ratio (more than 10%) when no VBC was added in the first stage, no particles were observed under a microscope.

In the first instance, 80% of the total VBC in the monomer feed was employed in the first stage (Table 4.5) in all cases except for a St/VBC ratio of 90/10. Highly monodisperse particles were obtained in the case of NA99 (Figure 4.15 and Table 4.5), unfortunately when the total VBC content greater than 25%, no particles were observed under the microscope. Figure 4.14 (a) shows a photograph of the reaction mixture taken of a polymerisation containing 50% of VBC based on monomer feed (Table 4.5; NA129). When this mixture was observed under a microscope no particles were observed. However, when the mixture was allowed to stand for a few hours, phase separation occurred and particles sedimented to the bottom of the vial (Figure 4.14 (b)). The particles were isolated by centrifuge and, surprising highly monodisperse particles (Figure 4.15 (d)) were produced, even though the yield of the particles was very poor and the small particle sizes obtained (Table 4.5). In order to get a high yield, the VBC ratio in the second stage was decreased to between 30% - 5%. Although, highly monodisperse particles were successfully formed in all cases, (Figure 4.15), the yields obtained were still poor (between 45%-14%; Table 4.5).

For high VBC contents (>25% based on monomer feed), with either low or high ratios of VBC in the second stage, the nucleation can be observed around 15 minutes after polymerisation. Unfortunately, upon the second addition of monomer (more than 80% of VBC based on the total VBC in the monomer feed), no particles can be observed at the end of the reaction. This result contradicts previous reports from other research groups in which the presence of comonomer in the second stage should not interfere with the nucleation stage.<sup>[7, 9-10]</sup>

In the case of 5% and 10% of VBC (based on monomer feed) (Table 4.5; NA99 and NA106), the ratio of VBC in the second stage was increased to 80% and 50%. In both cases, similar results were obtained in which monodisperse particles were obtained in satisfactory yield (Figure 4.15 (b-i and b-ii); Table 4.5). For every case, the average particle size recorded was around 2  $\mu\text{m}$ . Overall, the results shows that ADP less effective to produce satisfactory products when the high VBC content used in the reaction. Even though in some case monodisperse particles still possible produced, but the yield decreased upon increasing the VBC content.

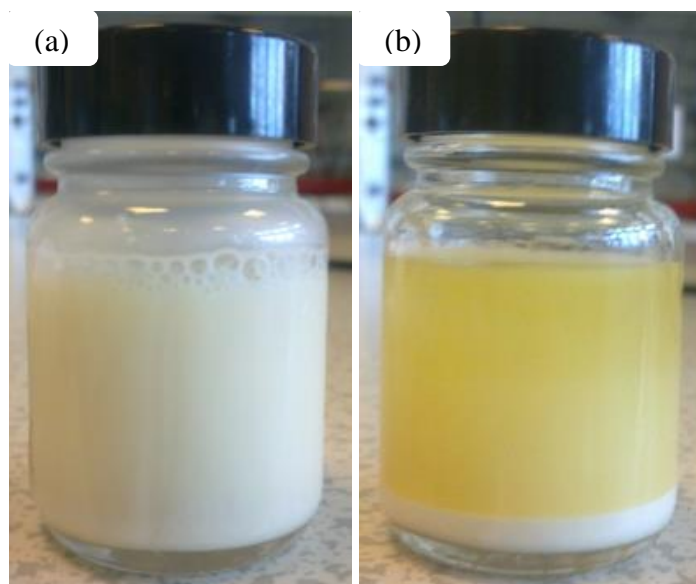


**Figure 4.14: Images of reaction mixture after polymerisation with 50% of VBC (NA129): (a) Before precipitation, and (b) After precipitation.**

**Table 4.5: Characterisation data for polymers synthesised during experiments to explore the effect of the VBC ratio in a second stage with varying VBC content and fixed EGDMA content (0.1 wt%). [a] Mass of St +VBC=100% total monomer feed in the feed. [b] Percentage of VBC based on total VBC in the feed. [c] Average particle diameter  $\pm$  standard deviation (S.D.) calculated from the image analysis in SEM (using Minitab software).**

St/VBC ratio <sup>a</sup>	Sample	VBC ratio (%) in 2 <sup>nd</sup> stage <sup>b</sup>	Average particles size ( $\mu\text{m}$ ) <sup>c</sup>	Yield (%)	Remarks
95/05	NA99	80	2.50 $\pm$ 0.42	63	Nearly monodisperse
90/10	NA106	50	2.03 $\pm$ 0.12	63	Nearly monodisperse
75/25	NA104	80	N/A	N/A	No particles observed under microscope at the end of the reaction
	NA83	20	2.45 $\pm$ 0.06	68	Nearly monodisperse
	NA128	5	1.47 $\pm$ 0.29	45	Nearly monodisperse
50/50	NA105	80	N/A	N/A	No particles observed at the end of reaction
	NA129	5	1.87 $\pm$ 0.10	18	Nearly monodisperse
25/75	NA86	30	2.11 $\pm$ 0.33	14	Nearly monodisperse

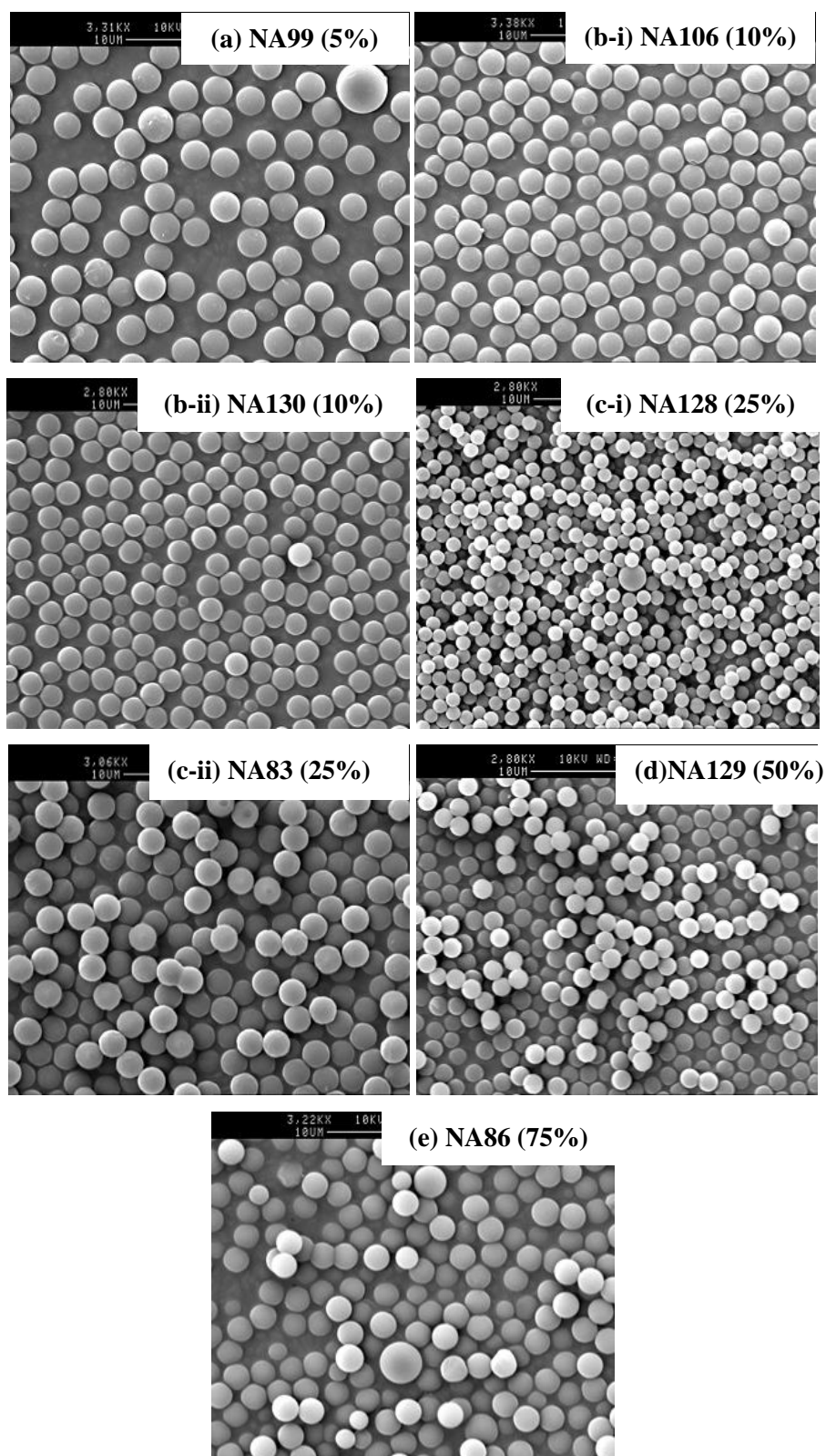


**Figure 4.15: SEM images of poly(St-co-VBC-co-EGDMA) particles prepared with varying VBC contents and fixed EGDMA content (0.1 wt%). VBC ratio in a second stage: (a) 80%; (b-i) 50%; (b-ii) 5%; (c-i) 20%; (c-ii) 5%; (d) 5% and (e) 30%.**

Figure 4.16 shows the FTIR spectra of the poly(*St-co-VBC-co* EGDMA) particles produced. The signal at  $1265\text{ cm}^{-1}$  is ascribed to chloromethyl groups derived from VBC residues in the precursors. As expected, with increasing VBC content in monomer feed, the intensity of this signal increases, although no signal can be seen for the 25% and 50% VBC content polymers. This surprising result, which is backed up with elemental microanalysis data, suggests lower VBC contents in the products than would be expected based on monomer feed compositions. The signal at  $1730\text{ cm}^{-1}$  in spectra can be seen clearly; this arise from the ester groups of EGDMA residues.

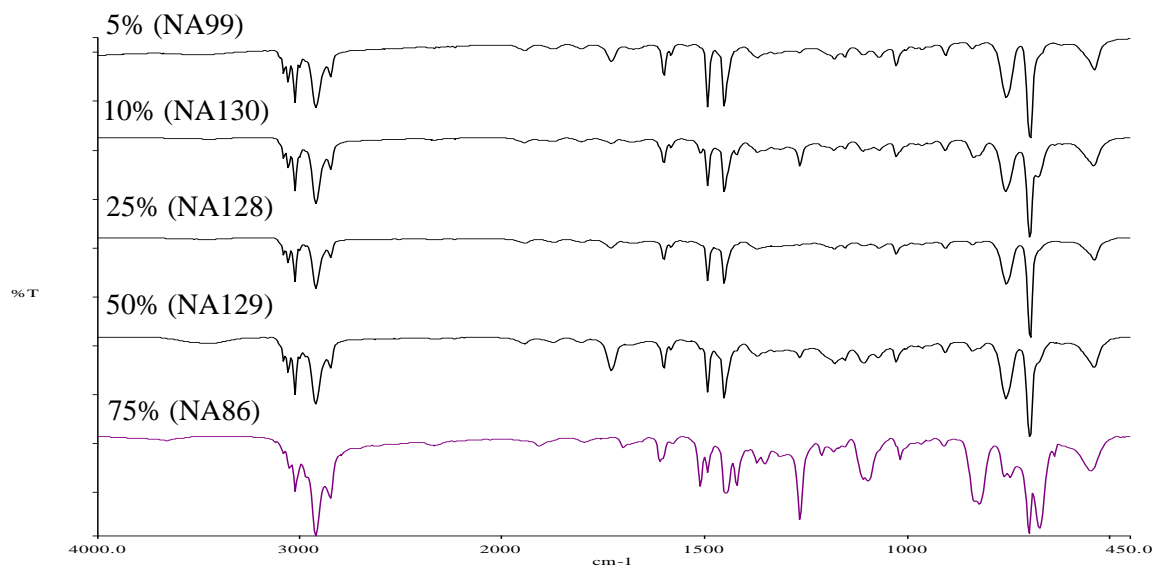


**Figure 4.16: FTIR spectra of poly(*St-co-VBC-co* EGDMA) particles prepared with varying VBC contents.**

**Table 4.6: Characterisation data for polymers synthesised during experiments to explore the effect of the VBC ratio in a second stage in a two-stage ADP. [a] Mass of St +VBC=100% total monomer feed in the feed.[b] based on total monomer in the feed.**

Sample	St/VBC ratio <sup>a</sup> (%)	Crosslinker <sup>b</sup> (wt%)	Elemental microanalysis					
			Expected			Found		
			%C	%H	%Cl	%C	%H	%Cl
NA99	95/05	0.1	90.0	7.5	2.0	88.9	7.3	1.4
NA106	90/10	0.1	88.3	7.4	4.0	90.8	7.6	2.0
NA128	75/25	0.1	82.9	6.9	10.1	90.1	7.5	0.8
NA115	50/50	0.1	72.3	6.3	18.4	72.6	6.0	11.7
NA131	25/75	0.1	68.9	6.0	30.1	73.5	6.2	15.7

#### 4.5.10 Effect of Crosslinker Content

In the literature, many researchers have reported that dispersion polymerisations encounters problem when crosslinker is present at the beginning of the polymerisation. This problem can be prevented by delaying the addition of the crosslinker until after the nucleation stage is over.<sup>[2]</sup> In this study, EGDMA was added in a delayed addition to prevent inter- or intramolecular-crosslinking of molecules during the nucleation stage.

As shown in Figure 4.17, although very good quality, nearly monodisperse particles were obtained when low levels of crosslinker were added (0.1 wt%) in the second stage, when the concentration of EGDMA was increased up to 1 wt%, odd shaped particles (raspberry shaped), deformation and coagulum were obtained (Figure 4.18 and Table 4.6). The surfaces of the crosslinked particles also became rough and contaminated, however, for NA125, particles with good shape and quality were obtained, but the yield was very low (4%) (Table 4.7).

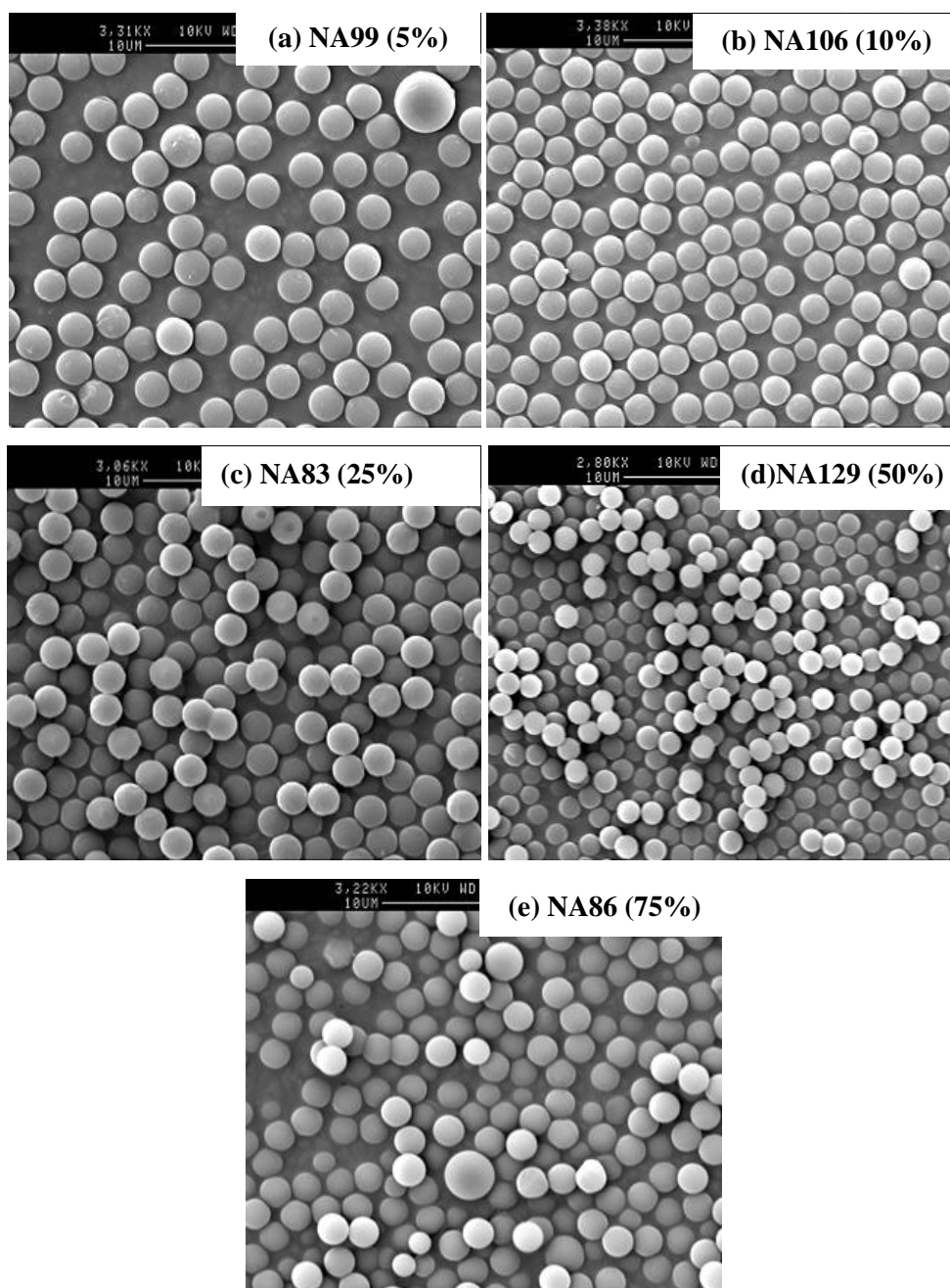


**Figure 4.17:** SEM images of poly(St-co-EGDMA-co-VBC) particles with 0.1 wt% of EGDMA at varying St/VBC ratios. Values in the brackets are percentage of VBC in the monomer feed.

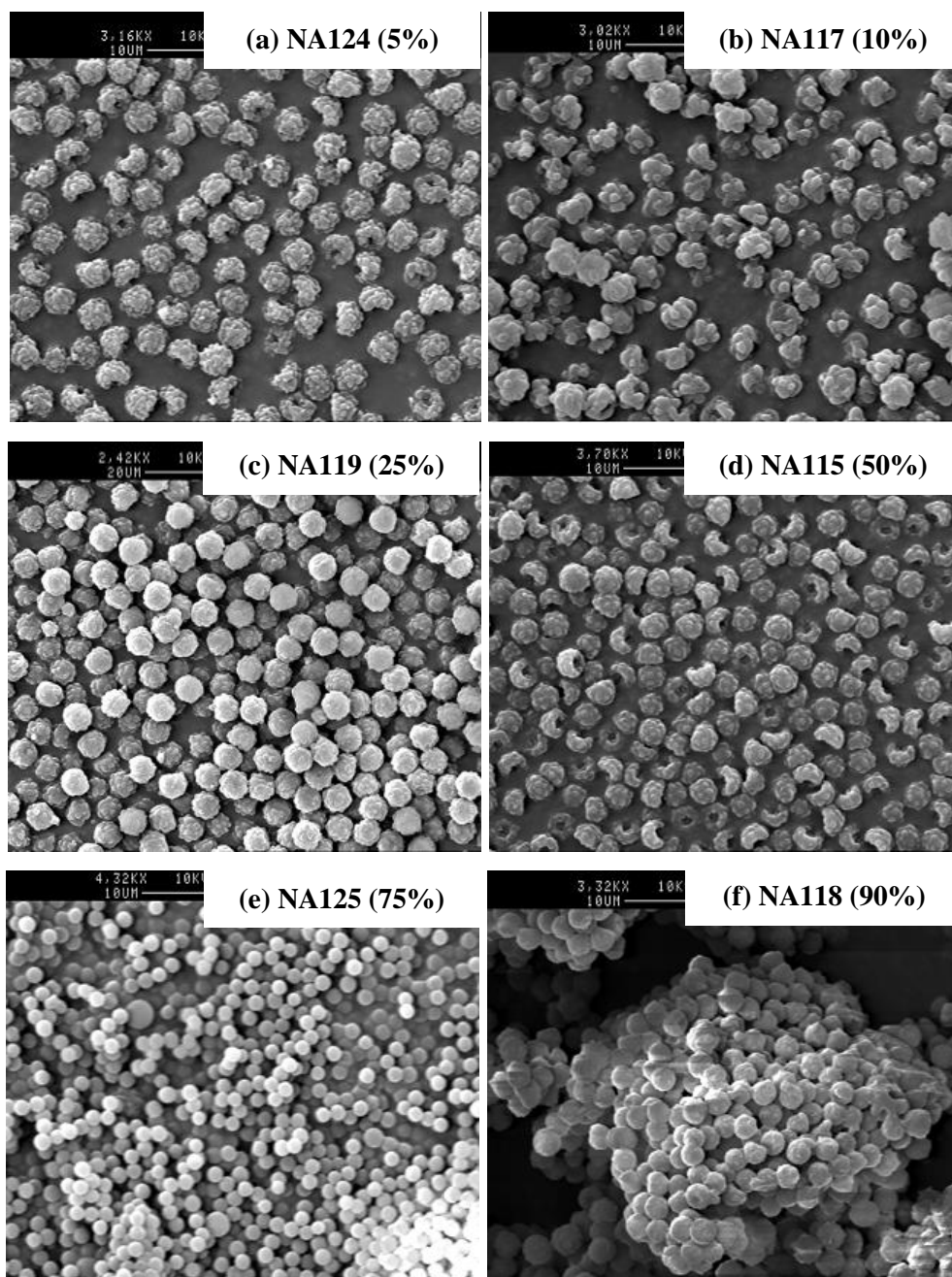


**Figure 4.18:** SEM images of poly(St-co-EGDMA-co-VBC) particles with 1 wt% of EGDMA at varying St/VBC ratios. Values in the brackets are percentage of VBC in the monomer feed.

**Table 4.7: Characterisation data for ADP precursor particles prepared with varying EGDMA content in the monomer feed. [a] Mass of St +VBC=100% total monomer feed in the feed, with varying EGDMA content (0.1 wt% and 1 wt% ), respectively.**

St/VBC ratio <sup>a</sup>	Sample	Crosslinker content (% wt)	Yield (%)	Remarks
95/05	NA99	0.1	63	Nearly monodisperse
	NA124	1	61	Raspberry shapes
90/10	NA106	0.1	63	Nearly monodisperse
	NA117	1	74	Raspberry shapes
75/25	NA83	0.1	68	Nearly monodisperse
	NA119	1	80	Raspberry shapes
50/50	NA129	0.1	18	Nearly monodisperse
	NA115	1	54	Raspberry shapes
25/75	NA86	0.1	14	Nearly monodisperse
	NA125	1	4	Spherical particles, nearly monodisperse
10/90	NA118	1	N/A	Coagulated particles

#### 4.6 Conclusions

It can be said that lightly crosslinked polymer resins have been successfully synthesised by aqueous dispersion polymerisation (ADP) *via* a two-stage/delayed addition methodology. Various parameters were probed in order to optimise the polymerisation conditions in order to synthesise good quality particles.

In ADP, the presence of water in the polymerisation medium, even in a low amount, can have a big effect on the nucleation stage. Prolonged nucleation times occurred due to the polymerisation medium becoming more polar and influencing the solubility of monomers, stabiliser, co-stabiliser as well as initiator. In contrast to NAD, the nucleation stage in ADP took approximately 45 minutes (when stirring from the beginning of the polymerisation), compared to 5 minutes for NAD polymerisations.

Prolonged nucleation times contributed to the possibility of second generation particles being produced.

Stirring also influences the nucleation stage; nucleation takes longer when stirring from the beginning of the polymerisation, however when stirring was started 1.5 hours after the start of polymerisation, nucleation was observed after approximately 15 minutes. A similar result was obtained when there was no stirring over the of the polymerisation, however the possibility of secondary nucleation is higher.

Linear polymer precursors synthesised in a two-stage (delayed addition) and one-stage polymerisation were not much different to one another; second generation (small) particles were generated in both reactions. However, when the crosslinker (EGDMA) was added to a two-stage polymerisation, spherical particles were obtained with a narrow particle size distribution.

Styrene also has an influence upon the final products. When styrene was present in a second monomer addition, the quality of the final product decreased. In contrast, VBC present either in a first stage or a second stage (in two-stage polymerisation) did not exert any significant changes on the final products. However, when the VBC content, based on the monomer feeds was greater than 25%, the yield of the products decreased even though the particles still retained their quality and uniformity.

Lastly, similarly to NAD polymerisation, when EGDMA contents increase the quality of the final product is decreased. In this case, very low amounts of EGDMA (0.1 wt%) were successfully employed in the reaction mixture in order to obtain narrow particle size distribution particles with, at the same time, retention of the high quality of the particles.

## References

- [1] J. S. Song, L. Chagal and M. A. Winnik, *Macromolecules* **2006**, *39*, 5729-5737.
- [2] J. S. Song and M. A. Winnik, *Macromolecules* **2005**, *38*, 8300-8307.
- [3] C. K. Ober and K. P. Lok, *Macromolecules* **1987**, *20*, 268-273.
- [4] M. Okubo, K. Ikegami and Y. Yamamoto, *Colloid Polym. Sci.* **1989**, *167*, 193-200.
- [5] J. Lee and M. Senna, *Colloid Polym. Sci.* **1995**, *273*, 76-82.
- [6] H. Ahmad, B. M. Chaki, M. M. Rahman, M. A. J. Miah and K. Tauer, *e-Polymers* **2007**, *80*, 1-13.
- [7] J. S. Song and M. A. Winnik, *Polymer* **2006**, *47*, 455-461.
- [8] J. W. Kim, B. S. Kim and K. D. Suh, *Colloid Polym. Sci.* **2000**, *278*, 591-595.
- [9] J. S. Song and M. A. Winnik, *Macromolecules* **2009**, *39*, 8318-8325.
- [10] J. S. Song, F. Tronc and M. A. Winnik, *Polymer* **2006**, *47*, 817-825.

## ***CHAPTER FIVE***

## **5.0 Summary**

Hypercrosslinked polymers have been prepared by extensive, post-polymerisation crosslinking, using Friedel-Crafts alkylations, of gel-type, non-aqueous dispersion (NAD) precursors in a swollen state. Such hypercrosslinked materials have remarkably high specific surface areas ( $\sim 1,600 \text{ m}^2/\text{g}$ ). The effect of swelling time, stirring, reaction temperature, reaction time, EGDMA content and solvent system were investigated in an optimisation of the hypercrosslinking chemistry. Since spherical NAD precursors which were hypercrosslinked in 1,2-dichloroethane were found to not retain their spherical shape, variations to the classical hypercrosslinking chemistry were sought. In this regard, NAD precursors were treated with a sub-stoichiometric amount of Lewis acid catalyst in a non-swelling solvent, to deliver lightly hypercrosslinked derivatives. These lightly hypercrosslinked derivatives were then fully hypercrosslinked using the classical hypercrosslinking chemistry. Under optimised reaction conditions, spherical and nearly monodisperse hypercrosslinked polymers could be prepared successfully. The specific surface areas of the hypercrosslinked particles prepared in this manner ranged from  $572 \text{ m}^2/\text{g}$  to  $1165 \text{ m}^2/\text{g}$ , with synthetic control over the specific surface areas of the products being entirely possible. As an alternative to the hypercrosslinking of gel-type, non-aqueous dispersion (NAD) precursors, the hypercrosslinking of swellable precursors synthesised by aqueous dispersion polymerisation (ADP) was also investigated.

## **5.1 Introduction to Hypercrosslinked Polymers**

Hypercrosslinked polymers have attracted significant levels of attention due to their striking features, such as high specific surface areas, amphipathic character, , chemical and mechanical stability. Hypercrosslinked polymers have considerable scope for exploitation in separation science applications, but also for hydrogen storage in the context of the hydrogen economy.

## **5.2 Aims Of Work**

The aims of the work programme described in this Chapter were to optimise the reaction for the hypercrosslinking of swellable, gel-type poly(St-co-VBC-co-EGDMA) precursors which had been obtained *via* NAD polymerisation (refer to Chapter Three). This was achieved by manipulating various reaction parameters, with a key goal being to produce spherical, preferably monodisperse, hypercrosslinked particles with high specific surface areas. As was discussed in Chapter Three, the NAD precursor particles which were synthesised were of good quality and close to monodisperse. Unfortunately, particle quality tended to be degraded as a result of hypercrosslinking, and ways to circumvent this problem were sought. In this regard, several reaction variables were investigated, including the solvent system, temperature, swelling time, stirring, and crosslinker.

## **5.3 Experimental**

### **5.3.1 Materials**

The reagents that were used in the hypercrosslinking reactions were anhydrous 1,2-dichloroethane (DCE) (99.8% grade), heptane (99% grade), hexane (99%), methanol (99.7 grade) and iron (III) chloride (97% grade), all of which were supplied by Sigma-Aldrich. All reagents were used as received.

### **5.3.2 Equipment**

The hypercrosslinked polymers were performed in a three-necked, round-bottomed flask fitted with a condenser, overhead stirrer and two-blade PTFE-type stirrer. The reaction vessel was immersed in a thermostatically controlled oil bath.

### **5.3.3 Characterisation**

The hypercrosslinked particles were characterised using the following methods.

### **5.3.3.1 Scanning Electron Microscopy (SEM)**

SEM was carried out using a Cambridge S-90. SEM micrographs were acquired at an accelerating voltage of 10.0 kV. A thin layer of sample was deposited onto a steel stub, which had been coated previously with conductive (copper), double-sided adhesive tape. Gold coating of the immobilised sample was then carried out. Coated samples were placed inside the SEM chamber and a vacuum was applied; this vacuum evacuated the chamber of any small particles that may have deflected the electrons and affected the SEM image that was obtained.

### **5.3.3.2 Fourier-Transform Infra-Red (FT-IR) Spectroscopy**

All FT-IR spectra were recorded on a Perkin-Elmer 1600 series FT-IR Spectrometer. The method that was used involved placing polymer beads between two diamond plates in a diamond compression cell. The sample was scanned with a resolution of  $4\text{ cm}^{-1}$ ; an average of 16 scans was taken per sample.

### **5.3.3.3 Optical Microscopy**

Optical microscopy (Olympus Vanox, Japan) was used to visualise the polymer particles the end of reactions. A few drops of a polymer dispersion were deposited onto a microscope slide and the particles imaged once the solvent had evaporated.

### **5.3.3.4 Elemental Microanalysis**

A small sample of resin (30 mg) was submitted to the Microanalysis Laboratory at Strathclyde University and C, H and N contents were determined simultaneous in a Perkin Elmer 2400 analyser. The samples were wrapped in tin foil and combusted at  $1800\text{ }^{\circ}\text{C}$  in pure oxygen. The combustion products were catalysed and interferences removed before being swept into a detector zone where each element was separated and eluted as  $\text{CO}_2$ ,  $\text{H}_2\text{O}$  and  $\text{NO}_2$ . The signals were converted to a percentage of the elements.

For Cl analysis, approximately 5 mg of the sample was weighed into ashless filter paper, which was then fastened to a platinum rod. The sample was then combusted in an oxygen-filled flask containing a weak solution of H<sub>2</sub>O<sub>2</sub> (oxygen flask combustion method) and left to sit for 30 minutes. During this time, any halogen present is adsorbed into the solution in the form of halide. After adding 80 mL of ethanol and adjusting the pH to between 1.5 and 2, the resultant solution was titrated with mercuric nitrate solution using diphenylcarbazone as the indicator.

### **5.3.3.5 Nitrogen Sorption Porosimetry Analysis**

Nitrogen sorption porosimetry was used to determine the specific surface area of the polymers from nitrogen sorption data in the lower range of the sorption isotherm. This method derives accurate and reliable data both theoretically and practically.

The porosimeter which was used was a Micromeritics ASAP 2010 BET ANALYZER. Prior to use, the samples (0.3 g – 0.4 g) were heated overnight in a vacuum oven at ~ 40 °C to ensure that all the gas molecules, moisture, and residual solvent had been removed from the samples. After the degassing process, the samples were analysed with computer control Module ASAP 2010 Version 2.00 to give the specific surface areas.

### **5.3.3.6 Solubility Tests**

~ 20 mg of NAD precursor was added into a small vial containing 5 mL of solvent and then left overnight. The samples was then observed under visual inspection and imaged under an optical microscope.

## **5.4 Procedure/Methodology**

### **5.4.1 Synthesis of Gel-Type, NAD Precursor Particles**

All the stabiliser, co-stabiliser, initiator and styrene, half of the VBC and half of the ethanol were added into a 500 mL five-necked, round-bottomed flask fitted with an

overhead stirrer, condenser and nitrogen inlet. Once a homogenous solution had formed at room temperature, the solution was bubbled with nitrogen gas at room temperature for 30 minutes. The flask was then placed into an oil bath set at 70 °C, and stirred mechanically using a four bladed PTFE stirrer at 160 rpm. EGDMA and the second half of the VBC were dissolved in the second half of the ethanol at 70 °C under nitrogen. One hour after the start of the polymerisation, the hot solution containing EGDMA and VBC was added into the reaction flask. The reaction was continued for a further 24 hours. The particles that were obtained were centrifuged for 10 minutes at 3,000 rpm, and then washed 2 times in ethanol and 2 times in methanol (the particles were suspended in the appropriate wash solvent and centrifuged between each washing step). The particles were isolated by vacuum filtration on a 0.22 µm nylon membrane filter and dried overnight *in vacuo* (60 mbar) at 40 °C.

#### **5.4.2 Partial Hypercrosslinking of NAD Precursor Particles**

NAD precursor particles (1.5 g) were added into a round-bottomed flask which contained hexane (40 mL), and left to wet for 2 hours. The mixture was then cooled on an ice bath (~4 °C) before a sub-stoichiometric amount of FeCl<sub>3</sub> was added. FeCl<sub>3</sub> was allowed to disperse uniformly in the mixture for 2 hours before the mixture was heated to 60 °C for 18 hours. Stirring was applied continuously over the reaction course. The final products were filtered using vacuum filtration on a 0.22 µm nylon membrane filter, and then washed with MeOH and several times with aqueous HNO<sub>3</sub> (pH 2). They were then extracted overnight with acetone in a Soxhlet extractor, and dried *in vacuo* (60 mbar) at 40 °C overnight.

#### **5.4.3 Hypercrosslinking of NAD Particles**

Partially hypercrosslinked particles (1.5 g) were added into a round-bottomed flask which contained DCE (40 mL) and left to swell fully under nitrogen for 1 hour. Then, FeCl<sub>3</sub> (in a 1:1 molar ratio of CH<sub>2</sub>Cl:FeCl<sub>3</sub>) suspended in DCE (40 mL) was added. The mixture was then heated rapidly to 80 °C. The reaction was continued for

18 hours, with continuous stirring over the entire reaction course. The hypercrosslinked particles were filtered using vacuum filtration on a 0.22  $\mu\text{m}$  nylon membrane filter, and then washed with MeOH and several times with aqueous  $\text{HNO}_3$  (pH 2). They were then extracted overnight with acetone in a Soxhlet extractor, and dried *in vacuo* (60 mbar) at 40  $^\circ\text{C}$  overnight.

## 5.5 Results and Discussion

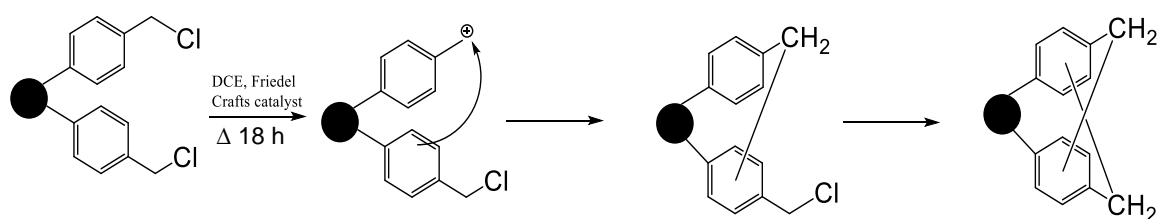


**Figure 5.1:** Hypercrosslinking of gel-type precursor particles *via* Friedel-Crafts alkylations.

Figure 5.1 shows the hypercrosslinking reaction scheme. Methylene bridges are installed between adjacent aromatic residues whilst the polymer particle is in a swollen state. The methylene bridges prevent network collapse upon removal of the solvent. This process imparts microporosity into the polymer. It is important to appreciate the fact that the methylene bridges are set in place throughout the entire bead and not only at the surface, *i.e.*, Figure 5.1 is a mere schematic representation.

## 5.6 Hypercrosslinking of Non-Aqueous Dispersion Precursor Particles

In the present study, gel-type precursor beads were synthesised by the non-aqueous dispersion (NAD) polymerisation of VBC, St and EGDMA, with ethanol as the inert diluent. Note that the same concentration of EGDMA (1 wt% based on total monomer feed) was used in all polymerisations to deliver products with the same nominal crosslink density.

### 5.6.1 Effect of Swelling Time on the Hypercrosslinked Particles

Gel-type particles might be expected to be the most appropriate precursors for hypercrosslinking reactions because such particles are easily swollen and are already in a convenient beaded form. However, since hypercrosslinking reactions are normally performed in thermodynamically good solvents, the highly swollen chloromethylated particles with low crosslink density used in this work were found to be susceptible to agglomeration.<sup>[1]</sup> Part of the reason for this may be that a soluble portion of the particles is solubilised during the swelling process, and this soluble portion is able to exit from the particles. It was a significant technical challenge to generate hypercrosslinked polystyrenes in this way without any agglomeration.

Table 5.1 shows the synthesis data for the NAD precursor particles and their corresponding hypercrosslinked particles. Unsurprisingly, the VBC content of the swellable precursors mirrors the VBC content in the monomer feed, and the specific surface areas of the hypercrosslinked polymers produced is directly proportional to the VBC content of the swellable precursors. Moreover, the higher the VBC content of the swellable precursor the smaller the mean pore diameter of the hypercrosslinked product. Upon hypercrosslinking, a substantial fall in the chlorine content was observed for all polymers (Table 5.1), which implied that methylene bridge formation is an efficient process. Nevertheless, a low proportion of the chloromethyl groups normally survived the hypercrosslinking process, as evidenced by the chlorine contents of the products and their FT-IR spectra. These unreacted chloromethyl moieties can be exploited in post-hypercrosslinking chemical modification reactions, provided that they are not located within inaccessible regions of the particles.

For the swellable precursor particles, nitrogen sorption porosimetry experiments showed that, as expected, they had very low specific surface areas ( $< 5 \text{ m}^2/\text{g}$ ) in the dry state (Table 5.2). In other words, the swellable precursor particles were essentially non-porous in the dry-state. However, following hypercrosslinking, a remarkable increase in specific surface area was observed, with BET specific surface areas of up to  $\sim 1600 \text{ m}^2/\text{g}$  being recorded (Table 5.2). Such high specific surface area

are consistent with polymers having a high micropore content. Table 5.2 also shows that swellable precursors with higher chloromethyl contents give rise to hypercrosslinked products with higher specific surface areas. Clearly, this is one way in which the porosity of the hypercrosslinked products can be tuned.

Polymers HXLNA70 and HXLNA71 were found to have a negative C-value, which means that such particles exhibit monolayer nitrogen sorption (particles exhibiting multilayer nitrogen sorption have positive C-values). This means that the nitrogen sorption is better described by the Langmuir model, and that it is more appropriate to quote the Langmuir specific surface area for those particles (Table 5.2) rather than the BET specific surface area.

All the hypercrosslinked particles had a mean pore size which was in the mesopore range, with mean pore sizes of between 2 nm and 7 nm being recorded. Presumably, given the typical distribution of pore sizes in polymers of this type, there is a significant micropore content, and this contributes to the high specific surface area.

As was discussed in Chapter 3, the NAD precursors synthesised in neat ethanol were found to be nearly monodisperse. Unfortunately, the quality of the particles was diminished upon hypercrosslinking, and we ascribed this to the presence of a soluble component dissolving and leaching out of the particles during the hypercrosslinking process. The presence of the soluble portion of polymer is perhaps not so surprising given the low level EGDMA (1 wt%) present in the monomer feed. All the SEM images presented in Figure 5.2 show hypercrosslinked particles with rough, contaminated surfaces. The particles are also no longer spherical and there is evidence of chemical aggregation. Irrespective of this, even although the particles were not spherical in shape they still had well-developed pore structures (the specific surface areas of the hypercrosslinked polymers were  $> 1000 \text{ m}^2/\text{g}$  when the VBC content in the monomer feed was  $> 50\%$ ; Table 5.2).

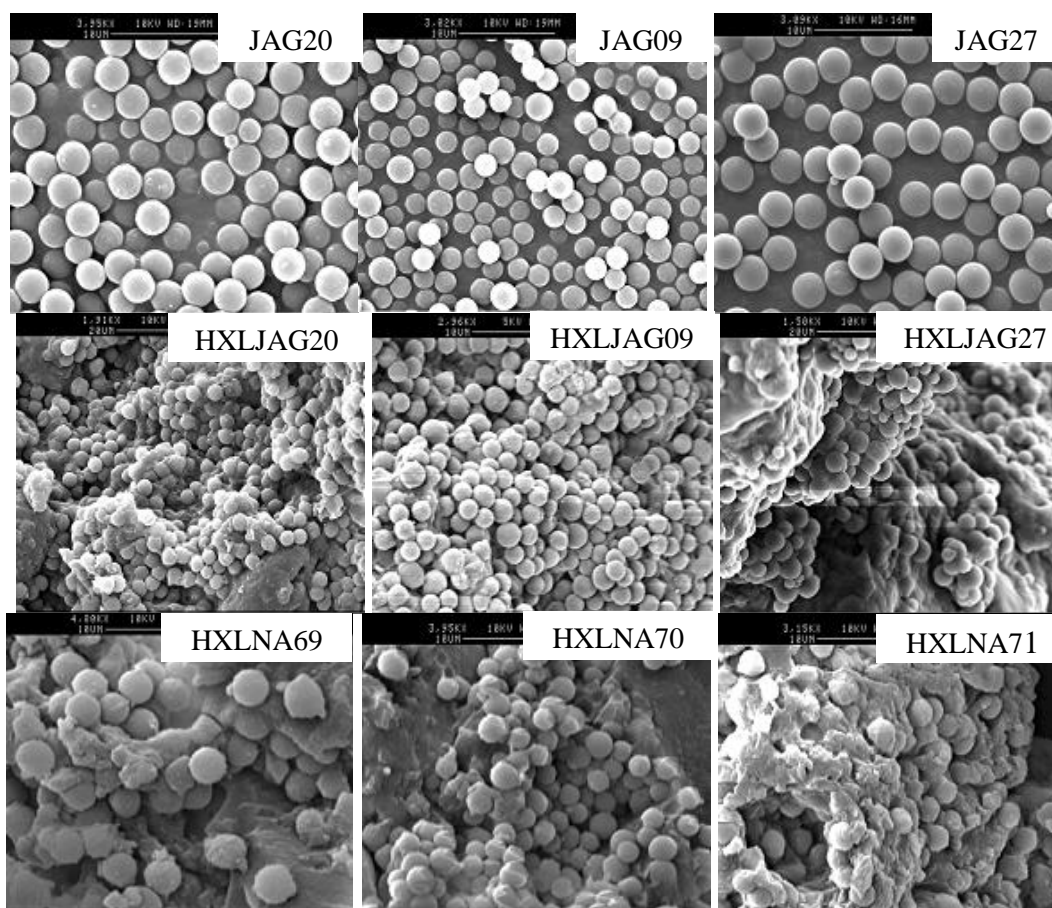


**Figure 5.2: SEM images of poly(St-co-VBC-co-EGDMA) precursor particles prepared by NAD polymerisation with different St/VBC feed ratios and fixed EGDMA content (1 wt%); JAG20, JAG09 and JAG27, and their hypercrosslinked derivatives; HXLJAG20, HXLJAG09, HXLJAG27 hypercrosslinked after 60 min swelling time; HXLNA69, HXLNA70 and HXLNA71 hypercrosslinked after 15 min swelling time at 80 °C in DCE/Heptane (100/0) respectively.**

**Table 5.1: Synthesis data for NAD particles and their hypercrosslinked derivatives at different swelling times. [a] HXLNA69, HXLNA70, HXLNA71 are derived from JAG20, JAG09 and JAG27 respectively.[b] Mass of St +VBC = 100% total monomer feed in the feed; EGDMA is 1 wt% based on total monomer in the feed. [c] Average particle diameter  $\pm$  standard deviation (S.D.) calculated from the image analysis in SEM (using Minitab software). [d] For the hypercrosslinked particles relative to the mass of the corresponding NAD (non-hypercrosslinked) precursor particles.**

Sample	St/VBC feed ratio (w/w) <sup>b</sup>	Swelling time (min)	Temp (°C)	Stirring	DCE/Heptane ratio (v/v)	Microanalysis						Average particle size ( $\mu\text{m}$ ) <sup>c</sup>	Yield (%)
						Expected (%)			Found (%)				
						C	H	Cl	C	H	Cl		
JAG20	10/90	N/A	N/A	N/A	N/A	72.9	6.1	20.7	72.4	5.9	19.6	2.40 $\pm$ 0.40	89
JAG09	25/75	N/A	N/A	N/A	N/A	76.0	6.4	17.3	76.3	6.5	15.6	2.40 $\pm$ 0.30	97
JAG27	50/50	N/A	N/A	N/A	N/A	81.3	6.8	11.5	81.1	6.6	10.7	3.40 $\pm$ 0.60	83
HXLJAG20	10/90	60	80	YES	100/0	91.9	7.3	trace	85.9	6.8	3.44	2.30 $\pm$ 0.19	78 <sup>d</sup>
HXLJAG09	25/75	60	80	YES	100/0	91.9	7.7	trace	89.2	7.7	trace	2.30 $\pm$ 0.40	76 <sup>d</sup>
HXLJAG27	50/50	60	80	YES	100/0	92.0	7.7	trace	90.1	7.1	trace	4.16 $\pm$ 0.96	77 <sup>d</sup>
HXLNA69 <sup>a</sup>	10/90	15	80	YES	100/0	90.7	6.7	trace	86.4	6.1	4.7	2.24 $\pm$ 0.20	67 <sup>d</sup>
HXLNA70 <sup>a</sup>	25/75	15	80	YES	100/0	90.7	6.1	trace	80.0	5.4	2.9	1.92 $\pm$ 0.29	90 <sup>d</sup>
HXLNA71 <sup>a</sup>	50/50	15	80	YES	100/0	90.7	6.1	trace	85.8	6.0	1.5	2.57 $\pm$ 0.20	90 <sup>d</sup>

**Table 5.2: Porosimetry-derived characterisation data for NAD precursor particles and their hypercrosslinked derivatives synthesised in DCE using different swelling times. Data computed from the N<sub>2</sub> sorption isotherms and BET theory.[a] HXLNA69, HXLNA70, HXLNA71 are derived from JAG 20, JAG09 and JAG27 respectively.**

Sample	BET (m <sup>2</sup> /g)	Langmuir (m <sup>2</sup> /g)	C Value	Pore volume (cm <sup>3</sup> /g)	Pore size	
					adsorption (nm)	desorption (nm)
JAG20	~2	~2	N/A	N/A	N/A	N/A
JAG09	~2	~2	N/A	N/A	N/A	N/A
JAG27	~2	~2	N/A	N/A	N/A	N/A
HXLJAG20	1460	2019	134	1.42	4.95	3.44
HXLJAG09	1122	1545	153	0.95	4.45	2.35
HXLJAG27	784	1077	219	0.52	3.47	2.88
HXLNA69 <sup>a</sup>	1559	2455	185	2.11	6.58	4.57
HXLNA70 <sup>a</sup>	1107	1717	-529	0.86	3.89	3.31
HXLNA71 <sup>a</sup>	411	626	-161	0.27	3.27	2.89

### **5.6.2 Effect Upon the Hypercrosslinked Particles of Stirring During Hypercrosslinking**

The purpose of this study in this section is to investigate the effect of stirring on the hypercrosslinked particles during hypercrosslinking. Since the NAD precursor particles size decreased when they contacted with DCE, probably due to diffusion of soluble polymer out of the particles, thus, it may be valuable to probe that stirring may increase the rate of diffusion of soluble polymer during hypercrosslinking reaction.

From Figure 5.3, it appears that the particle quality was better when no stirring was applied (HXLNA62, HXLNA61 and HXLNA60) compared to the analogous situation where stirring was applied (HXLNA69, HXLNA70 and HXLNA71). This is probably because particle coalescence is more likely in the absence of stirring/mixing.

Even although poorer quality particles were obtained when no stirring was applied, the specific surface areas of the products were still high; specific surface areas of up to 1559 m<sup>2</sup>/g were recorded (Table 5.4). Unsurprisingly, therefore, significant drops in the chlorine contents were observed upon hypercrosslinking (Table 5.3).

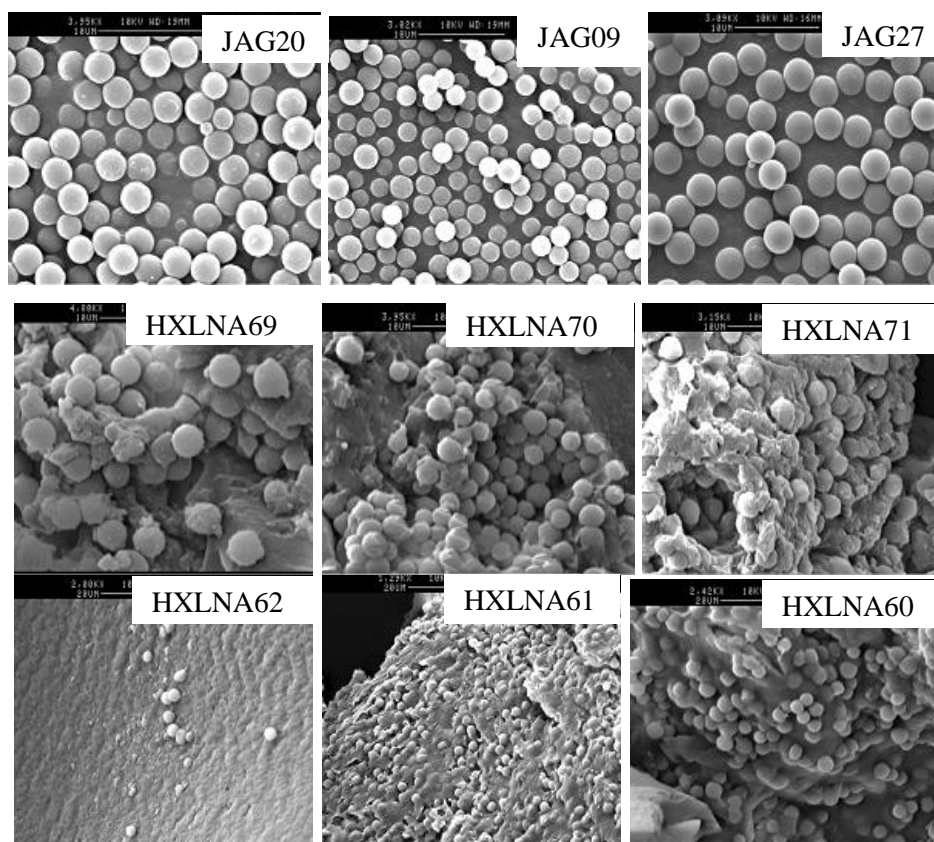


**Figure 5.3: SEM images of poly(St-co-VBC-co-EGDMA) precursor particles prepared by NAD polymerisation with different St/VBC feed ratios and fixed EGDMA content (1 wt%); JAG20, JAG09 and JAG27 and their hypercrosslinked derivatives; HXLNA62, HXLNA61, HXLNA60 synthesised without stirring; HXLNA69, HXLNA70 and HXLNA71 synthesised whilst stirring, in DCE at 80 °C.**

**Table 5.3: Synthesis data for NAD precursor particles and their hypercrosslinked derivatives synthesised either with or without stirring at 80 °C in DCE. [a] Mass of St +VBC = 100% total monomer feed in the feed; EGDMA is 1 wt% based on total monomer in the feed. [b] Average particle diameter  $\pm$  standard deviation (S.D.) calculated from the image analysis in SEM (using Minitab software). [c] For the hypercrosslinked particles relative to the mass of the corresponding the NAD (non-hypercrosslinked) precursor particles.**

Sample	St/VBC feed ratio (w/w) <sup>a</sup>	Swelling time (min)	Temp (°C)	Stirring	DCE/Heptane ratio (v/v)	Microanalysis						Average particle size ( $\mu\text{m}$ ) <sup>b</sup>	Yield (%)
						Expected (%)			Found (%)				
						C	H	Cl	C	H	Cl		
JAG20	10/90	N/A	N/A	N/A	N/A	72.9	6.1	20.7	72.4	5.9	19.6	2.40 $\pm$ 0.40	89
JAG09	25/75	N/A	N/A	N/A	N/A	76.0	6.4	17.3	76.3	6.5	15.6	2.40 $\pm$ 0.30	97
JAG27	50/50	N/A	N/A	N/A	N/A	81.3	6.8	11.5	81.1	6.2	10.7	3.40 $\pm$ 0.60	83
HXLNA69	10/90	15	80	YES	100/0	90.7	6.7	trace	86.4	6.1	4.7	2.24 $\pm$ 0.20	67 <sup>c</sup>
HXLNA70	25/75	15	80	YES	100/0	90.7	6.1	trace	80.0	5.4	2.9	1.92 $\pm$ 0.29	90 <sup>c</sup>
HXLNA71	50/50	15	80	YES	100/0	90.7	6.1	trace	85.8	6.0	1.5	2.57 $\pm$ 0.20	90 <sup>c</sup>
HXLNA62	10/90	15	80	NO	100/0	90.7	6.7	trace	76.9	6.3	4.9	1.94 $\pm$ 0.30	87 <sup>c</sup>
HXLNA61	25/75	15	80	NO	100/0	90.9	6.1	trace	87.3	7.1	0.9	2.43 $\pm$ 0.40	87 <sup>c</sup>
HXLNA60	50/50	15	80	NO	100/0	91.1	7.0	trace	78.9	6.4	3.7	2.23 $\pm$ 0.30	87 <sup>c</sup>

**Table 5.4: Porosimetry-derived characterisation data for NAD precursor particles and their hypercrosslinked derivatives synthesised either with or without stirring at 80 °C in DCE. Data computed from nitrogen sorption isotherms and BET theory.**

Sample	BET (m <sup>2</sup> /g)	Langmuir (m <sup>2</sup> /g)	C Value	Pore volume (cm <sup>3</sup> /g)	Pore size	
					Adsorption (nm)	desorption (nm)
JAG20	~2	~2	N/A	N/A	N/A	N/A
JAG09	~2	~2	N/A	N/A	N/A	N/A
JAG27	~2	~2	N/A	N/A	N/A	N/A
HXLNA69	1559	2455	185	2.11	6.58	4.57
HXLNA70	1107	1717	-529	0.86	3.89	3.31
HXLNA71	411	625	-161	0.27	3.27	2.89
HXLNA62	1441	2268	223	1.68	5.75	4.16
HXLNA61	633	972	-170	0.42	3.31	3.05
HXLNA60	1159	1814	994	1.23	5.30	3.78

### **5.6.3 Effect of Hypercrosslinking Temperature Upon the Hypercrosslinked Particles**

The temperature at which the hypercrosslinking reaction was carried out was varied to ascertain whether this would have an effect on the quality and porous character of the hypercrosslinked microspheres. The reaction temperature of the hypercrosslinking reaction was reduced from 80 °C to 60 °C. Unsurprisingly, the hypercrosslinking reaction was slower at the lower temperature; the products derived from the hypercrosslinking reactions conducted at 60 °C had a higher chlorine content, consistent with an incomplete hypercrosslinking reaction.

The effect of changing the hypercrosslinking temperature upon the specific surface area is less clear cut and somewhat difficult to explain. However, yet again there is a direct relationship between the chlorine content of the swellable precursor and its hypercrosslinked derivative; the highest specific surface areas are recorded for the swellable precursors which have the highest chlorine content.

Of most interest, arguably, was the effect of temperature upon the quality of the hypercrosslinked particles. However, the hypercrosslinking reaction temperature did not appear to have a discernible effect on the quality of the particles, at least within the temperature range studied (Figure 5.4). Nevertheless, all the particles produced had high specific surface areas and mean pore sizes close to 2 nm.

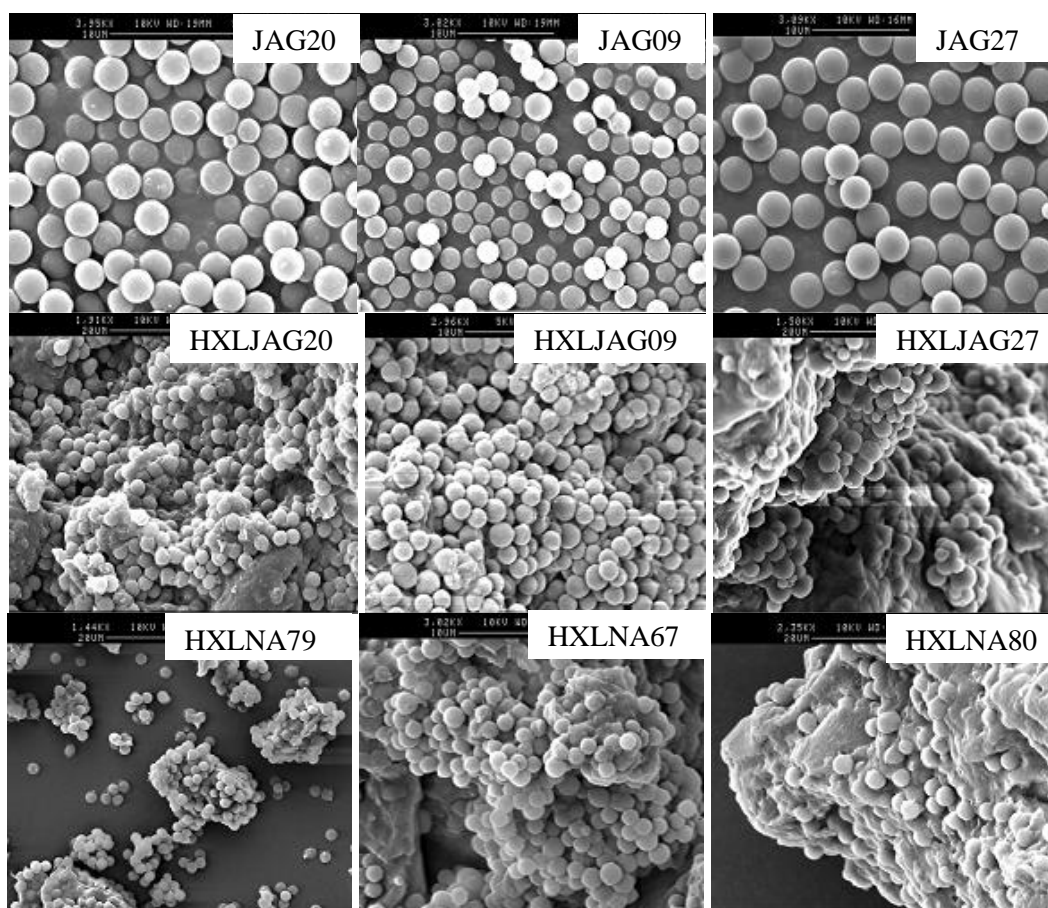


**Figure 5.4:** SEM images of poly(*St-co-VBC-co-EGDMA*) precursor particles prepared by NAD polymerisation with different *St/VBC* feed ratios and fixed *EGDMA* content (1 wt%); JAG20, JAG09 and JAG27 and their hypercrosslinked derivatives; HXLJAG20, HXLJAG09, HXLJAG27 hypercrosslinked at 80 °C; HXLNA79, HXLNA67 and HXLNA80 hypercrosslinked at 60 °C, in DCE.

**Table 5.5: Synthesis data for NAD precursor particles and their hypercrosslinked derivatives which were hypercrosslinked at different temperatures in DCE. [a] Mass of St +VBC = 100% total monomer feed in the feed; EGDMA is 1 wt% based on total monomer in the feed. [b] Average particle diameter  $\pm$  standard deviation (S.D.) calculated from the image analysis in SEM (using Minitab software). [c] For the hypercrosslinked particles relative to the mass of the corresponding NAD (non-hypercrosslinked) precursor particles.**

Sample	St/VBC ratio (w/w)	Swelling time (min)	Temp (°C)	Stirring	DCE/Heptane ratio (v/v)	Microanalysis						Average particle size ( $\mu\text{m}$ ) <sup>b</sup>	Yield (%)
						Expected (%)			Found (%)				
						C	H	Cl	C	H	Cl		
JAG20	10/90	N/A	N/A	N/A	N/A	72.9	6.1	20.7	72.4	5.9	19.6	2.40 $\pm$ 0.40	89
JAG09	25/75	N/A	N/A	N/A	N/A	76.0	6.4	17.3	76.3	6.5	15.6	2.40 $\pm$ 0.30	97
JAG27	50/50	N/A	N/A	N/A	N/A	81.3	6.8	11.5	81.1	6.2	10.7	3.40 $\pm$ 0.60	83
HXLJAG20	10/90	60	80	YES	100/0	91.9	7.3	trace	85.9	6.8	trace	2.50 $\pm$ 0.19	78 <sup>c</sup>
HXLJAG09	25/75	60	80	YES	100/0	92.0	7.7	trace	89.2	7.7	trace	2.30 $\pm$ 0.40	76 <sup>c</sup>
HXLJAG27	50/50	60	80	YES	100/0	92.0	7.7	trace	90.1	7.1	trace	3.16 $\pm$ 0.96	77 <sup>c</sup>
HXLNA79	10/90	60	60	YES	100/0	91.9	7.7	trace	85.9	6.1	3.5	2.19 $\pm$ 0.16	80 <sup>c</sup>
HXLNA67	25/75	60	60	YES	100/0	90.9	6.1	trace	87.1	6.6	3.2	1.80 $\pm$ 0.23	53 <sup>c</sup>
HXLNA80	50/50	60	60	YES	100/0	92.0	7.7	trace	89.5	6.7	2.0	2.50 $\pm$ 0.17	80 <sup>c</sup>

**Table 5.6: Porosimetry-derived characterisation data for NAD precursor particles and their hypercrosslinked derivatives which were hypercrosslinked at different temperatures in DCE. Data computed from nitrogen sorption isotherms and BET theory.**

Sample	BET ( $\text{m}^2/\text{g}$ )	Langmuir ( $\text{m}^2/\text{g}$ )	C value	Pore volume ( $\text{cm}^3/\text{g}$ )	Pore size	
					adsorption (nm)	desorption (nm)
JAG20	~2	~2	N/A	N/A	N/A	N/A
JAG09	~2	~2	N/A	N/A	N/A	N/A
JAG27	~2	~2	N/A	N/A	N/A	N/A
HXLJAG20	1460	2019	134	1.42	4.95	3.44
HXLJAG09	1122	1545	153	0.95	4.45	2.35
HXLJAG27	784	1077	219	0.52	3.47	2.88
HXLNA79	1299	2030	1009	0.99	4.88	3.86
HXLNA67	1099	1715	-1160	1.11	5.27	3.73
HXLNA80	646	992	-166	0.99	3.11	3.06

#### **5.6.4 Effect Upon the Hypercrosslinked Particles by Stirring at 60 °C During Hypercrosslinking**

As has been discussed in previous section, when the hypercrosslinking reaction was carried out at low temperature, the specific surface area of the hypercrosslinked particles produced was also low (Table 5.5) even although high yields were obtained. Thus, once again the effect of stirring was probed to see if it had an effect on the final products when at the reaction temperature was 60°C.

As one can see in Table 5.7, the yield of product obtained in the hypercrosslinking reaction was higher when no stirring was applied. This may be because stirring encourages the exit of soluble material from the particles. However, those particles which were prepared with stirring did have higher specific surface areas (Table 5.8) and correspondingly lower chlorine contents (Table 5.7).

All the hypercrosslinked particles showed satisfactory specific surface areas ( $>1000 \text{ m}^2/\text{g}$ ) when the VBC content was over 50%. In terms of pore size and volume, minor differences were observed. In terms of particle quality, stirring did not have any obvious effect; in all cases the hypercrosslinked particles did not retain the spherical shape of the swellable precursors, but beads can be seen clearly in the case of HXLNA79 (Figure 5) when stirring was applied.

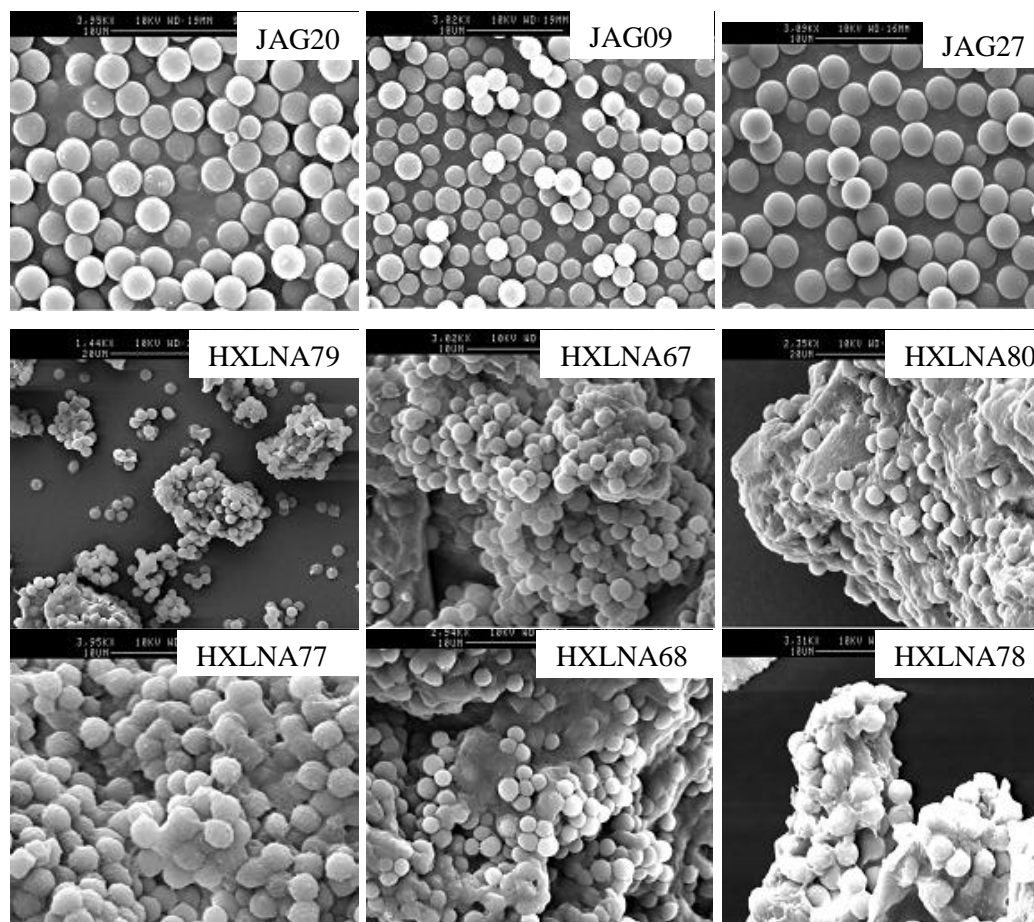


**Figure 5.5:** SEM images of poly(*St-co-VBC-co-EGDMA*) precursor particles prepared by NAD polymerisation with different *St/VBC* feed ratios and fixed *EGDMA* content (1 wt%); JAG20, JAG09 and JAG27 and their hypercrosslinked derivatives; HXLNA79, HXLNA67, HXLNA80 hypercrosslinked with stirring; HXLNA77, HXLNA68 and HXLNA78 hypercrosslinked without stirring, at 60 °C in DCE.

**Table 5.7: Synthesis data for NAD precursors and their hypercrosslinked derivatives prepared with and without stirring during hypercrosslinking at 60 °C in DCE. [a] Mass of St +VBC = 100% total monomer feed in the feed; EGDMA is 1 wt% based on total monomer in the feed. [b] Average particle diameter ± standard deviation (S.D.) calculated from the image analysis in SEM (using Minitab software). [c] For the hypercrosslinked particles relative to the mass of the corresponding NAD (non-hypercrosslinked) precursor particles.**

Sample	St/VBC feed ratio (w/w) <sup>a</sup>	Swelling time (min)	Temp (°C)	Stirring	DCE/Heptane ratio (v/v)	Microanalysis						Average particle size (µm) <sup>b</sup>	Yield (%)
						Expected (%)			Found (%)				
						C	H	Cl	C	H	Cl		
JAG20	10/90	N/A	N/A	N/A	N/A	72.9	6.1	20.7	72.4	5.9	19.6	2.40±0.40	89
JAG09	25/75	N/A	N/A	N/A	N/A	76.0	6.4	17.3	76.3	6.5	15.6	2.40±0.30	97
JAG27	50/50	N/A	N/A	N/A	N/A	81.3	6.8	11.5	81.1	6.2	10.7	3.40±0.60	83
HXLNA79	10/90	60	60	YES	100/0	91.9	7.7	trace	85.9	6.1	3.5	2.19±0.16	80 <sup>c</sup>
HXNAL67	25/75	60	60	YES	100/0	90.9	6.1	trace	87.1	6.6	3.2	1.80±0.23	53 <sup>c</sup>
HXNAL80	50/50	60	60	YES	100/0	92.0	7.7	trace	89.5	6.7	2.0	2.50±0.17	80 <sup>c</sup>
HXLNA77	10/90	60	60	<b>NO</b>	100/0	90.7	6.7	trace	84.2	6.3	6.0	2.27±0.17	90 <sup>c</sup>
HXLNA68	25/75	60	60	<b>NO</b>	100/0	90.9	6.1	trace	86.7	6.6	4.1	1.99±0.28	67 <sup>c</sup>
HXLNA78	50/50	60	60	<b>NO</b>	100/0	91.9	7.7	trace	90.0	6.8	1.2	2.55±0.16	90 <sup>c</sup>

**Table 5.8: Porosimetry-derived characterisation data for NAD precursors and their hypercrosslinked derivatives prepared with or without stirring at 60 °C in DCE. Data computed from nitrogen sorption isotherms and BET theory.**

Sample	BET (m <sup>2</sup> /g)	Langmuir (m <sup>2</sup> /g)	C value	Pore volume (cm <sup>3</sup> /g)	Pore size	
					adsorption (nm)	desorption (nm)
JAG20	~2	~2	N/A	N/A	N/A	N/A
JAG09	~2	~2	N/A	N/A	N/A	N/A
JAG27	~2	~2	N/A	N/A	N/A	N/A
HXLNA79	1299	2030	1009	0.99	4.88	3.86
HXLNA67	1099	1715	-1160	1.11	5.27	3.73
HXLNA80	646	992	-166	0.99	3.11	3.06
HXLNA77	1120	1750	-10017	0.99	5.22	3.84
HXLNA68	1140	1727	-932	1.11	5.21	3.69
HXLNA78	603	922	-152	0.99	3.04	3.10

### 5.6.5 Effect of Stirring During Swelling

Since the particles quality did not have any significant effect when stirring or without stirring was applied either during hypercrosslinking or at low temperature (as has been discussed in previous section), therefore, in this section another attempt was made to study effect of stirring during swelling with aim to delay rate of diffusion soluble particles out from NAD precursor during swelling.

Figures 5.6 and 5.7 show SEM images of particles acquired before and after hypercrosslinking reactions. The hypercrosslinked particles in Figure 5.6 were synthesised in the absence of stirring during swelling, whilst Figure 5.7 shows hypercrosslinked particles which were synthesised with stirring during swelling. As can be seen, when stirring was applied during swelling the overall quality of the particles was improved slightly (Figure 5.7; HXLNA182); the HXLNA182 particles were spherical in shape and the particles' surfaces were smooth, even though some aggregation was apparent. For the situation where stirring was not applied during swelling (Figure 5.6; HXLNA172), the particles lost their spherical shape, plus surface contamination and particle aggregation were apparent.

The SEM images also show that the quality of the hypercrosslinked particles was decreased when the hypercrosslinking reaction was performed at room temperature (HXLNA181) or the reaction time was short (HXLNA179). Tables 5.9 and 5.10 show the synthesis and characterisation data for the hypercrosslinked polymers which were prepared either with or without stirring during swelling. The overall effects upon specific surface area are minimal.

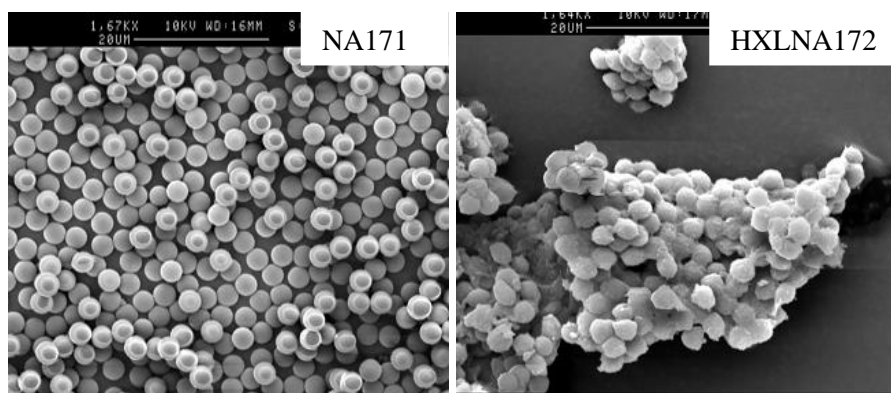


Figure 5.6: SEM images of precursor particles prepared by NAD polymerisation at fixed EGDMA content (1 wt%) and St/VBC ratio (90/10), NA171, and its hypercrosslinked derivative HXLNA172 prepared with no stirring during swelling time. Hypercrosslinking was at 80 °C for 18 h.

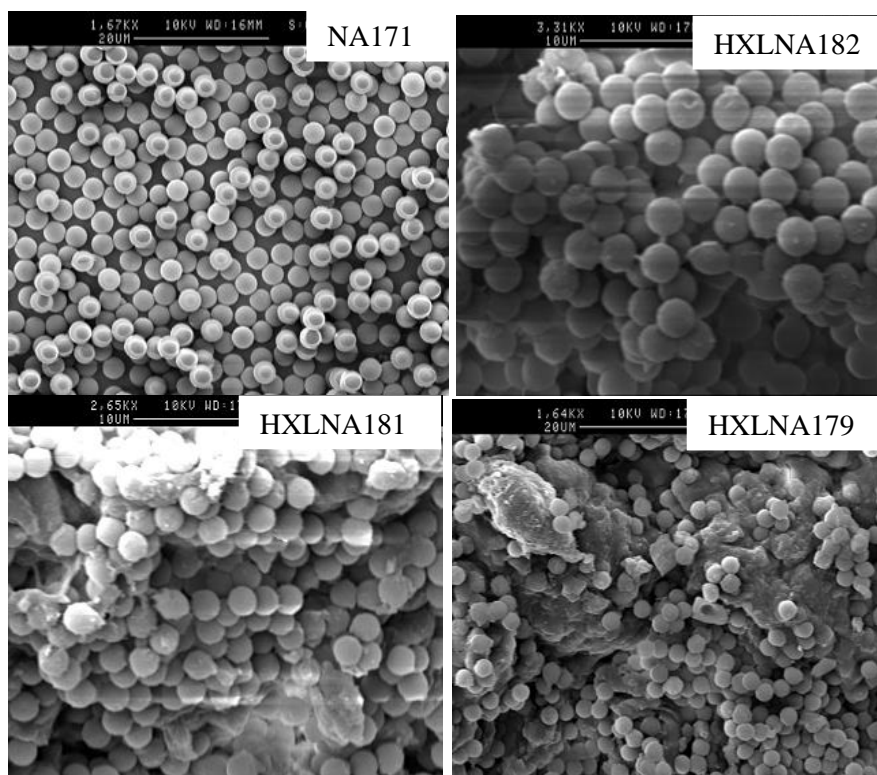


Figure 5.7: SEM images of precursor particles prepared by NAD polymerisation at fixed EGDMA content (1 wt%) and St/VBC ratio (90/10), NA171, and its hypercrosslinked derivatives: HXLNA182 (80 °C, 18 h), HXLNA181 (RT, 18 h) and HXLNA179 (RT, 30 min), prepared with stirring during swelling.

**Table 5.9: Synthesis data for an NAD precursor and its hypercrosslinked derivatives prepared with and without stirring during swelling. Hypercrosslinking at 80 °C in DCE. St/VBC: 10/90 and EGDMA is 1 wt% based on total monomer in the feed. [a] Average particle diameter  $\pm$  standard deviation (S.D.) calculated from the image analysis in SEM (using Minitab software). [b] For the hypercrosslinked particles relative to the mass of the corresponding NAD (non-hypercrosslinked) precursor particles.**

Sample	Reaction		Stirring during swelling	Microanalysis						Average particle size ( $\mu\text{m}$ ) <sup>a</sup>	Yield (%)
	Temp (°C)	time (min)		Expected (%)			Found (%)				
				C	H	Cl	C	H	Cl		
NA171	75	24	N/A	89.1	7.5	36.2	73.0	6.1	23.4	2.50 $\pm$ 0.19	89
HXLNA172	80	1080	NO	93.3	6.8	trace	86.2	6.7	2.6	3.02 $\pm$ 0.68	78 <sup>b</sup>
HXLNA182	80	1080	YES	91.9	7.7	trace	88.9	6.2	4.3	2.77 $\pm$ 0.17	83 <sup>b</sup>
HXLNA181	RT	1080	YES	91.9	7.7	trace	83.5	6.1	5.9	2.77 $\pm$ 0.17	83 <sup>b</sup>
HXLNA179	RT	30	YES	91.9	7.3	trace	82.6	6.7	7.1	2.65 $\pm$ 0.13	96 <sup>b</sup>

**Table 5.10: Porosimetry-derived characterisation data for an NAD precursor and its hypercrosslinked derivatives prepared with stirring during swelling. Hypercrosslinking at 80 °C in DCE. Data computed from nitrogen sorption isotherms and BET theory.**

Sample	BET ( $\text{m}^2/\text{g}$ )	Langmuir ( $\text{m}^2/\text{g}$ )	C value	Pore		
				volume ( $\text{cm}^3/\text{g}$ )	adsorption (nm)	desorption (nm)
NA171	~2	~2	N/A	N/A	N/A	N/A
HXLNA172	1258	1741	130	1.42	5.62	4.03
HXLNA182	1344	2106	667	1.56	5.68	4.17
HXLNA181	1038	1615	-467	0.85	4.06	3.46
HXLNA179	718	1104	-136	0.49	3.24	3.21

### 5.6.6 Effect of Solvent System on the Hypercrosslinking of Particles

The pioneering hypercrosslinking work carried out by Davankov<sup>[2]</sup> involved linear polystyrene dissolved in DCE. Thus the choice of an appropriate thermodynamically 'good' solvent for gel-type polymers, as well as a solvent which is compatible with Friedel-Crafts catalysts, becomes a key factor in order to get high efficiency reactions. In the present work, DCE was used as a swelling solvent in hypercrosslinking reactions, however in an attempt to suppress the dissolution of a soluble component present in the precursors, and thereby improve the quality of the hypercrosslinked products, a mixed solvent system (DCE/heptane) was also evaluated. It should be noted that heptane is a non-solvent for polystyrene. A thermodynamically good solvent, DCE, and a thermodynamically bad solvent, heptane, were used in combination to swell poly(St-co-VBC-co-EGDMA) in a controlled fashion, with the goal being to produce good quality, *i.e.*, spherical, hypercrosslinked particles. Table 5.11 shows the specific surface areas of various hypercrosslinked particles which were hypercrosslinked either in neat DCE or in a 50/50 (v/v) mixture of DCE/heptane.

DCE is a thermodynamically good solvent for polystyrene and has been shown to give high specific surface area products in hypercrosslinking reactions when used as a swelling solvent,<sup>[2-5]</sup> compared to other solvent.<sup>[6-7]</sup> Similar results were obtained in the present work; when hypercrosslinking was performed in neat DCE the specific surface areas of the porous products were more than 1000 m<sup>2</sup>/g, as shown in Table 5.11, with the exception of HXLJAG27 where the VBC content in the monomer feed was 50%. Clearly, the more swollen the precursor the higher the SSA of the hypercrosslinked product. This is another way to tune the porosity of the products.

When the mixed solvent system was used to swell the precursor particles (Table 5.11), the precursor particles were swollen less efficiently due to the presence of heptane and this is manifested in products with lower SSA and higher mean pore size. The solubility of the catalyst may also be lower in the mixed solvent system. Nevertheless, the hypercrosslinked particles produced in this manner still had respectable SSAs. Their chlorine contents were higher than for those polymers hypercrosslinked in the presence of met DCE, and this may reflect lower swelling by the mixed solvent and reduced accessibility of catalyst to functional groups during the hypercrosslinking process.

Figure 5.6 shows the SEM images of poly(St-*co*-VBC-*co*-EGDMA) from this series taken before and after hypercrosslinking. The NAD precursor particles are close to monodisperse, however the quality of the particles was diminished by the hypercrosslinking process. Somewhat surprisingly, the hypercrosslinked particles which were synthesised in the binary solvent mixture were of the lower quality. Satisfactory yields were obtained for all the hypercrosslinked particles produced (Table 5.10).

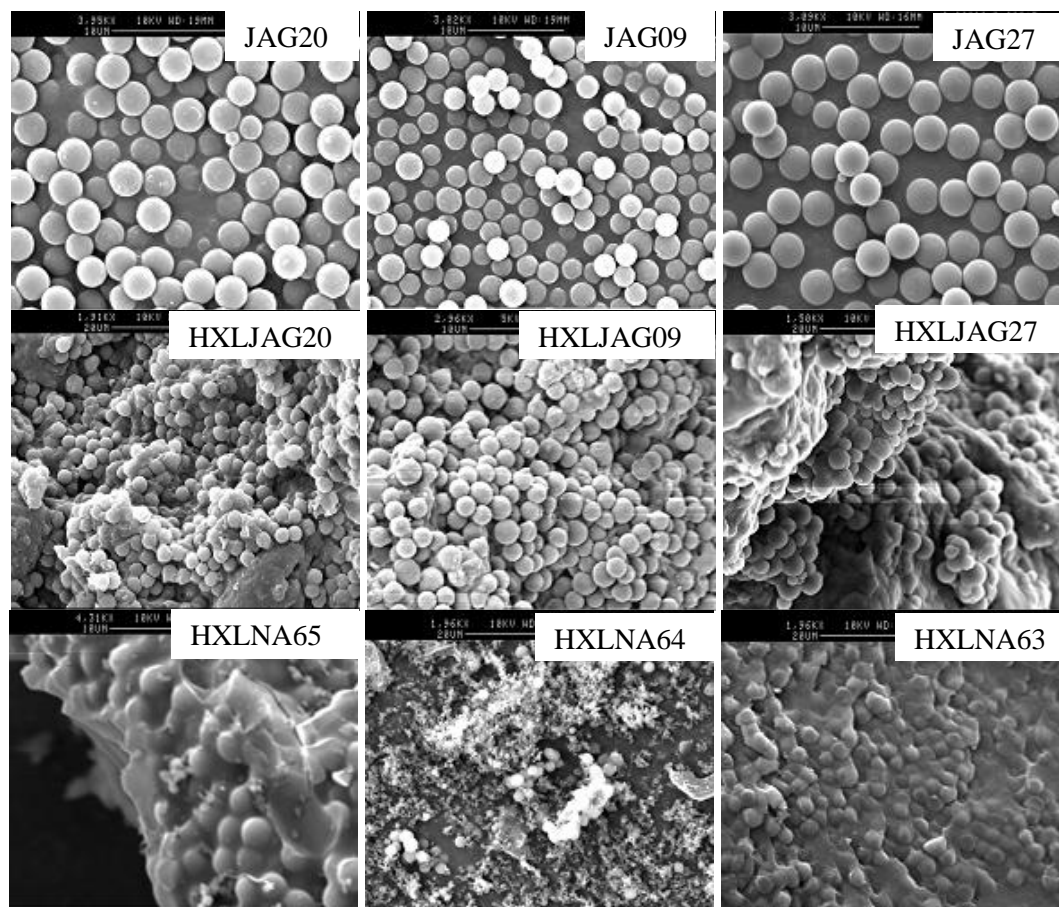


**Figure 5.8:** SEM images of poly(*St-co-VBC-co-EGDMA*) precursor particles prepared by NAD polymerisation with different *St/VBC* w/w ratios and fixed *EGDMA* content (1 wt%); JAG20, JAG09 and JAG27, and their hypercrosslinked derivatives synthesised in different solvent system: HXLJAG20, HXLJAG09 and HXLJAG27 in DCE/Heptane (100/0 v/v); HXLNA65, HXLNA64 and HXLNA63 in DCE/Heptane (50/50 v/v), at 80 °C.

**Table 5.11: Synthesis data of NAD precursors and their hypercrosslinked derivatives hypercrosslinked at 80 °C in either neat DCE or in a mixture of DCE and heptane. [a] Mass of St +VBC = 100% total monomer feed in the feed; EGDMA is 1 wt% based on total monomer in the feed. [b] Average particle diameter ± standard deviation (S.D.) calculated from the image analysis in SEM (using Minitab software). [c] For the hypercrosslinked particles relative to the mass of the corresponding NAD (non-hypercrosslinked) precursor particles.**

Sample	St/VBC feed ratio (w/w) <sup>a</sup>	Swelling time (min)	Temp (°C)	Stirring	DCE/Heptane ratio (v/v)	Microanalysis						Average particle size (µm) <sup>b</sup>	Yield (%)
						Expected (%)			Found (%)				
						C	H	Cl	C	H	Cl		
JAG20	10/90	N/A	N/A	N/A	N/A	72.9	6.1	20.7	72.4	5.9	19.6	2.40±0.40	89
JAG09	25/75	N/A	N/A	N/A	N/A	76.0	6.4	17.3	76.3	6.5	15.6	2.40±0.30	97
JAG27	50/50	N/A	N/A	N/A	N/A	81.3	6.8	11.5	81.1	6.2	10.7	3.40±0.60	83
HXLJAG20	10/90	60	80	YES	100/0	91.9	7.3	trace	85.9	6.8	trace	2.30±0.19	78 <sup>c</sup>
HXLJAG09	25/75	60	80	YES	100/0	91.9	7.3	trace	89.2	7.70	trace	2.30±0.40	76 <sup>c</sup>
HXLJAG27	50/50	60	80	YES	100/0	92.0	7.7	trace	90.1	7.1	trace	4.16±0.96	77 <sup>c</sup>
HXLNA65	10/90	60	80	YES	<b>50/50</b>	90.7	6.7	trace	72.9	6.7	6.2	2.31±0.12	73 <sup>c</sup>
HXLNA64	25/75	60	80	YES	<b>50/50</b>	90.9	6.1	trace	82.0	6.7	2.2	1.67±0.36	80 <sup>c</sup>
HXLNA63	50/50	60	80	YES	<b>50/50</b>	91.1	7.0	trace	90.6	7.1	0.6	2.82±0.32	87 <sup>c</sup>

**Table 5.12: Porosimetry-derived characterisation data NAD precursors and their hypercrosslinked derivatives, hypercrosslinked at 80 °C in either neat DCE or DCE/Heptane (50/50), Data computed from nitrogen sorption isotherms and BET theory.**

Sample	BET (m <sup>2</sup> /g)	Langmuir (m <sup>2</sup> /g)	C value	Pore volume (cm <sup>3</sup> /g)	Pore size	
					adsorption (nm)	desorption (nm)
JAG20	~2	~2	N/A	N/A	N/A	N/A
JAG09	~2	~2	N/A	N/A	N/A	N/A
JAG27	~2	~2	N/A	N/A	N/A	N/A
HXLJAG20	1460	2019	134	1.42	4.95	3.44
HXLJAG09	1122	1545	153	0.95	4.45	2.35
HXLJAG27	784	1077	219	0.52	3.47	2.88
HXLNA65	925	1420	-118	0.75	4.50	5.11
HXLNA64	940	1431	-127	0.86	5.17	5.56
HXLNA63	611	940	-237	0.54	4.54	4.59

### **5.6.7 Effect of Stirring and a Mixed Solvent System on the Hypercrosslinking of Particles**

As has been discussed in previous sections, stirring and mixed solvent system did not have significant effect in terms of the quality particles. Therefore, in this section, a study of effect of stirring in mixed solvents system was carried out in order to improve the quality of hypercrosslinked particles

Table 5.12 shows the porosimetry-derived characterisation data for the hypercrosslinked polymers synthesised in the mixed solvent system. Here, the effect of stirring was also assessed. As can be seen from Table 5.13 the yields of products obtained with and without stirring were similar (80%). From the elemental microanalysis results for the particles hypercrosslinked in the mixed solvent system, it can be seen that the consumption of chlorine was higher when the hypercrosslinking reaction was stirred. However, stirring had no obvious effect on the SSAs of the products.

Figure 5.9 shows the SEM images of swellable precursors and their hypercrosslinked derivatives prepared in the mixed solvent system either with or without stirring. Although high yields of products (> 80%) were obtained in all cases, the quality of the particles was very variable. HXLNA65 was of good quality.

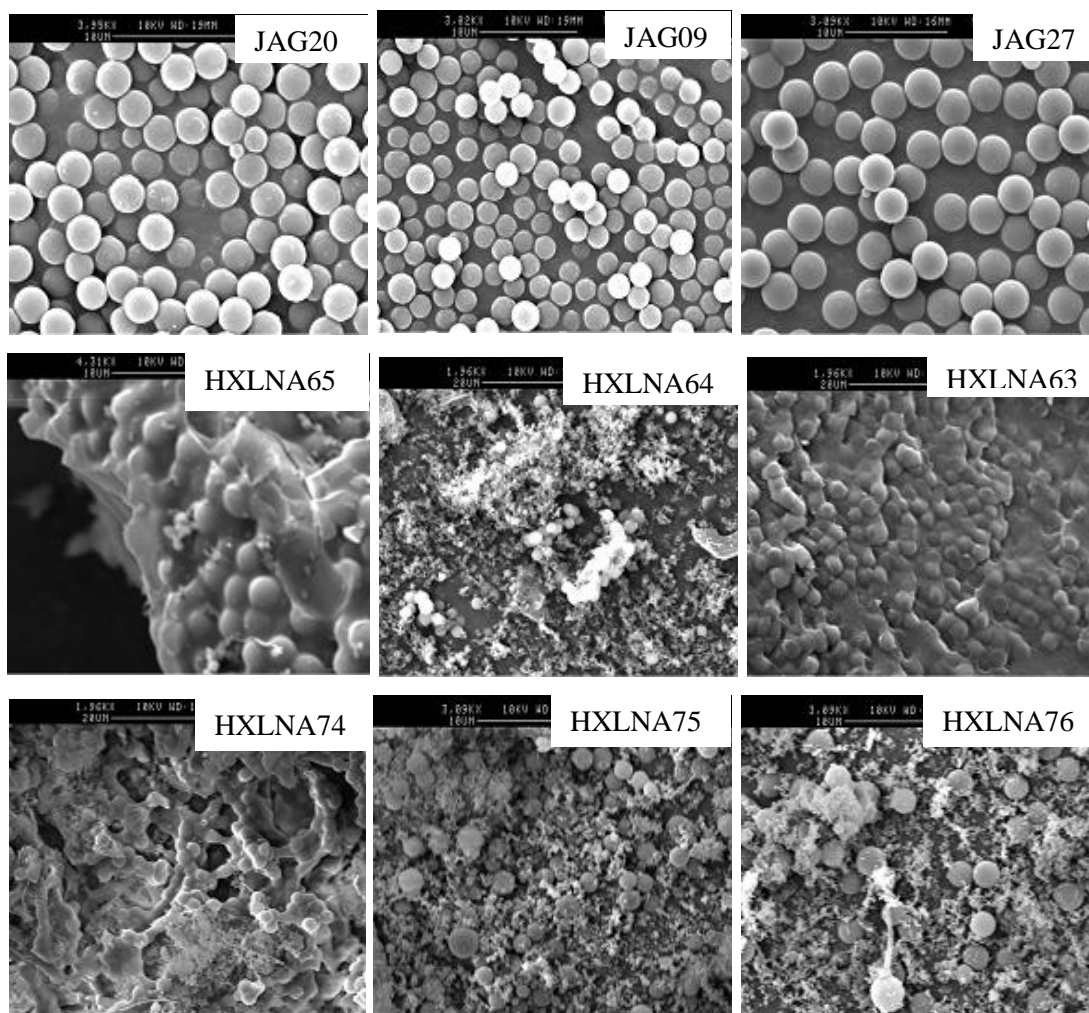


**Figure 5.9:** SEM images of poly(*St-co-VBC-co-EGDMA*) precursor particles prepared by NAD polymerisation with different *St/VBC* w/w ratios and fixed *EGDMA* content (1 wt%); JAG20, JAG09 and JAG27, and their hypercrosslinked derivatives: HXLNA65, HXLNA64 and HXLNA63 prepared with stirring; HXLNA74, HXLNA75 and HXLNA76 prepared without stirring, at 80 °C in DCE/heptane.

**Table 5.13: Synthesis and characterisation data for NAD precursor particles and their hypercrosslinked derivatives prepared with and without stirring during the reaction course, at 80 °C in a mixed solvent system. [a] Mass of St +VBC = 100% total monomer feed in the feed; EGDMA is 1 wt% based on total monomer in the feed. [b] Average particle diameter ± standard deviation (S.D.) calculated from the image analysis in SEM (using Minitab software). [c] For the hypercrosslinked particles relative to the mass of the corresponding the NAD (non-hypercrosslinked) precursor particles.**

Sample	St/VBC feed ratio (w/w) <sup>a</sup>	Swelling time (min)	Temp (°C)	Stirring	DCE/Heptane ratio (v/v)	Microanalysis						Average particle size (µm) <sup>b</sup>	Yield (%)
						Expected (%)			Found (%)				
						C	H	Cl	C	H	Cl		
JAG20	10/90	N/A	N/A	N/A	N/A	72.9	6.1	20.7	72.4	5.9	19.6	2.40±0.40	89
JAG09	25/75	N/A	N/A	N/A	N/A	76.0	6.4	17.3	76.3	6.5	15.6	2.40±0.30	97
JAG27	50/50	N/A	N/A	N/A	N/A	81.3	6.8	11.5	81.1	6.2	10.7	3.40±0.60	83
HXLNA65	10/90	60	80	YES	50/50	90.7	6.7	trace	72.9	6.7	6.2	2.31±0.12	73 <sup>c</sup>
HXLNA64	25/75	60	80	YES	50/50	90.9	6.1	trace	82.0	6.7	2.2	1.67±0.36	80 <sup>c</sup>
HXLNA63	50/50	60	80	YES	50/50	91.1	7.0	trace	90.6	7.1	0.6	2.82±0.32	87 <sup>c</sup>
HXLNA74	10/90	60	80	<b>NO</b>	50/50	90.7	6.7	trace	86.2	6.0	5.8	2.28±0.10	80 <sup>c</sup>
HXLNA75	25/75	60	80	<b>NO</b>	50/50	90.9	6.1	trace	89.3	6.4	4.3	1.95±0.40	80 <sup>c</sup>
HXLNA76	50/50	60	80	<b>NO</b>	50/50	91.1	7.0	trace	91.8	6.9	2.1	2.45±0.24	80 <sup>c</sup>

**Table 5.14: Porosimetry-derived characterisation data for NAD precursor particles and their hypercrosslinked derivatives prepared with and without stirring at 80 °C in DCE/Heptane (50/50). Data computed from nitrogen sorption isotherms and BET theory.**

Sample	BET (m <sup>2</sup> /g)	Langmuir (m <sup>2</sup> /g)	C value	Pore volume (cm <sup>3</sup> /g)	Pore size	
					adsorption (nm)	Desorption (nm)
JAG20	~2	~2	N/A	N/A	N/A	N/A
JAG09	~2	~2	N/A	N/A	N/A	N/A
JAG27	~2	~2	N/A	N/A	N/A	N/A
HXLNA65	925	1420	-118	0.75	4.50	5.11
HXLNA64	940	1431	-127	0.86	5.17	5.56
HXLNA63	611	940	-237	0.54	4.54	4.59
HXLNA74	837	1277	-130	0.69	4.60	5.25
HXLNA75	820	1260	-169	0.81	5.76	6.11
HXLNA76	607	931	-159	0.99	4.67	4.77

### 5.6.8 Effect of EGDMA Content of the Particles

The crosslinker content is an important variable in the production of swellable precursors by NAD polymerisation, but potentially also for the hypercrosslinked products derived therefrom. Unfortunately, raising the crosslinker (EGDMA) content to 6 wt% in the monomer feed had a negative impact upon the quality of the NAD precursor particles (Figure 5.10). Although such precursors could be hypercrosslinked, albeit in a poor yield (Table 5.14), the products were of low porosity (< 30 m<sup>2</sup>/g). Presumably, this observation is reflective of the fact that the precursors do not swell effectively in DCE due to their higher crosslink density. The inefficient consumption of the chlorine in NA55 during hypercrosslinking arises for the very same reason.

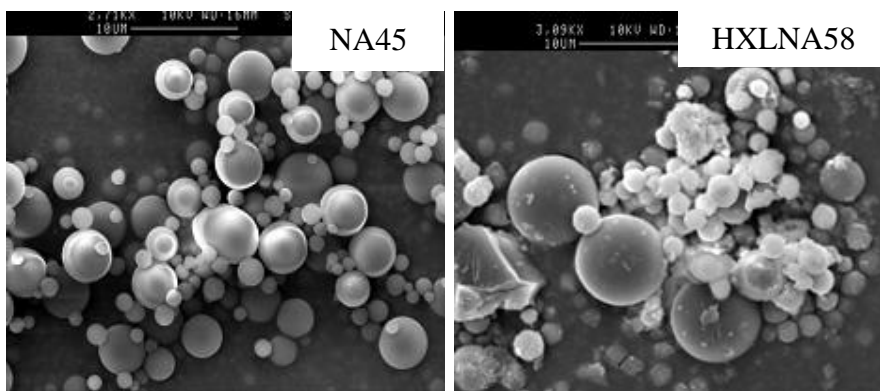


**Figure 5.10: SEM images of poly(St-co-VBC-co-EGDMA) precursor particles prepared by NAD polymerisation with a fixed St/VBC feed ratio (50/50) and fixed EGDMA content (6 wt%); NA45, and the hypercrosslinked derivative prepared without stirring; HXLNA58, in DCE at 80 °C.**

**Table 5.15: Synthesis data for NAD precursor particles and their derivatives hypercrosslinked at 80 °C in DCE. [a] Mass of St +VBC = 100% total monomer feed in the feed. [b] Average particle diameter ± standard deviation (S.D.) calculated from the image analysis in SEM (using Minitab software). [c] For the hypercrosslinked particles relative to the mass of the corresponding NAD (non-hypercrosslinked) precursor particles.**

Sample	St/VBC feed ratio (w/w) <sup>a</sup>	EGDMA Content (wt%)	Swelling time (min)	Temp (°C)	Stirring	DCE/Heptane ratio (v/v)	Microanalysis						Average particle size <sub>b</sub> (µm)	Yield (%)
							Expected (%)			Found (%)				
							C	H	Cl	C	H	Cl		
JAG27	50/50	1	N/A	N/A	N/A	N/A	81.3	6.8	11.5	81.1	6.2	10.7	3.40±0.60	83
NA45	50/50	6	N/A	N/A	N/A	N/A	81.3	6.8	11.5	86.3	7.1	11.4	3.41±0.58	13
HXLNA78	50/50	1	60	80	NO	100/0	91.9	7.7	trace	90.0	6.8	1.5	2.55±0.16	90 <sup>c</sup>
HXLNA58	50/50	6	60	80	NO	100/0	91.9	7.7	trace	67.4	5.4	4.6	3.13±2.05	1 <sup>c</sup>

**Table 5.16: Porosimetry-derived characterisation data for NAD precursor particles and their hypercrosslinked derivatives prepared with different EGDMA contents at 80 °C in DCE. Data computed from nitrogen sorption isotherms and BET theory.**

Sample	BET (m <sup>2</sup> /g)	Langmuir (m <sup>2</sup> /g)	C value	Pore volume (cm <sup>3</sup> /g)	Pore size	
					adsorption (nm)	desorption (nm)
NA45	~2	N/A	N/A	N/A	N/A	N/A
NA45	~2	N/A	N/A	N/A	N/A	N/A
HXLNA78	603	922	-152	0.99	3.04	3.10
HXLNA58	29	47	61	0.06	9.74	7.14

### 5.6.9 Effect of Hypercrosslinking Reaction Time on Specific Surface Area and Chlorine Content

The dependence of the specific surface area and chlorine content of hypercrosslinked polymers with respect to the hypercrosslinking reaction time is depicted in Figure 5.11. As the chlorine content falls the specific areas rises, as chloromethyl residues are converted into methylene bridges. The reaction rate is relatively fast; hypercrosslinked polymers with SSAs in excess of 1000 m<sup>2</sup>/g are delivered in around one hours. The conversion of chloromethyl into methylene bridges can be monitored conveniently by FT-IR spectroscopy (Figure 5.12); as the hypercrosslinking reaction proceeds the absorption bands at 1265 cm<sup>-1</sup> and 676 cm<sup>-1</sup>, which are ascribed to chloromethyl groups, diminish steadily in intensity. After 30 minutes, or so, the rate of loss of chlorine slowed down, since the formation of methylene bridges through hypercrosslinking changed the accessibility of the remaining chloromethyl groups. A similar result was reported by Veverka *et al.*<sup>[8]</sup> Nevertheless, from 30 minutes of reaction time onwards the chlorine content continued to fall and the SSA continued to rise. A hypercrosslinked polymer with an SSA of ~ 1,500 m<sup>2</sup>/g was isolated after a hypercrosslinking time of 1440 minutes (i.e., 24 hours).

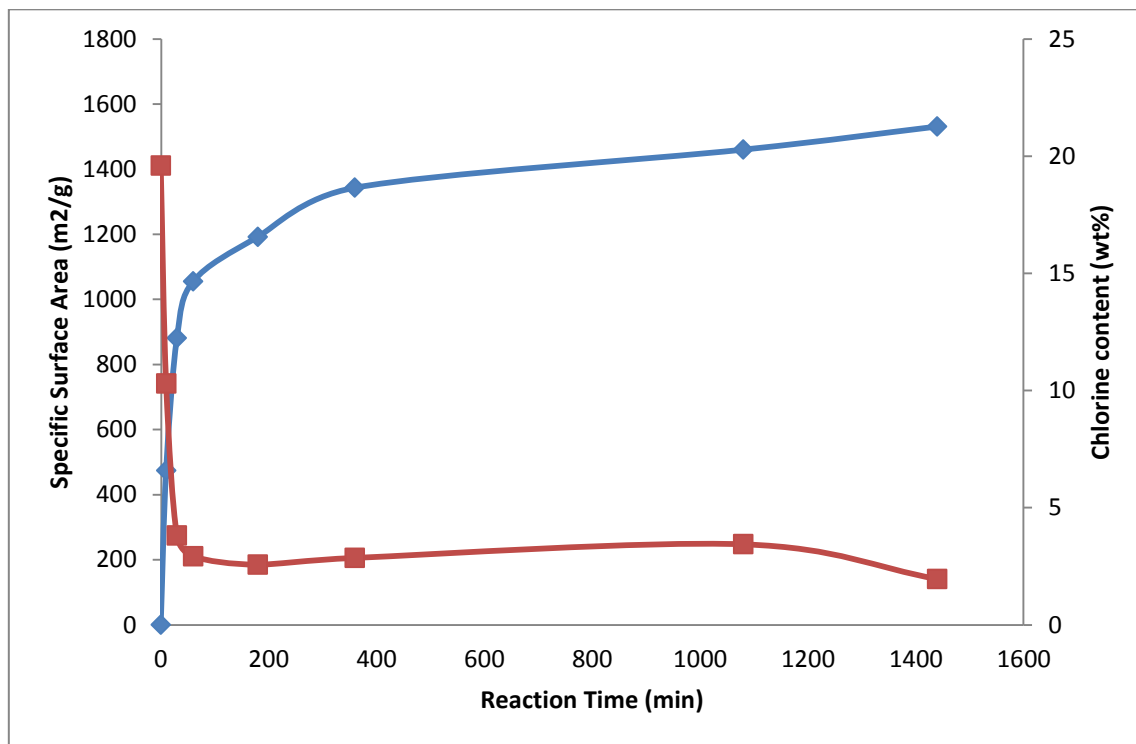


**Figure 5.11: Dependence of the specific surface area (blue line) and chlorine content (red line) of the hypercrosslinked particles on the hypercrosslinking reaction time. HXLNA136 (10 min); HXLNA137a (30 min); HXLNA135a (60 min) HXLNA135b (180 min); XHLNA135c (360 min); HXLJAG23 (1080 min) and HXLNA137b (1440 min).**

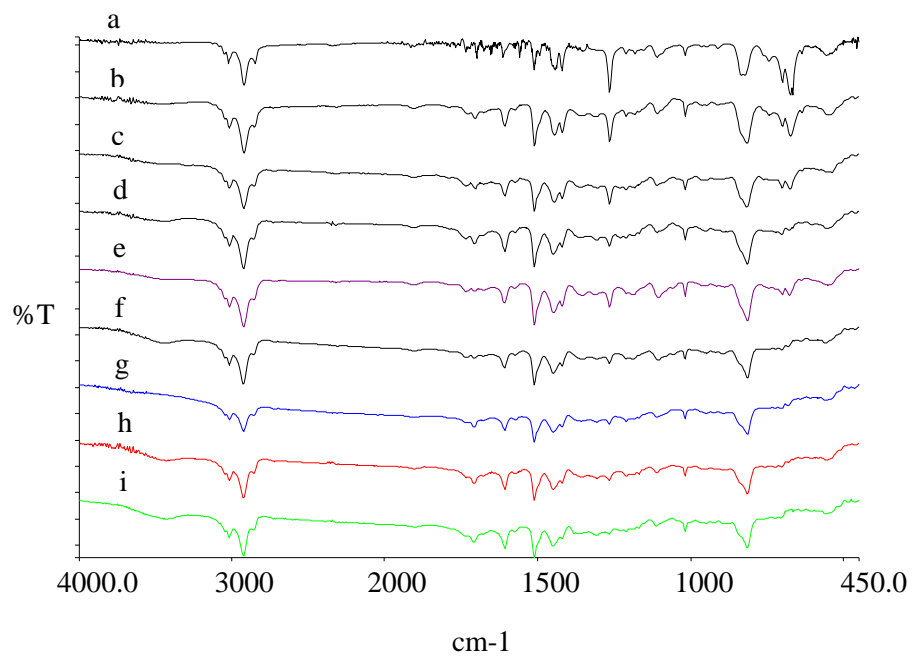


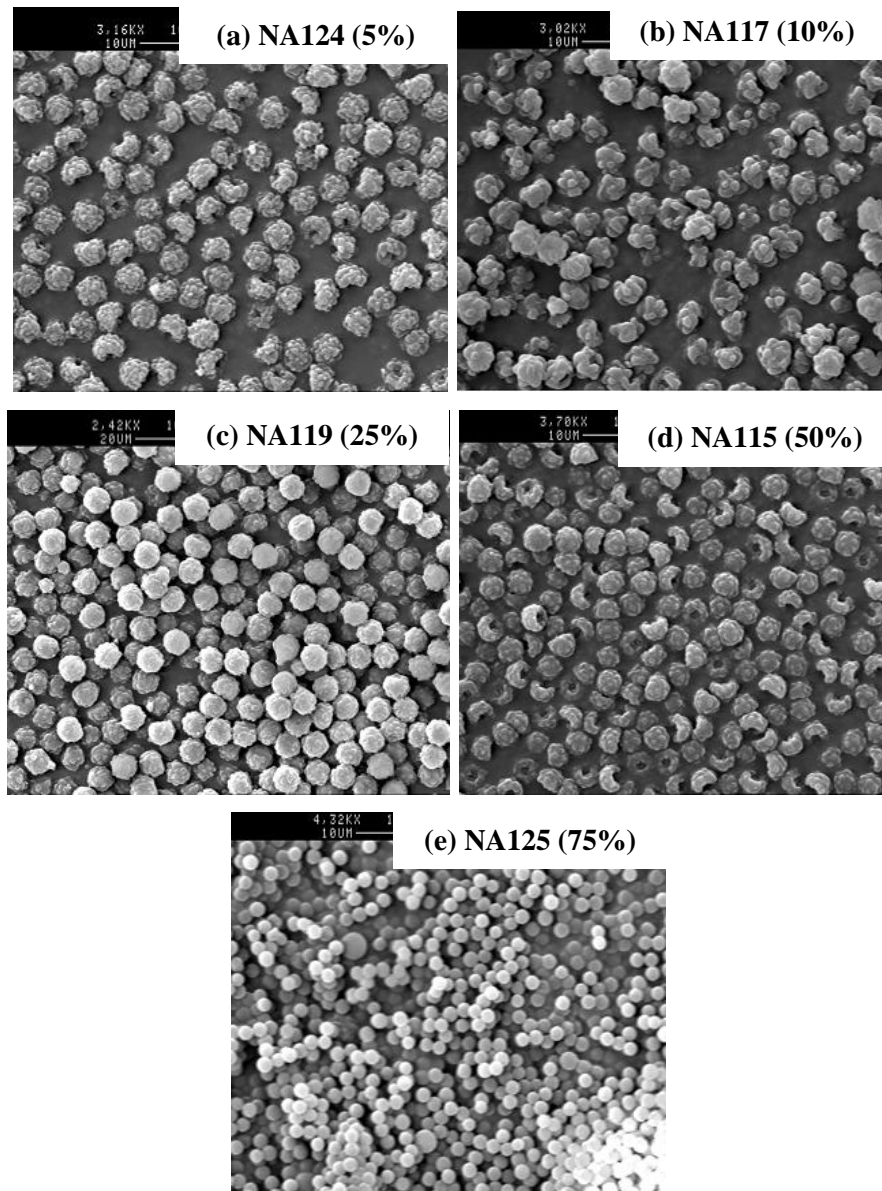
**Figure 5.12: FT-IR spectra of hypercrosslinked particles with fix EGDMA contents (1 wt%) and St/VBC = 10/90 prepared with variable hypercrosslinking reaction times; (a) Precursor (b) 10 min (c) 15 min (d) 30 min (e) 60 min (f) 180 min (g) 360 min (h) 1080 min and (i) 1440 min.**

## 5.7 Hypercrosslinking of Aqueous Dispersion Polymerisation (ADP) Precursor Particles

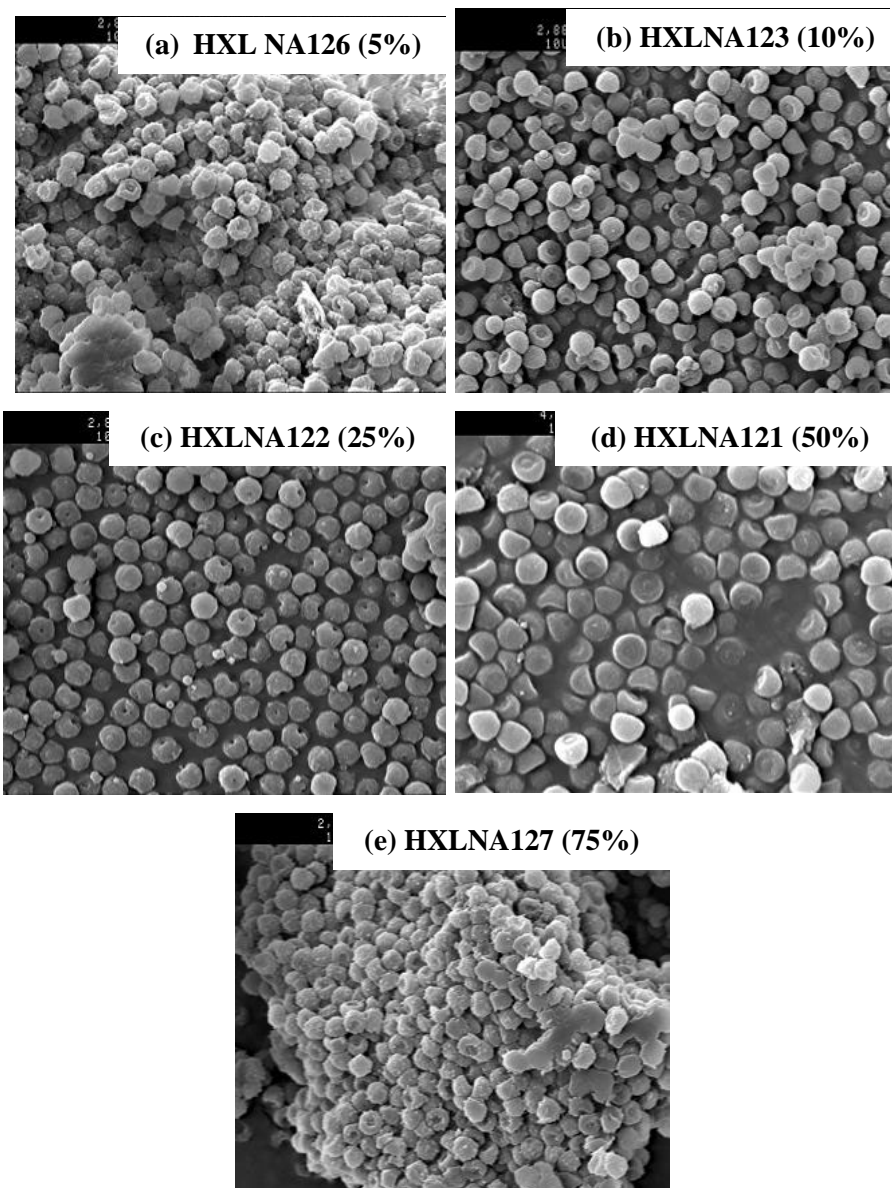
For the precursor particles synthesised by ADP which were described earlier, it was found that when the crosslinker content in the monomer feed was increased up to 1 wt%, then particles with extraordinary raspberry shapes were obtained, as is shown in Figure 5.13. The exception to this was polymer NA125, which was synthesised using 75% VBC in the monomer feed; the surfaces of the NA125 particles were smooth and the particles were spherical. All the particles synthesised by ADP were around 2  $\mu\text{m}$  (Table 5.17). Irrespective of their shape and form, all these particles were hypercrosslinked.

Figure 5.14 shows SEM images of the hypercrosslinked particles obtained upon hypercrosslinking of the swellable ADP precursors. It can be seen that the particles which contained 5% and 75% VBC in the monomer feed, NA124 and NA125, respectively, appeared to be aggregated. However, the particles which had intermediate VBC contents (10%, 25% and 50%) retained their integrity upon hypercrosslinking and were not noticeably aggregated. Some of the particles displayed remarkable surface features. For example, some particles has very striking depressions/holes on their surfaces. It is not at all obvious why these features should exist/persist.

Through nitrogen sorption porosimetry analysis it was found that hypercrosslinked particles based upon ADP precursors had lower SSAs than hypercrosslinked particles based upon NAD precursors (Table 5.17). Unsurprisingly, precursors with lower VBC contents gave rise to hypercrosslinked products with lower SSAs, and precursors with higher VBC contents gave rise to hypercrosslinked products with higher SSAs. SSAs up to  $\sim 800 \text{ m}^2/\text{g}$  were recorded for polymers of this type.



**Figure 5.13: SEM images of swellable poly(St-co-VBC-co-EGDMA) particles prepared by ADP with 1 wt% of EGDMA at varying St/VBC ratios (VBC content in monomer feed is shown in brackets).**



**Figure 5.14: SEM images of hypercrosslinked poly(St-co-VBC-co-EGDMA) particles with 1 wt% of EGDMA at varying St/VBC ratios (VBC content in monomer feed is shown in brackets)**

**Table 5.17: Synthesis data for ADP particles hypercrosslinked at 80 °C in DCE. [a] Mass of St +VBC = 100% total monomer feed in the feed. [b] Average particle diameter  $\pm$  standard deviation (S.D.) calculated from the image analysis in SEM (using Minitab software).[c] For the hypercrosslinked particles relative to the mass of the corresponding ADP (non-hypercrosslinked) precursor particles.**

Sample	St/VBC feed ratio (w/w) <sup>a</sup>	Microanalysis						Average particle size ( m) <sup>b</sup>	Yield (%) <sup>c</sup>
		Expected (%)			Found (%)				
		C	H	Cl	C	H	Cl		
HXLNA126	95/05	88.8	8.2	trace	86.2	7.2	0.8	2.09 $\pm$ 0.20	40
HXLNA123	90/10	91.9	7.7	trace	86.7	7.2	1.0	2.02 $\pm$ 0.12	50
HXLNA122	75/25	89.1	7.4	trace	84.3	6.8	1.8	2.19 $\pm$ 0.35	60
HXLNA121	50/50	89.0	7.1	trace	85.5	7.0	2.2	1.53 $\pm$ 0.10	90
HXLNA127	25/75	76.3	6.5	trace	83.5	6.5	2.3	2.10 $\pm$ 0.30	77

**Table 5.18: Porosimetry-derived characterisation data for swellable ADP precursor and their derivatives which were hypercrosslinked at 80 °C in DCE. Data computed from nitrogen sorption isotherms and BET theory.**

Sample	St/VBC feed ratio (w/w) <sup>a</sup>	BET (m <sup>2</sup> /g)	Langmuir (m <sup>2</sup> /g)	Pore volume (cm <sup>3</sup> /g)	Pore size (nm)	
					Adsorption	Desorption
NA124	95/05	N/A	N/A	N/A	N/A	N/A
NA117	90/10	N/A	N/A	N/A	N/A	N/A
NA119	75/25	N/A	N/A	N/A	N/A	N/A
NA115	50/50	N/A	N/A	N/A	N/A	N/A
NA125	25/75	N/A	N/A	N/A	N/A	N/A
HXLNA126	95/05	0.8	0.9	3.58	N/A	N/A
HXLNA123	90/10	0.1	0.2	3.99	N/A	N/A
HXLNA122	75/25	3	4	10.3	3.12	3.82
HXLNA121	50/50	547	744	2.44	3.58	2.97
HXLNA127	25/75	803	1100	3.58	5.07	3.91

## 5.8 Optimisation

Thus far, various strategies have been explored in an attempt to retain the high quality of swellable precursor particles through a hypercrosslinking process, including exploring the effects of stirring and changes to the swelling solvent. Disappointingly, this was met with only limited success, therefore a radically different strategy was evolved and implemented. The new strategy aimed to partially hypercrosslink the precursors in a non-swelling solvent, in order to stabilise the particles, and then to complete the hypercrosslinking process in a good solvent. This strategy is outlined schematically in Figure 5.15. Here, the NAD precursor particles are partially hypercrosslinked in hexane using a low amount of  $\text{FeCl}_3$ ; after isolation, these partially hypercrosslinked particles and then hypercrosslinked fully in DCE using a stoichiometric amount of catalyst.

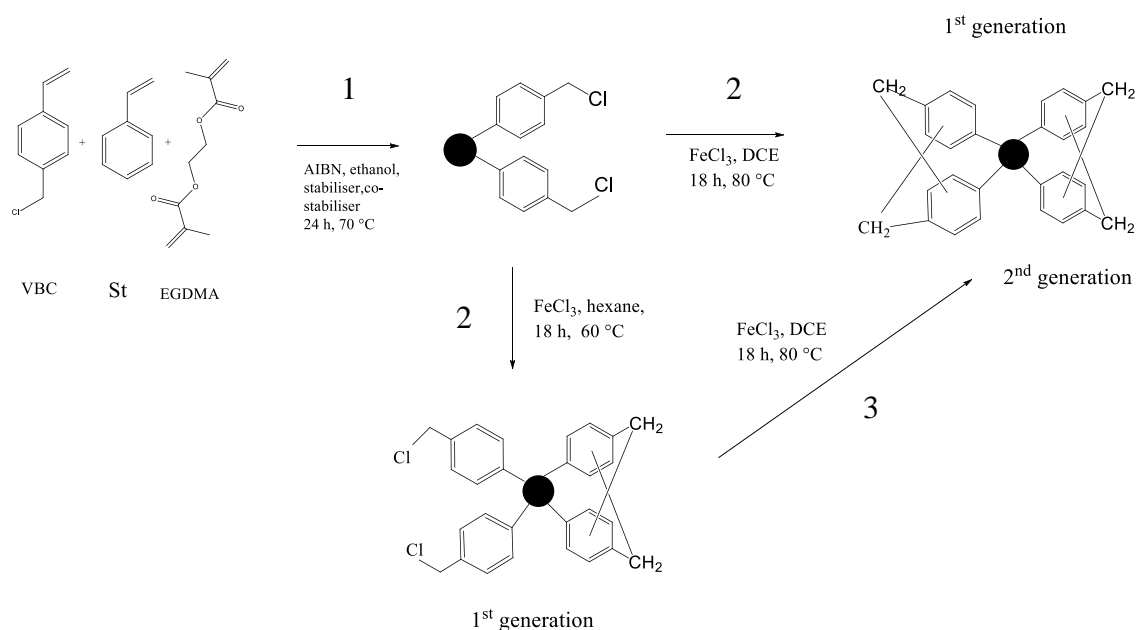


**Figure 5.15: Schematic representation of a one-step and a two-step hypercrosslinking process.**

### 5.8.1 Partial Hypercrosslinking of Swellable Precursors

In order to test the above hypothesis/strategy, a few attempts were made. In an initial attempt, the partial hypercrosslinking reactions were performed in heptane at either 80 °C or at room temperature (PHXLNA187 and PHXLNA188, respectively) in the presence of 2 mol% FeCl<sub>3</sub> (relative to number of moles of chloromethyl residues). Pleasingly, in Figure 5.16 it can be seen that the particles retained their spherical shape during the partial hypercrosslinking process even although there were occasional signs of aggregation. This was a very encouraging outcome. FT-IR spectroscopy revealed the expected drop in intensity of chloromethyl-derived bands (at 1265 cm<sup>-1</sup> and 673 and 702 cm<sup>-1</sup> Figure 5.18; (a) and (b)), and the partial hypercrosslinking gave beaded products which remained swellable in DCE, as was planned. Unfortunately, as well as being swellable the partially hypercrosslinked particles appeared to be soluble to some extent. The best results, in terms of particle quality, were obtained when the partial hypercrosslinking reaction was performed at ambient temperatures. The final products were non-porous in the dry-state; the SSAs of the partially hypercrosslinked particles were ~2 m<sup>2</sup>/g.

The alcohols ethanol and methanol were also tested as solvent media in which to perform the partial hypercrosslinking reaction, because both methanol and ethanol are non-solvents for polystyrene. Unfortunately, no hypercrosslinking was observed in either solvent, thus acetylacetone (acac) in methanol was used instead to help to solubilise the catalyst. Interestingly, with acac as an additive, partial hypercrosslinking of the particles was observed. As is depicted in Figure 5.16 (PHXLNA189), the partially hypercrosslinked particles obtained through this method were of very good quality. The hypercrosslinking reaction could be monitored in the usual manner using FT-IR spectroscopy. In Figure 5.17 (c), it can be seen that the intensities of the bands at 1265 cm<sup>-1</sup>, 702 and 673 cm<sup>-1</sup> are reduced upon hypercrosslinking, and that this structural change is reflected by the elemental microanalysis data (Table 5.19). Unfortunately, when the partially hypercrosslinked products were placed into contact with DCE they still swelled extensively and dissolved gradually. This evidence suggests that even the percentage of FeCl<sub>3</sub> was increased to up to 16.5 mol% (relative to the number of moles of chloromethyl

residues), the conversion of the chloromethyl groups to methylene bridges is still too low to stabilise the particles in DCE. Jiang and co-workers<sup>[9]</sup> reported that FeCl<sub>3</sub> was a superior catalyst for the alkylation of small molecules when in the presence of acac. However, in the present study, the partial hypercrosslinking process was not sufficiently advanced to stabilise the particles. The SSAs of these partially hypercrosslinked particles was ~2 m<sup>2</sup>/g.

Ahn *et al.*<sup>[10]</sup> reported upon successful hypercrosslinking in hexane. Their hypercrosslinked products had respectable specific surface area (> 600 m<sup>2</sup>/g). Thus, hexane was screened as a solvent in the present work. Accordingly, partial hypercrosslinking reactions were performed in hexane, either at ambient temperature or at 60 °C, in the presence of 11 mol% FeCl<sub>3</sub> (relative to the number of moles or chloromethyl residues). Very pleasingly now, the final products isolated from both reactions were of very good quality and in a spherical form (Figure 5.16; PHXLNA190 and PHXLNA191). When the partial hypercrosslinking reaction was carried out at ambient temperature, the colour of the particles was found to change from white to pale brown, whereas when the same reaction was carried out at 60 °C the colour of the particles changed from white to brown. From the FT-IR spectra (Figure 5.17 (d) and (e)), it can be seen that the intensities of the diagnostic bands at 1265, 702 and 673 cm<sup>-1</sup> diminish most markedly when the reaction was performed at 60 °C. A similar picture emerges when the elemental microanalysis data is analysed; for PHXLNA190, the chlorine content was reduced by 21% upon reaction, however the chlorine content fell by 50% when the reaction was carried out at 60 °C (PHXLNA191). The hypercrosslinking reaction is therefore faster at the higher temperature, and by a measurable amount.

For PHXLNA194, the chlorine content was decreased by ~19% when the reaction was allowed to proceed for 30 minutes at room temperature, but when the NAD precursor particles were partially hypercrosslinked at the same temperature but with a much longer reaction time (up to 18 hours), almost 44% of the chlorine groups were successfully converted to methylene bridges (Table 5.19). Thus, although

slower hypercrosslinking was observed at room temperature, methylene bridge formation still ensued in an efficient manner.

In all cases, the particles were non-porous in the dry state (the SSAs were around 2 m<sup>2</sup>/g), the yields were satisfactory and the particle size ranges of the partially hypercrosslinked products were similar to the precursors (Table 5.19). Most importantly, however, was the observation that when the final products were placed into contact with DCE, the particles were found to be stable. Thus, it has been possible to obtain particles which are stable in DCE using this partial hypercrosslinking strategy, and these partially hypercrosslinked particles were taken forward to reactions involving full/exhaustive hypercrosslinking.

**Table 5.19: Synthesis data for the partial hypercrosslinking of swellable precursors in non-swelling solvents. [a] percentage of FeCl<sub>3</sub> used relative to the number of moles of chloromethyl residues.**

Sample	Method	Solvent	FeCl <sub>3</sub> (mol%) <sup>a</sup>	Remarks
PHXLNA187	The precursor particles were left contact with heptane for 1 h Heptane containing FeCl <sub>3</sub> then added into reaction flask Reaction was allowed to proceed at 80 °C for 18 h	Heptane	2	Soluble in DCE Spherical Pale brown Some particles coagulated
PHXLNA188	The precursor particles were left in contact with Heptane for 1 h Heptane containing FeCl <sub>3</sub> then added into reaction flask Reaction was allowed to proceed at RT for 18 h	Heptane	2	Soluble in DCE Spherical Pale brown
PHXLNA189	Lewis acid-assisted Brønsted acid (LBA) FeCl <sub>3</sub> and acac was added into a mixture of precursor and methanol The reaction was allowed to proceed at RT for 18 h <sup>[9]</sup>	Methanol	16.5	Soluble in DCE Spherical Pale brown
PHXLNA190	The precursor particles were left in contact with hexane for 2 h Then the mixture was cooled in an ice bath before FeCl <sub>3</sub> added FeCl <sub>3</sub> left to disperse uniformly in the mixture for 2 h Then the reaction was allowed to proceed at RT for 18 h <sup>[10]</sup>	Hexane	11	Disperse in DCE Spherical Pale brown

**Table 5.19: Synthesis data for the partial hypercrosslinking of swellable precursors in non-swelling solvents. [a] percentage of FeCl<sub>3</sub> used relative to the number of moles of chloromethyl residues. (Cont).**

Sample	Method	Solvent	FeCl <sub>3</sub> (mol%) <sup>a</sup>	Remarks
PHXLNA191	The particles were left in contact with hexane for 2 h Then the mixture was cooled in an ice bath before FeCl <sub>3</sub> added FeCl <sub>3</sub> left to disperse uniformly in the mixture for 2 h Then the reaction was allowed to proceed at 80 °C for 18 h <sup>[10]</sup>	Hexane	11	Disperse in DCE Spherical Brown
PHXLNA194	The particles were left in contact with hexane for 2 h Then the mixture was cooled in an ice bath before FeCl <sub>3</sub> added FeCl <sub>3</sub> left to disperse uniformly in the mixture for 2 h Then the reaction was allowed to proceed at RT for 30 min <sup>[10]</sup>	Hexane	11	Disperse in DCE Spherical Pale brown
PHXLNA195	The particles were left in contact with hexane for 2 h Then the mixture was cooled in an ice bath before FeCl <sub>3</sub> added FeCl <sub>3</sub> left to disperse uniformly in the mixture for 2 h Then the reaction was allowed to proceed at RT for 18 h <sup>[10]</sup>	Hexane	5	Disperse in DCE Spherical Pale brown

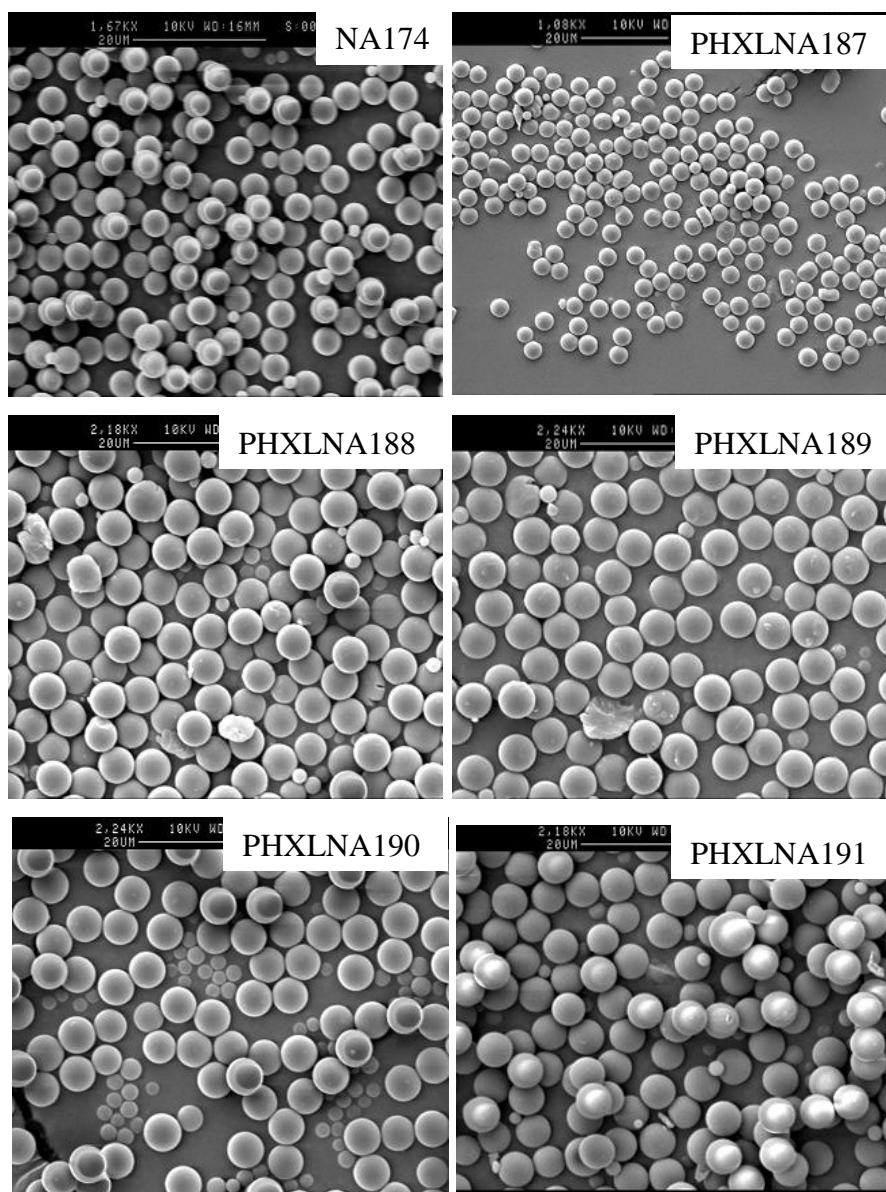


**Figure 5.16:** SEM images of NAD precursor particles (NA174) and their partially hypercrosslinked derivatives (PHXLNA187-PHXLNA191) prepared using different non-swelling solvent in the partial hypercrosslinking step. (a) PHXLNA187-PHXLNA188 in heptane (2 wt% of  $\text{FeCl}_3$ ), (b) PHXLNA189 in methanol (16.5 wt% of  $\text{FeCl}_3$ ) and (c) PHXLNA190-PHXLNA191 in hexane (11 wt% of  $\text{FeCl}_3$ ).

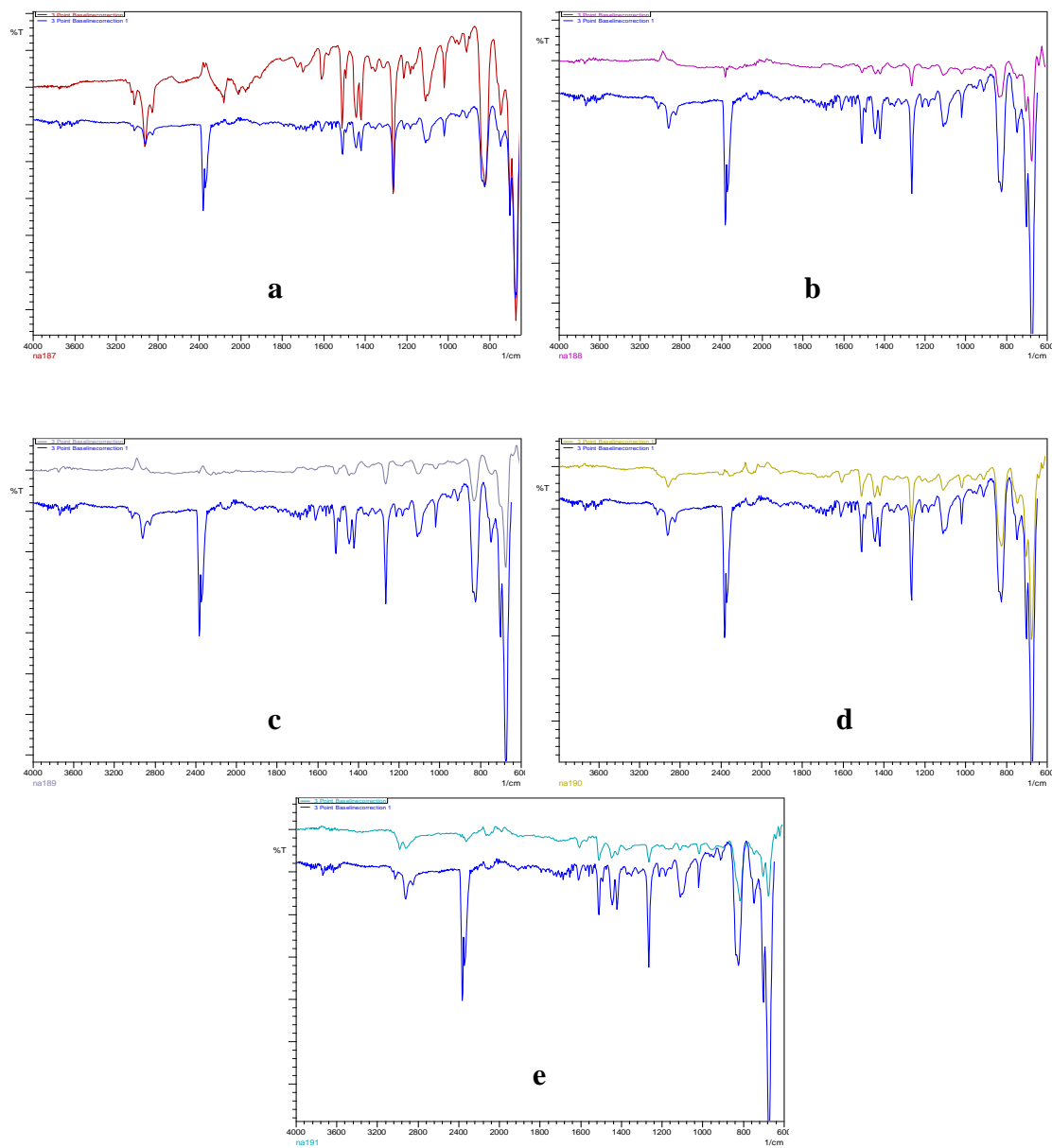


**Figure 5.17:** FT-IR spectra of NAD precursor particles (blue line) and partially hypercrosslinked particles prepared using different synthesis approaches in different non-swelling solvents. [a] NA174 and PHXLNA187, [b] NA174 and PHXLNA188, [c] NA174 and PHXLNA189, [d] NA174 and PHXLNA190 and [e] NA174 and PHXLNA191.

**Table 5.20: Characterisation data for polymer synthesised *via* partial hypercrosslinking reactions. [a] % Cl content after reaction. [b] Computed from nitrogen sorption isotherms and BET theory. [c] For the hypercrosslinked particles relative to the mass of the corresponding NAD (non-hypercrosslinked) precursor particles. [d] NAD precursor particles. [e] % Cl content before reaction.**

Sample	Cl content (%) <sup>a</sup>	SSA (m <sup>2</sup> /g) <sup>b</sup>	Particle size range (μm)	Yield (%) <sup>c</sup>
NA174 <sup>d</sup>	22.4 <sup>e</sup>	~2	1.35-4.26	85
PHXLNA187	13.7	~2	1.45-4.28	81
PHXLNA188	19.5	~2	1.68-4.26	83
PHXLNA189	19.0	~2	1.35-4.18	82
PHXLNA190	17.7	~2	1.52-4.24	84
PHXLNA191	11.2	~2	1.43-4.42	78
NA171 <sup>d</sup>	23.4 <sup>e</sup>	~2	2.91-3.82	89
PHXLNA194	18.9	~2	2.91-3.60	96
PHXLNA195	13.1	~2	2.91-3.90	93

### 5.8.2 Full/Exhaustive Hypercrosslinking of Partially Hypercrosslinked Particles

Since partially hypercrosslinked particles which were stable when in contact with DCE had been successfully produced, the next step was to expose the partially hypercrosslinked particles to an exhaustive hypercrosslinking process, in an attempt to introduce porosity whilst at the same time preserving particle quality. In this regard, a series of partially hypercrosslinked polymers were fully hypercrosslinked using a typical hypercrosslinking method. First of all, PHXLNA190, a partially hypercrosslinked polymer which contained 17.7% of chlorine, was fully hypercrosslinked in DCE (HXLNA193). As is shown in Figure 5.18 and Table 5.20, particles of good quality were produced, although there was still some observable decrease in quality. Loss of chloromethyl groups through hypercrosslinking could once again be followed using FT-IR spectroscopy (Figure 5.18, light blue line). The bands in the FR-IR spectrum at 673, 702 and 1265 cm<sup>-1</sup> diminish in intensity upon hypercrosslinking. From the elemental microanalysis results (Table 2.20), it can be seen that around 21% of the chloromethyl

groups are consumed by the end of the partial hypercrosslinking reaction, and around 54% of the chloromethyl groups by the end of the second hypercrosslinking reaction.

The particle colour changed from white to pale brown as a result of the partial hypercrosslinking reaction, and from pale brown to dark brown as a result of the full/exhaustive hypercrosslinking reactions. These colour changes are believed to arise due to the presence of catalyst residues in the reaction products. In many respects colour in the final products is not important, provided that they are porous, thus we were extremely pleased to find that the SSA of the particles rose dramatically as a result of the second hypercrosslinking step, from ~ 2 m<sup>2</sup>/g for the partially hypercrosslinked material to 1165 m<sup>2</sup>/g for the fully hypercrosslinked material (Table 5.20). The yields of products were also highly satisfactory.

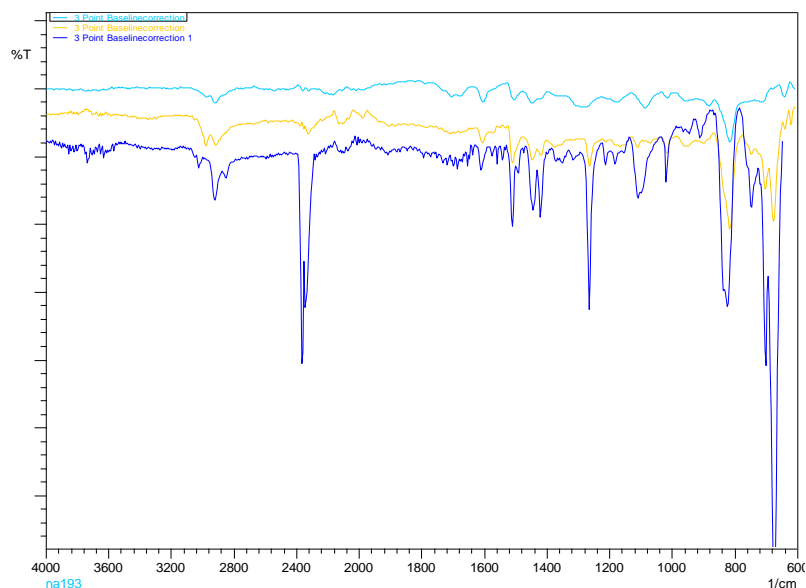


**Figure 5.18: FT-IR spectra of NAD precursor particles (blue line), their partially hypercrosslinked derivatives which were hypercrosslinked at RT (brown line) and their fully hypercrosslinked derivatives (pale blue line).**

Second of all, PHXLNA191, which was a partially hypercrosslinked polymer which had been partially hypercrosslinked at 60 °C, was hypercrosslinked fully. As can be seen in

Figure 5.19 the fully hypercrosslinked product was of high quality, although the quality was still lower than that of the swellable precursor. From the FTIR spectrum (Figure 5.20, pink line), it can be seen that the bands at 673, 702 and 1265  $\text{cm}^{-1}$  diminish in intensity upon hypercrosslinking. The chlorine content of the product also falls compared to the starting material(s) (Table 5.21). Once again, the colour of the particles was changed to dark brown, and nitrogen sorption porosimetry showed that porosity has been imparted into the particles ( $\text{SSA} = 571 \text{ m}^2/\text{g}$ ; Table 5.21). The SSA of HXLNA192 is lower than the SSA of HXLNA193, presumably because the partial hypercrosslinking of the former was more extensive than the partial hypercrosslinking of the latter. This suggestion is borne out by the elemental microanalysis data. Nevertheless, the yield and the quality of the particles was again highly satisfactory.

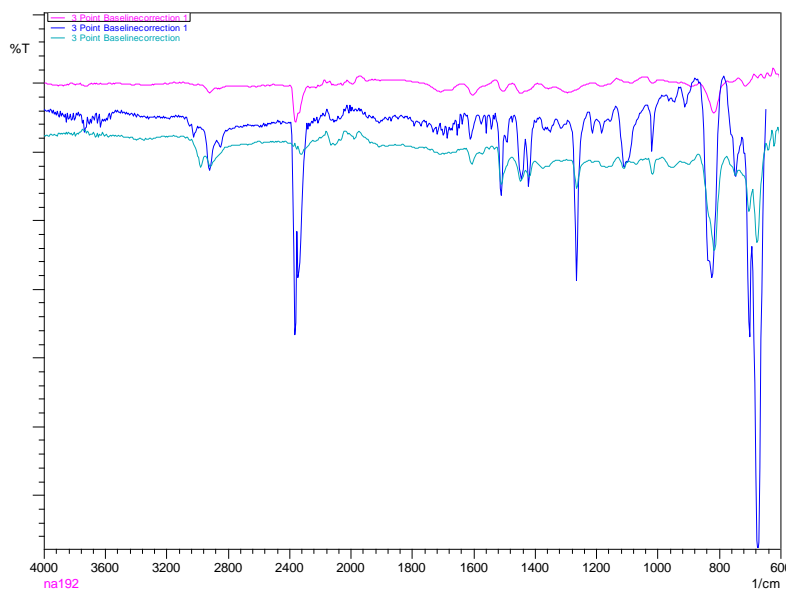


**Figure 5.19: FT-IR spectra of NAD precursor particles (blue line), their partially hypercrosslinked derivatives where the partial hypercrosslinking has been conducted at 60 °C (green line), and the fully hypercrosslinked derivative (pink line).**

Third of all, the effect of changing the reaction conditions for the full/exhaustive hypercrosslinking step was explored using the same common starting material (PHXLANA194). When the full/exhaustive hypercrosslinking step was carried out at 80

°C for 18 hours (HXLNA196), the chlorine content fell to 1.5% and the SSA increased dramatically to 1325 m<sup>2</sup>/g. In contrast, when the full/exhaustive hypercrosslinking step was carried out at room temperature for 24 hours (HXLNA199), the chlorine content fell to 8.1% and the SSA rose to below 1,000 m<sup>2</sup>/g, which was indicative of less extensive hypercrosslinking. Nevertheless, it is interesting to note that high SSAs can be imparted into such products even at room temperature.

Finally, for the case of PHXLNA195, which contained 13.1% of chlorine and was non-porous in the dry state, it could be transformed into fully a polymer (HXLNA197) with high porosity (1258 m<sup>2</sup>/g) by hypercrosslinking at 80 °C for 18 hours. The particle quality is also excellent, thus a robust synthetic strategy would appear to be in place.

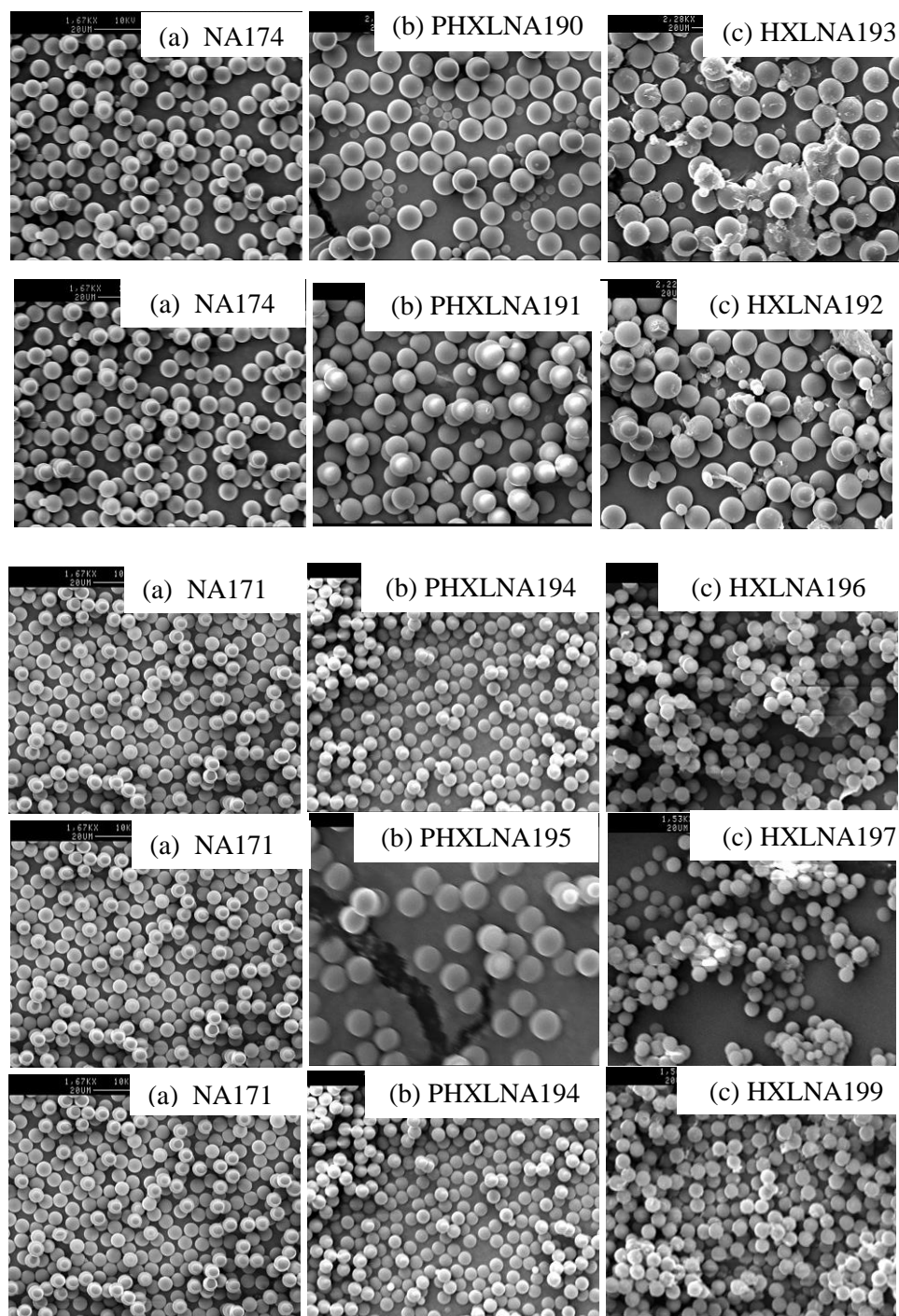


**Figure 5.20: SEM images of NAD precursor particles, their partially hypercrosslinked derivatives and their fully hypercrosslinked derivatives. (a) NA174 and NA 171- NAD precursor particles. (b) PHXLNA190 (11 wt% of FeCl<sub>3</sub>, RT, 18 h), PHXLNA191 (11 wt% of FeCl<sub>3</sub>, 80 °C, 18 h), PHXLNA194 (11 wt% of FeCl<sub>3</sub>, RT, 30 min), PHXLNA195 (5 wt% of FeCl<sub>3</sub>, RT, 18 h) - partially hypercrosslinked particles, and (c) HXLNA193 HXLNA192, HXLNA196, HXLNA197 and HXLNA199 - fully hypercrosslinked particles.**

**Table 5.21: Characterisation data for swellable precursors, their partially hypercrosslinked derivatives and their fully hypercrosslinked derivatives. [a] Porosity data computed from nitrogen sorption isotherms and BET theory. [b] For the partially hypercrosslinked particles relative to the mass of the corresponding NAD (non-hypercrosslinked) precursor particles, or for the fully hypercrosslinked particles relative to the mass of the corresponding partially hypercrosslinked particles.**

	Sample	SSA (m <sup>2</sup> /g) <sup>a</sup>	Pore volume (cm <sup>3</sup> /g)	Pore size		Cl content (%)	Particle size range (µm)	Yield (%) <sup>b</sup>	Colour
				Adsorption (nm)	Desorption (nm)				
1 <sup>st</sup> step	NA174	~2	N/A	N/A	N/A	22.4	1.35-4.26	85	White
2 <sup>nd</sup> step	PHXLNA190	~2	N/A	N/A	N/A	17.7	160.4-25	84	Pale brown
3 <sup>rd</sup> step	HXLNA193	1165	0.63	3.48	3.05	9.6	1.35-4.37	87	Dark brown
1 <sup>st</sup> step	NA174	~2	N/A	N/A	N/A	22.4	1.35-4.26	85	White
2 <sup>nd</sup> step	PHXLNA191	~2	N/A	N/A	N/A	11.2	1.43-4.42	78	Brown
3 <sup>rd</sup> step	HXLNA192	571	0.99	2.71	3.63	7.9	1.35-4.21	90	Dark brown
1 <sup>st</sup> step	NA171	~2	N/A	N/A	N/A	23.4	2.91-3.82	89	White
2 <sup>nd</sup> step	PHXLNA194	~2	N/A	N/A	N/A	18.9	2.91-3.60	96	Pale brown
3 <sup>rd</sup> step	HXLNA196	1324	0.71	3.39	2.73	1.5	2.91-3.90	90	Brown
1 <sup>st</sup> step	NA171	~2	N/A	N/A	N/A	23.4	2.91-3.82	89	White
2 <sup>nd</sup> step	PHXLNA194	~2	N/A	N/A	N/A	18.9	2.91-3.60	96	Pale brown
3 <sup>rd</sup> step	HXLNA199	943	0.54	3.64	2.88	8.1	2.91-3.97	85	Brown
1 <sup>st</sup> step	NA171	~2	N/A	N/A	N/A	23.4	2.91-3.82	89	White
2 <sup>nd</sup> step	PHXLNA195	~2	N/A	N/A	N/A	13.1	2.66-3.63	93	Pale brown
3 <sup>rd</sup> step	HXLNA197	1258	0.87	0.63	0.62	3.0	2.91-3.95	93	Brown

Note: (a) Reaction conditions in partial hypercrosslinking step - PHXLNA190 (11% of FeCl<sub>3</sub>, RT, 18 h); PHXLNA191 (11% of FeCl<sub>3</sub>, 80 °C, 18 h); PHXLNA194 (RT, 30 min); PHXLNA195 (5% of FeCl<sub>3</sub>, RT, 18 h)

179 (b) Reaction conditions in full hypercrosslinking step - HXLNA193 (80 °C, 18 h); HXLNA192 (80 °C, 18 h); HXLNA196 (80 °C, 18 h); HXLNA197 (80 °C, 18 h); HXLNA199 (RT, 24 h)

## 5.9 Conclusions

In this Chapter, which is one of the most important Chapters in the entire thesis, swellable precursor particles were converted into highly porous polymer particles using Friedel-Crafts alkylation-mediated hypercrosslinking reactions. These hypercrosslinking reactions were fast (highly porous polymer networks were delivered in a few minutes) and efficient (the yields of products were very high). Hypercrosslinked products with specific surface areas approaching  $2,000 \text{ m}^2/\text{g}$  were prepared readily in this way.

Unfortunately, synthesising the hypercrosslinked products in a well-defined beaded format, where the particle size distributions were narrow, was found to be a far from trivial task, and a lot of time and effort was invested in this endeavour. When swellable precursor particles, which had been synthesised by dispersion polymerisation, were subjected to classical hypercrosslinking conditions, the hypercrosslinked products were normally polydisperse, showed signs of aggregation and signs of contamination, even when the swellable precursor particles were of highly quality. This deterioration in particle quality was ascribed to a soluble portion of the swellable precursors dissolving out of the swellable particles during hypercrosslinking, leading to both particle-particle couple (*i.e.*, particle aggregation) and surface contamination of particles.

In an attempt to improve the quality of the hypercrosslinked particles a number of experimental variables were studied, including the hypercrosslinking reaction temperature, the effect of stirring, the nature of the swelling solvent and the crosslink density of the swellable precursor particles. Unfortunately, and in spite of many experiments, it was not possible to produce high quality particles in a reliable manner. Nevertheless, the following conclusions could be drawn from this extensive study: 1) Stirring during hypercrosslinking is generally better than hypercrosslinking without stirring; 2) A highly compatible swelling solvent (DCE) yields hypercrosslinked polymers which are more porous than those polymers synthesised in the presence of a less compatible (binary) solvent (DCE/heptane); 3) Raising the hypercrosslinking temperature noticeably increased the rate of methylene bridge formation; 4) Swellable

precursors of higher crosslink density (*e.g.*, 6% EGDMA) were found to retain the quality of the particles better than swellable precursors of lower crosslink density, however, the SSAs of such hypercrosslinked polymers were low, relatively speaking. 5) Swellable particles produced by ADP delivered hypercrosslinked products with lower SSAs than their NAD counterparts, probably due to the lower chloromethyl contents of the precursors.

With the failure of the systematic study to deliver uniformly-sized hypercrosslinked particles, an alternative synthetic strategy was devised. This synthetic strategy which was evolved involved the partial hypercrosslinking of swellable precursor using a sub-stoichiometric amount of Friedel-Crafts catalyst in a non-swelling solvent. The purpose of this step was to stabilise the particles before placing them into a swelling solvent. With the partially hypercrosslinked particles in hand, they were thereafter converted into fully hypercrosslinked particles by bringing them into contact with stoichiometric amounts of catalyst in a swelling solvent. Very pleasingly, not only could hypercrosslinked products with SSAs well in excess of 1,000 m<sup>2</sup>/g be produced in this way, but the particle quality was also very good. The particles were isolated in beaded form and had narrow particle size distribution. This research breakthrough paves the way for the synthesis of functionalised hypercrosslinked polymers in a well-defined beaded form, and this subject is the focus of the following two chapters in this thesis.

## References

- [1] Q. Liu, *Macromol. Chem. Phys.* **2010**, *211*, 1012–1017.
- [2] V. A. Davankov, M. M. Llyn, M. P. Tsyurupa, G. I. Timofeeva and L. V. Dubrovina, *Macromolecules* **1996**, *29*, 8398-8402.
- [3] D. C. Sherrington, *Chem. Commun.* **1998**, 2275-2285.
- [4] S. Shen, X. Zhang and L. Fan, *Mater. Lett.* **2008**, *62*, 2392-2394.
- [5] N. Fontanals, R. M. Marcé, P. A. G. Cormack, F. Borrull and D. C. Sherrington, *J. Chromatogr. A* **2008**, *1191*, 118-123.
- [6] Q. Liu, L. Wang, A. Xiao, H. Yu, Q. Tan, J. Ding and G. Ren, *J. Phys. Chem. C* **2008**, *112*, 13171–13174.
- [7] J.-H. Ahn, J.-E. Jang, C.-G. Oh, S.-K. Ihm, J. Cortez and D. C. Sherrington, *Macromolecules* **2006**, *39*, 627–632.
- [8] P. Veverka and K. Jeřábek, *React. Funct. Polym.* **1999**, *41*, 21-24.
- [9] Z. Y. Jiang, J. R. Wua, L. Lia, X. H. Chena, G. Q. Laia, J. X. Jianga, Y. Luc and L. W. Xua, *Cent. Eur. J. Chem.* **2010**, *8*, 669-673.
- [10] J. H. Ahn, J. E. Jang, C. G. Oh, S. K. Ihm, J. Cortéz and D. C. Sherrington, *Macromolecules* **2006**, *39*, 627-631.

***CHAPTER SIX<sup>[1-2]</sup>***

**6.0 Summary**

Sulfonated, hypercrosslinked (HXLNAD-SCX) polymers have been prepared by treating polymeric precursors with concentrated sulfuric acid (95-97%), in order to produce resins with strong cation-exchange character. The presence of sulfonic acid groups was verified by infrared spectroscopy, and the IEC of the polymers quantified by acid-base titrations. The effect of reaction time and the concentration of the sulfonating agent on the properties of the S-HXL polymers were examined. Varying the reaction time, from 3 hours to 18 hours, and varying the concentration of sulfuric acid, was found to influence the IEC as well as the specific surface area of the polymers. Although side-reactions were apparent in some of these reactions, at shorter reaction times and lower concentrations of sulfuric acid polymers with satisfactory IEC and specific surface areas were still obtained. Optimised sulfonation conditions were applied to the production of S-HXL polymers with varying specific surface areas, and interesting and useful products produced.

**6.1 Introduction to Strong Cation-Exchange Resins**

Strong cation-exchange (SCX) resins typically derive their functionality from the presence of sulfonic acid groups. The ionisation state of this type of resin is independent of pH across a wide pH range, therefore they can operate at most pH values and splits salts, but they do require substantial amounts of regenerant, achieved by contacting with strong acid solution after exhaustion. This resin is the resin of choice for many applications in solid-phase extraction (SPE) applications. Also, they can be exploited as heterogeneous catalysts, and in this context offer several distinct advantages over homogeneous acid catalysts.

**6.2 Aims of Work**

In this work, the aims have been focused on the preparation of sulfonated hypercrosslinked polymers (strong cation-exchange resins) with tuneable ion-

exchange capacity (IEC) and specific surface area. To achieve this, hypercrosslinked polymers were treated with concentrated sulfuric acid as a sulfonating agent, with an important variable being the reaction time. The resultant sulfonated particles were characterised using SEM, acid-base titrations, nitrogen sorption porosimetry and FT-IR spectroscopy.

## **6.3 Experimental**

### **6.3.1 Materials**

The reagents used in the sulfonation reactions were 1,2-dichloroethane (DCE) (99.8% grade) and concentrated sulfuric acid (95-97%), both supplied by Sigma-Aldrich, and distilled water. All reagents were used as received.

### **6.3.2 Equipment**

Sulfonation reactions were performed in a three-necked, round-bottomed flask fitted with condenser, overhead stirrer and a two-blade, PTFE-type stirrer. The reaction vessel was immersed in a thermostatically-controlled oil bath.

### **6.3.3 Characterisation**

The characterisation methods used are as detailed below.

### **6.3.4 Scanning Electron Microscopy (SEM)**

SEM was carried out using a Cambridge S-90. Micrographs were acquired at an accelerating voltage of 10.0 kV. A thin layer of sample was deposited onto a steel stub, which had been coated previously with conductive (copper), double-sided adhesive tape. Gold coating of the immobilised sample was then carried out. Coated samples were placed inside the SEM chamber and a vacuum was applied; this vacuum evacuated the chamber of any small particles that may have deflected the electrons and affected the SEM image that was obtained.

### **6.3.5 Fourier-Transform Infra-Red (FT-IR) spectroscopy**

All FT-IR spectra were recorded using a Perkin-Elmer 1600 series FTIR Spectrometer. The method that was used involved placing polymer beads between two diamond plates in a diamond compression cell. The sample was scanned with a resolution of  $4\text{ cm}^{-1}$ ; an average of 16 scans was taken per sample.

### **6.3.6 Elemental Microanalysis**

A small sample of each resin (30 mg) was submitted to the Microanalysis Laboratory at Strathclyde University, and C, H and N contents were determined simultaneously using a Perkin Elmer 2400 analyser. The samples were wrapped in tin foil and combusted at  $1,800\text{ }^{\circ}\text{C}$  in pure oxygen. The combustion products were catalysed and interferences removed before being swept into a detector zone where each element was separated and eluted as  $\text{CO}_2$ ,  $\text{H}_2\text{O}$  and  $\text{NO}_2$ . The signals were converted to a percentage of the elements.

For Cl analysis, approximately 5 mg of the sample was weighed into ashless filter paper, which was then fastened to a platinum rod. The sample was then combusted in an oxygen-filled flask containing a weak solution of  $\text{H}_2\text{O}_2$  (oxygen flask combustion method) and left to sit for 30 minutes. During this time, any halogen present is adsorbed into the solution in the form of halide. After adding 80 mL of ethanol and adjusting the pH to between 1.5 and 2, the resultant solution was titrated with mercuric nitrate solution using diphenylcarbazone as the indicator.

### **6.3.7 Nitrogen Sorption Porosimetry Analysis**

Nitrogen sorption porosity was used to determine the specific surface areas of the polymers from nitrogen sorption data in the lower range of the sorption isotherm. This method derives accurate and reliable data both theoretically and practically.

The porosimeter which was used was a Micromeritics ASAP 2010 BET ANALYZER. Prior to use, the samples (0.3 – 0.4 g) were heated overnight in a

vacuum oven at ~ 40 °C to ensure that all the gas molecules, moisture, and residual solvent had been removed from the samples. After the degassing process, the samples were analysed with computer control Module ASAP 2010 Version 2.00 to give the specific surface area data.

### **6.3.8 Titration Analysis**

Approximately 0.05 g of a resin sample was weighed and added into a 100 mL beaker containing a 2 N sodium chloride solution (10 mL). The slurry was stirred periodically and left for one hour to allow for the displacement of H<sup>+</sup> from the resin. Thereafter, the slurry was titrated slowly with a 0.1 N standardized sodium hydroxide (NaOH) solution using a pH meter to follow the change in pH. The ion-exchange capacity of the resins (IEC, mmol/g) was determined graphically.

## **6.4 Procedure/Methodology**

### **6.4.1 Synthesis of Precursor Gel-Type NAD Polymers**

All the stabiliser, co-stabiliser, initiator and styrene, half of the VBC and half of the ethanol were added into a 500 mL five-necked, round-bottomed flask fitted with an overhead stirrer, condenser and nitrogen inlet. Once a homogenous solution had formed at room temperature, the solution was bubbled with nitrogen gas at room temperature for 30 minutes. The flask was then placed into an oil bath set at 70 °C, and stirred mechanically using a four-bladed PTFE stirrer at 160 rpm. EGDMA and the second half of the VBC were dissolved in the second half of the ethanol at 70 °C under nitrogen. One hour after the start of the polymerisation, the hot solution containing EGDMA and VBC was added into the reaction flask. The reaction was continued for a further 24 hours. The particles that were obtained were centrifuged for 10 minutes at 3,000 rpm and then washed 2 times in ethanol and 2 times in methanol (the particles were suspended in the appropriate wash solvent and centrifuged between each washing step). The particles were filtered using vacuum filtration on a 0.22 µm nylon membrane filter and dried overnight in *vacuo* (60 mbar) at 40 °C.

#### 6.4.2 Partial Hypercrosslinking of NAD Precursor Polymers

NAD precursor particles (1.5 g) were added into a round-bottomed flask containing hexane (40 mL) and left in contact with the hexane for 2 hours. The mixture then was cooled in an ice bath (~4 °C) before a small amount of FeCl<sub>3</sub> (2% - 16.5 mol% relative to the number of moles of chloromethyl residues) was added in order to stabilise the final particles when contacted with DCE in fully hypercrosslinking reaction. FeCl<sub>3</sub> was allowed to disperse uniformly throughout the mixture for 2 hours before the reaction vessel was heated to 60 °C for 18 hours. Stirring was applied continuously during the reaction course. The final product was filtered using vacuum filtration on a 0.22 µm nylon membrane filter, and then washed with MeOH and several times with aqueous HNO<sub>3</sub> (pH 2) before being extracted overnight with acetone in a Soxhlet extractor. The product was dried in *vacuo* (60 mbar) at 40 °C overnight.

#### 6.4.3 Hypercrosslinking of NAD Polymers

NAD precursor particles (1.5 g) were added into a round-bottomed flask containing DCE (40 mL) and left to swell fully under nitrogen for 1 hour. Then, FeCl<sub>3</sub> (in a 1:1 molar ratio of CH<sub>2</sub>Cl:FeCl<sub>3</sub>) suspended in DCE (40 mL) was added. The mixture was then heated rapidly to 80 °C. The reaction was allowed to continue for 18 hours, whilst stirring continuously during the course of the reaction. The hypercrosslinked particles were filtered using vacuum filtration on a 0.22 µm nylon membrane filter and washed with MeOH and then washed several times with aqueous HNO<sub>3</sub> (pH 2). They were then extracted overnight with acetone in a Soxhlet extractor, and dried overnight in *vacuo* (60 mbar) at 40 °C.

#### 6.4.4 Sulfonation of Hypercrosslinked Polymers

In a typical sulfonation reaction, the hypercrosslinked particles (0.5 g) were added into a round-bottomed flask containing DCE (30 mL) and left to wet under nitrogen for 1 hour. Then, sulfuric acid was added. The mixture was then heated rapidly to 60 °C under nitrogen, with continuous mechanical stirring during the reaction. The

sulfonated hypercrosslinked particles were then allowed cool on an ice-water bath to quench the reaction, washed with an excess of distilled water until the washings were neutral pH, and then filtered using vacuum filtration on a 0.22  $\mu\text{m}$  nylon membrane filter. They were then dried overnight in *vacuo* (60 mbar) at 40 °C.

## 6.5 Results and Discussion

In order to prepare sulfonated hypercrosslinked polymers, two synthetic strategies were followed, as is depicted in Figure 6.1. Either swellable NAD precursors were synthesised and hypercrosslinked fully in a Davankov-type reaction<sup>[3]</sup> prior to sulfonation (a three-step strategy) or the swellable NAD precursors were contacted with a non-swelling solvent and a small amount of  $\text{FeCl}_3$  to achieve partial hypercrosslinking before being fully hypercrosslinked using the classical Davankov chemistry (a four-step strategy). The hypercrosslinked products obtained were then sulfonated, using concentrated sulfuric acid as the sulfonating agent.

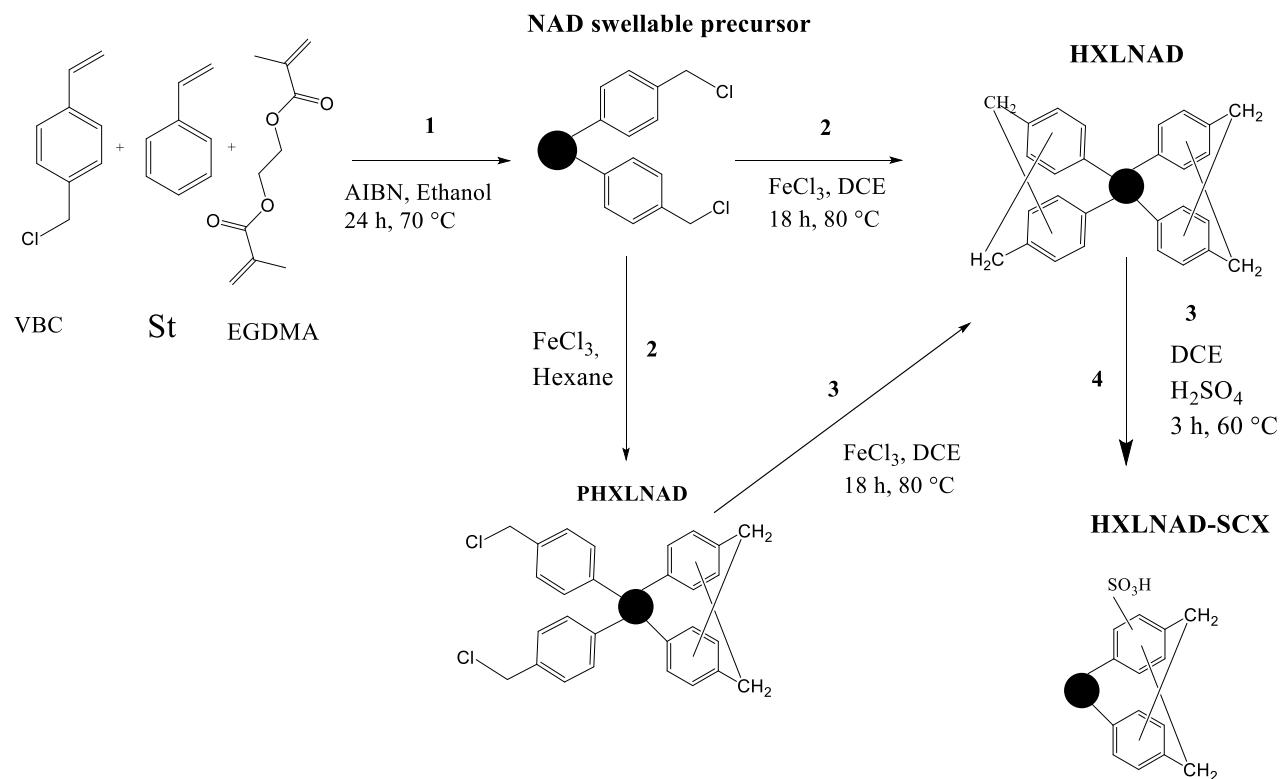
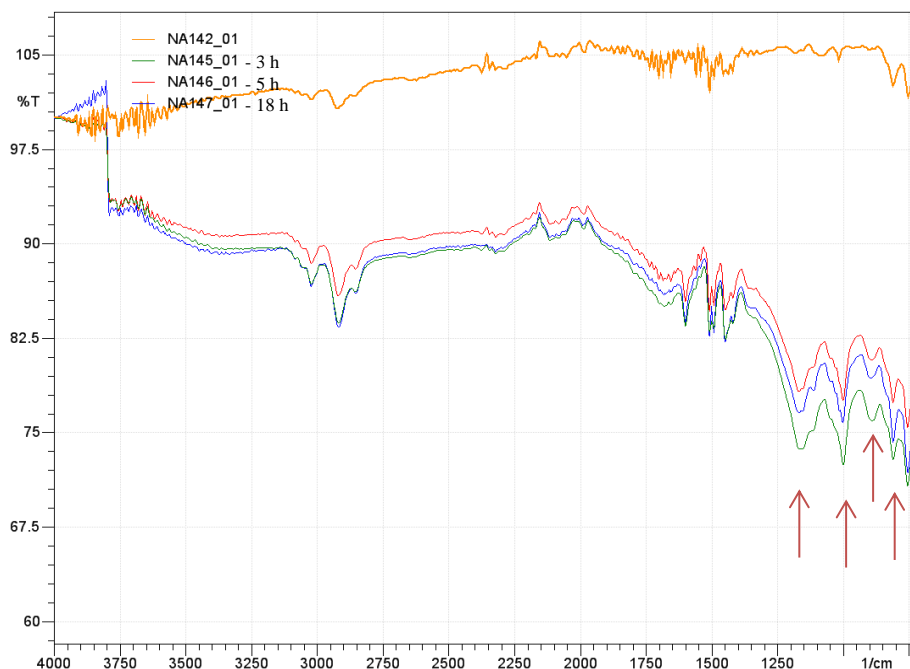


Figure 6.1: Reaction schemes showing the two distinct routes into the production of sulfonated hypercrosslinked (HXLNAD-SCX) polymer.

## 6.5.1 Three Step Strategy for the Production of Sulfonated Hypercrosslinked Polymers

### 6.5.1.1 FT-IR Analysis

Figure 6.2 shows the infrared spectra of NA142 (unsulfonated polymer) and sulfonated polymers: NA145 (3 h), NA146 (5 h) and NA147(18 h) which were treated with 5 mL of sulfuric acid at different reaction time; a few additional bands appeared in the spectra of the sulfonated hypercrosslinked (HXLNAD-SCX) polymers compared to the spectrum of the unsulfonated polymer (as indicated by the red arrows at 1174, 1000, 892 and 812  $\text{cm}^{-1}$ ). These new bands are all consistent with sulfonation: the band at 1174  $\text{cm}^{-1}$  is ascribed to symmetric stretching vibration of S=O; the bands at 1000, 892, and 812  $\text{cm}^{-1}$  are ascribed to sulfonate groups attached to an aryl ring. All the spectra were similar even when the reactions were carried out for different reaction times. A similar outcome was observed for an HXLNAD-SCX polymer which was treated with 530 mL of sulfuric acid, as is shown in Figure 6.3. Diagnostic bands appear at 827, 892 and 1002  $\text{cm}^{-1}$  (circled), and S=O bands can be observed at 1123 and 1086  $\text{cm}^{-1}$  and all the spectra also show the similar pattern when the sulfonation were carried out at different reaction times.



**Figure 6.2:** FT-IR spectra of a hypercrosslinked polymer and its sulfonated derivatives produced at different reaction times in the presence of 5 mL of sulfuric acid at 60 °C: NA142 (HXL polymer) and NA146-NA147 (HXLNAD-SCX polymers).

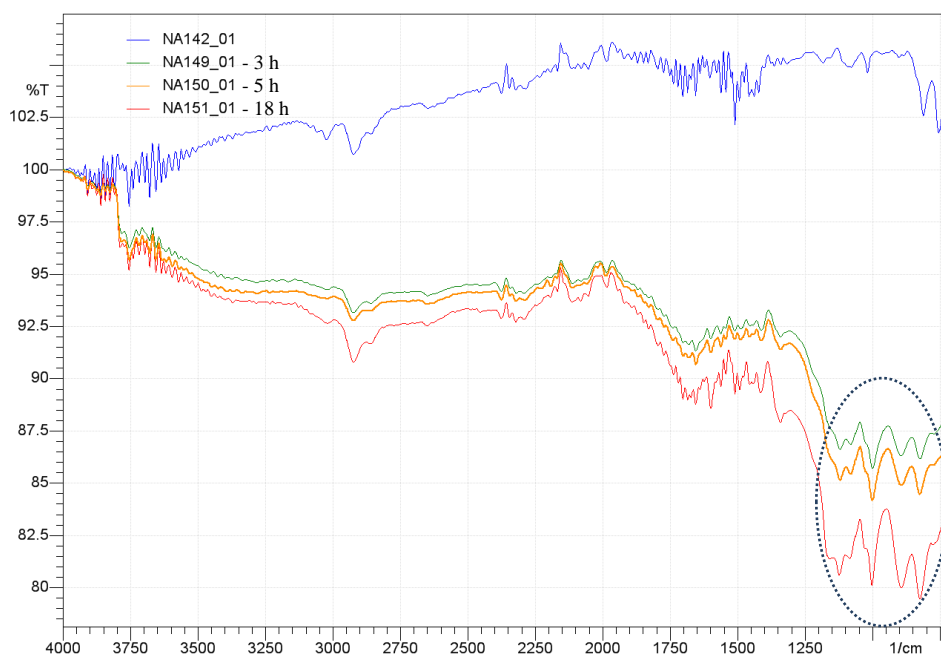


**Figure 6.3: FT-IR spectra of hypercrosslinked polymer and its sulfonated derivatives synthesised at different reaction times in the presence of 30 mL of sulfuric acid at 60 °C: NA142 (HXL polymer) and NA149-NA151 (HXLNAD-SCX polymers).**

### 6.5.1.2 Ion-Exchange Capacity (IEC)

The time duration of the sulfonation reaction was one of the important reaction variables which could be used to control the sulfonic acid group content within the sulfonated polymers. In the present study, hypercrosslinked polymers were sulfonated with different concentrations of sulfuric acid ( $\text{H}_2\text{SO}_4$ ) for different reaction times, at 60 °C, to produce sulfonated hypercrosslinked (HXLNAD-SCX) polymers with various IEC. The IEC was determined by titration analysis. Figure 6.4 depicts the variation of IEC with reaction times of 3 h, 5 h and 18 h, respectively. The IEC reached after a reaction time of three hours was around 2.1 mmol/g. However, extending the reaction times beyond three hours led to a decrease in the IEC rather than an increase in the IEC. This may be due to the formation of non-ionisable, sulfur containing side-products such as sulfone bridges, or as a result of desulfonation. Similar results have been reported elsewhere in the literature.<sup>[4]</sup> Irrespective of this point, it is clear that hypercrosslinked polymers with respectable IECs can be synthesised using this methodology.

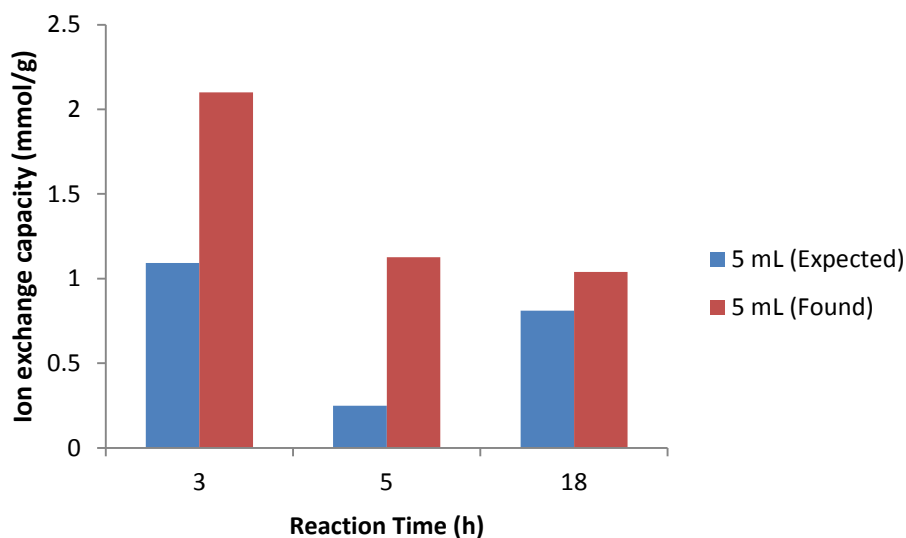


**Figure 6.4: Dependence of IEC on reaction time in the presence of 5 mL of sulfuric acid at 60 °C.**

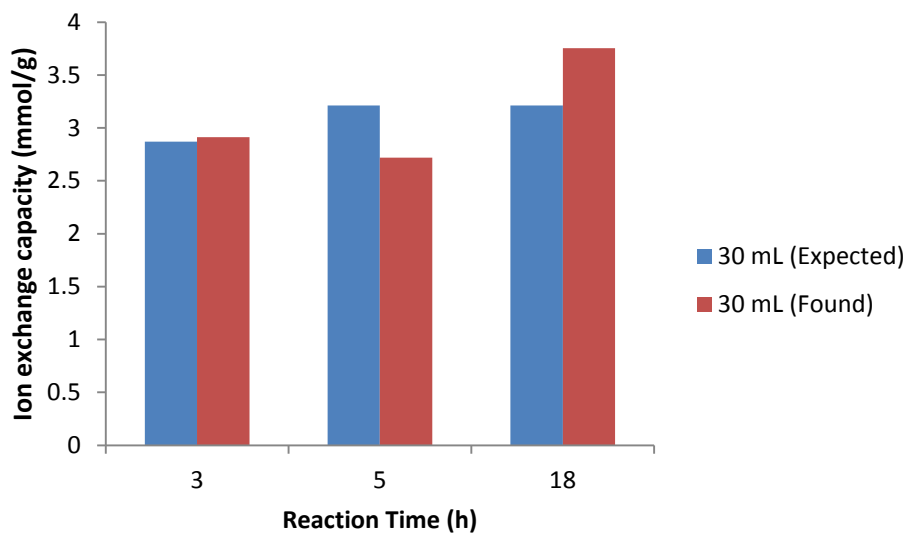


**Figure 6.5: Dependence of IEC on reaction time in the presence of 30 mL of sulfuric acid at 60 °C.**

Similar results were obtained when a higher amount of sulfuric acid was used (30 mL) although, unsurprisingly higher IECs were realisable. As is shown in Figure 6.5, the IEC after three hours of reaction was close to 3 mmol/g. A marginal fall in IEC was apparent upon increasing the reaction time to four hours, however an IEC of close to 4 mmol/g was possible when the reaction time was 18 hours.

It should be noted for both cases (5 mL and 30 mL of sulfuric acid) expected ion exchange capacities appear to be lower than the found values. It is unclear why such thing happens. It is, presumably, for IEC that determined by titration, in an ionic solution (i.e NaCl as ionic solution used in the determined of IEC), the sulfonic group ionised and it interchanged its' counterion (i.e H<sup>+</sup>) with another cationic counterion (i.e Na<sup>+</sup>). Thus, the greater interchange of the counterions appeared providing the higher IEC. It is contrast if IEC calculated based on sulfur content that found in elemental analysis. However, the expected IECs and the found one are still in reasonable good agreement.

### **6.5.1.3 Physical Form of Sulfonated Hypercrosslinked Polymers**

Figures 6.6 and 6.7 show the SEM micrographs of polymers taken before and after the various sulfonation reactions. From these images, it can be seen that the swellable NAD particles (JAG27) were of very good quality. Unfortunately, after hypercrosslinking the quality of the beads was diminished, and some particles were aggregated. The HXLNAD-SCX polymers were similar in quality to their hypercrosslinked precursors; beads are evident, but so too are aggregated beads.

Inspection of the SEM images acquired for the sulfonated microparticles suggests that the particle quality is decreased as the reaction time is decreased, especially at the higher amount of sulphuric acid. One can speculate as to why this might be the case, however Malik<sup>[5]</sup> had similar observations during a study which involved the sulfonation of porous styrene-divinylbenzene copolymers with concentrated sulfuric acid; he ascribed the effects to oxidative side-reactions, and had spectroscopic evidence in support of this. In the present study, FT-IR bands in the 1655 cm<sup>-1</sup> to 1850 cm<sup>-1</sup> region may suggest similar phenomena (Figure 6.3).

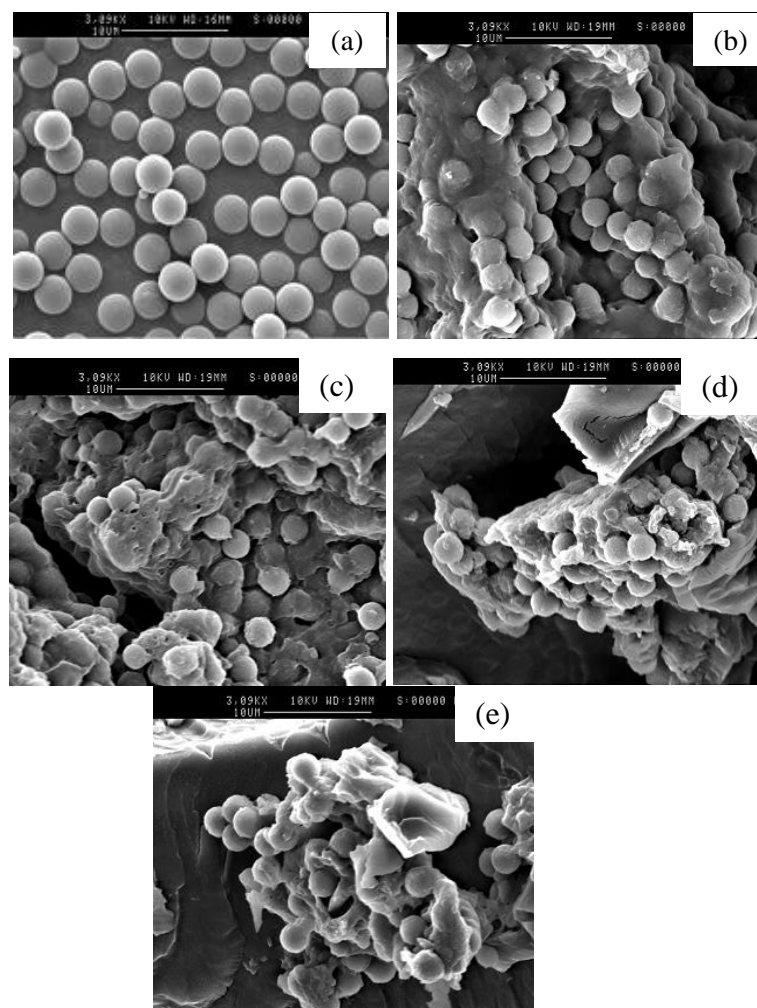


**Figure 6.6: SEM images of (a) swellable NAD precursor JAG27, (b) hypercrosslinked polymer NA142 and its derivatives after sulfonation reactions (c-e) at a fixed amount of sulfuric acid (5 mL) and at different reaction times: (c) NA145 - 3 h, (d) NA146 - 5 h and (e) NA146 - 18 h, respectively.**

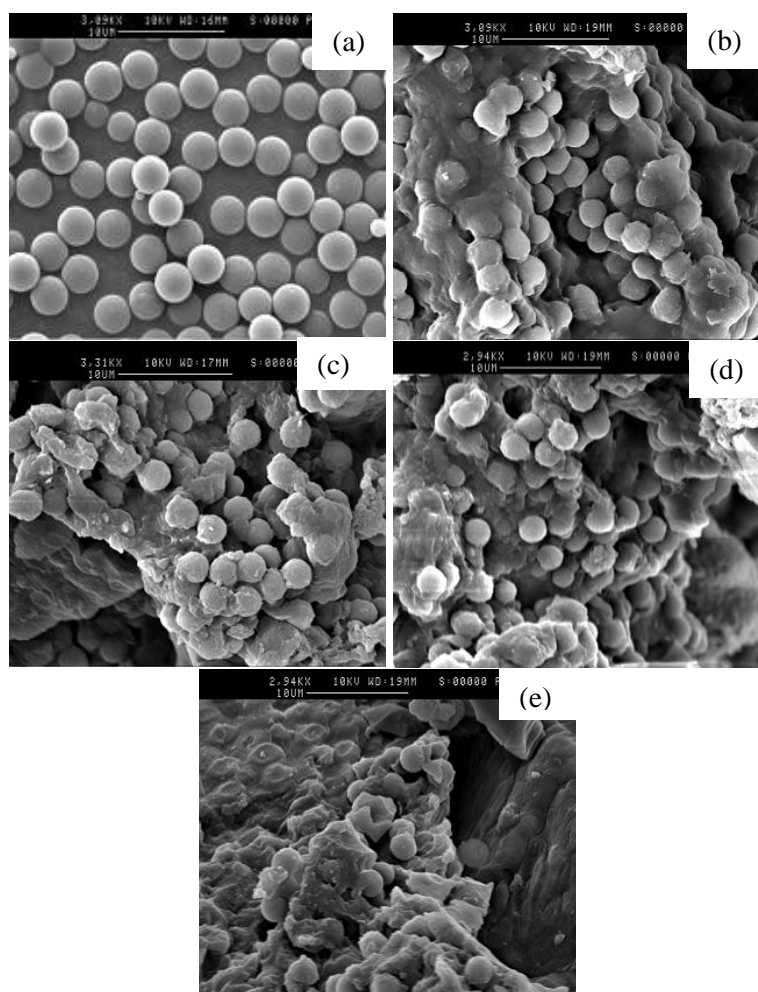


**Figure 6.7:** SEM images of (a) swellable NAD precursor JAG27 (b) hypercrosslinked polymer NA142 and its derivatives after sulfonation (c-e) at a fixed amount of sulfuric acid (30 mL) and at different reaction times: (c) NA151 - 3 h, (d) NA149 - 5 h and (e) NA150 - 18 h, respectively.

#### 6.5.1.4 Specific Surface Area of Sulfonated Hypercrosslinked Polymers

The specific surface areas (SSAs) of the sulfonated hypercrosslinked (HXLNAD-SCX) polymers were measured by nitrogen sorption porosimetry analysis. As is depicted in Figure 6.8, the SSA of the hypercrosslinked polymer prior to sulfonation was 667 m<sup>2</sup>/g. Unfortunately, upon sulfonation the SSA always fell, and very

dramatically in the case of those polymers sulfonated using a higher level of sulphuric acid. For the polymer sulfonated using a lower level of sulphuric acid, the SSA of the sulfonated product was  $\sim 345 \text{ m}^2/\text{g}$  when the reaction time was 3 hours, but then increased ( $\sim 500 \text{ m}^2/\text{g}$ ) and decreased again ( $\sim 107 \text{ m}^2/\text{g}$ ) when yet longer reaction times were employed (5 and 18 hours, respectively). A decrease in specific surface area is to be expected, however the variability is surprising and difficult to explain. For the polymer sulfonated using a higher level of sulfuric acid, the sulfonated products always have very low dry-state specific surface areas, irrespective of the reaction time (Figure 6.8). This may be due to pore blocking as a result of sulfone bridge formation<sup>[6]</sup> (Figure 6.9) and sulfonic acid group insertion or, as described previously, oxidative side-reactions leading to collapse of the microporous networks. Somewhat similar results were reported elsewhere.<sup>[7]</sup> Furthermore, replacement of H by either  $\text{SO}_3\text{H}$  or a sulfone bridge reduces the pore phase volume and thus increases the polymer apparent density,<sup>[88]</sup> although this effect in isolation is unlikely to be able to account for the dramatic effects on SSA which were observed.

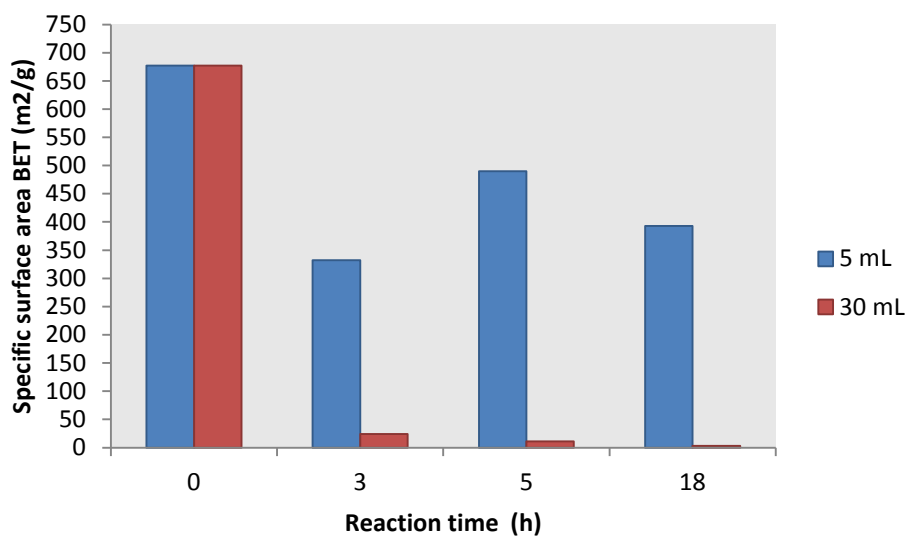


**Figure 6.8:** Specific surface areas (SSA) of sulfonated polymers obtained upon treatment of a non-sulfonated precursor with variable amount of sulfuric acid and for different reaction times.

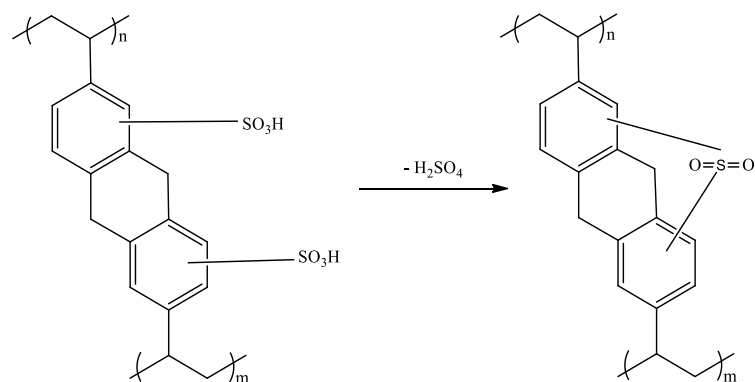


**Figure 6.9: Highly schematic representation of a sulfone-bridge forming reaction.**

As is presented in Table 6.1, satisfactory yield of final product was obtained (more than 80%) when the reaction time was 18 hours in all cases except NA147. Meanwhile, the sulfur content increased in all cases within the same time-frame. This shows that the sulfur content in the products increased as the reaction time was extended. Although the HXLNAD-SCX polymers isolated after longer reaction time were non-porous in the dry state, these polymers still had higher IECs, as is depicted in Figure 6.4. This may imply that the polymers, contrary to expectations for a heavily crosslinked hypercrosslined polymers, these particular polymers are swellable to some extent.

**Table 6.1: Synthesis data for sulfonated hypercrosslinked polymers prepared with different reaction time and varying amounts of sulfuric acid. [a] Based on 1:1 molar ratio  $C_{17}H_{16}:C_{17}H_{17}SO_3$**

Sample	$H_2SO_4$ (mL)	Reaction time (h)	Mass of Starting material (g)	Max. Theor. Yield (g) <sup>a</sup>	Product Yield (g)	Product Yield (%)	Microanalysis	
							Expected S (%)	Found S (%)
NA145	5	3	0.5000	0.684	0.6037	88	10.6	3.5
NA146	5	5	0.5000	0.684	0.6073	89	10.6	0.8
NA147	5	18	0.4989	0.682	0.5149	76	10.6	2.6
NA151	30	3	0.5073	0.600	0.6939	87	10.6	9.2
NA149	30	5	0.5254	0.719	0.7042	98	10.6	10.3
NA150	30	18	0.5153	0.700	0.7048	99	10.6	10.3

### 6.5.1.5 Sulfonation of Other Hypercrosslinked Polymers

In the optimisation study just described, sulfonated polymers with satisfactory IEC values were obtained when the sulfonation reactions were performed using 30 mL of sulfuric acid for a period of 3 hours. Therefore, other hypercrosslinked polymers, besides JAG27, were sulfonated under analogous conditions. The polymers selected for this study had variable SSAs. Figure 6.10 shows SEM images of these polymers before and after sulfonation. From these images it can be seen that the particle quality is reduced upon hypercrosslinking, but that the particle quality is retained during the sulfonation reactions. For the HXLNAD-SCX polymers, rough particle surfaces can be observed together with some evidence of aggregation, however the particle quality is, generally speaking, satisfactory.

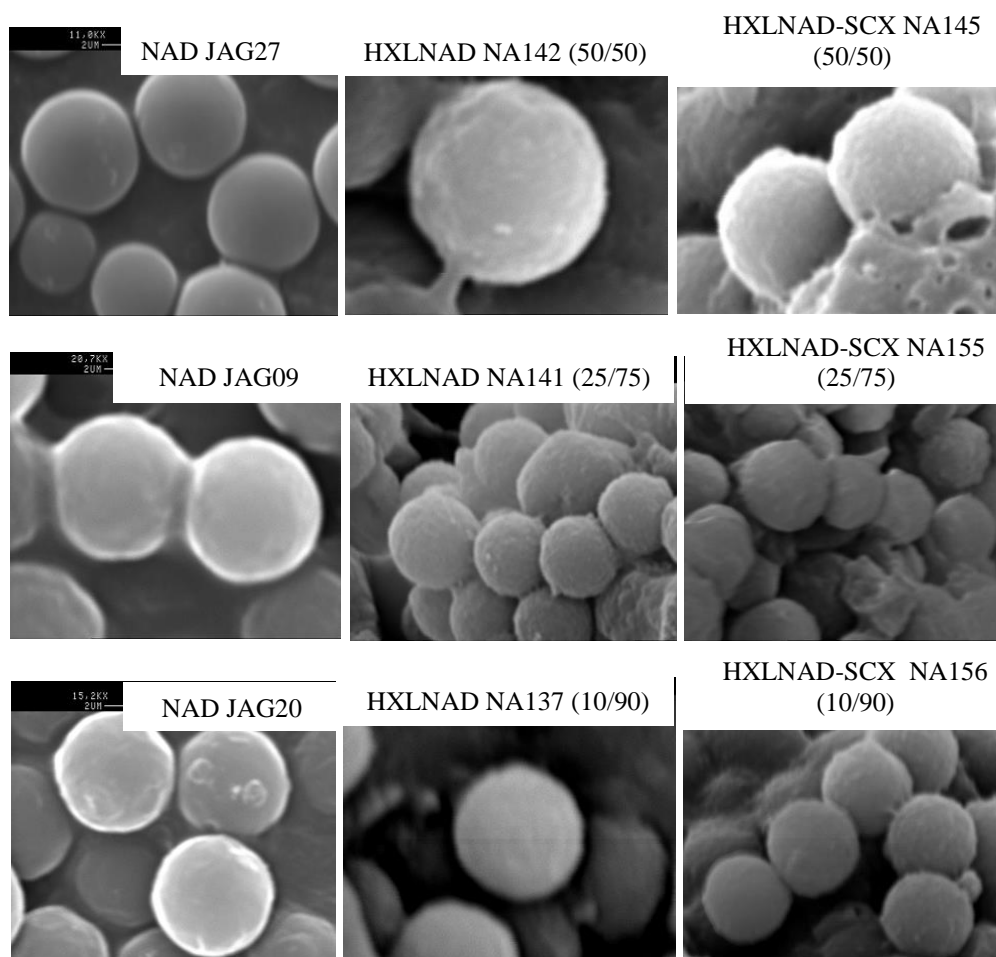


**Figure 6.10: SEM images of sulfonated hypercrosslinked polymers derived from a range of hypercrosslinked precursors (value in the bracket shows the percentage of St/VBC used in synthesis of swellable NAD precursor).**

The IEC values for three of the HXLNAD-SCX polymers (75%, 50% and 90% of VBC content in the NAD precursors) were measured and found to be satisfactory, with an average IEC value of 2.12 mmol/g, where the HXLNAD-SCX polymer containing 75% of VBC gave rise to the highest IEC (2.3 mmol/g) (Figure 6.11). The polymers were found to increase in mass upon sulfonation (Table 6.2), which is consistent with successful sulfonation, with the sulphur contents rising accordingly. Figure 6.12 shows the specific surface areas of the different HXLNAD-SCX polymers. As expected, upon sulfonation the SSA was found to decrease, by approximately 50% in each case. Similar as discussed in previous section, even though the expected ion exchange capacities appear to be lower than the values calculated from elemental analysis, but the values are in reasonable good agreement.

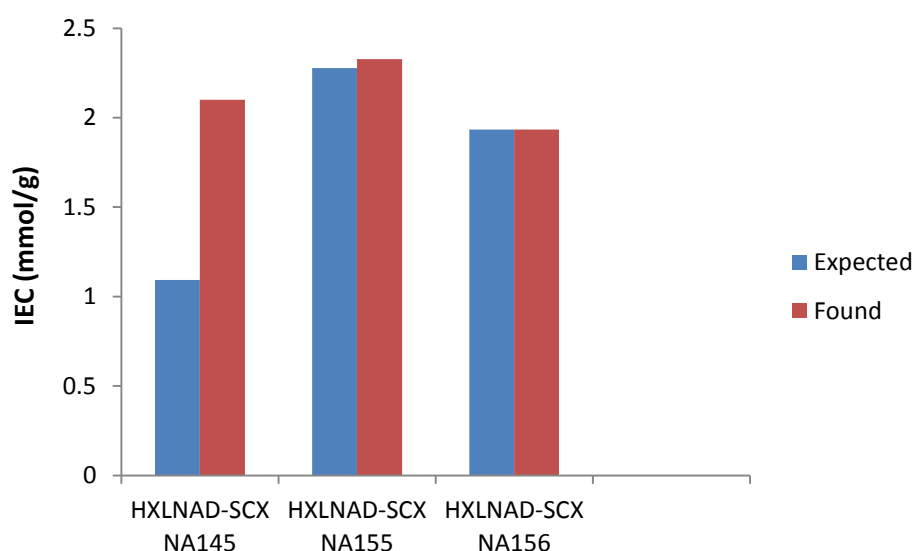


**Figure 6.11: Ion-exchange capacity of different sulfonated hypercrosslinked polymers.**

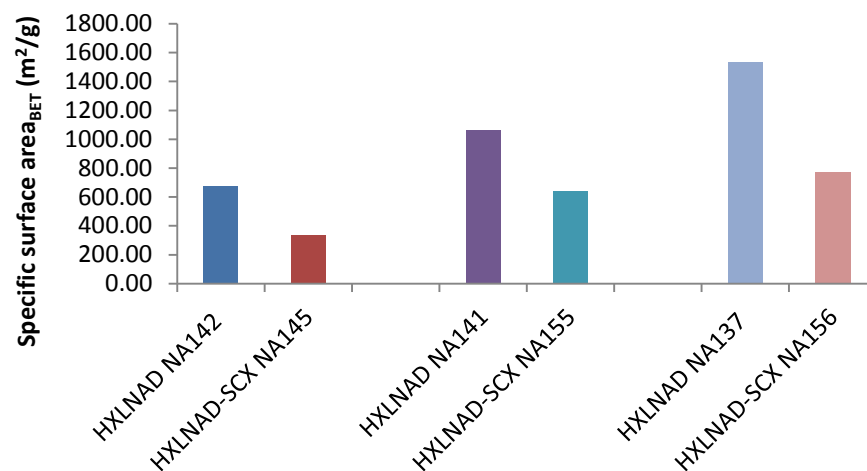


**Figure 6.12:** Specific surface area data for the different sulfonated hypercrosslinked polymers.

**Table 6.2:** Synthesis data for sulfonated hypercrosslinked polymer. [a] Based on 1:1 molar ratio  $C_{17}H_{16}:C_{17}H_{17}SO_3$ .

Sample	Mass of Starting material (g)	Max. Theor. Yield (g) <sup>a</sup>	Product Yield (g)	Product Yield (%)	Microanalysis		Average particle size (μm)
					Expected S (%)	Found S (%)	
NA145	0.5000	0.684	0.6037	89	10.6	3.5	2.02 ± 0.25
NA155	0.4401	0.602	0.5067	84	10.6	7.3	2.19 ± 0.27
NA156	0.5307	0.725	0.6303	87	10.6	6.2	2.51 ± 0.31

### 6.5.2 Four Step Strategy for the Production of Sulfonated Hypercrosslinked Polymers

Figure 6.13 shows the SEM images of the sulfonated hypercrosslinked polymers that were produced *via* the four step synthetic strategy, where NAD precursor particles (NA171) were partially hypercrosslinked (PHXLNA198) prior to full hypercrosslinking with an appropriate mass of iron (III) chloride in DCE (HXLNA196) and then sulfonated (HXLNAD-SCXNA198). The SEM images show that the sulfonated hypercrosslinked polymers were delivered in high quality.

Table 6.3 shows the characterisation data for the sulfonated particles produced *via* a four step synthetic strategy. The mean particle diameter for all samples was between 3.30 to 3.35  $\mu\text{m}$ , and the particles had narrow particle size distributions. Furthermore, the yields that were obtained were also satisfactory. As expected, the specific surface areas fell upon sulfonation, however HXLNAD-SCX NA198 still has a high specific surface so retains a well-developed pore network in the dry state. The IEC for the sulfonated hypercrosslinked polymer was also satisfactory (1.28 mmol/g), and this tallied with the elemental microanalytical data. Presently, these particles are also undergoing evaluation as ion-exchange resins in the laboratory of a collaborator.

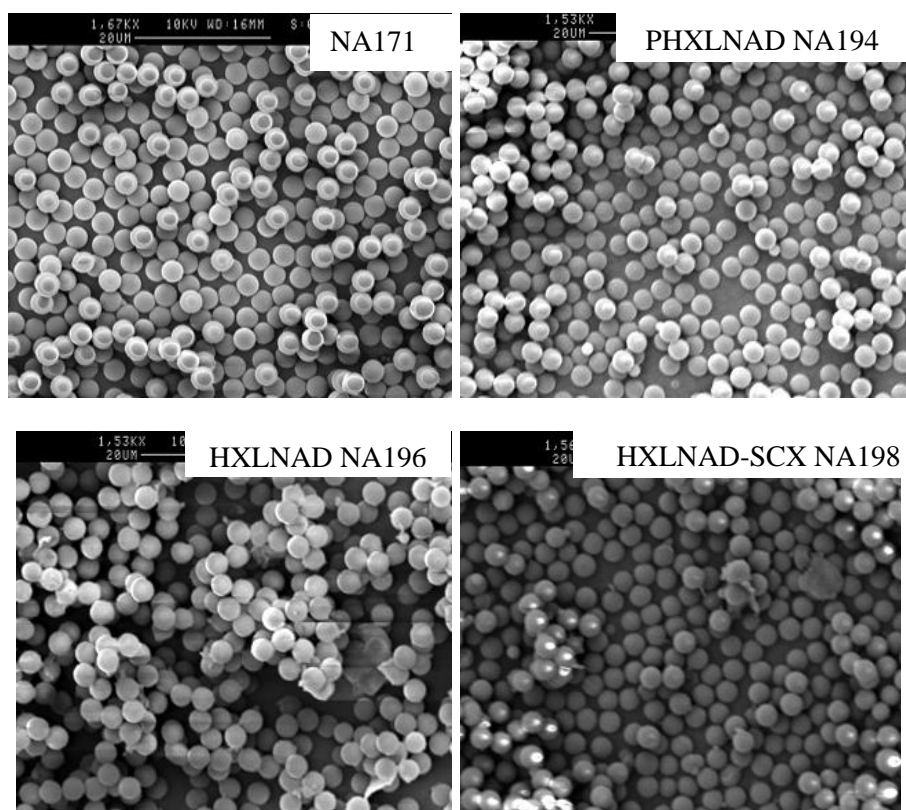


**Figure 6.13: SEM images of sulfonated hypercrosslinked polymers synthesised *via* a four step synthetic strategy. NA171 - NAD precursor particles; PHXLNAD NA194 - partially hypercrosslinked particles; HXLNAD NA196 - fully hypercrosslinked particles and HXLNAD-SCX NA198 - sulfonated hypercrosslinked particles.**

**Table 6.3: Characterisation data for sulfonated hypercrosslinked polymers produced *via* a four step synthetic strategy.**

	1 <sup>st</sup> step	2 <sup>nd</sup> step	3 <sup>rd</sup> step	4 <sup>th</sup> step
Sample	NA171	PHXLNA194	HXLNA196	HXLNAD-SCXNA198
SSA <sub>BET</sub> (m <sup>2</sup> /g)	~2	~2	1324	871
IEC (mmol/g)	N/A	N/A	N/A	1.28
Cl (%)	23.4	18.9	3.1	3.1
S (%)	N/A	N/A	N/A	0.68
Average particle size (μm)	3.30±0.20	3.07±0.40	3.53±0.20	3.56±0.20
Yield (%)	89	96	90	76

## 6.6 Conclusions

Strong cation-exchange resins have been prepared using a three step synthetic strategy, where swellable NAD precursors were synthesised, hypercrosslinked and then sulfonated using concentrated sulfuric acid. It was possible to control the level of sulfonation by control of the reaction conditions. Extending the reaction time did not benefit the sulfonation reaction; IECs tended to fall after extended reaction times, as did the SSAs. Optimised sulfonation conditions were evolved nevertheless, and a range of hypercrosslinked particles, of varying SSA, sulfonated under the optimised conditions. Useful particles with satisfactory ion-exchange capacity were produced.

Sulfonated, hypercrosslinked particles of the highest quality were synthesised *via* a four step synthetic strategy. Very high quality sulfonated hypercrosslinked polymer microspheres were successfully prepared in this way. The IEC values were acceptable and they retained a well-developed pore structure in the dry state and presently, these particles are undergoing evaluation as ion-exchange resins in the laboratory of a collaborator.

## References

- [1] D. Bratkowska, R. M. Marcé, P. A. G. Cormack, D. C. Sherrington, F. Borrulla and N. Fontanals, *J. Chromatogr. A* **2010**, *1217*, 1575-1582.
- [2] P. A. G. Cormack, A. Davies and N. Fontanals, *React. Func. Polym.* **2012**, *72*, 939-946.
- [3] V. A. Davankov, M. M. Llyin, M. P. Tsyurupa, G. I. Timofeeva and L. V. Dubrovina, *Macromolecules* **1996**, *29*, 8398-8402.
- [4] N. Shibuyal and R. S. Porter, *Macromolecules* **1992**, *25*, 6495-6499.
- [5] M. A. Malik, *Ind. Eng. Chem. Res.* **2009**, *48*, 6961-6965.
- [6] C. R. Martins, G. Ruggeri and M. A. D. Paoli, *J. Braz. Chem. Soc.* **2003**, *14*, 797-802.
- [7] N. Walsby, M. Paranen, J. Juhanoja and F. Sundholm, *J. Appl. Polym. Sci.* **2000**, *81*, 1572-1579.
- [8] F. M. B. Coutinho, R. R. Souza and A. S. Gomes, *Eur. Polym. J.* **2004**, *40*, 1525-1532.

## ***CHAPTER SEVEN<sup>[1-3]</sup>***

**7.0 Summary**

A series of strong anion-exchange resins was prepared by the amination of hypercrosslinked polymers bearing pendent chloromethyl moieties, using dimethylbutylamine as an aminating agent. The reaction conditions were optimised in an attempt to achieve the highest ion-exchange capacity (IEC) whilst retaining the quality, integrity and porosity of the particles during the amination process. The aminated hypercrosslinked polymers obtained were analysed by FT-IR spectroscopy, SEM, elemental microanalysis and nitrogen sorption porosimetry.

**7.1 Introduction to Strong Anion-Exchange Resins**

Strong anion-exchange (SAX) resins typically derive their functionality from quaternary ammonium exchange sites. There are two main groups of strong anion-exchange sites: (a) the sites have three alkyl groups attached to the nitrogen centre, and (b) an ethyl moiety replaces one of the three alkyl groups. This type of resin can be used across a wide pH range and, after exhaustion, can be regenerated with concentrated sodium hydroxide, for example, to convert the exhausted resin back to its hydroxide form.

**7.2 Aims of Work**

The aims of this work were to synthesise hypercrosslinked polymers with strong anion-exchange character (HXLNAD-SAX) by treating hypercrosslinked microparticles with dimethylbutylamine as an aminating agent. The hypercrosslinked microparticles were obtained by the exhaustive hypercrosslinking of swellable precursors in a swollen state. The aminated hypercrosslinked particles prepared were then characterised to evaluate their ion-exchange capacity and morphology.

## **7.3 Experimental**

### **7.3.1 Materials**

The reagents used in the amination reactions were dried toluene ( $\geq 99.3\%$  grade) supplied by Aldrich, *N,N*-dimethylbutylamine (DMBA) (99% grade) and methanol (99.7% grade) supplied by Sigma-Aldrich, sodium hydrogen carbonate (99.7% grade) supplied by VWR and distilled water. All reagents were used as received.

### **7.3.2 Equipment**

The amination of hypercrosslinked polymers was performed in a three-necked, round-bottomed flask fitted with condenser, overhead stirrer and a two-blade PTFE-type stirrer. The reaction vessel was immersed in a thermostatically-controlled oil bath.

### **7.3.3 Characterisation**

The aminated particles were characterised using the following methods.

#### **7.3.3.1 Scanning Electron Microscopy (SEM)**

SEM was carried out using a Cambridge S-90. SEM micrographs were acquired at an accelerating voltage of 10.0 kV. A thin layer of sample was deposited onto a steel stub, which had been coated previously with conductive (copper), double-sided adhesive tape. Gold coating of the immobilised sample was then carried out. Coated samples were placed inside the SEM chamber and a vacuum was applied; this vacuum evacuated the chamber of any small particles that may have deflected the electrons and affected the SEM image that was obtained.

#### **7.3.3.2 Fourier-Transform Infra-Red (FT-IR) Spectroscopy**

All FTIR spectra were recorded on a Perkin-Elmer 1600 series FTIR Spectrometer. The method that was used involved placing polymer beads between two diamond plates in a diamond compression cell. The sample was scanned with a resolution of  $4\text{ cm}^{-1}$ ; an average of 16 scans was taken per sample.

### **7.3.3.3 Elemental Microanalysis**

A small sample of each resin (30 mg) was submitted to the Microanalysis Laboratory at Strathclyde University and C, H and N contents determined simultaneously using a Perkin Elmer 2400 analyser. The samples were wrapped in tin foil and combusted at 1800 °C in pure oxygen. The combustion products were catalysed and interferences removed before being swept into a detector zone where each element was separated and eluted as CO<sub>2</sub>, H<sub>2</sub>O and NO<sub>2</sub>. The signals were converted to a percentage of the elements.

For Cl analysis, approximately 5 mg of the sample was weighed into ashless filter paper, which was then fastened to a platinum rod. The sample was then combusted in an oxygen-filled flask containing a weak solution of H<sub>2</sub>O<sub>2</sub> (oxygen flask combustion method) and left to sit for 30 minutes. During this time, any halogen present is adsorbed into the solution in the form of halide. After adding 80 mL of ethanol and adjusting the pH to between 1.5 and 2, the resultant solution was titrated with mercuric nitrate solution using diphenylcarbazone as the indicator.

### **7.3.3.4 Nitrogen Sorption Porosimetry Analysis**

Nitrogen sorption porosimetry was used to determine the specific surface areas of the polymers from nitrogen sorption data in the lower range of the sorption isotherm. This method delivers accurate and reliable data both theoretically and practically.

The porosimeter which was used was a Micromeritics ASAP 2010 BET ANALYZER. Prior to use, the samples (0.3 g – 0.4 g) were degassed and heated overnight in a vacuum oven (60 mbar) at ~ 40 °C to ensure that all the gas molecules, moisture, and residual solvent had been removed from the samples. After the degassing process, the samples were analysed with computer control Module ASAP 2010 Version 2.00 to give the specific surface areas.

## **7.4 Procedure/Methodology**

### **7.4.1 Synthesis of Gel-Type NAD Precursor Polymers**

All the stabiliser, co-stabiliser, initiator and styrene, half of the VBC and half of the ethanol were added into a 500 mL five-necked, round-bottomed flask fitted with an overhead stirrer, condenser and nitrogen inlet. Once a homogenous solution had formed at room temperature, the solution was bubbled with nitrogen gas at room temperature for 30 minutes. The flask was then placed into an oil bath set at 70 °C, and stirred mechanically using a four bladed PTFE stirrer at 160 rpm. EGDMA and the second half of the VBC were dissolved in the second half of the ethanol at 70 °C under nitrogen. One hour after the start of the polymerisation, the hot solution containing EGDMA and VBC was added into the reaction flask. The reaction was continued for a further 24 hours. The particles that were obtained were centrifuged for 10 minutes at 3,000 rpm and then washed 2 times in ethanol and 2 times in methanol (the particles were suspended in the appropriate wash solvent and centrifuged between each washing step). The particles were filtered using vacuum filtration on a 0.22 µm nylon membrane filter and dried overnight in *vacuo* (60 mbar) at 40 °C.

### **7.4.2 Hypercrosslinking of NAD Precursor Polymers**

NAD precursor particles (1.5 g) were added into a three-necked, round-bottomed flask containing DCE (40 mL) and left to swell fully under nitrogen for 1 hour. Then, FeCl<sub>3</sub> (in a 1:1 molar ratio of CH<sub>2</sub>Cl:FeCl<sub>3</sub>) suspended in DCE (40 mL) was added. The mixture was then heated rapidly to 80 °C. The reaction was allowed to continue for 18 hours, with continuous stirring throughout. The hypercrosslinked particles were filtered and washed with MeOH and then washed several times with aqueous HNO<sub>3</sub> (pH 2). They were then extracted overnight with acetone in a Soxhlet extractor and dried overnight in *vacuo* (60 mbar) at 40 °C.

### 7.4.3 Amination of Hypercrosslinked Polymers

For a typical amination reaction, hypercrosslinked polymer particles (~ 0.5 g) and dried toluene (80 mL) were placed in a three-necked, round-bottomed flask (100 mL) and the mixture left under N<sub>2</sub> for 1 hour to wet the beads. Then, dimethylbutylamine (DMBA) (in a 5 or 10% molar excess relative to –CH<sub>2</sub>Cl groups) was added into the reaction vessel. The mixture then was heated rapidly to 85 °C and kept at this temperature for 18 h. The aminated beads were filtered and washed with toluene, MeOH, MeOH:H<sub>2</sub>O (1:2 ratio) and then washed several times with aqueous 5% (w/v) NaHCO<sub>3</sub> (pH 9) and water. They were then extracted overnight with acetone in a Soxhlet extractor before drying overnight in *vacuo* (60 mbar) at 40 °C.

### 7.5 Results and Discussion

Figure 7.1 shows the synthetic steps involved in preparation of aminated hypercrosslinked polymers. In the first step, swellable NAD precursors were prepared *via* non-aqueous dispersion polymerisation, as discussed in Chapter Three, and then hypercrosslinked (refer to Chapter Five) to deliver hypercrosslinked polymers bearing residual, pendent chloromethyl moieties. The hypercrosslinked polymers were then aminated, using dimethylbutylamine as the aminating agent, in dried toluene at 85 °C for 18 hours.

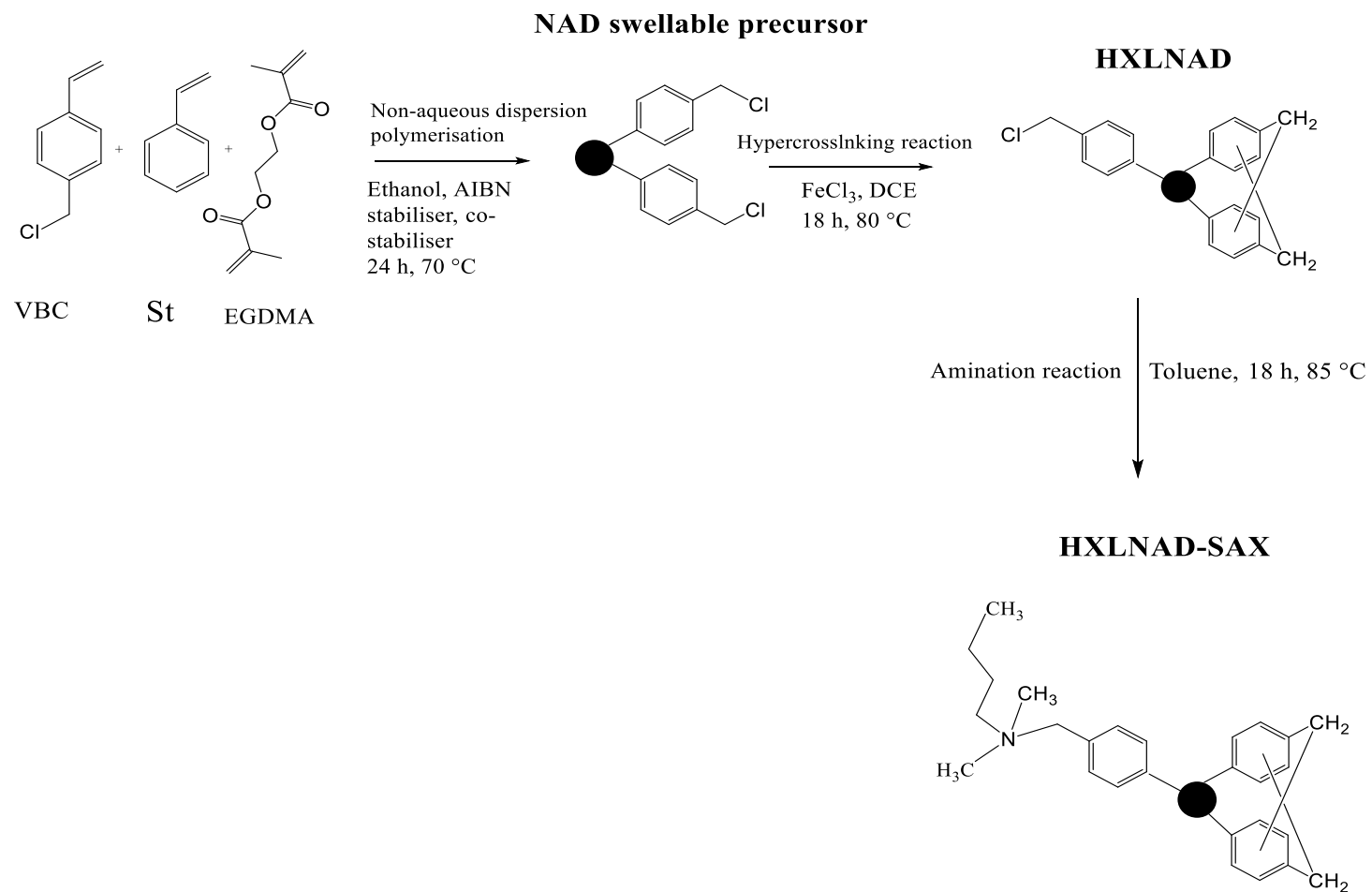


**Figure 7.1: Synthesis of aminated hypercrosslinked (HXLNAD-SAX) polymers *via* the amination of a hypercrosslinked precursor (HXLNAD**

### 7.5.1 FT-IR Spectroscopy

The FT-IR spectra of the hypercrosslinked polymer before and after the amination reactions are presented in Figure 7.2. The characteristic absorption bands at  $1265\text{ cm}^{-1}$  and  $733\text{ cm}^{-1}$  arise from stretching vibrations of C-Cl bonds. The  $975\text{ cm}^{-1}$  band is ascribed to a  $\text{CH}_2$  vibration,<sup>[4]</sup> present in the hypercrosslinked polymer before amination (green line). After amination, the bands at  $1265\text{ cm}^{-1}$  and  $733\text{ cm}^{-1}$  diminish significantly in intensity, except for polymer NA152 (blue line), and this is consistent with displacement of chloride by DMBA.

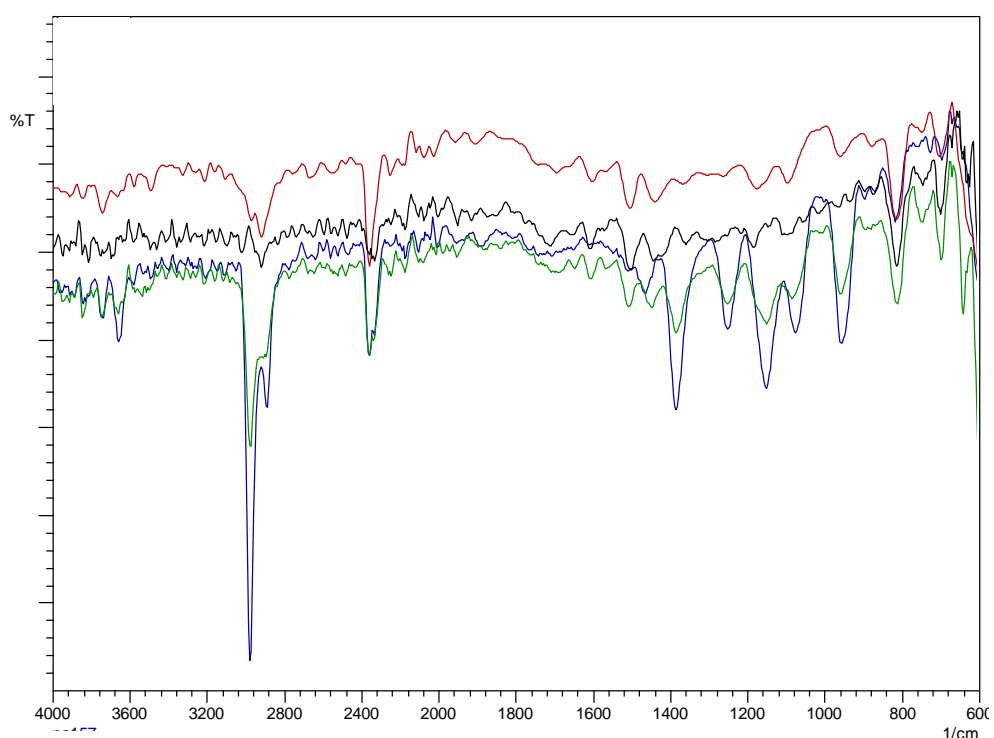


**Figure 7.2: FTIR spectra of a hypercrosslinked polymer and its aminated derivatives, with variable reaction times using a 5% molar excess of DMBA at  $85\text{ }^{\circ}\text{C}$ : NA141 (HXL polymer - green line); NA152-3 h (blue line), NA153-5 h (black line) and NA157-18 h (red line) are HXLNAD-SAX polymers.**

### 7.5.2 Specific Surface Areas of Aminated Hypercrosslinked Polymers

Figure 7.3 shows the specific surface areas of polymers before and after amination, where both the level of DMBA used and the reaction time has been varied. As can be seen, the specific surface area of the parent polymer prior to amination was around  $1,000\text{ m}^2/\text{g}$ . However, after the amination reaction, for all cases except where a 10%

molar excess of DMBA was used at a reaction time of 18 h, the specific surface areas were found to increase slightly. An increase in specific surface area is perhaps counter-intuitive, however similar observations have been reported in literature.<sup>[4-6]</sup>

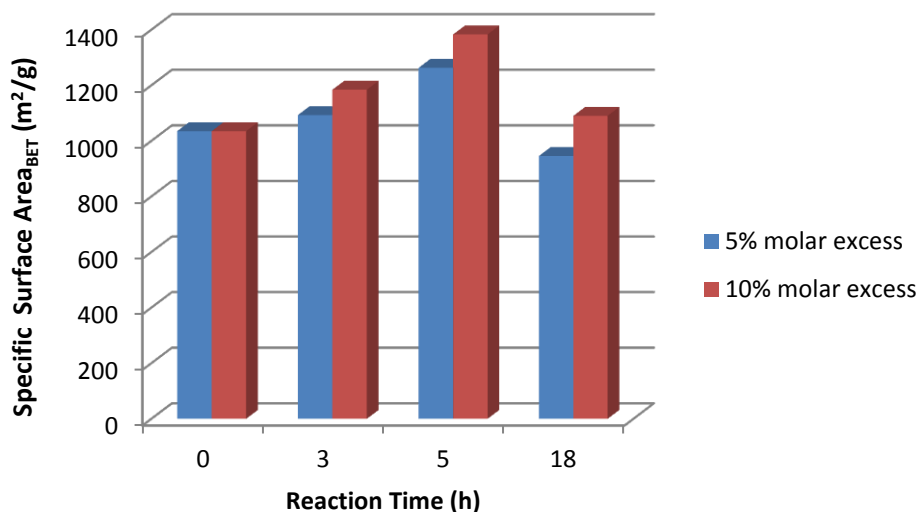


**Figure 7.3: Specific surface areas of aminated hypercrosslinked polymers prepared using various amount of DMBA and different reaction times.**

### 7.5.3 Ion Exchange Capacity (IEC) And Nitrogen Content

The ion-exchange capacities and nitrogen contents of the various aminated hypercrosslinked polymers are presented in Figure 7.4 and Table 7.1. From Figure 7.4, the ion-exchange capacities of both polymers produced using the three hour long reaction had an IEC of around 0.18 mmol/g. However, when the reaction time was extended to 5 hours the IEC fell to around 0.1 mmol/g but then increased again when the reaction time was extended to 18 hours. The overall effect of changing the relative amount of DMBA present in the reaction is minimal. The elemental microanalytical data shows that as the chlorine content falls the nitrogen content is increased. The changes in the chlorine and nitrogen contents are low, and this is reflected by the modest IEC values recorded. It should be noted that observed exchange capacities appear to be lower than the value calculated based on chlorine content in non-aminated hypercrosslinked particles. This is because not all of the

chloromethyl moieties are available/accessible for reaction with an amine nucleophile

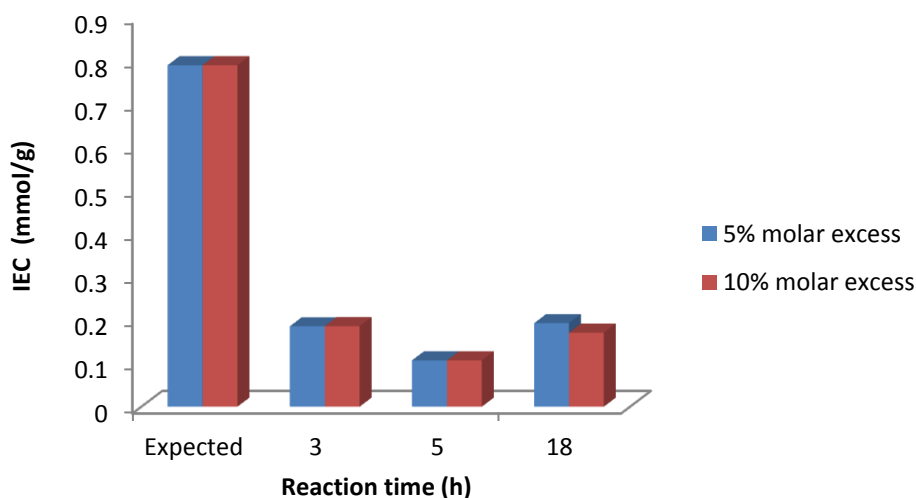


**Figure 7.4: Ion-exchange capacities of aminated hypercrosslinked polymers prepared using various amount of DMBA and variable reaction times.**

**Table 7.1: Synthesis data for aminated hypercrosslinked polymers prepared using various amount of DMBA and variable reaction times. [a] Based on 1:1 molar ratio of  $C_9H_9Cl:C_{15}H_{24}N$ .**

Reaction time (h)	Sample	Yield (%) <sup>a</sup>	Elemental Microanalysis (%)	
			Cl (Found)	N (Found)
<b><u>5% molar excess</u></b>				
0	HXLNAD NA141	88	2.80	0.36
3	HXLNAD-SAX NA152	76	2.60	0.62
5	HXLNAD-SAX NA153	65	trace	0.51
18	HXLNAD-SAX NA157	65	2.28	0.63
<b><u>10% molar excess</u></b>				
0	HXLNAD NA141	88	2.80	0.36
3	HXLNAD-SAX NA158	66	1.28	0.62
5	HXLNAD-SAX NA159	66	2.17	0.51
18	HXLNAD-SAX NA160	76	1.79	0.60

#### 7.5.4 Physical Form of Aminated Hypercrosslinked Polymers

In terms of the physical form of the particles, the shapes of the particles were changed upon hypercrosslinking, as was discussed in Chapter 5, however there were no obvious changes in the particles as a consequence of the amination process (Figures 7.6. and 7.6). This was entirely as expected.

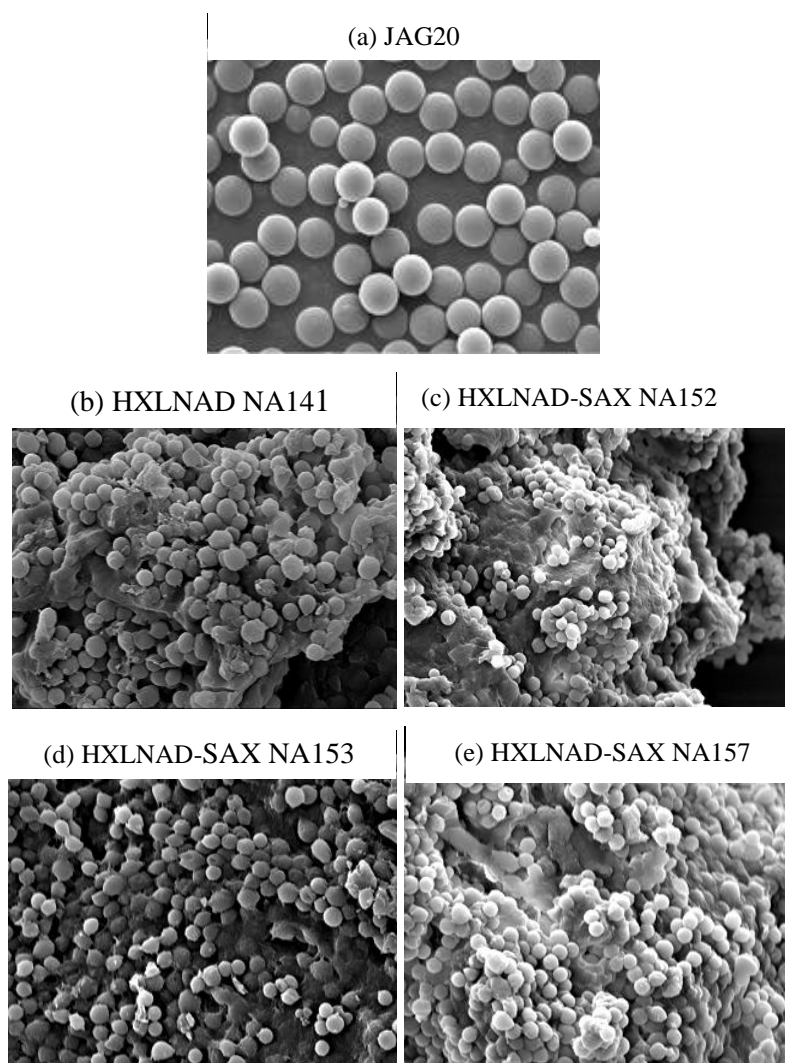


**Figure 7.5: SEM images of (a) swellable NAD precursor, (b) hypercrosslinked polymer and (c)–(e) hypercrosslinked polymers aminated with 5% molar excess of DMBA at different reaction times: HXLNAD-SAX NA152-3 h, HXLNAD-SAX NA153-5 h and HXLNAD-SAX NA157-18 h, respectively.**

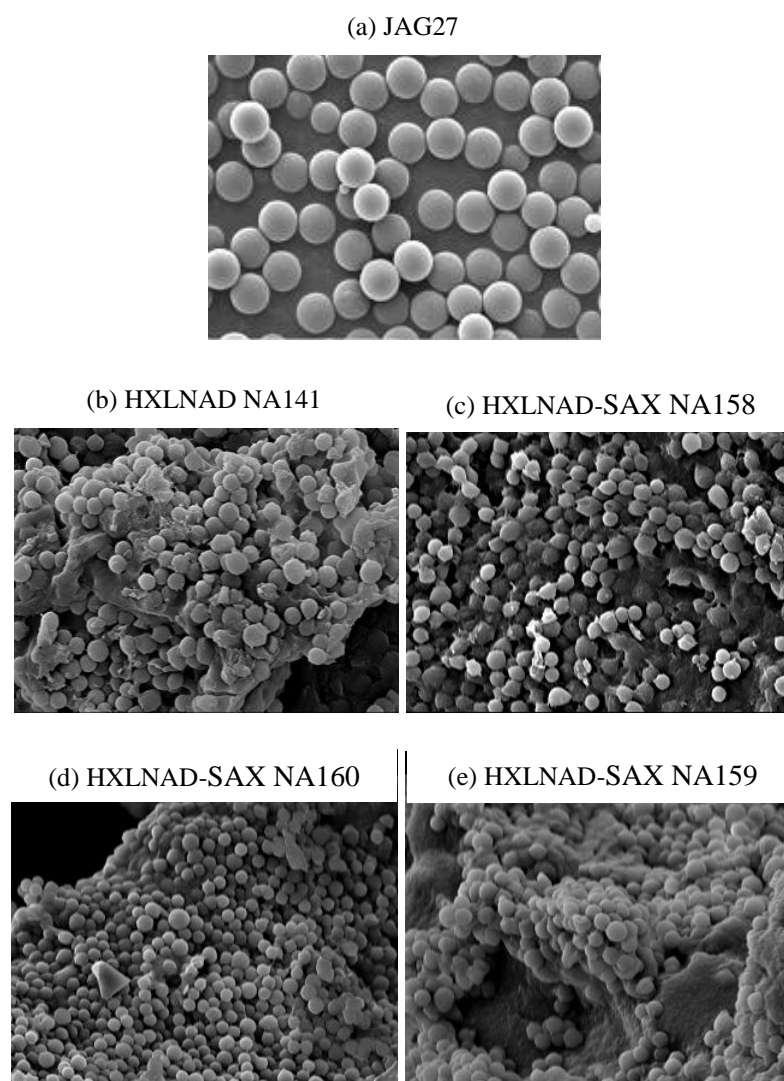


**Figure 7.6: SEM images of (a) swellable NAD precursor, (b) hypercrosslinked polymer and (c)-(e) hypercrosslinked polymers aminated with 10% molar excess of DMBA at different reaction times: HXLNAD-SAX NA158-3 h, HXLNAD-SAX NA159-5 h and HXLNAD-SAX NA160-18 h, respectively.**

### 7.5.5 Amination of Hypercrosslinked Polymers With Variable Chloromethyl Contents

In this section, the amination of hypercrosslinked polymers with variable chloromethyl contents was studied in an attempt to synthesise aminated hypercrosslinked polymers with higher IECs and higher specific surface areas. Figure 7.7 shows the specific surface areas of three aminated hypercrosslinked

polymers. Prior to amination, the hypercrosslinked polymers were prepared by controlling the residual chloromethyl content of the polymers by varying the reaction time during the hypercrosslinking reaction, before taking these polymers with variable chloromethyl contents forward to amination reactions with dimethylbutylamine. As can be seen, the non-aminated hypercrosslinked polymers all had high specific surface areas, but in every case the SSA was decreased relative to the parent polymers. This was expected, however it was pleasing to note that all of the aminated products still retained well-developed pore structures in the dry state.

Table 7.2 shows the synthesis data for the aminated hypercrosslinked polymers. Upon amination, the chlorine contents fall, as would be expected. The ion-exchange capacities are variable, however the data does show that it is possible to control to some extent the IEC by means of this synthetic strategy, which is a useful outcome.

It is unclear why polymer NA168 had the highest IEC of all. It should be pointed out that NA168 had the lowest chlorine content and the highest nitrogen content, and the higher the nitrogen content the higher the IEC that can be realised, so this result is not ambiguous. From this observation for NA168, it can be concluded that the majority of functional groups were accessible and that hypercrosslinked polymers with respectable IECs can be successfully functionalised using this methodology. Overall, the expected IECs and the found IECs are in reasonable good agreement.

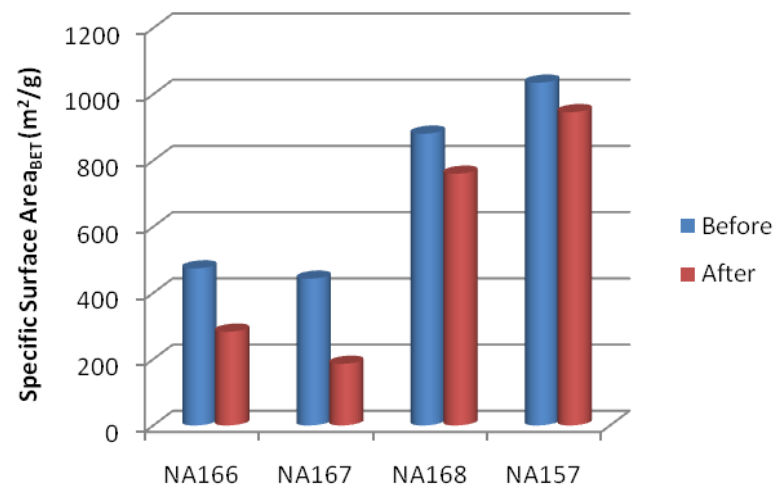


**Figure 7.7:** Specific surface areas of hypercrosslinked polymers before and after amination of polymers with variable chloromethyl contents.

**Table 7.2:** Synthesis data for aminated hypercrosslinked polymer at different chlorine residue and fixed 5% molar excess of DMBA. [a] Based on 1:1 molar ratio of C<sub>9</sub>H<sub>9</sub>Cl:C<sub>15</sub>H<sub>24</sub>N.

Sample	Yield (%) <sup>a</sup>	Microanalysis (%)				IEC (mmol/g)	
		Cl (Before)	Cl (After)	N (before)	N (After)	(Expected)	(Found)
NA166 (HXLNA136-10 min)	99	10.3	2.34	2.93	2.09	2.901	1.493
NA167 (HXLNA137-15 min)	98	4.40	3.13	1.25	1.84	1.294	1.314
NA168 (HXLNA137-30 min)	84	3.81	1.04	1.08	3.59	1.073	2.564
NA157 (HXLNA141-1080 min)	65	2.80	2.28	0.80	0.63	0.789	0.193

## 7.6 Conclusions

A series of aminated hypercrosslinked polymers has been synthesised successfully in good yields by treating chloromethyl-containing hypercrosslinked polymers with dimethylbutylamine (DMBA), to deliver strong anion-exchanger resins. The effect of varying the DMBA level and reaction time was studied; IECs of close to 0.2 mmol/g were recorded, however changing the level of DMBA employed had minimal effect.

In an attempt to synthesise aminated hypercrosslinked polymers with yet higher IECs, the effect of varying the chloromethyl content of the non-aminated polymers was studied. Porous polymers with IECs close to 1.5 mmol/g could be prepared in this way, and it was possible to tune, to some extent, the IEC achieved.

Overall, aminated hypercrosslinked polymers with satisfactory ion-exchange capacities have been prepared. These polymers have potential application as strong anion-exchange resins, and will be evaluated as such in the future.

## References

- [1] N. Fontanals, P. A. G. Cormack, D. C. Sherrington, R. M. Marcé and F. Borrulla, *J. Chromatogr. A* **2010**, *1217*, 2855-2861.
- [2] N. Fontanals, P. A. G. Cormack and D. C. Sherrington, *J. Chromatogr. A* **2008**, *1215*, 21-28.
- [3] D. Bratkowska, A. Davies, N. Fontanal, P. A. G. Cormack, F. Borrull, D. C. Sherrington and R. M. Marcé, *J. Sep. Sci.* **2012**, *35*, 2621-2628.
- [4] J. Liu, J. Yao, H. Wang and K. Y. Chan, *Green Chem.* **2006**, *8*, 368-371.
- [5] J. H. Hong, M. C. Park, S. K. Hong and B. S. Kim, *J. Appl. Polym. Sci.* **2009**, *112*, 830-834.
- [6] H. Xu and X. Hu, *React. Funct. Polym.* **1999**, *42*, 235-242.

## ***CHAPTER EIGHT***

## **8.0 Conclusions**

In the research work described in this thesis, dispersion polymerisation was the method of choice for the production of swellable polymer microparticles bearing chemical functionality which renders them amenable to post-polymerisation hypercrosslinking. Dispersion polymerisation was selected for this task because it is well-suited to the production of lightly crosslinked (swellable) microparticles, the methodology produces high-solids dispersions, and it is scalable. Both conventional dispersion polymerisation and aqueous dispersion polymerisation were evaluated.

Dispersion polymerisation was found to be very sensitive to small changes in the reaction conditions, thus a lot of time and effort was invested in the optimisation of synthetic protocols which would deliver swellable precursor particles of good quality and narrow particle size distributions. The dispersion medium, monomer concentration, initiator concentration, level of crosslinker in the feed and stirrer type were all found to affect the outcomes of the polymerisations. Of particular note are the findings that delaying the addition of crosslinker until after the particles had nucleated yielded particles of better quality, and that increasing the monomer and initiator concentrations simultaneously gave larger particles. As a result of the optimisation work performed, reliable and robust dispersion polymerisation conditions were identified which enabled the copolymerisation of styrene and vinylbenzyl chloride, in the presence of low levels of crosslinker, on a multi-gram scale; the beaded products obtained were isolated in good yields and were of high quality. The typical mean particle diameters were in the low micron range, and the particles were non-porous in the dry state (since they were gel-type).

Subsequently, the swellable precursor particles were converted into highly porous polymer particles using Friedel-Crafts alkylation-mediated hypercrosslinking reactions which exploited the pendent chloromethyl groups present in the precursor particles. These hypercrosslinking reactions were fast (highly porous polymer

networks were delivered in a few minutes) and efficient (the yields of products were very high), and products with SSAs approaching 2,000 m<sup>2</sup>/g were prepared readily.

Unfortunately, synthesising the hypercrosslinked products in a well-defined beaded format, where the particle size distributions were narrow, was found to be a far from trivial task, and a lot of time and effort was invested into this important endeavour. When swellable precursor particles, which had been synthesised by dispersion polymerisation, were subjected to classical hypercrosslinking conditions, the hypercrosslinked products were normally polydisperse, showed signs of aggregation and signs of contamination, even when the swellable precursor particles were of highly quality. This deterioration in particle quality was ascribed to a soluble portion of the swellable precursors dissolving out of the swellable particles during hypercrosslinking, leading to both particle-particle couple (*i.e.*, particle aggregation) and surface contamination of particles.

Many attempts were made at improving the quality of the particles produced *via* the hypercrosslinking chemistry, and this extensive study included varying, *inter alia*, the reaction temperature, the dispersion medium, the mixing and the crosslink density of the swellable precursor. Unfortunately, wholly satisfactory outcomes were not realised; the systematic study failed to deliver uniformly-sized hypercrosslinked particles. Thus, an alternative synthetic strategy was devised. The new synthetic strategy which was evolved involved the partial hypercrosslinking of swellable precursors using a sub-stoichiometric amount of Friedel-Crafts catalyst in a non-swelling solvent. The purpose of this step was to stabilise the particles before placing them into a swelling solvent. With the partially hypercrosslinked particles in hand, they were thereafter converted into fully hypercrosslinked particles by bringing them into contact with stoichiometric amounts of catalyst in a swelling solvent. Very pleasingly, not only could hypercrosslinked products with SSAs well in excess of 1,000 m<sup>2</sup>/g be produced in this way, but the particle quality was also very good. The particles were isolated in beaded form and had narrow particle size distributions. This research breakthrough paves the way for the synthesis of functionalised hypercrosslinked polymers in a well-defined beaded form.

The hypercrosslinking study revealed that it was very easy to tune the porosity of the hypercrosslinked products. Even although the hypercrosslinking reactions were very fast, reaction time is an important variable since the SSA increases as the hypercrosslinking reaction proceeds. However, controlling the ratio of styrene to VBC in the monomer feed, and varying the swelling extent of the precursor particles through changes in the dispersion medium, can also be used to tune porosity.

In the final part of this study, and with a view towards applications, functional groups were introduced into hypercrosslinked microparticles *via* post-hypercrosslinking chemical modification reactions. Functional groups with ion-exchange character were targeted, and in this regard hypercrosslinked particles with sulfonic acids groups and quaternary ammonium groups were synthesised. Porous polymer particles with satisfactory ion-exchange capacities could be produced in this way, with good options for control over ion-exchange capacity and particle quality.

### **8.1 Future Work**

The research work described in this thesis has set in place a range of facile, versatile and cost-effective synthetic methodologies of the production of highly porous, functionalised polymer particles in a well-defined beaded form. As such, a broad range of applications are suggested, and an important part of the future work will be to exploit the particles in terms of applications. Particles with narrow particles size distributions are especially well-suited to column-based (flow-through) separation science applications. However, the particles are by no means restricted to this field of use. For example, exploitation of the porous polymers as polymer supports for catalyst immobilisation or solid-phase organic synthesis are every bit as enticing.

Porous polymer microparticles with both strong cation exchange and strong anion exchange character have been synthesised. We have recently begun to explore the potential of these ion-exchangers as novel sorbents in solid-phase extraction. The particles are particularly attractive for solid-phase extraction applications because the

ion-exchange character is wrapped up in particles with high SSAs (hence high sorption capacity) and low particle size (hence high chromatographic efficiency).